

**APPLICATION OF BIOCATALYSTS FOR THE SUSTAINABLE  
POTENTIAL DRUGS**

**A Thesis Submitted**

**IN PARTIAL FULFILLMENT OF THE REQUIREMENTS**

**FOR THE DEGREE OF**

**DOCTOR OF PHILOSOPHY**

**IN**

**BIO-CHEMISTRY**

**BY**

**AMOL GULAB KHATIK**

**Admission No: 18SBAS3060004**

**Supervisor**

**Dr. Arvind Kumar Jain**

**Professor and Dean**

**School of Basic and Applied Sciences**

**Galgotias University**

**Greater Noida**



**SCHOOL OF BASIC AND APPLIED SCIENCES**

**GALGOTIAS UNIVERSITY (UP), INDIA**

**2023**

## CANDIDATE'S DECLARATION

I hereby certify that the work presented in the thesis, entitled “**Application of Biocatalysts for the Sustainable Potential Drugs**” in the fulfilment of the requirements for the award of the degree of Doctor of Philosophy in Biochemistry, School of Basic and Applied Sciences, Galgotias University, Greater Noida is an authentic record of my own work carried out during a period from **April, 2019** to **March, 2023** under the supervision of **Dr. Arvind Kumar Jain**, Professor and Dean, School of Basic and Applied Sciences, Galgotias University Greater Noida.

The matter embodied in this thesis by me is not have been submitted in part or full to any other university or institute for the award of any degree.

**(Amol Gulab Khatik)**

This is to certify that above statement made by the candidate is correct to the best of my knowledge.

**Supervisor**

**Dr. Arvind Kumar Jain**  
**Professor and Dean**  
**School of Basic and Applied Sciences**  
**Galgotias University**  
**Greater Noida**

The Ph. D. Viva- Voice examination of **Amol Gulab Khatik**, Research Scholar has been held on

Sign of Supervisor

Sign of External

## ABSTRACT

Biocatalytic synthesis is an efficient synthesis of chiral building blocks of pharmaceutical, agrochemical and fine chemicals intermediates. This research work elicits mainly on exploring novel route of synthesis for the applications of biocatalyst using nitrilases, ketoreductases and transaminases. Ketoreductases application for the chiral selective reduction of tert-butyl[5-(4-cyanobenzoyl)-2-fluorophenyl]carbamate to tert-butyl{5-[(4-cyanophenyl)(hydroxy)methyl]-2-fluorophenyl}carbamate. Commercially available enzymes were screened and the process optimised for commercial applications using ES-KRED-213 enzyme from syncozyme. The optimisation study includes co-solvent, pH, temperature for the reaction, substrate loading, enzyme loading and yield of the product. The purity of tert-butyl{5-[(4-cyanophenyl)(hydroxy)methyl]-2-fluorophenyl}carbamate formed was >99% (RP-HPLC), and chiral purity >99% (NP-HPLC). The recovered product was confirmed and characterized with instrumental analysis using HPLC analysis, specific optical rotation, melting point and boiling point, LC-MS, ATR-FTIR,  $^1\text{H}$  NMR, and  $^{13}\text{C}$  NMR.

Transaminase application for the chiral selective transamination of 1-(3-methylphenyl) ethan-1-one to (1*R*)-(3-methylphenyl)ethan-1-amine using ATA-025 from codexis. Commercially available enzymes screened and optimised the process for the commercial application. The variable such as co-solvent, enzyme loading, substrate loading, temperature, and pH for development of process displaying maximum conversion with good product formation and higher yield were optimized using one factor at a time approach and numerical optimization with Box Behnken Design, respectively. The purity of recovered product (1*R*)-(3-methylphenyl)ethan-1-amine formed was  $\geq 99\%$  (RP-HPLC), and chiral purity  $\geq 98.5\%$  (Chiral-GC), and it was also confirmed and characterized with instrumental methods using melting point, LC-MS, ATR-FTIR, and  $^1\text{H}$  NMR.

Nitrilases application for hydroxylation of 2-chloroisonicotinonitrile to 2-chloroisonicotinic acid using ES-NIT-102 from syncozyme. Commercially available nitrilases screened and optimised the commercially viable process cross linked enzyme aggregates (nitrilase-CLEAs) by fractional precipitation with *iso*-propanol, and cross linked with glutaraldehyde. The nitrilase-CLEAs prepared with optimized 35 mM glutaraldehyde for 120 min cross linking time had 82.36±4.45% residual activity and displayed type-II structural CLEAs formation as confirmed by particle size, SEM, FTIR, and SDS-PAGE analysis. Nitrilase-CLEAs had superior pH and temperature stability, showed a shift in optimal temperature by 5°C, and retained nearly 1.5 to 1.7 folds activity over free nitrilase at 50°C and 55°C after more than 9 h incubation. Nitrilase-CLEAs showed reduced affinity and decreased conversion of substrate as indicated by slightly higher  $K_m$  values by 5.19% and reduced  $V_{max}$  by 17%. Further, these nitrilase-CLEAs used for hydroxylation of 2-chloroisonicotinonitrile to 2-chloroisonicotinic acid. Nitrilase-CLEAs were catalytically active for 3 cycles showcasing 81% conversion, 75.53 g/L product formation and 66.42% yield. The recovered product was confirmed by HPLC, FTIR, LC-MS, and  $^1H$  NMR, and displayed >99% purity.

**Key words:** Transaminase; Transamination; Ketoreductase; Reduction; Nitrilase; Cross linked enzyme aggregates; Hydroxylation.

## **DEDICATION**

Every Challenging work needs self-efforts as well as guidance and blessings of elders especially those who were very close to our heart.

My humble efforts, “I dedicate to the loving memory of my Late. father”.

**“Gulab N. Khatik”**

Who formed part of my vision. The happy memory of my father still provides persistent inspiration for my journey in this life.

I also dedicate my efforts to my Sweet and loving

**“BROTHER, MOTHER, SISTERS & WIFE”**

Whose affection, love, encouragement, prays of days & night make me able to get such success and honour.

Along with all my hardworking Teachers, Family & Friends

## ACKNOWLEDGEMENT

With immense pleasure and deep sense of gratitude, I wish to express my sincere thanks to my research guide **Dr. Arvind Kumar Jain**, Dean and Professor, School of Basic and Applied Sciences, Galgotias University, Greater Noida, Gautam Buddha Nagar, (UP) India, without his motivation and continuous encouragement, this research would not have been successfully completed.

I am grateful to our Honourable chancellor **Mr. Sunil Galgotia**, Galgotias University, Vice chancellor **Prof. (Dr.) Mallikharjuna Babu Kayala**, Galgotias University, for motivating us to carry out this research in Galgotias University, Greater Noida by providing us the sophisticated infrastructural facilities, and many other resources needed for my research.

I thank internal members, Professors, for their valuable suggestions and helping me throughout my research, encouragement, and support. I express my sincere thanks to the Doctoral Committee members, for their guidance throughout my research period.

I am Sincerely thankful to **Dr. Sawraj Singh** (Technical director of Iosynth Labs Pvt Ltd. Bangalore) and **Dr. Abhijeet Bhimrao Muley** for their constant support to complete this study.

I wish to extend my profound sense of gratitude to my family members for all the sacrifices they made during my research and providing me the moral support.

Date: 01/03/2023

**AMOL GULAB KHATIK**

## Approval Sheet

This Thesis entitled “**Application of biocatalysts for the sustainable potential drugs**” written by Mr. Amol Gulab Khatik for the approval of the award of the degree of Doctor of Philosophy in Biochemistry.

**Examiner**

.....  
.....  
.....

**Supervisor**

.....  
.....  
.....

**Supervisor**

.....  
.....  
.....

Date: .....

Place: .....

## **Statement of Thesis Preparation**

1. Thesis title: **“Application of biocatalysts for the sustainable potential drugs”**
2. Degree for which the thesis is submitted: **Doctor of Philosophy**
3. Thesis Guide was referred to for preparing the thesis.
4. Specifications regarding thesis format have been closely followed.
5. The contents of the thesis have been organized based on the guidelines.
6. The thesis has been prepared without resorting to plagiarism.
7. All sources used have been cited appropriately.
8. The thesis has not been submitted elsewhere for a degree.



## LIST OF FIGURES

Figure 1.1 Schematic representation of the reaction diagram.....	1
Figure 1.2 Protein structure representing Primary, secondary tertiary and quaternary structures.....	4
Figure 1.3 Reaction mechanism of Alcohol dehydrogenas.....	6
Figure 1.4 Mechanism of hydride transfer to carbonyl carbon from NAD(P)H .....	8
Figure 1.5 Mechanism of transaminase enzyme.....	14
Figure 1.6 Approaches for application of transaminases.....	15
Figure 1.7 Nitrilase based conversion of nitriles to carboxylic acid and ammonia.....	16
Figure 2.1 Typical image of the Thermomixer .....	24
Figure 2.2 Typical images of micropipettes .....	25
Figure 2.3 Typical image of rotary evaporator .....	26
Figure 2.4 Typical image of the HPLC.....	27
Figure 2.5 Typical image on Chromatogram related terms .....	28
Figure 2.6 Image of normal phase HPLC column .....	31
Figure 2.7 Image of reverse phase HPLC column.....	31
Figure 2.8 Typical image of Gas chromatography .....	33
Figure 2.9 Typical image of GC column .....	34
Figure 2.10 Typical image of the polarimeter .....	36
Figure 2.11 Typical image of the Melting Point Apparatus .....	37
Figure 2.12 Schematic diagram of LC-MS setup .....	38
Figure 2.13 Typical image of LC-MS.....	38
Figure 2.14 Typical image of FTIR .....	39
Figure 2.15 Typical image of NMR spectrometer .....	40
Figure 2.16 Typical image of DLS-Particle size analyzer.....	41

Figure 2.17 Typical image of scanning electron microscope .....	42
Figure 2.18 Typical image of vertical electrophoretic unit.....	43
Figure 2.19 Typical image of centrifuge.....	44
Figure 3.1 Reverse phase HPLC chromatogram of tert-butyl[5-(4-cyanobenzoyl)-2-fluoro phenyl] carbamate .....	52
Figure 3.2 Reverse phase HPLC chromatogram of tert-butyl{5-[(4-cyanophenyl) (hydroxy) methyl]-2-fluorophenyl}carbamate .....	53
Figure 3.3 Chiral HPLC chromatogram of tert-butyl{5-[(4-cyanophenyl)(hydroxy)methyl]-2- fluoro phenyl}carbamate .....	54
Figure 3.4 <sup>1</sup> H NMR profile of tert-butyl[5-(4-cyanobenzoyl)-2-fluorophenyl]carbamate .....	55
Figure 3.5 LC-MS spectra of tert-butyl[5-(4-cyanobenzoyl)-2-fluorophenyl]carbamate .....	56
Figure 3.6 LC-MS spectra of tert-butyl{5-[(4-cyanophenyl)(hydroxy)methyl]-2-fluoro phenyl} carbamate.....	57
Figure 3.7 Reaction pathway for ketoreductase mediated chiral selective reduction of tert- butyl [5-(4-cyanobenzoyl)-2-fluorophenyl]carbamate to tert-butyl {5-[(S)-(4-cyano phenyl) (hydroxy)methyl]-2-fluorophenyl}carbamate using glucose and glucose dehydrogenase system.....	59
Figure 3.8 Reaction pathway for ketoreductase mediated chiral selective reduction of tert- butyl [5-(4-cyanobenzoyl)-2-fluorophenyl]carbamate to tert-butyl {5-[(S)-(4- cyanophenyl) (hydroxy)methyl]-2-fluorophenyl}carbamate using iso-propanol as co- factor recycling.....	59
Figure 3.9 Effect of addition of co-solvents on chiral selective reduction of tert-butyl [ 5-(4-cyanobenzoyl)-2-fluorophenyl]carbamate to tert-butyl {5-[(S)-(4-cyanophenyl) (hydroxy)methyl]-2-fluorophenyl}carbamate .....	63

Figure 3.10 Effect of temperature on chiral selective reduction of tert-butyl [5-(4-cyanobenzoyl)-2-fluorophenyl]carbamate to tert-butyl {5-[(S)-(4-cyanophenyl)(hydroxy)methyl]-2-fluoro phenyl}carbamate .....	65
Figure 3.11 Effect of operating pH on chiral selective reduction of tert-butyl [5-(4-cyanobenzoyl)-2-fluorophenyl]carbamate to tert-butyl {5-[(S)-(4-cyanophenyl) (hydroxy) methyl]-2-fluoro phenyl}carbamate.....	67
Figure 3.12 Effect of enzyme loading on chiral selective reduction of tert-butyl [5-(4-cyanobenzoyl)-2-fluorophenyl]carbamate to tert-butyl {5-[(S)-(4-cyanophenyl) (hydroxy) methyl]-2-fluoro phenyl}carbamate.....	67
Figure 3.13 Effect of substrate loading on chiral selective reduction of tert-butyl [5-(4-cyanobenzoyl)-2-fluorophenyl]carbamate to tert-butyl {5-[(S)-(4-cyanophenyl) (hydroxy)methyl]-2-fluoro phenyl}carbamate.....	69
Figure 3.14 Time course of reaction on gram scale progression with temperature.....	70
Figure 3.15 Time course of reaction on gram scale progression with enzyme loading.....	72
Figure 3.16 Time course of reaction on gram scale progression with substrate loading.....	73
Figure 3.17 HPLC profile of tert-butyl {5-[(S)-(4-cyanophenyl)(hydroxy)methyl]-2-fluoro phenyl}carbamate.....	74
Figure 3.18 Reverse phase HPLC chromatogram of tert-butyl[5-(4-cyanobenzoyl)-2-fluorophenyl]carbamate.....	75
Figure 3.19 Normal phase HPLC chromatogram of single isomer of tert-butyl{5-[(4-cyanophenyl)(hydroxy)methyl]-2-fluorophenyl}carbamate.....	75
Figure 3.20 Normal phase HPLC chromatogram of racemic tert-butyl{5-[(4-cyanophenyl) (hydroxy)methyl]-2-fluorophenyl}carbamate .....	76
Figure 3.21 LC profile of tert-butyl{5-[(4-cyanophenyl)(hydroxy)methyl]-2-fluorophenyl}carbamate in LC-MS .....	77

Figure 3.22 Mass fraction profile tert-butyl{5-[(4-cyanophenyl)(hydroxy)methyl]-2-fluorophenyl} carbamate .....	78
Figure 3.23 FTIR spectra of tert-butyl{5-[(4-cyanophenyl)(hydroxy)methyl]-2-fluorophenyl} carbamate.....	80
Figure 3.24 <sup>1</sup> H NMR in DMSO of tert-butyl {5-[(S)-(4-cyanophenyl)(hydroxy)methyl]-2-fluorophenyl} carbamate .....	82
Figure 3.25 <sup>13</sup> C NMR in DMSO of tert-butyl {5-[(S)-(4-cyanophenyl)(hydroxy)methyl]-2-fluorophenyl} carbamate .....	83
Figure 4.1 Route of synthesis for Chiral selective transamination of (1R)-(3-methylphenyl)ethan-1-amine from 1-(3-methylphenyl)ethan-1-one .....	96
Figure 4.2 Effect of addition of co-solvents on chiral selective transamination of (1R)-(3-methylphenyl)ethan-1-amine from 1-(3-methylphenyl)ethan-1-one .....	99
Figure 4.3 Influence of enzyme loading on chiral selective transamination of 1-(3-methylphenyl)ethan-1-one to (1R)-(3-methylphenyl)ethan-1-amine.....	101
Figure 4.4 Influence of substrate loading on chiral selective transamination of 1-(3-methylphenyl)ethan-1-one to (1R)-(3-methylphenyl)ethan-1-amine.....	102
Figure 4.5 Influence of operating temperature on chiral selective transamination of 1-(3-methylphenyl)ethan-1-one to (1R)-(3-methylphenyl)ethan-1-amine.....	103
Figure 4.6 Influence of medium pH on chiral selective transamination of 1-(3-methylphenyl)ethan-1-one to (1R)-(3-methylphenyl)ethan-1-amine .....	105
Figure 4.7 Response surface plots (3D and 2D) representing the effect of interaction of enzyme loading and substrate loading on the response 1 (Conversion, %) during chiral selective transamination of (1R)-(3-methylphenyl)ethan-1-amine from 1-(3-methylphenyl).....	113

Figure 4.8 Response surface plots (3D and 2D) representing the effect of interaction of enzyme loading and temperature on the response 1 (Conversion, %) during chiral selective transamination of (1R)-(3-methylphenyl)ethan-1-amine from 1-(3-methylphenyl)ethan-1-one.....	113
Figure 4.9 Response surface plots (3D and 2D) representing the effect of interaction of enzyme loading and pH on the response 1 (Conversion, %) during chiral selective transamination of (1R)-(3-methylphenyl)ethan-1-amine from 1-(3-methylphenyl)ethan-1-one .....	114
Figure 4.10 Response surface plots (3D and 2D) representing the effect of interaction of substrate loading and temperature on the response 1 (Conversion, %) during chiral selective transamination of (1R)-(3-methylphenyl)ethan-1-amine from 1-(3-methylphenyl)ethan-1.....	114
Figure 4.11 Response surface plots (3D and 2D) representing the effect of interaction of substrate loading and pH on the response 1 (Conversion, %) during chiral selective transamination of (1R)-(3-methylphenyl)ethan-1-amine from 1-(3-methylphenyl)ethan-1-one.....	115
Figure 4.12 Response surface plots (3D and 2D) representing the effect of interaction of temperature and pH on the response 1 (Conversion, %) during chiral selective transamination of (1R)-(3-methylphenyl)ethan-1-amine from 1-(3-methylphenyl)ethan-1-one .....	115
Figure 4.13 Response surface plots (3D and 2D) representing the effect of interaction of enzyme loading and substrate loading on the response 2 (Yield, %) during chiral selective transamination of (1R)-(3-methylphenyl)ethan-1-amine from 1-(3-methylphenyl)ethan-1-on .....	118

Figure 4.14 Response surface plots (3D and 2D) representing the effect of interaction of enzyme loading and temperature on the response 2 (Yield, %) during chiral selective transamination of (1R)-(3-methylphenyl)ethan-1-amine from 1-(3-methylphenyl)ethan-1-one .....	118
Figure 4.15 Response surface plots (3D and 2D) representing the effect of interaction of enzyme loading and pH on the response 2 (Yield, %) during chiral selective transamination of (1R)-(3-methylphenyl)ethan-1-amine from 1-(3-methylphenyl)ethan-1-one .....	119
Figure 4.16 Response surface plots (3D and 2D) representing the effect of interaction of substrate loading and temperature on the response 2 (Yield, %) during chiral selective transamination of (1R)-(3-methylphenyl)ethan-1-amine from 1-(3-methylphenyl)ethan-1-one .....	119
Figure 4.17 Response surface plots (3D and 2D) representing the effect of interaction of substrate loading and pH on the response 2 (Yield, %) during chiral selective transamination of (1R)-(3-methylphenyl)ethan-1-amine from 1-(3-methylphenyl)ethan-1-one .....	120
Figure 4.18 Response surface plots (3D and 2D) representing the effect of interaction of temperature and pH on the response 2 (Yield, %) during chiral selective transamination of (1R)-(3-methylphenyl)ethan-1-amine from 1-(3-methylphenyl)ethan-1-one .....	120
Figure 4.19 LC profile of 1-(3-methylphenyl)ethan-1-one after LC-MS analysis .....	127
Figure 4.20 LC profile of (1R)-(3-methylphenyl)ethan-1-amine after LC-MS analysis .....	128
Figure 4.21 LC mass profile of 1-(3-methylphenyl)ethan-1-one .....	129
Figure 4.22 LC mass profile of (1R)-(3-methylphenyl)ethan-1-amine .....	130
Figure 4.23 <sup>1</sup> H NMR spectra of 1-(3-methylphenyl)ethan-1-one .....	132
Figure 4.24 <sup>1</sup> H NMR spectra of (1R)-(3-methylphenyl)ethan-1-amine .....	133

Figure 4.25 FTIR spectra of 1-(3-methylphenyl)ethan-1-one .....	135
Figure 4.26 FTIR spectra of (1R)-(3-methylphenyl)ethan-1-amine .....	136
Figure 4.27 RP-HPLC profile of 1-(3-methylphenyl)ethan-1-one .....	137
Figure 4.28 RP-HPLC profile of (1R)-(3-methylphenyl)ethan-1-amine .....	138
Figure 4.29 HPLC profile of transamination reaction with around 55-60% conversions .....	138
Figure 4.30 Chiral GC profile of (1R)-(3-methylphenyl)ethan-1-amine .....	139
Figure 4.31 Chiral GC profile of (R,S)-(3-methylphenyl)ethan-1-amine .....	140
Figure 4.32 Effect of enzyme loading in transamination of 1-(3-methylphenyl)ethan-1-one to (1R)-(3-methylphenyl)ethan-1-amine .....	142
Figure 4.33 Effect of substrate loading in transamination of 1-(3-methylphenyl)ethan-1-one to (1R)-(3-methylphenyl)ethan-1-amine .....	143
Figure 4.34 Effect of operating temperature in transamination of 1-(3-methylphenyl)ethan-1- one to (1R)-(3-methylphenyl)ethan-1-amine .....	144
Figure 4.35 Effect of medium pH in transamination of 1-(3-methylphenyl)ethan-1-one to (1R)-(3-methylphenyl)ethan-1-amine .....	145
Figure 5.1 Chromatograms of standard mandelonitrile (0.25 mg/mL in 0.1% trifluoroacetic acid in water (60%) and acetonitrile (40%)) on HPLC .....	158
Figure 5.2 Chromatograms of standard mandelic acid (0.25 mg/mL in 0.1% trifluoroacetic acid in water (60%) and acetonitrile (40%)) on HPLC .....	158
Figure 5.3 Chromatograms of enzymatic reaction with around 90% conversion on HPLC system .....	159
Figure 5.4 Effect of miscible organic solvents on the recovery of nitrilase activity .....	160
Figure 5.5 Effect of glutaraldehyde concentration (mM), on the preparation of nitrilase- CLEAs .....	161
Figure 5.6 Effect of Cross-linking time (min) on the preparation of nitrilase-CLEAs .....	162

Figure 5.7 Instrumental characterization particle size distribution of nitrilase-CLEAs .....	163
Figure 5.8 Scanning electron microscopic image of nitrilase-CLEAs at 1500 × magnification .....	164
Figure 5.9 FTIR spectra of free nitrilase and nitrilase-CLEAs.....	165
Figure 5.10 SDS-PAGE analysis of free nitrilase and nitrilase-CLEAs. Lane A: standard molecular weight markers, Lane B: free nitrilase, and Lane C: nitrilase-CLEAs.....	167
Figure 5.11 Lineweaver-Burk plot for determination of kinetic parameters of free nitrilase and nitrilase-CLEAs .....	168
Figure 5.12 Effect of operating pH on activity of free nitrilase and nitrilase-CLEAs.....	169
Figure 5.13 pH stability of free nitrilase and nitrilase-CLEAs.....	170
Figure 5.14 Effect of operating temperature on activity of free nitrilase and nitrilase-CLEAs .....	171
Figure 5.15 Thermal stability of free nitrilase .....	172
Figure 5.16 Thermal stability of nitrilase-CLEAs .....	172
Figure 5.17 Reaction pathway of hydroxylation of 2-chloroisonicotinonitrile to 2- chloroisonicotinic acid with nitrilase.....	174
Figure 5.18 Chromatograms of standard 2-chloroisonicotinonitrile (0.25 mg/mL in 0.1% trifluoroacetic acid in water (60%) and acetonitrile (40%)) on HPLC system .....	174
Figure 5.19 Chromatograms of standard 2-chloroisonicotinic acid (0.25 mg/mL in 0.1% trifluoroacetic acid in water (60%) and acetonitrile (40%)) on HPLC system .....	175
Figure 5.20 Chromatograms of enzymatic reaction with around 40% conversion on HPLC system.....	175
Figure 5.21 Effect of nitrilase-CLEAs loading on conversion of 2-chloroisonicotinonitrile to 2-chloroisonicotinic acid .....	176



Figure 5.22 Effect of temperature with incubation time on conversion of 2-chloroisonicotinonitrile to 2-chloroisonicotinic acid using nitrilase CLEA.....	177
Figure 5.23 FTIR spectra of 2-chloroisonicotitrile and 2-chloroisonicotinic acid.....	178
Figure 5.24 LC profile of 2-chloroisonicotinic acid in LC-MS.....	179
Figure 5.25 Mass fractions of 2-chloroisonicotinic acid on LC-MS spectra.....	179
Figure 5.26 <sup>1</sup> H NMR spectra of 2-chloroisonicotinonitrile.....	180
Figure 5.27 <sup>1</sup> H NMR spectra of 2-chloroisonicotinic acid.....	181

## LIST OF TABLES

Table 1.1 Enzyme classification .....	5
Table 1.2 Nitrilase non-selective application.....	17
Table 1.3 Nitrilase enantio-selective application.....	18
Table 1.4 Nitrilase chemo-selective application.....	19
Table 1.5 Nitrilase regio-selective application .....	20
Table 2.1 Column chemistry and mode of separation .....	30
Table 2.2 List of HPLC column used in research work.....	32
Table 2.3 GC column used in research work.....	35
Table 3.2.4 Screening of ketoreductases for reduction of tert-butyl [5-(4-cyanobenzoyl)-2-fluorophenyl] carbamate to tert-butyl {5-[(S)-(4-cyanophenyl)(hydroxymethyl)-2-fluorophenyl] carbamate.....	60
Table 4.1 Experimental range levels of parameters for chiral selective transamination of 1-(3-methylphenyl)ethan-1-one to (1R)-(3-methylphenyl)ethan-1-amine Experimental range levels of parameters for chiral selective transamination of 1-(3-methylphenyl)ethan-1-one.....	90
Table 4.2 Transaminase screening screening for transamination of 1-(3-methyl phenyl)ethan-1-one to (1R)-(3-methyl phenyl)ethan-1-amine .....	98
Table 4.3 Effect of transamination parameters on conversion, product formation, product recovery, and yield after of chiral selective transamination of 1-(3-methylphenyl)ethan-1-one to (1R)-(3-methylphenyl)ethan-1-amine .....	106
Table 4.4 Combined transformation parameters according to Box Behnken design and the corresponding response as enzymatic conversion (%) and yield (%) in chiral selective transamination of 1-(3-methylphenyl)ethan-1-one to (1R)-(3-methylphenyl)ethan-1-amine .....	108

Table 4.5 ANOVA for response surface quadratic model of response 1 (Conversion, %) in chiral selective transamination of 1-(3-methylphenyl)ethan-1-one to (1R)-(3-methylphenyl)ethan-1-amine.....	111
Table 4.6 ANOVA for response surface quadratic model of response 2 (Yield, %) in chiral selective transamination of 1-(3-methyl phenyl) ethan-1-one to (1R)-(3-methyl phenyl) ethan-1-amine .....	116
Table 4.7 Coefficient of all the term in polynomial model at $p < 0.05$ and the corresponding ANOVA data associated with the consequences of transamination parameters on conversion (%) and yield (%).....	121
Table 4.8 The set of constraints for different factors and responses for developing the reaction conditions .....	125
Table 5.1 Screening of nitrilases for hydroxylation of 2-chloro-isonicotinonitrile to 2-chloro-isonicotinic acid.....	156
Table 5.2 Reusability profile of nitrilase-CLEAs for hydroxylation of 2-chloroisonicotinonitrile to 2-chloroisonicotinic acid indicating conversion of substrate to product (%), product formation (g/L) and product yield (%).....	182

## LIST OF TERMS AND ABBREVIATIONS

FPLC	Fast protein liquid chromatography
MALDI-TOF-MS	Matrix assisted laser desorption ionization- time of flight mass spectrometry
UV Vis	Ultraviolet visible
NMR	Nuclear magnetic resonance
CD	Circular dichroism
3D	Three dimensional
IUBMB	International Union of Biochemistry and Molecular Biology
EC	Enzyme commission
API	Active pharmaceutical ingredient
NAD	Nicotinamide adenine dinucleotide
NADP	Nicotinamide adenine dinucleotide phosphate
FAD	Flavin adenine dinucleotide
ADH	Alcohol dehydrogenase
PLP	pyridoxal 5'-phosphate
( <i>S</i> )	Sinister configuration
( <i>R</i> )	Rectus configuration
L	Levorotatory
D	Dextrorotatory
MTCC	Microbial type culture collection
ATCC	American type culture collection
KR	Kinetic resolution
AS	Asymmetric synthesis

DKR	Dynamic kinetic resolution
GDH	Glucose dehydrogenase
TA	Transaminase
DLS	Dynamic light scattering
SEM	Scanning electron microscope
FTIR	Fourier transform infrared
ATR	Attenuated total reflection
SDS-PAGE	Sodium dodecyl-sulfate polyacrylamide gel
HPLC	High performance liquid chromatography
LC-MS	Liquid chromatography mass spectrometry
GC	Gas chromatography
CLEA	Cross-linked enzyme aggregates
DMSO	Dimethyl sulfoxide
HCl	Hydrochloric acid
μL	Microliter
Mg	Milligram
mM	Millimolar
RPM	Rotation per minute
RSM	Response surface methodology
RP	Reverse phase
NP	Normal phase
FID	Flame ionization detector

PDA detector	Photodiode detector
UV detector	Ultraviolet detector
KRED	Ketoreductase
ANOVA	Analysis of variance
BBD	Box Behnken design
NaCl	Sodium chloride
NaOH	Sodium hydroxide
NR	Not Reported
CA	Carboxylic acid
Ferment.	Fermentation
IUBMB	International Union of Biochemistry and Molecular Biology
-NH <sub>2</sub>	Amine
TFA	Trifluoroacetic acid

## LIST OF PUBLICATIONS

1. **Khatik AG, Jain AK, Muley AB; “Preparation, characterization and stability of cross linked nitrilase aggregates (nitrilase–CLEAs) for hydroxylation of 2-chloroiso nicotinonitrile to 2-chloroisonicotinic acid”, *Bioprocess and Biosystems Engineering*; Published online: 13 August 2022; <https://doi.org/10.1007/s00449-022-02766-0> (IF= 3.4). **SCI****
2. **Khatik AG, Jain AK, Muley AB; “Transaminases mediated chiral selective synthesis of (1R)-(3-methylphenyl)ethan-1-amine from 1-(3-methylphenyl)ethan-1-one: Process minutiae, optimization, characterization, and ‘What If Studies’”, *Bioprocess and Biosystems Engineering*; Published online: 3 December 2022; <https://doi.org/10.1007/s00449-022-02824-7> (IF= 3.4). **SCI****
3. **Khatik AG, Jain AK, Muley AB; “Ketoreductase assisted synthesis of chiral selective tert-butyl{5-[(4-cyanophenyl)(hydroxy)methyl]-2-fluorophenyl} carbamate: Process minutiae, optimization and characterization”, *Chemical Papers*; Published online:19 January 2023; <https://doi.org/10.1007/s11696-023-02698-3> (IF= 2.1). **SCI****
4. **Khatik AG, Jain AK, Tiwari RK; “Review on Nitrilase enzyme”, *Chemical Papers* (Communicated) (IF= 2.1). **SCI****
5. **Khatik AG, Jain AK, Nadar SS; “Immobilized ketoreductase application to meet the challenges for sustainable potential drugs”, *International journal of biological macromolecules*; (Communicated) (IF= 8.0). **SCI****
6. **Khatik AG, Jain AK; “Industrial application of racemase enzymes”, *Macromolecules* (In progress) (IF= 6.0). **SCI****

## Patents

7. **Amol Gulab Khatik**, Dr. Arvind Kumar Jain

Title of invention: **“Preparation, characterization and stability of cross linked nitrilase aggregates (nitrilase–CLEAs) for hydroxylation of 2-chloroisonicotinonitrile to 2-chloroisonicotinic acid”** Published online: 7 October 2022;  
Application Number: 202221054882 A

8. **Amol Gulab Khatik**, Dr. Arvind Kumar Jain

Title of invention: **“Synthesis of chiral compound tert-butyl{5-[(4-cyanophenyl)(hydroxy)methyl]-2-fluorophenyl}carbamate via novel and green enzymatic route at industrial scale”** Published online: 10 December 2022; Application Number: 202211071408

## International Conference

9. **Amol Gulab Khatik**, Dr. Arvind Kumar Jain . **“Ketoreductase assisted synthesis of chiral selective tert-butyl{5-[(4-cyanophenyl)(hydroxy)methyl]-2-fluorophenyl}carbamate: Process minutiae, optimization and characterization”**.  
**International Conference on Advanced Materials for Next Generation** on 29 and 30 September 2021 at Galgotias University.

<https://doi.org/10.33263/Proceedings35.030> Volume 3, Issue 5, 2021, 30;

**Application.** 29 and 30 September, 2021 at Galgotias University



## **Book Chapter**

- 10. Amol Khatik, Arvind K. Jain; “Biological and Enzymatic approach in green technologies”, for the book “Green Chemistry: A Path to Sustainable Development”. Publisher: Elsevier (In progress)**

## Contents

CANDIDATE’S DECLARATION .....	i
ABSTRACT.....	ii
DEDICATION.....	iv
ACKNOWLEDGEMENT .....	v
Approval Sheet.....	vi
Statement of Thesis Preparation .....	vii
LIST OF FIGURES .....	viii
LIST OF TABLES.....	xvii
LIST OF TERMS AND ABBREVIATIONS .....	xix
LIST OF PUBLICATIONS .....	xxii
Chapter 1.....	1
1.1 Introduction.....	1
1.2 Enzyme as biological catalyst.....	1
1.3 Types of protein.....	3
1.4 Oxido-reductases .....	6
1.5 Transferase.....	13
1.6 Hydrolase.....	16
Chapter 2.....	22
2.1. Material and methods .....	22
2.2 Substrates, products, and enzymes .....	22
2.3 Coenzymes and cofactors .....	23

2.4	Chemicals for assay .....	23
2.5	Reagents for the reaction buffer and other preparations.....	23
2.6	Instruments .....	24
Chapter 3.....		45
3.1.	Introduction .....	45
3.2	Material and Methods .....	47
3.2.1	Screening of ketoreductases for reduction tert-butyl[5-(4-cyanobenzoyl)-2-fluorophenyl]carbamate to tert-butyl {5-[(4-cyanophenyl) (hydroxy) methyl] -2- fluorophenyl }carbamate .....	47
3.2.2	Screening of co-solvents.....	48
3.2.3	Optimization of process parameters .....	48
3.2.4	Time course reactions on gram scale.....	49
3.2.5	Instrumental characterization .....	50
3.2.6	Statistical analysis.....	51
3.3	Results and discussion .....	51
3.3.1	Screening of ketoreductases for reduction of tert-butyl[5-(4-cyanobenzoyl)-2-fluorophenyl]carbamate to tert-butyl {5-[(4-cyanophenyl) (hydroxy) methyl] -2- fluorophenyl }carbamate .....	58
3.3.2	Effect of co-solvents .....	63
3.3.3	Optimization of process parameters .....	65
3.3.4	Time course reactions on gram scale.....	69

3.3.5	Instrumental characterization of tert-butyl{5-[(4-cyanophenyl)(hydroxy)methyl]-2-fluorophenyl}carbamate .....	74
3.4	Conclusion .....	84
Chapter 4	.....	85
4.1	Introduction.....	85
4.2	Material and Methods .....	88
4.2.1	Enzyme Screening for transamination of 1-(3-methylphenyl)ethan-1-one to (1 <i>R</i> )-(3-methylphenyl)ethan-1-amine.....	88
4.2.2	Screening of co-solvents.....	88
4.2.3	Optimization of process parameters .....	89
4.2.3.1	One factor at a time application.....	89
4.2.3.2	Statistical application using central composite pattern.....	90
4.2.4	Instrumental characterization .....	92
4.2.4.1	Reverse phase HPLC .....	92
4.2.4.2	Chiral analysis by GC.....	92
4.2.4.3	Confirmation and characterization of 1-(3-methylphenyl)ethan-1-one to (1 <i>R</i> )-(3-methylphenyl)ethan-1-amines .....	93
4.2.5	Time course reactions on gram scale.....	93
4.2.6	Statistical analysis.....	94
4.3	Result and discussion.....	95
4.3.1	Screening of transaminases for transamination of 1-(3-methylphenyl)ethan-1-one to (1 <i>R</i> )-(3-methylphenyl)ethan-1-amine.....	95

4.3.2	Screening of co-solvents.....	98
4.3.3	Optimization of process parameters .....	100
4.3.3.1	1 factor at a time approach .....	100
4.3.3.2	Statistical approach using Box Behnken Design.....	107
4.3.4	Instrumental characterization of 1-(3-methyl phenyl) ethan-1-one and (1 <i>R</i> )-(3-methyl phenyl) ethan-1-amine.....	126
4.3.4.1	Boiling point.....	126
4.3.4.2	LC-MS analysis .....	126
4.3.4.3	NMR analysis .....	131
4.3.4.4	FTIR analysis.....	134
4.3.4.5	HPLC analysis .....	137
4.3.4.6	Chiral analysis by GC.....	139
4.3.5	Time course reactions on gram scale for ‘What If studies’ .....	141
4.3.5.1	Progress of reaction with enzyme loading.....	141
4.3.5.2	Progress of reaction with substrate loading .....	142
4.3.5.3	Progress of reaction with temperature .....	143
4.3.5.4	Progress of reaction with medium pH .....	144
4.4	Conclusion .....	145
Chapter 5.....		147
5.1	Introduction.....	147
5.2	Material and methods .....	150

5.2.1	Screening of nitrilases for hydroxylation of 2-chloro isonicotinonitrile to 2 – chloro isonicotinic acid.....	150
5.2.2	Preparation of nitrilase-CLEAs .....	151
5.2.2.1	Step 1: Precipitation of nitrilase .....	151
5.2.2.2	Step 2: Cross-linking of nitrilase .....	151
5.2.3	Determination of nitrilase activity and protein content .....	152
5.2.4	Instrumental characterization .....	152
5.2.5	Kinetic parameters of free nitrilase and nitrilase-CLEAs.....	153
5.2.6	Biochemical characterization .....	153
5.2.6.1	pH optima and pH stability.....	153
5.2.6.2	Temperature optima and thermal stability.....	153
5.2.6.3	Application of free-nitrilase and nitrilase-CLEAs for hydroxylation of 2-chloro isonicotinonitrile to 2-chloro isonicotinic acid.....	153
5.2.6.4	Instrumental characterization of 2-chloroisonicotinonitrile and 2-chloroiso nicotinic acid.....	154
5.2.7	Reusability studies of nitrilase-CLEAs .....	155
5.2.8	Statistical analysis.....	155
5.3	Results and discussion .....	155
5.3.1	Screening of nitrilases for hydroxylation of 2-chloro isonicotinonitrile to 2- chloroiso nicotinic acid.....	155
5.3.2	Preparation of nitrilase-CLEAs .....	157
5.3.3	Precipitation of nitrilase.....	159

5.3.4	Cross-linking of nitrilase .....	160
5.3.5	Instrumental characterization of Nitrilase CLEAs .....	163
5.3.5.1	Particle size and morphology of nitrilase-CLEAs .....	163
5.3.5.2	FTIR analysis.....	165
5.3.5.3	SDS PAGE analysis.....	166
5.3.6	Kinetic constants.....	167
5.3.7	Biochemical characterization .....	169
5.3.7.1	pH optima and pH stability.....	169
5.3.7.2	Temperature optima and thermal stability.....	171
5.3.8	Hydroxylation of 2-chloro-4-cyanopyridine (2-chloro isonicotinonitrile) to 2-chloro pyridine-4-carboxylic acid (2-chloro isonicotinic acid).....	173
5.3.8.1	Effect of enzyme loading.....	175
5.3.8.2	Effect of reaction temperature .....	176
5.3.9	Instrumental characterization of 2-chloro isonicotinonitrile to 2-chloro isonicotinic acid.....	177
5.3.9.1	Functional group confirmation by FTIR .....	177
5.3.9.2	Mass confirmation by LC-MS.....	178
5.3.9.3	Structural confirmation by NMR.....	180
5.3.10	Reusability of nitrilase-CLEAs .....	181
5.4.	Conclusion .....	183
Chapter 6.....		184
6.1. Summary .....		184

6.2	Future prospects.....	188
	REFERENCES .....	190



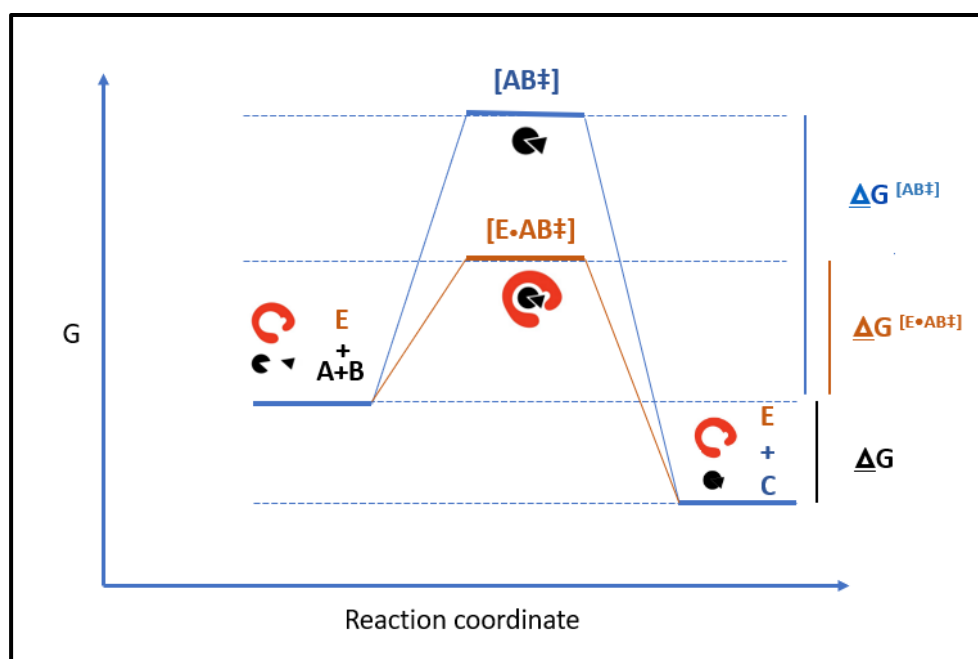
## **CHAPTER-1**

### **INTRODUCTION**

# Chapter 1

## 1.1 Introduction

Conventional chemistry processes require complex synthetic reactions which utilise a high quantity of energy and raw materials. As time passes, evolution created millions of micro-organisms having enzymes known to catalyse xenobiotic compounds. Enzymes are natural biocatalysts for the transformation of organic compounds [1]. Enzymes are naturally occurring catalysts for the transformations with specificity and selectivity. Specificity and selectivity include chemo-, regio-, enantio-selectivity and specificity [2]. Additionally, enzymes have rate enhancement capability compared to non-catalysed reactions in the range of  $10^7$  to  $10^{19}$ -fold increase explained in *figure 1.1* [3,4]



*Figure 1.1 Reaction diagram of enzyme catalysed reaction*

## 1.2 Enzyme as biological catalyst

Biocatalytic processes are competitive to multilevel classical chemistry using isolated enzymes or living cells at ambient temperature in aqueous medium. This

shows the positive impact on lower energy consumption and less pollutant deriving process [5]. Mentioned benefit of the enzymes in the organic transformation becomes the competitive for the replacement of traditional catalytic synthesis of new chirally selective components likes -amines, -alcohols, and -carboxylic acids at large scale applications in active pharmaceutical ingredients (APIs), food industries and fine chemicals [6].

There are various challenges in application of enzymes in chemical synthesis such as stability of enzymes in reaction medium, high cost of enzymes and product inhibition. Biocatalysis is further divided into enzymatic process and ferment. process. In ferment. process whole cells with pre-owned enzymes [7], and enzymatic synthesis uses purified enzyme isolated from micro-organism uses to carry out the reaction. In ferment. process whole cells use to performing several conversions by using the energy generated by living microorganisms. The micro-organisms are grown using the feed and the desired product is separated from the rest of ferment. medium. Best example of ferment. is the bioethanol production from the sugar fermentation [8]. Other mode of biocatalysis is by using the purified enzymes as a catalyst. For the reaction isolated enzymes processed using immobilised and stabilised using stabilisers to sustain in continuous processes and specified and highly selective biocatalytic process.

Kirchoff's in 1811 first introduced the concept of Enzyme catalysis. but the word '-catalysis' was given by Berzelius in year 1838, and "protein" word was introduced by Kunhe in 1864. Today's biocatalysis is based on the hypothesis proposed by Michaelis and Menten in the year 1913. Enzymes are selective in nature and specific (Lock and key mechanism) in their actions. Enzymes acts by lowering the activation energy without consuming itself in the reaction. Enzymes undergo a conformational change during the biocalytic process. These enzymes produce minimum waste by

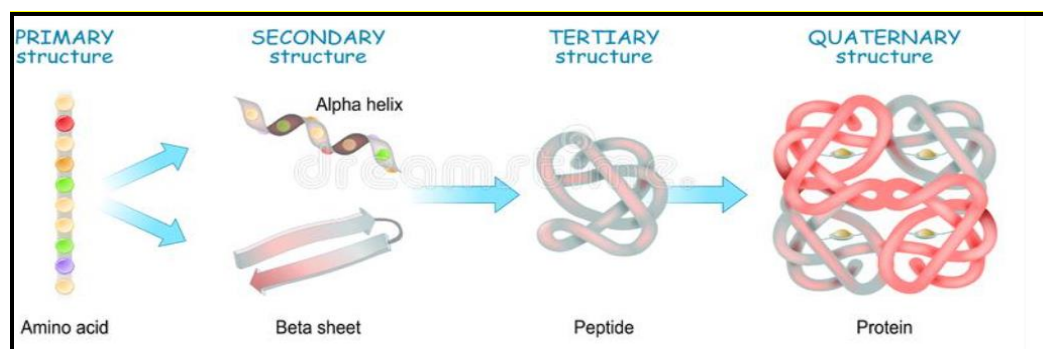
consuming low amount of energy at neutral pH, atmospheric pressure, and ambient temperature. To perform the effective process needs to optimise the reaction pH, temperature, and stability of the enzyme in solvent needs to be optimized.

Resolution of chiral building blocks of pharmaceuticals, agricultural fine chemicals which includes carboxylic acids, amines and CA by tightly binding the active catalytic site to one of the isomers with lock and key mechanism whereas another isomer will not bind. The use of enzymes for resolution of pharmaceutical intermediates is demanding alternative to chemically conventional synthesis methods [9]. Enzymes from the micro-organisms, fungi, yeast, plant, and animal sources are mainly used for the biocatalysis Enzyme purification mainly needs chromatographic technique such as FPLC. Others techniques of concentration such as salting in and salting out, precipitation using co-solvent, membrane techniques like ultra-filtration and removal of small molecules and salts by dialysis or frozen techniques such as lyophilisation. Purified or partially purified enzyme are characterised by techniques such as electrophoretic techniques, MALDI-TOF-MS, UV Vis spectroscopy, CD and fluorescent spectrometry and structural characterization by NMR spectrometry or crystallographic x-ray studies. Functioning characterization such as optimum conditions determinations such as assorted temperatures and pH. Fundamentally, enzymes are proteins containing chains of amino acids in linear forms which folds to form 3D structure of enzyme.

### **1.3 Types of protein**

Proteins are divided into four types based on their protein's structure (*figure 1.2*): -primary, -secondary, -tertiary, and -quaternary. The primary protein structure is amino acids linked with peptide chains, the secondary structures of protein containing the  $\alpha$ -helices or sheets of  $\beta$ -pleated which are linked together with hydrogen bonding. The tertiary structures of protein is the 3-dimensinal arrangement

of a protein moiety with additional attractive forces such as vander val, hydrogen bonds between the  $\alpha$ -helices or the sheets of  $\beta$ -pleated and the quaternary structures of protein is of several protein molecules together. From the entire structure of protein only active site consisting of few amino acids are responsible for the catalysis. There are some exceptions having coenzymes and cofactors which are useful for maintaining structures of protein and the pocket of active site formed by amino acid sequence. Coenzymes are low molecular weight organic molecules which are non-protein parts which may be or may not be take part in the active activator site of the enzyme but enhances the stability and solubility of the enzyme. Cofactors are metal ions and. The cofactors are untidily or rigidly bound to the protein molecule via electron pair or non-electron pair bonding and provide stability to the enzyme and its active site. In some enzymes cofactors and coenzymes are essentially required for its activity. Once cofactor or coenzyme separated from enzyme moiety enzyme will not show the activity and hence decrease the activity.



*Figure 1.2 Protein structure representing Primary, secondary tertiary and quaternary structures*

### Enzymes Classification

To get uniformity, enzymes nomenclature appointed the Committee IUBMB in the year 1984. The nomenclature shows commission number is allocated to enzymes according to their category of action with further subclasses and sub-classes, this

type of classification simplified the identification procedure and maintained the identity of enzyme within the enzyme pool called as enzyme commission (EC) number. This enzyme classification within a group is divided into 4-numbers, where the 1<sup>st</sup> number represents general class of enzymes, the 2<sup>nd</sup> number represents the sub-class of the enzymes and it will change with general class of enzymes, the 3<sup>rd</sup> number representing sub-subclasses and the 4<sup>th</sup> number representing specific enzyme having particular identity of each enzyme. Enzymes are classified into six main classes. There are six main classes of enzymes, as in *table 1.1*

*Table 1.1 Enzyme classification*

EC	Enzyme Type	Reaction Type	Reference
1	Oxidoreductases	Redox reactions, Oxygenation or hydrogenation of substrate	Serra et al.,2005
2	Transferases	Transfer of group(s) from one molecule to another molecule	Breuer and Hauer, 2003; Daines et al., 2004
3	Hydrolases	Cleavage of group(s) in a molecule	Pandey et al, 1999 Serra et al.,2005 Daines et al., 2004
4	Lyases	Addition of double bond(s) to a molecule	Breuer and Hauer, 2003;
5	Isomerases	Several types of isomerization	Maru et al, 2002;
6	Ligases	Formation of bonds (synthetases)	Turner, 2000; Daines et al., 2004

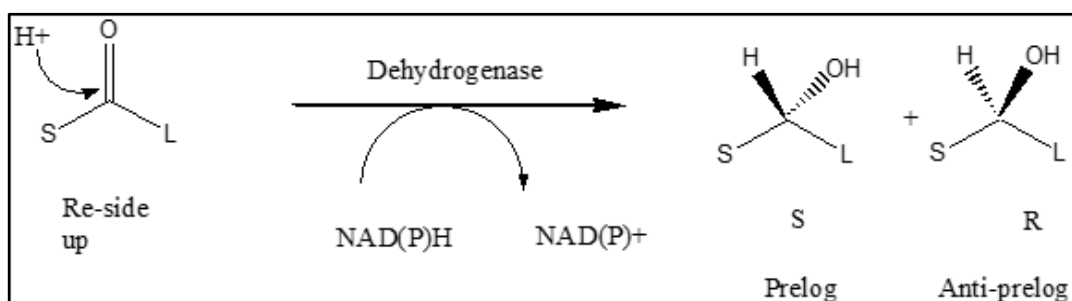
The present **research work** on the application of enzymes **Reductases**, **Transferases** and **Nitrilases** in the synthesis of API to enhance insight of researchers from academic and industrial into the subject matter, operation for addressing global challenges such as climate change, substitution of fossil fuels,

improvement in resource efficiency and elimination of hazardous chemicals from the synthetic processes.

#### 1.4 Oxido-reductases

Commonly called as dehydrogenase or oxidases. Enzymes of the class oxidoreductase acts by removing hydrogen atoms and electrons from the reactant. Cofactors are required for the enzymes of this class for accepting the hydrogen and electrons from the reactant.

Chiral selective reduction of ketone is demanded in the industries from the prochiral -ketones as chiral -alcohols are the constituents of API intermediates in pharmaceutical industries, agro-chemicals, and fine chemical industries [10-12]. The synthesis of chiral alcohols is with asymmetric reduction by chemical synthesis, or the racemic resolution of racemic mixtures mainly performed by metal or chemical catalysts or enzyme catalysts. Researchers having more attention towards the asymmetric synthesis using ketoreductase/alcohol dehydrogenase as it acts on prochiral centre and yields a chiral selective alcohol [13]. The biocatalytic asymmetric synthesis route is more preferred than synthetic methods as shown in *figure 1.3*, which involves expensive chiral resolving reagents, difficult to perform process, use of unsafe chemical reagents, and heavy metals [13].



*Figure 1.3 Reaction mechanism of Alcohol dehydrogenase*

The biocatalytic processes attracting researchers because of their distinctive properties like sustainable, reducing the waste generation, and escape from the use of destructive and dangerous reagents. Pharmaceutical drugs having the chiral selective alcohols as their intermediates are Reyataz, Montelukast [14]. The alcohol dehydrogenases are broadly present in bacteria, fungi, yeast, insects, and plants. The alcohol dehydrogenases have broad substrate specificity such as aliphatic, and aromatic alcohols with use of cofactors classified as

#### **1.4.1 Types of oxido-reductase**

(a) NAD or NAD(P) -utilising dehydrogenases

(b) NAD(P)- without utilising dehydrogenases

(c) FAD- based alcohol oxidases.

##### **(a) NAD or NADP- utilising dehydrogenases:**

These are largest group of alcohol dehydrogenases. The enzymes of this class have considerable industrial importance, as they can perform both oxidative and reductive type of reactions using NADH or NADPH as a cofactor.

##### **(b) NAD(P)- without utilising alcohol dehydrogenases:**

These groups of enzymes use pyrroloquinoline quinone, heme, or F<sub>420</sub> as their cofactor. The ADH from *Paracoccus denitrificans* (methanol dehydrogenase) [15], *Acetobacter* and *Gluconobacter* sp. (ethanol dehydrogenase) and certain archaeobacteria belongs to this class.

##### **(c) FAD- based alcohol oxidases:**

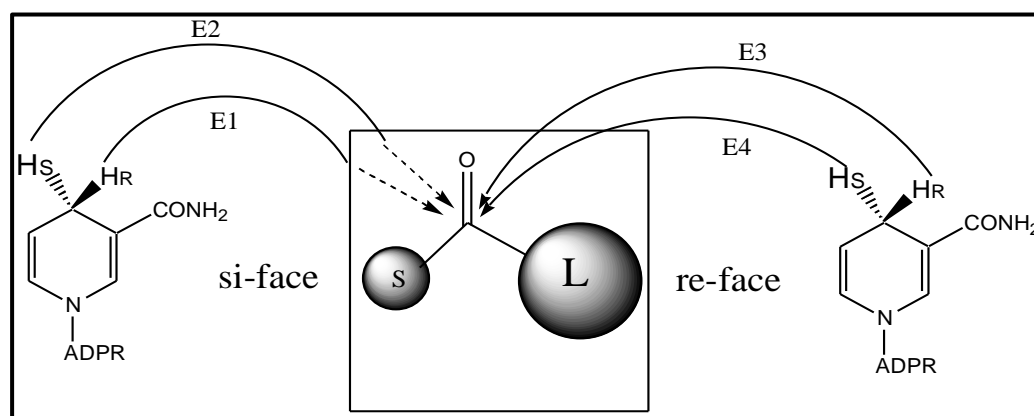
These enzymes catalyzes the oxidation of alcohols, example of oxidase is methanol oxidase from *Hansenula polymorpha* [16] and the veratryl alcohol oxidase from fungi



for lignin degradation. Alcohol dehydrogenases or Aldo-keto reductases, responsible for the stereo-selective reductions of prochiral -ketone to chiral -alcohols.

### 1.4.2 Mechanism of action of alcohol dehydrogenase

The chirality of product alcohol solely depends upon the face of hydride addition to the  $sp^2$  hybridized carbonyl carbon [17]. Hydride transfer from coenzyme, NAD(P)H, to the substrates explained by four stereochemical patterns. The hydride ion attack on either *si*-face or *re*-face of the carbonyl species forming (*R*) and (*S*)-alcohols, respectively are shown in *figure 1.4*



*Figure 1.4 Mechanism of hydride transfer to carbonyl carbon from NAD(P)H*

The orientation of the substrate binding to the enzyme determines the face of hydride attack, the enzyme selectivity defines the formation of pro-(*R*)-hydride or pro-(*S*)-hydride from coenzyme. With the enzymes E1 and E2, hydride binding the *si*-face of the carbonyl group, and with the enzymes E3 and E4, the hydride binding the *re*-face, leading to the conformation of (*R*)-alcohol and (*S*)-alcohol, respectively. AHDs from *Pseudomonas* sp., *Lactobacillus kefir*, etc. are examples of E1 type [18], whereas glycerol dehydrogenase from *Geotrichum candidum* and dihydroxyacetone reductase from *Mucor javanicus* are E2 enzymes [19]. ADHs from yeast and horse liver are E3 types [20], while E4 enzymes are not reported yet. The ketone reduction

by dehydrogenase are conforming to the Prelog's rule and predominantly leads to the generation of (*S*)-alcohol.

Biotransformation processes utilize various biocatalyst formulations, from partially purified or purified enzymes to whole cells, either free or immobilized in inert support, depending on the nature of the reaction. Enzymes can act on variety of unnatural substrates by using expensive natural cofactors in stoichiometric amounts [21]. The coenzymes can be regenerated for the next cycle of the reaction. There have been many approaches developed for cofactor recycling. The use of co-substrates as alcohols, sugars, amino acids, etc. is a classical approach for this.

Alcohols such as ethanol and isopropanol have been commonly used with dehydrogenases since the single enzyme can perform oxidation and reduction reactions. For example, isopropanol used with ADH of *Geotrichum candidum* yielded 72% (*S*)-2-hexanol with 99% *ee* [22] Sugars, glucose, and glucose-6-phosphate are used for the revival of cofactor. The chiral selective reductions of various -ketones by glucose dehydrogenase of *Candida magnolia* was improved by the addition of glucose [23] Similarly, glutamic acid with glutamate dehydrogenase used for the regeneration of NADH [24]. Various newer techniques, such as electrochemical, photochemical, as well as organometallic approaches are being used for coenzyme regeneration. The electrochemical approach is considered as a promising and sustainable technology but despite many efforts, it suffered from low productivities and low overall stability making this technique difficult on a commercial scale.

In a reported process, regeneration of NADH by using rhodium complex (coupling agent) in the chiral selective reduction of 3-methyl cyclohexanone with thermophilic ADH from *Thermus* sp., good productivity, and stereoselectivity (96% *de*) was obtained [25]. Photochemical methods were developed as an environment-friendly

system, that employs light energy for recycling of NAD(P)H or flavin in photosynthetic microorganisms. The acetophenone reduction using a *cyanobacterium* was improved (96→99% *ee*) under illumination. Similarly, reduction of keto-isophorone using *Bacillus subtilis* derived old yellow enzyme homolog was enhanced with light energy [26]. Overall, the industrially viable method for the *in vivo* recycling of coenzyme is lacking.

In the cell, cellular machinery regenerates the cofactor, avoiding the addition of expensive cofactor or their recycling systems. Also, the natural environment inside the cell provides higher stability to the enzyme [27]. Microbial cells can be used in the form of live cell, lyophilized powder, or immobilized on various support for recycling the enzyme and requirement of the process. Generally, growing cells are not preferred due to higher side product formation, moreover, the growth conditions for cells usually different than that of reaction. The recent studies suggest that with optimization the byproduct generation can be reduced and found to be better than free enzymatic processes. Lyophilized cells are easy to handle, stable during storage, and considered as “off the shelf biocatalyst”, but a decrease in the enzyme’s activity during the lyophilization is of concern. The utilization of immobilized enzymes in the processes allows reusability with improved operational stability, and cost reduction [28].

To design a whole-cell catalyst, an efficient microbial culture is screened first, and the enzyme production is optimized by medium designing and optimizing the fermentation parameters (time of fermentation, temperature, fluid dynamic conditions, pH, inducers application, type of reactor, gas-liquid mass transfer conditions, etc.). Further, genetic manipulation of the organism allows subsiding the undesired characteristics of the biocatalyst or even, improvement of biocatalyst stability, activity, and selectivity [29]. However, it is observed that whole-cell

microbial reduction has narrow substrate specificity, lower yield, lower productivity, and lack of selectivity due to binding of substrate to enzyme interrupted by the existence of different enzymes of the similar functions with varying stereoselectivity. Hence, the selection of a suitable microbial strain with superior selectivity and stereospecificity is a necessity for biocatalytic reduction process development. Also, these enzymes essentially require an aqueous medium to exhibit their enzyme activity, which also hinders the application since most of the pharmaceuticals or compounds of biological importance are hydrophobic in nature.

### 1.4.3 Application of oxido-reductase pharmaceutical industries

Microbial reduction of ketones to produce chiral alcohols has offered novel synthesis route for various industrially important modules. Several bio-reductions reports are available in the literatures [11, 30, 31] for the incorporation of chiral selective API and its intermediates. Baker's yeast was the first to use for asymmetric reductions of carbonyl moieties. For example, the enantio-selectivity was decreased due to the competition between different alcohol dehydrogenases. Several new strains were segregated and used in reductive reactions. *Thermoanaerobacter* sp. ADH expressed in *Escherichia coli* was applied for the selective -keto reduction of the ethyl 5-oxo-6-heptenoate to (*R*)-5-hydroxyhept-6-enonoate, however the *Lactobacillus brevis* ADH provided the opposite (*S*) enantiomer by Fischer and Pietruszka, in 2007. These essential chiral selective alcohols are used as intermediary in the synthesizing of prostaglandins, leukotrienes, isoprostanes, and atractyligenin. The chiral selective reductions with *Lactobacillus kefir* shows the (*R*) alcohol >99% *ee* of the 1-[3,5-bis(trifluoro methyl)phenyl]-ethanone, an intervening for tachykinin NK1 receptor [32]. The *Rhodococcus erythropolis* forms (*S*)-alcohol, an important interpose of pharmaceutical use [33]. Quinolone CA acid, a new antibacterial agent was synthesized by employing *Phaeocrepis* sp. JCM 1880 for the selective

ketoreduction of azaspiroketones [34]. (*S*)-6-[(4-methoxybenzyl) oxy]-1-trimethylsilyl-1-hexyn-3-ol was produced by stereoselective ketoreduction of the keto intermediate by *Pichia minuta* IAM 12215.

The (*R*) acetal alcohol was incorporated by selective ketoreduction of the acetal keto intermediary by *Yamadazyma farinose* NBRC 10896. Both intermediates were then used for the synthesis of modiolide A, an antibacterial and antifungal agent [19]. Recently, biocatalyst from adzuki bean (*Phaseolus angularis*) was stated for the enantioselective ketoreduction of substituted phenyl ketone compounds, heterocyclic ketones, and bicyclic ketones with higher substrate tolerance without compromising the enantioselectivity [30] *Trichosporon cutaneum* IAM 12206 and *Pichia minuta* IAM 12215 were selectively reduced many sterically hindered ketones such as isopropyl phenyl sulfonylmethyl ketones, to their corresponding chiral (*R*) alcohol and (*S*) alcohol, respectively [22, 35].

It is reported that diketones like ( $\pm$ )-bicyclo (2,2,2)-oct-7-ene-2,5-dione was reduced by genetic engineered recombinant yeast TMB4100 overexpressing YMR226c reductases gene from baker's yeast, (+)-endohydroxyketone and (-)-exo-hydroxyketone obtained with >99% and 84–98% *ee*, respectively [36]. Another diketone, 3,5-dioxo-6-(benzyloxy) hexanoic acid ethyl ester was also reduced to their comparable syn-(3*R*,5*S*)-diol by *Acinetobacter* sp. SC13874 [37]. The formed diol is transitional in the formation of HMG-CoA reductases inhibitor.

*Comamonas testosteroni* DSM 1455 was studied at higher substrate concentration for the reduction of  $\alpha$ -azido,  $\alpha$ -bromo and  $\alpha$ -nitro ketones. The chiral selective alcohols are essential for the production of  $\beta$ -aryl ethanol amines, and used in manufacture of several antihypertensive, antiarrhythmic, and antianginal drugs [38]. Asymmetric reduction of 2-bromo-4-fluoro acetophenone and their esters such as (*S*)-1-(2'-bromo-4'-fluoro phenyl) ethanol were obtained using microbial cultures as

*Candida sp.*, *Hansenula sp.* and *Pichia sp.* which were resulted in higher yield with very good enantioselectivity (>99 %) for this reaction envisaged earlier by R. N Patel and group [11].

Both enantiomers of chiral phenylethanols were essential intermediates in the preparation of various pharmaceutical and fine chemical compounds. Several microbial cultures like Baker's yeast [39], *Aspergillus terreus* CCT 4083 [40], *Alternaria alternate* EBK-4 [41], *Rhodoturula glutinis* EBK-2 [42], *Rhodoturula sp.* AS2.2241 [43], *Candida viswanathii* MTCC 5158 [44], etc. have been reported two microbial species, *Paracoccus pantotrophus* DSM 11072 and *Comamonas sp.* DSM 15091 for the syntheses of a variety of substrates where sterically hindered ketones and diketones such as methyl - aryl, methyl - alkyl, cyclic, and produced the chiral alcohols with an opposite Prelog configuration [38].

### 1.5 Transferase

The transferase are the enzymes performing transfer of chemical functional group from substrate to product using donor group (cosubstrate). Transaminases, for example, transfers an -amine group (-NH<sub>2</sub>) to the -ketone group for the formation of a desired amine.

Transaminases are having the potential for the formation of chiral selective -NH<sub>2</sub> [45, 46]. It has increased its demands in the industries as it acts on prochiral centre and synthesis of bioactive molecule with chiral selectivity (*figure 1.5*).

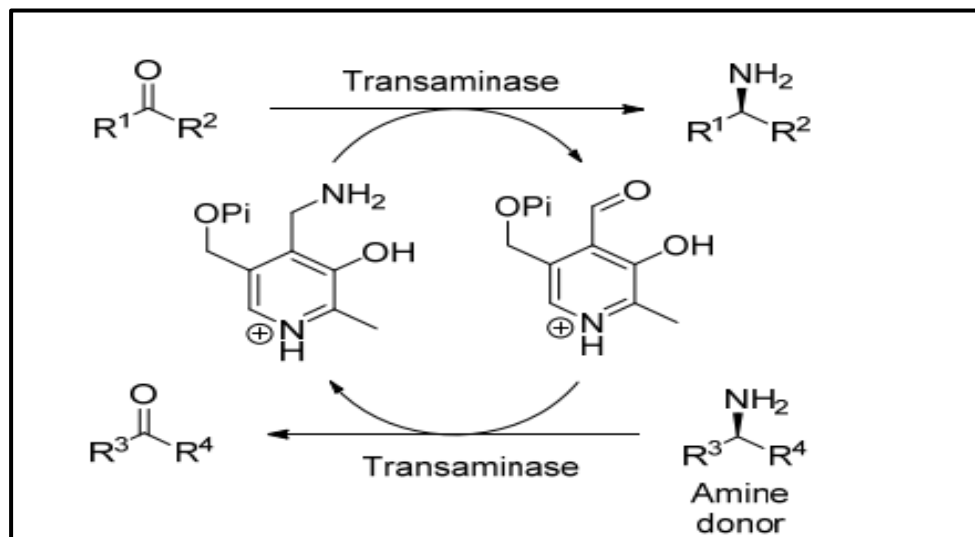


Figure 1.5 Transaminase enzyme mechanism

Building blocks of the pharmaceutical API are important because of its chiral centers. There are various classes of enzymes shows discrimination of enantiomers [47, 48]. Transaminases acts on the prochiral center and resulting product is chiral selective product.

In commercial scale synthesis of API intermediates having chiral amine group is very hazardous chemicals and high pressure and costly catalyst so transaminase catalysis has future for replacement for the development of industrially important chirally selective  $-NH_2$ . [49, 50] There are different types of approaches for the preparation of chirally selective  $-NH_2$  those are mentioned as follows. [45, 51-53] Details of the applications are explained in the *figure 1.6*

**1.5.1 Types of transaminases:** Are as follows. Typical schemes are shown in *figure 1.6*

(a) **Kinetic resolution:** In this approach undesired isomer of the amine species converted to keto form using transaminase species. This approach is not feasible as yield expected is 50%.

**(b) Asymmetric synthesis:** In this approach single step preparation of the chirally selective  $-NH_2$  from the  $-ketones$ . This approach has benefit over the other approaches i.e yield expected is matching with theoretical yields.

**(c) De-racemization of amine:** This is less explored approach

**(d) Racemization:** This is also less explored approach

### 1.5.2 Application of transaminase as presented in *figure 1.6*

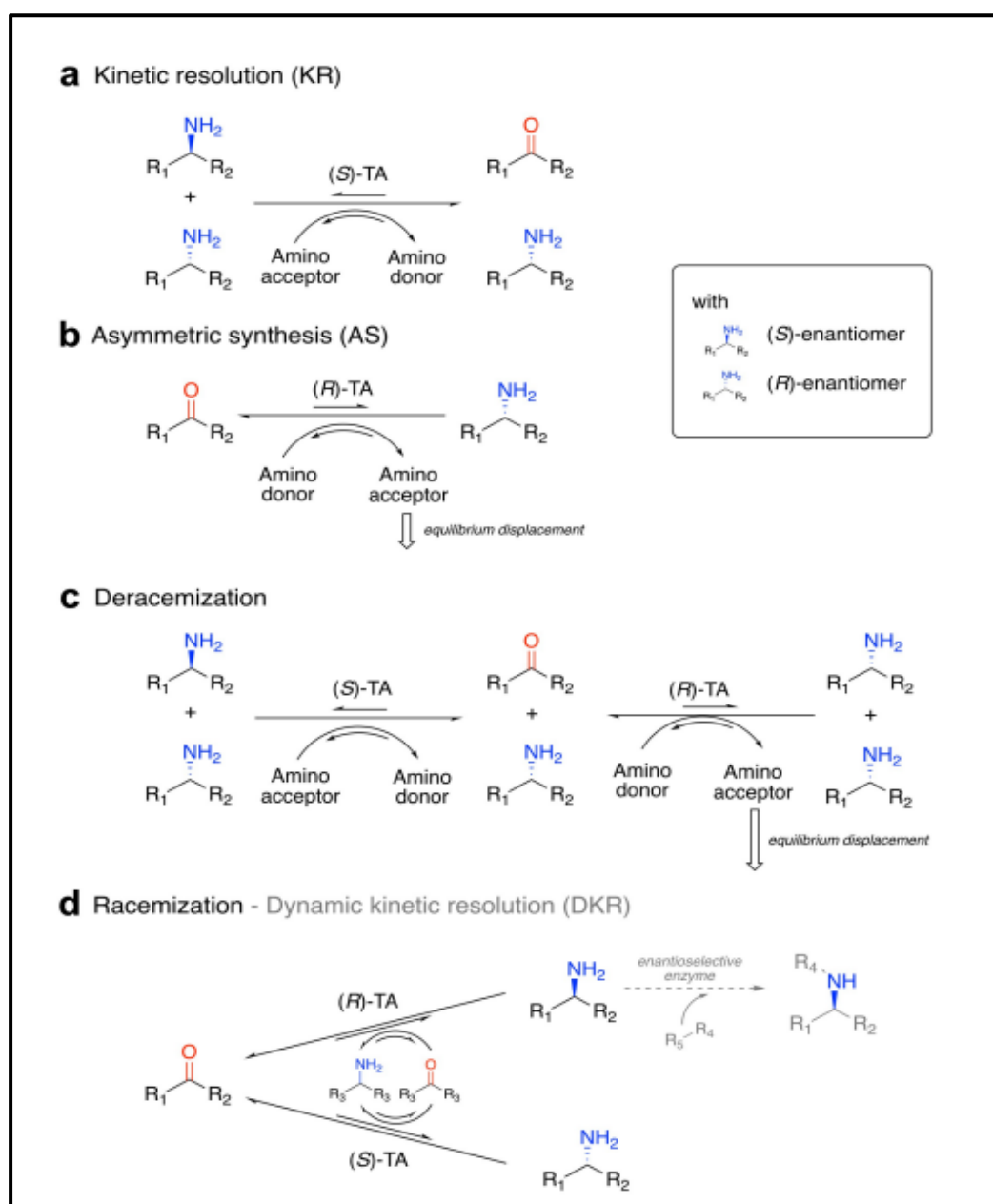


Figure 1.6 Approaches for application of transaminases



## 1.6 Hydrolase

Nitrilases are comes under the class of hydrolases. Hydrolysis of the -CN group perform by nitrilases to its CA and NH<sub>3</sub>. (figure 1.7)

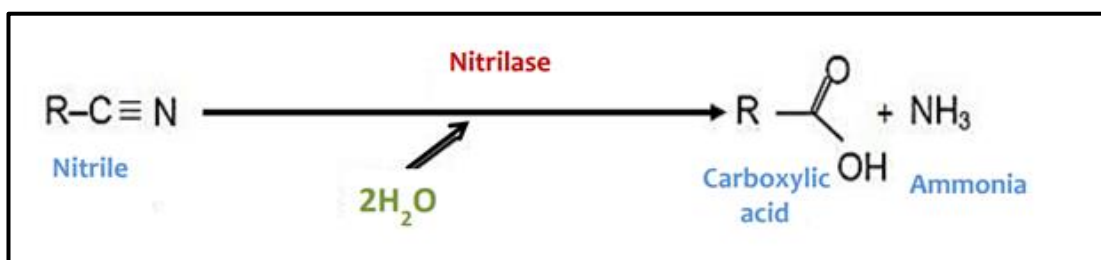


Figure 1.7 Nitrile hydrolysis to CA and NH<sub>3</sub> using Nitrilases

These enzymes found in the genomes of mammals, yeast, and plants, and their identification and characterization already reported. Over 30 nitrilases already identified since nitrilase activity was first discovered in plants in 1958 and in bacteria in 1964 [54]. Nitrilases have a diversified documented commercially useful petitions with the manufacturing of *R*- and *S*-Mandelic acid, *R*- and *S*- phenyllactic acid, and *R*- and *S*- 4 cyano 3 hydroxybutyric acid. However, only a few numbers of nitrilase applications have been carried out in manufacturing like generation of (*R*)-mandelic acid or 5-hydroxy pyrazine-2-CA and 6-hydroxy picolinic acid by Lonza and (*R*)-3-chloro mandelic acid by Mitsubishi Rayon Co. respectively [55]. The technical application of nitrilase has however, largely stands unexplored. Which appears due to several restrictions, which are frequently seen for enzymes relevant to biotechnology (poor enzymatic activity, low stability of enzyme, substrate compatibility towards buffer solutions, and non-enzymatic reaction). Many biotransformations using nitrilase enzymes have potentials for commercial production of API and their intermediates. It is usually necessary to modify or formulate the enzyme and enzymatic process reaction condition to fulfil industrial demands for chiral resolution. [56,57] Our goal is to provide a concise overview of recent developments in nitrilase uses in the generation of fine compounds and constituent

parts. The employment of nitrilase enzymes has been significantly expanded by several recent discoveries.

### 1.6.1 Applications of nitrilase enzymes

The examples of nitrilase applications against different substrates and their non-selective hydrolysis shown in *table 1.1*, Enantio-selective hydrolysis shown in *table 1.2*, Chemo-selective hydrolysis shown in *table 1.3*, Regio-selective hydrolysis shown in *table 1.4*

*Table 1.1 Nitrilase non-selective application*

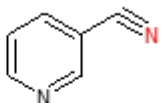
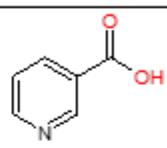
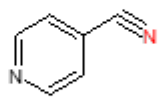
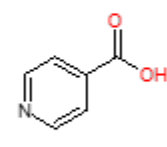
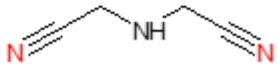
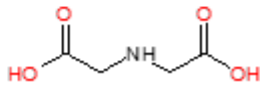
Source of nitrilase	Substrate	Product
<i>Rhodococcus rhodochrous J1</i> <i>Fusarium proliferatum ZJB-09150</i>		
<i>Nocardia globerula NHB-2</i> <i>Aspergillus niger K10</i> <i>Fusarium solani 01</i>		
<i>Alcaligenes faecalis ZJUTB10</i>		

Table 1.2 Nitrilase enantio-selective application

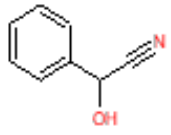
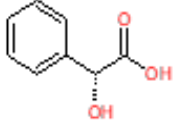
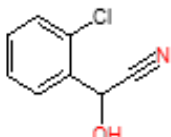
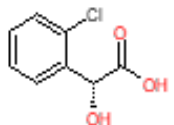
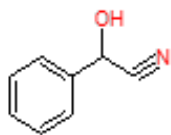
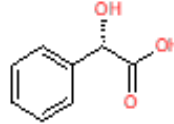
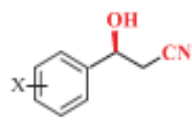
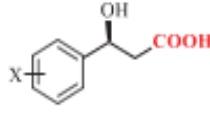
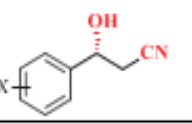
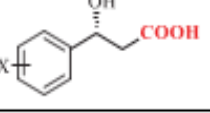
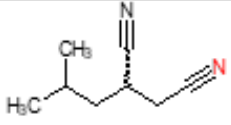
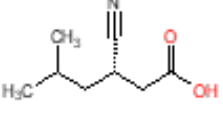
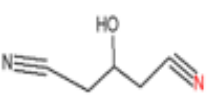
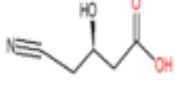
Source of nitrilase	Substrate	Product	Selectivity ( <i>ee</i> )
<i>Alcaligenes sp. MTCC 1067</i>			R (99.0%)
<i>Alcaligenes faecalis ECU040</i>			R (96.5%)
<i>Manihot esculenta</i> <i>Pseudomonas fluorescens EBC191</i>			S
<i>Bradyrhizobium japonicum strain</i> <i>USDAA110</i>			S (>95%)
<i>Synechocytis sp. Strain PCC 6803</i>			R (>98%)
<i>Arabidopsis thaliana</i>			3S (E>150)
<i>Diversa</i>			R (>99%)

Table 1.3 Nitrilase chemo-selective application

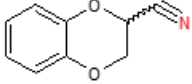
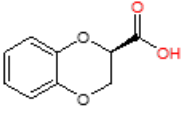
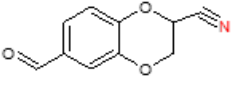
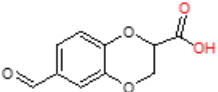
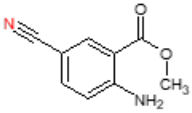
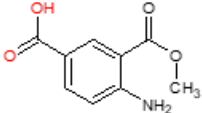
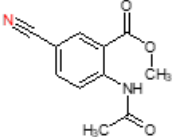
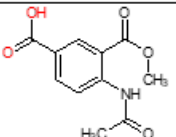
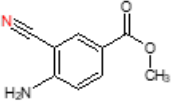
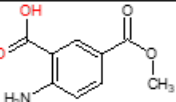
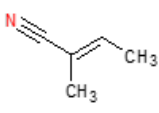
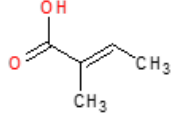
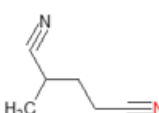
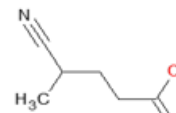
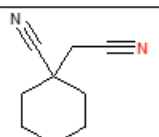
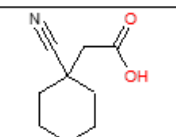

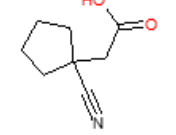
Source of nitrilase	Substrate	Product	Selectivity ( <i>ee</i> )
<i>Rhodococcus R312</i>			<i>R</i> (98%)
<i>Rhodococcus R312</i>			<i>R</i> (>99%)
<i>Rhodococcus sp. SRL4281</i>			<i>NR</i>
<i>Agrobacterium DSM6336</i>			<i>NR</i>
<i>Rhodococcus sp. SRL4281</i>			<i>NR</i>

Table 1.4 Nitrilase regio-selective application

Source of nitrilase	Substrate	Product	Selectivity ( <i>ee</i> )
<i>Acidovorax facilis</i> 72 W			<i>E</i>
Metagenomic libraries			<i>NR</i>
<i>Acidovorax facilis</i> ZJB09122			<i>NR</i>
<i>Bradyrhizobium japonicum</i> strain USDA110			<i>NR</i>

Conventional chemical processes are the basis of pharmaceutical agrochemical and fine chemical industries with complex chemical reactions consuming huge amount of energy and raw materials. As pollution control norms and regulatory requirement are forcing the commercial process towards the greener and environmentally friendly process. Biocatalysis, using enzymes helping to replace hazardous chemical steps in the routine chemical synthesis, is appearing as an as an economically and greener productive route for a variety of fine chemicals, active pharmaceuticals, and food intermediates.

### **Objective of the research work**

To develop the enzymatic route for the potential drugs and their intermediates.

To achieve the chiral selectivity without using the harsh chemicals.

To validate and assessment of the developed process or the commercial application.

## **CHAPTER-2**

### **MATERIAL AND METHODS**

## Chapter 2

### 2.1. Material and methods

Performing the study for the “applications of biocatalyst for the sustainable potential drugs”. The major requirements are enzymes and proposed substrates which are procured from the reliable sources are explained in detail as follows.

### 2.2 Substrates, products, and enzymes

#### 2.2.1 Substrates

Substrate tested against the enzymes are purchased as below.

- a) Substrate: (tert-butyl[5-(4-cyanobenzoyl)-2-fluorophenyl]carbamate) and product (tert-butyl{5-[(4-cyanophenyl)(hydroxy)methyl]-2-fluorophenyl}carbamate) for the screening of ketoreductase enzymes were synthesized and supplied by PVR scientific Nagpur.
- b) Substrate: 1-(3-Methylphenyl)ethan-1-one and product racemic 3-methylphenylethan-1-amine, and (1*R*)-(3-methylphenyl)ethan-1-amine for the screening of transaminase enzymes were purchased from Sigma Aldrich, Bangalore (India)
- c) Substrate: 2-chloroisonicotinonitrile and product 2-chloroisonicotinic acid for the screening of the nitrilase enzymes were purchased from the Sigma Aldrich Bangalore (India)

#### 2.2.2 Enzymes

- a) **Ketoreductase:** Ketoreductases screening kit was purchased from the Codexis Redwood City CA USA, Enzymicals-AG, Greifswald Germany, and SyncoZymes Co., Ltd. Shanghai China.
- b) **Transaminases:** Transaminases screening kit was purchased from the Codexis, Redwood City, CA USA.



- c) **Nitrilase:** Nitrilases screening kit was purchased from SyncoZymes Co., Ltd. Shanghai (China)

### **2.3 Coenzymes and cofactors**

- a) Cofactor: Nicotinamide adenine dinucleotide (NAD), nicotinamide adenine dinucleotidephosphate (NADP), and glucose dehydrogenase (GDH) were procured from Sigma, Bangalore (India)
- b) Coenzyme: pyridoxal-5-phosphate (PLP) were procured from SRL Pvt. Ltd., Mumbai (India)

### **2.4 Chemicals for assay**

- a. Mandelonitrile and mandelic acid for determination of enzyme activity was purchased from the Sigma Aldrich Bangalore (India)
- b. Crosslinking agent glutaraldehyde is purchased from the Sisco research laboratories India.

### **2.5 Reagents for the reaction buffer and other preparations**

- a. Monopotassium dihydrogen phosphate, dipotassium hydrogen phosphate and triethanolamine from the Merck India.
- b. Solvents and chemicals such as isopropyl alcohol, dichloromethane, methanol, ethanol, N, N-Dimethylformamide and Dimethyl sulphoxide and Monoisopropylamine were purchased from the Sisco research laboratories India.
- c. Water, Acetonitrile and Methanol were of HPLC grade and purchased from Rankem India.

## 2.6 Instruments

### a. Thermomixer

This device is known for its unique property of mixing mixtures with controlled temperature. This is the simple instrument with program keys for temperature and mixing parameters. Instrument provides accurate results in screening, assay results because of mixing and incubation for series of the samples remains same. The typical image of the Thermomixer (IKA MATRIX ORBITAL from IKA Germany) shown in *figure 2.1*



*Figure 2.1 Typical image of the Thermomixer*

**b. Micropipette**

These are easy to use and accurate laboratory equipment for measuring the small quantity of liquid samples. Micropipettes used in research laboratories due to its accuracy in measuring the preset small quantity of liquid solutions. The typical images of micropipettes (eppendorff) are shown in *figure 2.2*



*Figure 2.2 Typical images of micropipettes*

**c. Rotary evaporator**

This is typical chemistry lab instrument used for the removal of the relatively low boiling point solvent to sample under reduced pressure through the evaporation. Reduced pressure reduces the boiling point of the solvent than normal boiling point. Rotating the round bottom flask containing sample to be evaporated increases the surface area thus helps in increasing the rate of evaporation. The generated solvent vapours enter into the condenser, under cooling system vapour condenses into

solvent and collected into the receiver flask. The typical image of rotary evaporator model RV 8V from IKA Germany shown in *figure 2.3*



*Figure 2.3 Typical image of rotary evaporator*

**d. High performance liquid chromatography**

Analytical technique High performance liquid chromatography (HPLC) is used for the separation of components of the mixture with displaying the “chromatogram” is the result of chromatography and “chromatograph” is software to carry out separation. The typical image of the HPLC (Shimadzu LC-2030C 3D plus, Japan) shown in *figure 2.4*. The device responsible for the separation mixture of compound is” column”. The high-performance pumps are used for delivering solvent and sample to be separated at constant flow rate. The compounds dissolved in the solvents can be analysed with this technique.



*Figure 2.4 Typical image of the HPLC*

Analytical separation report is chromatogram which is two-dimensional plot showing concentration with the detector (signal intensity) against analysis time. The schematic representation and chromatogram related terms shown in *figure 2.5 and figure 2.6* respectively.

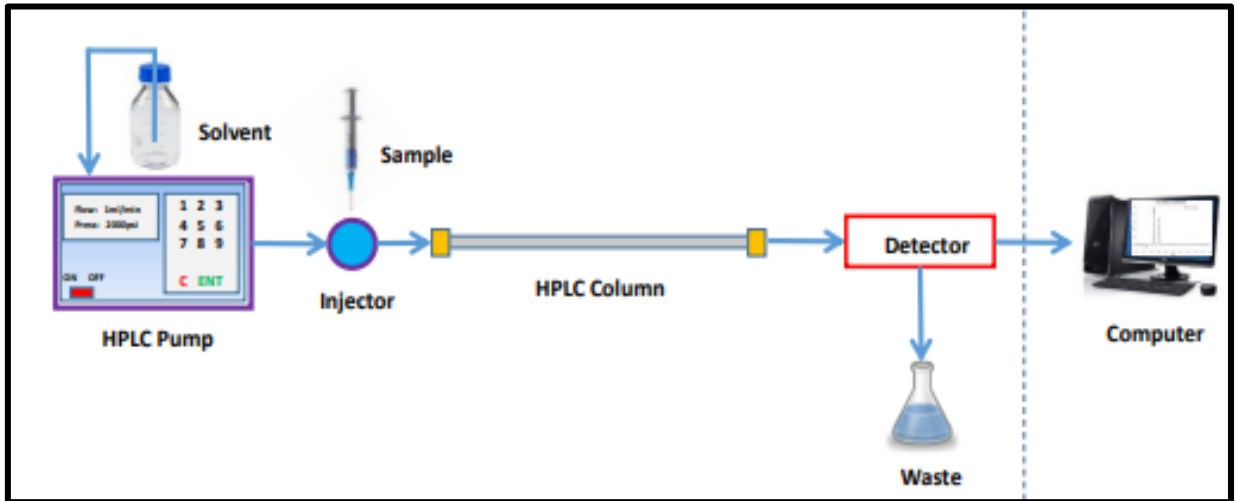


Figure 2.5 The schematic representation of HPLC

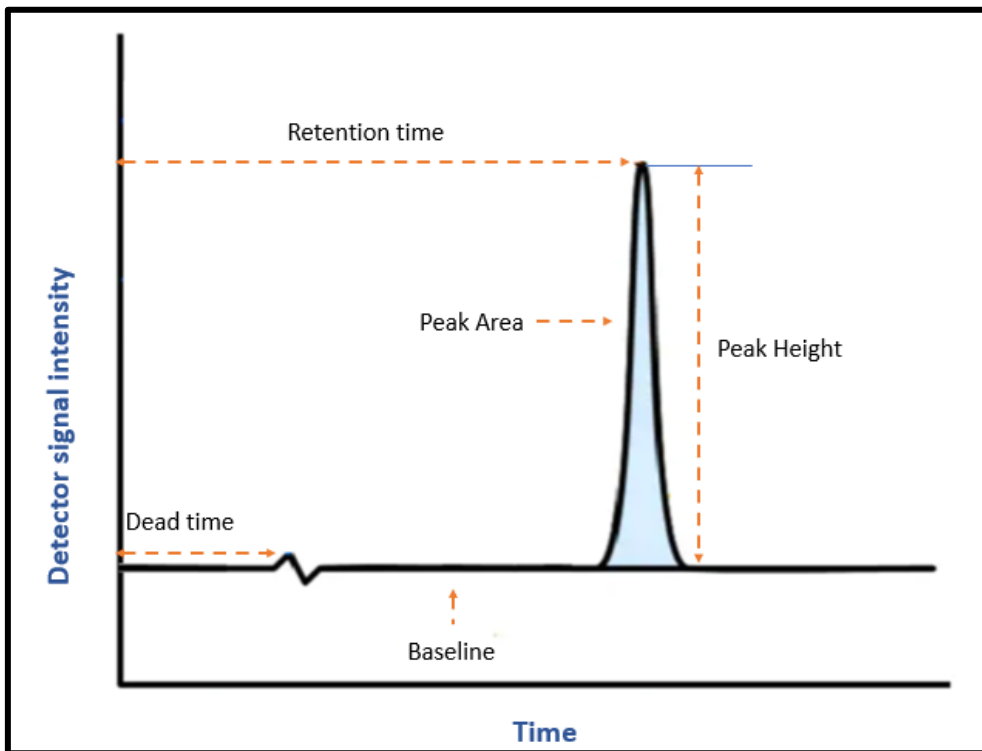


Figure 2.6 Image on chromatogram related terms

**e. HPLC column**

This is the main component of high-performance chromatographic technique for separating mixture of sample. The sample enters the column in the miscible form with solvent and separate out after coming out of it.

Inert material (Silica gel) is filled within the chromatographic column as it has porosity and particle size which helps in separating mixture of sample. This is called as a “stationary phase”.

HPLC columns have different length from 30 mm to 250 mm and particle size 3 $\mu$  to 5 $\mu$ . These factors are important for precise analytical method development. HPLC columns are separated according to the nature of compound to be separated and mobile phase.

The types of columns used for separating mixture of samples according to different mode of separation shown in *table 2.1*

Table 2.1 Column chemistry and mode of separation

<b>Mode of HPLC</b>	<b>Type of Stationary Phase (Column Chemistry)</b>	<b>Type of Mobile Phase</b>	<b>Elution order</b>
<b>NP (Normal Phase)</b>	<b>Polar</b> (Silica, Diol, CN etc.)	<b>Non-Polar</b> (Hexane mixed with methanol, ethanol or isopropyl alcohol)	More Hydrophobic First, More Hydrophilic Last (Decreasing order of hydrophobicity)
<b>RP (Reversed Phase)</b>	<b>Non-Polar</b> (C18, C8, C4 etc)	<b>Polar</b> (Milli q grade water mixed with acetonitrile, methanol or a small amount of tetrahydrofuran)	More Hydrophilic First, More Hydrophobic Last (Increasing order of hydrophobicity)

### 1. Normal phase HPLC column

In these types of columns stationary phase (Silica) is more polar than the mobile phase (solvent). Water has more polarity than silica, so it is not used and solvents like methylene chloride, hexane, chloroform are used as a solvent.

Mixture of sample having more polarity interact with polar stationary phase separates from the less polar component in the mixture of sample which interacts with the less polar mobile phase. Image of normal phase (CHIRACEL OD-H from Diacel corporation) HPLC column shown in *figure 2.7*





*Figure 2.7 Image of normal phase HPLC column*

These columns are frequently used in the separation of chiral compounds (API intermediates) in pharmaceutical industries.

## **2. Reverse phase HPLC column**

These columns are reverse of the normal phase columns. In this stationary phase is less polar compared to the mobile phase. C8, C18 and non-polar bonded hydrocarbons are commonly used as a stationary phase for reverse phase HPLC columns and water in the combination of organic solvents are used as mobile phase such as water: methanol, water: acetonitrile.

Mixture of sample separated based on polarity, but it is just opposite of the normal phase HPLC column. These columns are frequently used in pharmaceutical, agricultural and fine chemical industries. Image of the reverse phase (Atlantis-C18 from waters corporation) HPLC column shown in *figure 2.8*



*Figure 2.8 Image of reverse phase HPLC column*

### 3. Ion exchange HPLC column

Ionizing capability of the mixture of sample helps in separating the compounds with these columns. Stationary phase in these columns having acidic or basic with negative or positive charge and mobile phase is polar salt solution in water. Mixture of sample separates based on attractive ionic forces sample component and charged stationary phase.

### 4. Size exclusion HPLC column

Separation of mixture of sample based on porosity of the stationary phase particularly particle size. Polymers like polysaccharides and silica gel mixtures are used as stationary phase in these columns.

Mixture of sample separated based on small components enter inside pores while large components pass through the void space. Therefore, large component elutes first than the small component.

HPLC columns used in our research works are mentioned in *table 2.2*

*Table 2.2 List of HPLC column used in research work*

Sr. No	Name of Column	Manufacturer	Specification
1	Inert sustain	G L Sciences	AQ-C18 (5 $\mu$ m $\times$ 4.6 $\times$ 250 mm)
2	Ascentis Express	Sigma Aldrich	C-18 (2.7 $\mu$ m $\times$ 4.6 $\times$ 150 mm)
3	CHIRALCEL® OJ-RH	Diacel	5 $\mu$ m $\times$ 4.6 $\times$ 150 mm
4	Atlantis ® T3	Waters	C-18 (5 $\mu$ m $\times$ 4.6 $\times$ 250 mm)

## b. Gas Chromatography

Gas Liquid Chromatography is an analytical technique used for separating, identifying, and quantify the mixed of organic compounds by separation between the stationary phase of column and mobile phase i.e. gas within a column and elution according to boiling point of component of mixture.

Gas chromatography separation technique is suitable with organic compound having high volatility, thermal stability, and molecular weights below 1250 Da. Typical image of Gas chromatography (Shimadzu LC-2010 Pro) shown in *figure 2.9*



*Figure 2.9 Typical image of Gas chromatography*

The carrier gas plays a role of mobile phase for the separation of mixture of organic component which transports mixtures of components through the Gas chromatography

system, without reacting with component of mixtures. Syringe is used to inject the sample into Gas chromatography inlet, the component of mixtures gets vaporized and transferred to the analytical column (Typical image of GC column CP-Chirasil from Agilent corporation shown in *figure 2.10*). The separation of the component of mixture by their different interactions with the stationary phase. Finally, the detection by detector of the separated components after elution from the column. The GC column used in our study is shown in *table 2.3*



*Figure 2.10 Typical image of GC column CP-Chirasil*

Table 2.3 GC column used in research work

Sr. No	Name of Column	Manufacturer	Specification
1	CP-Chirasil Dex CB	Agilent	Length 25m, × Film 0.25µm × Diameter 0.25 mm

**g. Polarimeter**

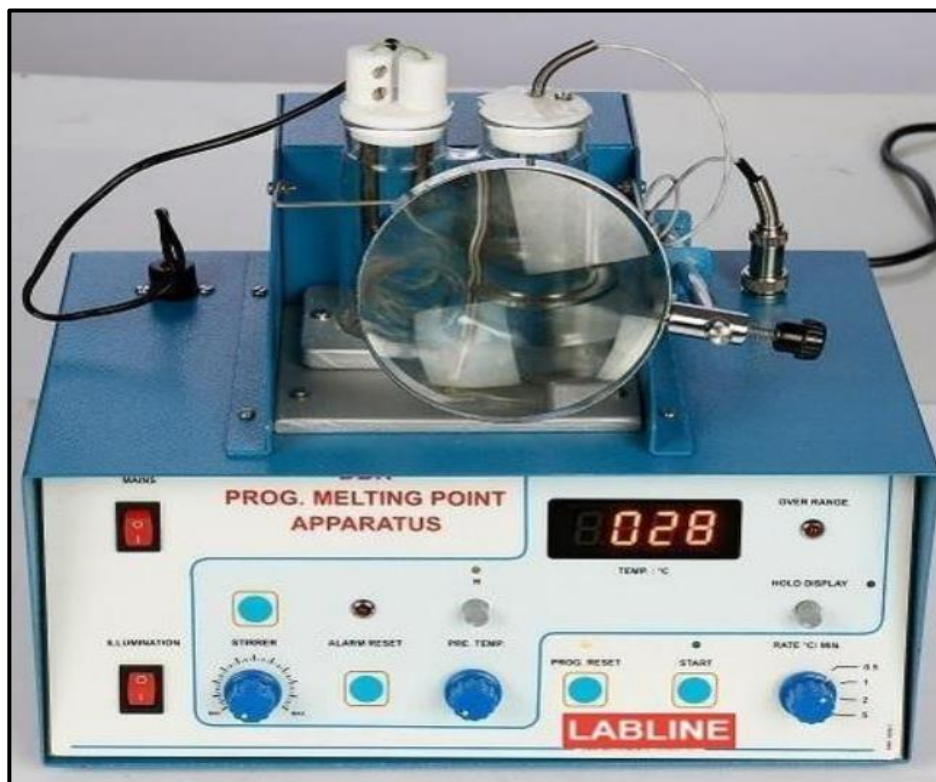
This instrument is used in the research laboratories, pharmaceuticals and fine chemical industries for measuring the optical purity of the molecules. In polarimeter the plane polarized light passes through the sample followed by the analyser and deviates from the optical path from zero position to optical rotation of the molecule. The photomultiplier detector produces the electrical signal having the frequency corresponding to the optical rotation of the molecule. The selected frequency circuit and power amplifier operates the servo motor and in turn the analyser until the optical zero position is regained. The analyser rotation is measured by an encoder and is shown on the digital display as optical rotation of the molecule. Typical image of the polarimeter (Model CDP-001 from Contech Instruments Ltd Mumbai, India) is shown in the *figure 2.11*



*Figure 2.11 Typical image of the polarimeter*

**h. Melting Point Apparatus**

Sample load into the sealed capillary tube which is then placed in the apparatus align for the heating bath. After this slowly increase the bath temperature and monitor the melting of the sample. The operator of the apparatus monitor the initiation of the melting and end point of the melting. Average reading of the sample is counted as the final melting point of the sample. Typical image of the melting Point Apparatus from Labline, Mumbai, India is shown in *figure 2.12*



*Figure 2.12 Typical image of the Melting Point Apparatus*

**i. Liquid chromatographic coupled mass detector**

LC-MS is a liquid chromatographic coupled with mass detector which works on the principle of HPLC followed by their mass-based detection. Although this technique is recently developed but attracting the researcher due to its unique properties such as sensitivity, selectivity and accuracy in detection. Schematic diagram of LC-MS setup shown in *figure 2.13* and typical image of LC-MS (LCMS-2020 from shimadzu, Japan) shown in *figure 2.14*

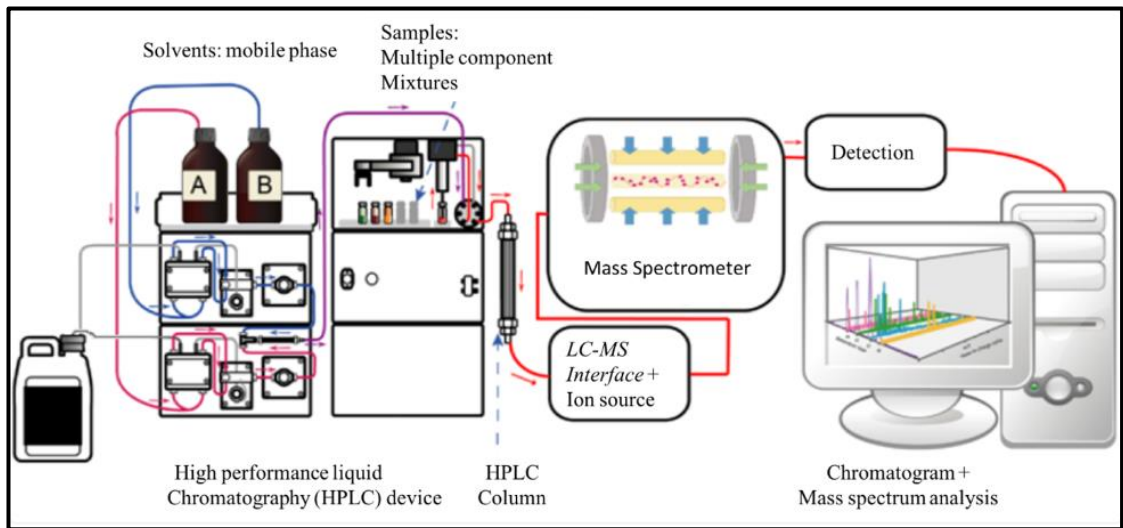


Figure 2.13 Schematic representation of LC-MS setup



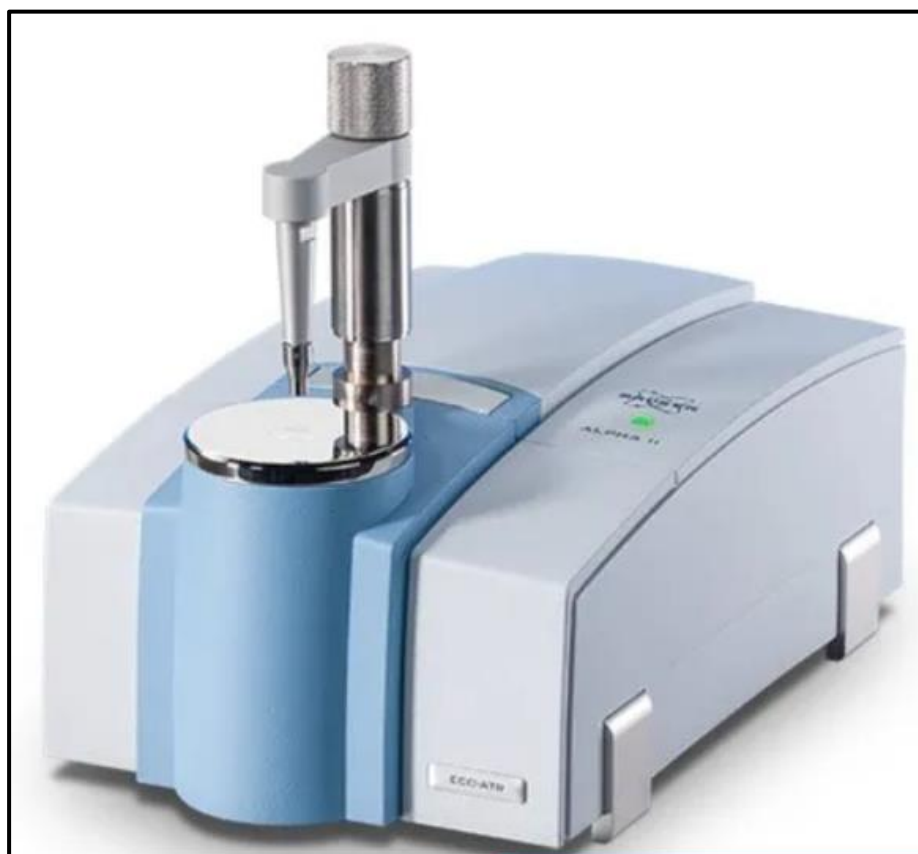
Figure 2.14 Typical image of LC-MS



**j. Fourier transform infrared spectrophotometer**

FTIR represents for “fourier transform infrared” and it is most commonly used technique infrared spectroscopy. Infrared (IR) radiations strike on the sample and few radiations get absorbed. The absorbed radiations on the sample are recorded. The different samples are varying in their structures and produces the different spectra, the spectra produced are different due to different functional group and different composition of the samples which is helpful to identify and distinguish from each other.

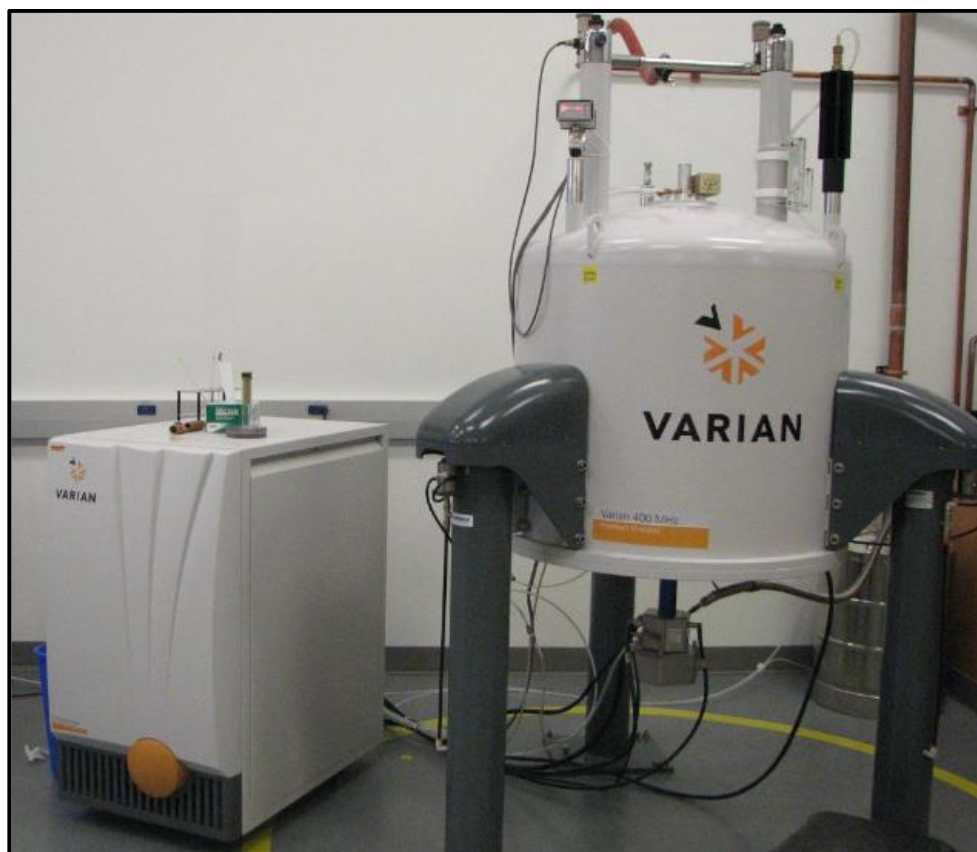
FTIR is the preferred method of infrared spectroscopy as it does not destroy the sample, faster, sensitive, and precise. FTIR spectroscopy is used in organic synthesis, pharmaceutical industry for identifying functional group of the investigational compound. Typical image of FTIR (Bruker Alpha II from Bruker Corporations, Germany) shown in *figure 2.15*



*Figure 2.15 Typical image of FTIR*

**k. Nuclear Magnetic Resonance Spectroscopy**

NMR used to determine content, purity, and molecular structure of investigational compound in research laboratories and industries. NMR can be used for the determination of molecular conformations in the solutions and to study the physical properties at the molecular level, includes conformational exchange, phase changes, solubility, and diffusion. According to the requirement various types of NMR techniques are available. Typical image of Varian 400 MR, NMR spectrometer shown in *figure 2.16*



*Figure 2.16 Typical image of NMR spectrometer*

**l. Dynamic light scattering - Particle size analyser**

DLS is technique used for the measurement of particle size and broadness and distribution of particles in the liquid solution. Dispersed systems like emulsion, suspension and liposome formulation preparations are based on the characteristics such as particle size and their distribution within the solution. DLS can measure the moving particles up to size 1  $\mu\text{m}$ . Typical image of DLS-Particle size analyser from Nanobrook 90 plus from PALS Instrument shown in *figure 2.17*



*Figure 2.17 Typical image of DLS-Particle size analyser*

**m. Scanning electron microscope**

SEM instrument with beam of high-energy electrons for the generation of variety signals on the focussed surface of solid sample. The signals generated by the interaction between sample and high energy electrons derived the information such as texture, chemical composition, morphology, and orientation of the sample. In

routine applications data is generated on the targeted surface area of the sample and 2-D image showing the spatial arrangement in the properties. In the routinely used SEM techniques approx.. 1 cm to 5 micron area can be scanned having magnification of 20 X to 30,000 X with spatial resolution of 50 to 100nm. The SEM is mainly useful in the studying of selected point of sample. This is specifically important to determination of chemical composition, morphology, and orientations of the investigational sample. Typical image of scanning electron microscope (Philips XL 30 SEM) shown in *figure 2.18*



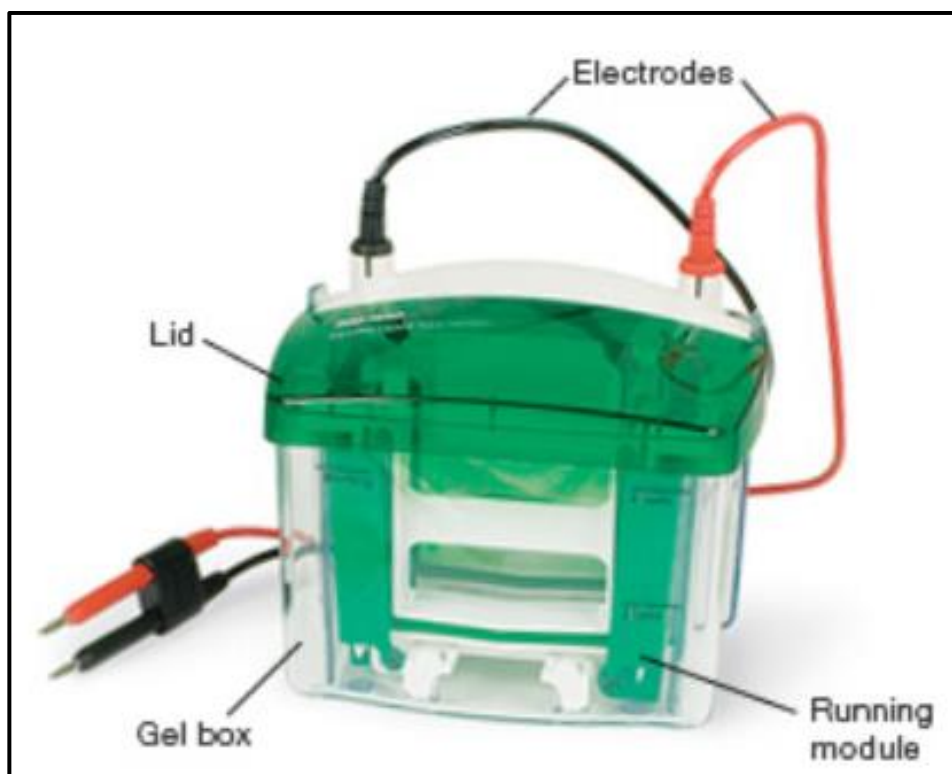
*Figure 2.18 Typical image of scanning electron microscope*

#### **n. Electrophoresis**

Proteins can be separated by electrophoresis under the influence of electric current through the gel matrix. The smaller molecules move faster due to less resistance from the gel matrix. Other influencing factors are the rate of migration through the gel matrix. Includes s the structure and charge on the proteins.

In SDS-PAGE, the use of sodium dodecyl sulfate or sodium lauryl sulfate and polyacrylamide gel protein molecules movements are based on the size of the proteins. It removes the influence of structure and charge of the protein as it acts as a detergent helping in denaturation the protein. Also breaks the disulphide linkages and unfold the protein structure into straight chains.

Typical image of vertical electrophoretic unit is shown in *figure 2.19*



*Figure 2.19 Typical image of vertical electrophoretic unit*

**o. Remi centrifuge**

Centrifuge is a device working on the principle of centrifugal force and density of the components in the fluid. The fluid under investigation is spined at high speed in centrifuged Typical image of centrifuge (Model C-24PLUS, Remi from Elektrotechnik, Ltd., India) shown in *figure 2.20*



*Figure 2.20 Typical image of centrifuge*

## **CHAPTER-3**

**SCREENING OF COMMERCIALY AVAILABLE REDUCTASE  
ENZYMES FOR THE CONVERSION OF TERT-BUTYL[5-(4-  
CYANOBENZOYL)-2-FLUOROPHENYL]CARBAMATE TO TERT-  
BUTYL {5-[(4-CYANOPHENYL)(HYDROXY) METHYL] -2-  
FLUOROPHENYL }CARBAMATE AND PROCESS OPTIMIZATION**

## Chapter 3

### 3.1. Introduction

Tert-butyl{5-[(4-cyanophenyl)(hydroxy)methyl]-2-fluorophenyl}carbamate is an important pharmaceutical entity and acts as a preliminary ingredient in the synthesis of drugs such as Citalopram [58], and Escitalopram oxalate [59] which are antidepressants acting specifically by inhibition of serotonin (5-HT) uptake. Tert-butyl{5-[(4-cyanophenyl)(hydroxy)methyl]-2-fluorophenyl}carbamate is also used in synthesis of different benzohydroxyls (specifically chlorobenzohydroxyls) which are intermediates in preparations of nefopam (analgesic, muscle relaxant, or antidepressant) [61]. These intermediates with –OH groups are generally synthesized by reduction of benzophenone families using oxo-binding and asymmetric reduction using ruthenium catalysts [62], amino acid-functionalized metal-organic frameworks [63], CBS (Corey–Bakshi–Shibata) catalyst [64], among many others reported in literature. In a recent review, [65] has explained different catalysts and the respective chemical approach for asymmetric reduction from prochiral ketones. The chemically reductive method requires protection of specific group, involves processing with harsh chemicals and conditions during its operation, limited substrate scope, and this leads to a product with reduced yield and some impurities [66]. In addition to the risks during processing and operation, there may be an extra burden environment, and can also cause deterioration of process reactor [67, 68]. In current times, the biocatalysis-based approaches using ketoreductases are attractive alternative to the chemical route of synthesis and/or process for reduction of pro-chiral ketones to optically pure chiral selective alcohols, due to high substrate specificity and precise selectivity (stereo-, chemo-, and regio-) of product [69].



Ketoreductases (EC Number 1.1.1.2) are related to short chain dehydrogenases or reductases family, which primarily utilize NADPH for stereo-specific reduction of  $\beta$ -ketoacyl intermediates. They have been further classified as type-A ketoreductases (generating l-hydroxyl substituents), type-B ketoreductases (generating d-hydroxyl substituents) and type-C ketoreductases (reductase-incompetent) [70]. The ketoreductases have gained enormous popularity due to their inimitable feature of reducing a broad domain of ketones and aldehydes, to yield important chiral selective alcohols [71]. Along with reduction of ketones and aldehydes, these enzymes also been used in reversible reactions i.e. oxidation of alcohols to produce ketones, aldehydes, and organic acid [72].

Now a days, ketoreductases have found industrial applications in the subsequent alcohol oxidations, and asymmetric reductions of pro-chiral ketones and aldehydes [73]. Previously, the ketoreductase mediated catalytic transformations have been industrially utilized to prepare an array of chiral synthons and/or active pharma ingredients, which includes (*S*)-Licarbazepine [74], (4*S*)-3-[(5*S*)-5-(4-fluorophenyl)-5-hydroxypentanoyl]-4-phenyl-1,3-oxazolidin-2-one [75], (*S*)-N-(2-(1-(3-ethoxy-4-methoxyphenyl)-2-(methylsulfonyl)ethyl)-1,3-dioxoisindolin-4-yl)acetamide [76], (*R*)-methyl mandelate, ethyl (*R*)-mandelate, (*S*)-N-benzyl-3-pyrrolidinol, and ethyl (*R*)-2-hydroxy-4-phenylbutyrate, [77], atorvastatin [78], Montelukast [79] and many others reported in literature. The industrial vitality of ketoreductases can be understood by the fact from rising number of innovative patents applied in recently by industries and academia which describe the processes for synthesizing valuable intermediates and compounds.

Here, in the said investigation, we have made an attempt to synthesize the chiral selective tert-butyl{5-[(4-cyanophenyl)(hydroxy)methyl]-2-fluorophenyl}carbamate *via* the reduction of tert-butyl[5-(4-cyanobenzoyl)-2-fluorophenyl]carbamate using

ketoreductase as a prominent biocatalysis. For this, we have firstly screened various ketoreductases from different sources for the said biotransformation. The best enzyme hit was taken forward and screening of different co-solvents and investigation of various process parameters (temperature, pH, enzyme loading, and substrate loading) were assessed for maximum conversion. In addition, the investigation of timely progress of reaction was performed with gram scale batches. Finally, the recovered product was confirmed with HPLC analysis, specific optical rotation, melting point and boiling point, LC-MS, ATR-FTIR, <sup>1</sup>H NMR, and <sup>13</sup>C NMR. According to our knowledge and gathered information's, the reduction of tert-butyl[5-(4-cyanobenzoyl)-2-fluorophenyl] carbamate to tert-butyl{5-[(4-cyanophenyl)(hydroxy)methyl]-2-fluorophenyl}carbamate using ketoreductases mediated approach is being reported for the first time in literature.

## **3.2 Material and Methods**

### **3.2.1 Screening of ketoreductases for reduction tert-butyl[5-(4-cyanobenzoyl)-2-fluorophenyl]carbamate to tert-butyl {5-[(4-cyanophenyl) (hydroxy) methyl] -2-fluorophenyl }carbamate**

A total of 92 ketoreductases were screened for selective reduction of tert-butyl[5-(4-cyanobenzoyl)-2-fluorophenyl]carbamate to tert-butyl{5-[(4-cyanophenyl)(hydroxy)methyl]-2-fluorophenyl}carbamate. For this, ketoreductase (20 mg) was added slowly with proper care to prevent foam formation in 900 µL buffer of potassium phosphate buffer with pH 7.5, 100 millimolar containing 2 mM-NAD, 2 mM-NADP, 2 mg GDH, and 10 mg glucose. After this, substrate (20 mg dissolved in 100 µL *iso*-propyl alcohol) was slowly added to this reaction medium which was incubated at 35±2<sup>0</sup>C on a thermomixer (Model Matrix Orbital Delta Plus, IKA Thermoshaker, Germany) for 24 hours at 1,000 rpm. The progress of the reaction was stopped by adjusting the pH to 2-2.5 with 6 Molar HCl solution, and the samples were extracted

in dichloromethane ( 3 X 1 mL). The collected organic layers were pooled together and dried by evaporation on rota evaporator with reduced pressure and analysed on reverse phase HPLC for conversion and normal phase HPLC for a chiral analysis.

### 3.2.2 Screening of co-solvents

The effect of addition of different co-solvents such as *iso*-propanol, dimethylsulfoxide, N,N-dimethylformamide, methanol and ethanol for selective reduction of tert-butyl[5-(4-cyanobenzoyl)-2-fluorophenyl]carbamate to tert-butyl{5-[(4-cyanophenyl)(hydroxy) methyl]-2-fluorophenyl}carbamate was assessed at 10% volume of the reaction volume. For this, the substrate solution was prepared by dissolving in co-solvent, added this substrate solution to the reaction mixture (mentioned above), and stirred at 220-240 rpm under ambient incubation conditions.

### 3.2.3 Optimization of process parameters

The process parameters optimization such as temperature, pH, enzyme loading, and substrate loading accomplice with reduction reaction were developed with approach using one factor at a time. The reaction mixture consisted of 9 mL buffer of potassium phosphate buffer 100 mM containing 2 mM-NADP, with enzyme (ES-KRED-213), substrate, incubated at specified temperature and pH, and stirred at 220-240 rpm. The ambient temperature for biotransformation was determined by incubating the reaction mixture in buffer of potassium phosphate 100 mM and pH 7 containing 2 mM-NADP, 10% enzyme loading, and 100 g/L substrate concentration at varying temperature (30<sup>0</sup>C, 40<sup>0</sup>C, and 50<sup>0</sup>C) for 12 hours. The medium pH was optimized by incubating the reaction mixture with buffer of potassium phosphate 100 mM containing 2 mM-NADP, 10% enzyme loading, and 100 g/L substrate concentration) with different pH (6, 7, 8, and 9) at optimized temperature for 12 hours. The ambient enzyme charging was assessed by nurturing the reaction medium in buffer of potassium phosphate 100 mM containing 2 mM-NADP, and

100 g/L substrate concentration at different enzyme loading (5%, 10%, 15% and 20%) at optimized temperature and pH for 12 h. Finally, the effective substrate concentration was determined by incubating the reaction medium with buffer of potassium phosphate 100 mM containing 2 mM-NADP at different substrate loading (50g/L, 100g/L, and 150g/L) at optimized temperature, pH, and enzyme loading for 12 hours.

#### **3.2.4 Time course reactions on gram scale**

The gram scale studies were performed by investigating the timely progress of reaction at different temperature (30<sup>0</sup>C, 40<sup>0</sup>C, and 50<sup>0</sup>C), enzyme loading (5%, 10%, 15% and 20%), and substrate loading 50g/L, 100g/L, and 150g/L). In a reaction vessel, 45 mL buffer of potassium phosphate 100 mM containing 2 mM-NADP, and enzyme (ES-KRED-213) were added and stirred at 220-240 rpm. The substrate was prepared by dissolving tert-butyl[5-(4-cyanobenzoyl)-2-fluorophenyl]carbamate in *iso*-propanol, and added slowly (dropwise) in the reaction vessel. The acetone generated during the progression of reduction reaction was removed by intermittently applying vacuum. After confirming complete conversion tert-butyl[5-(4-cyanobenzoyl)-2-fluoro phenyl] carbamate to tert-butyl{5-[(4-cyanophenyl)(hydroxy)methyl]-2-fluoro phenyl} carbamate with HPLC, the *iso*-propyl alcohol was removed from reaction mixture by distillation on rotary evaporator (model RV 8V, IKA® India Private Limited, Bangalore) at 45-50<sup>0</sup>C under vacuum. Finally added Hyflo powder 1 g to the reaction mixture, stirred for 30 min. and filtered through hyflo bed prepared on Whatman filter paper no. 42, and then hyflo cake formed was rinsed with ethyl acetate (25 mL). From the collected filtrate, the organic layer was separated using a separating funnel. The obtained water layer was washed again with 25 mL fresh ethyl acetate, mixed thoroughly, the ethyl acetate layer was recovered, and then the collected ethyl acetate layers were pooled together,

treated with activated carbon at 40-45<sup>0</sup>C for 1-1.5 h, filtered through hyflo bed and the clear filtrate was distilled on rota evaporator at 45-50<sup>0</sup>C under vacuum. The product formed *i.e.* tert-butyl{5-[(4-cyanophenyl) (hydroxy)methyl]-2-fluoro phenyl}carbamate was recovered, dried in vacuum tray dryer for 20-22 h at 30-35<sup>0</sup>C under vacuum, and the yield was calculated.

### **3.2.5 Instrumental characterization**

The quantification of conversion of substrate to product was done by reverse phase HPLC and chiral purity with normal phase HPLC.

#### **3.2.5.1 Reverse phase HPLC**

The dried samples were mixed and diluted to a final concentration of 0.25 mg/mL with acetonitrile. Finally filtered through 0.45 µm filter, and analysed on C18 column (Ascentis Express, C18 (2.7 µm × 4.6 × 150 mm)) using HPLC system (Shimadzu LC-2030C 3D plus, Japan). 10 mM ammonium acetate in water as mobile phase A and acetonitrile as mobile phase B, which was run in gradient mode (time: 0.01 min., A=98 and B=2; 20 min., A=20 and B=80; 28 min., A=20 and B=80; 28.1 min., A=98 and B=2; and 30 min., A=98 and B=2), injection volume= 10 µL, The temperature of column was 25±2<sup>0</sup>C, 0.8 mL/min was flow rate and detection at 200 nm with a run time of 30 min.

#### **3.2.5.2 Normal phase HPLC for a chiral analysis**

The chiral purity of isolated compound was enumerated with normal phase HPLC on CHIRALCEL® OJ-RH Column (Daicel chiral column (5 µm × 4.6 × 150 mm)) using HPLC Shimadzu LC-2030C 3D plus, Japan. The mobile phase A used was 0.1% trifluoroacetic acid in water and methanol in 30:70 (V/V) and mobile phase B was acetonitrile which was run in gradient mode (time: 0.01 min., A=100 and B=0; 20 min., A=100 and B=0; 25 min., A=10 and B=90; 28 min., A=10 and B=90; 30

min., A=100 and B=0), injection volume=20  $\mu$ L, column temperature was  $25\pm 2^{\circ}\text{C}$ , 0.5 mL/min. was flow rate, and detection at 200 nm with 30 minute run time.

### **3.2.5.3 Confirmation and characterization of tert-butyl{5- [(4-cyanophenyl)(hydroxy) methyl]-2-fluorophenyl} carbamate**

The confirmation and characterization of final recovered, and purified product was done by specific optical rotation (SOR), melting and boiling point, LCMS, FTIR, and NMR, along with HPLC. The specific optical rotation was analysed on digital Polarimeter (model CDP – 001, Contech Instruments Ltd., Navi Mumbai, India) at 1 g/100 mL dichloromethane. The melting and boiling point was determined on Digital Melting Point Apparatus (Labline, Mumbai, India). LC-MS was performed by using the same mobile phase on C18 column. The mass fragments of the compound were visualized with mass split in the instrument (LCMS 2020, Shimadzu, Japan). The distinctive, characteristic, functional, and structural moieties were determined on ATR-FTIR. The number of protons and carbons were determined by  $^1\text{H}$  NMR  $^{13}\text{C}$  NMR by dissolving it in deuterated chloroform ( $\text{CDCl}_3$ ).

### **3.2.6 Statistical analysis**

All the experimental reactions were carried out in triplicate and the obtained findings are expressed as average  $\pm$  standard errors. The obtained data was tested on Microsoft Excel, 2013, and SPSS Version16 by claiming one way ANOVA to assess the differences in mean and statistically significant differences amongst the observed average values established at  $p \leq 5\%$  and Dunnett's post hoc test.

## **3.3 Results and discussion**

The purity of substrate (tert-butyl[5-(4-cyanobenzoyl)-2-fluorophenyl]carbamate) and Racemic standard product (tert-butyl{5-[(4-cyanophenyl)(hydroxy)methyl]-2-fluoro phenyl}carbamate) as determined by supplier with reverse phase HPLC was  $> 97\%$  and  $>98\%$ , respectively (*figure 3.1 and figure 3.2*).

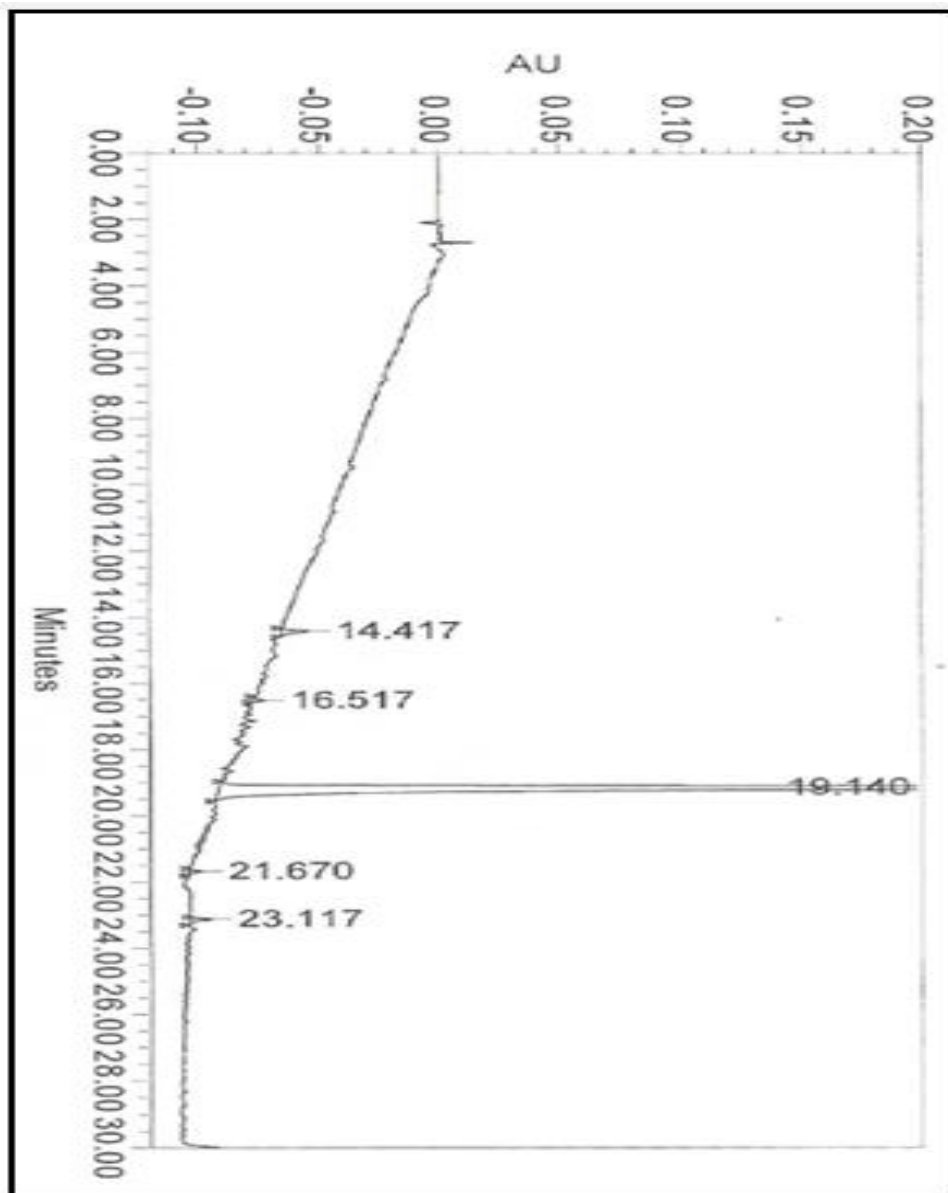


Figure 3.1 Reverse phase HPLC chromatogram of *tert*-butyl[5-(4-cyanobenzoyl)-2-fluorophenyl] carbamate

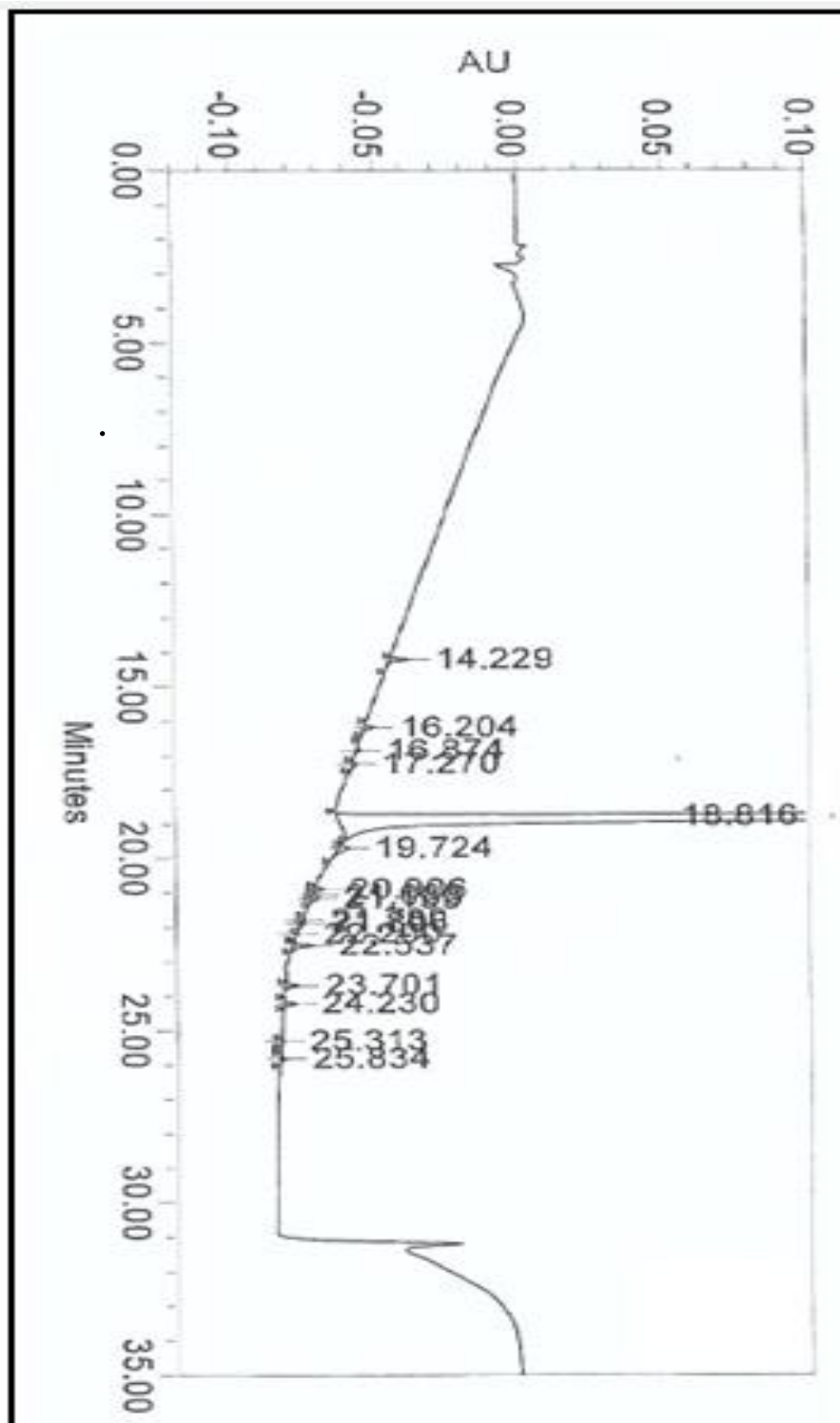
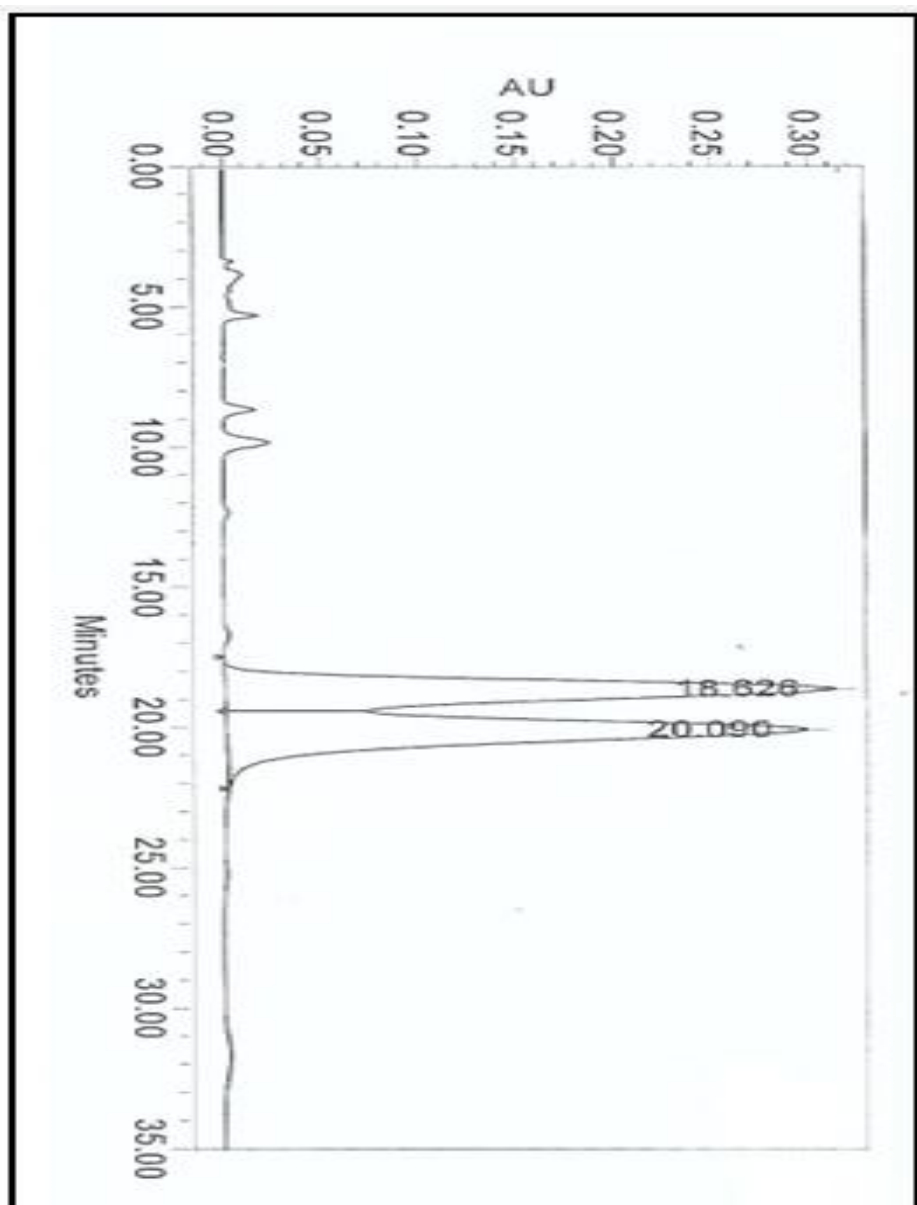


Figure 3.2 Reverse phase HPLC chromatogram of *tert*-butyl{5-[(4-cyanophenyl)(hydroxy)methyl]-2-fluorophenyl}carbamate

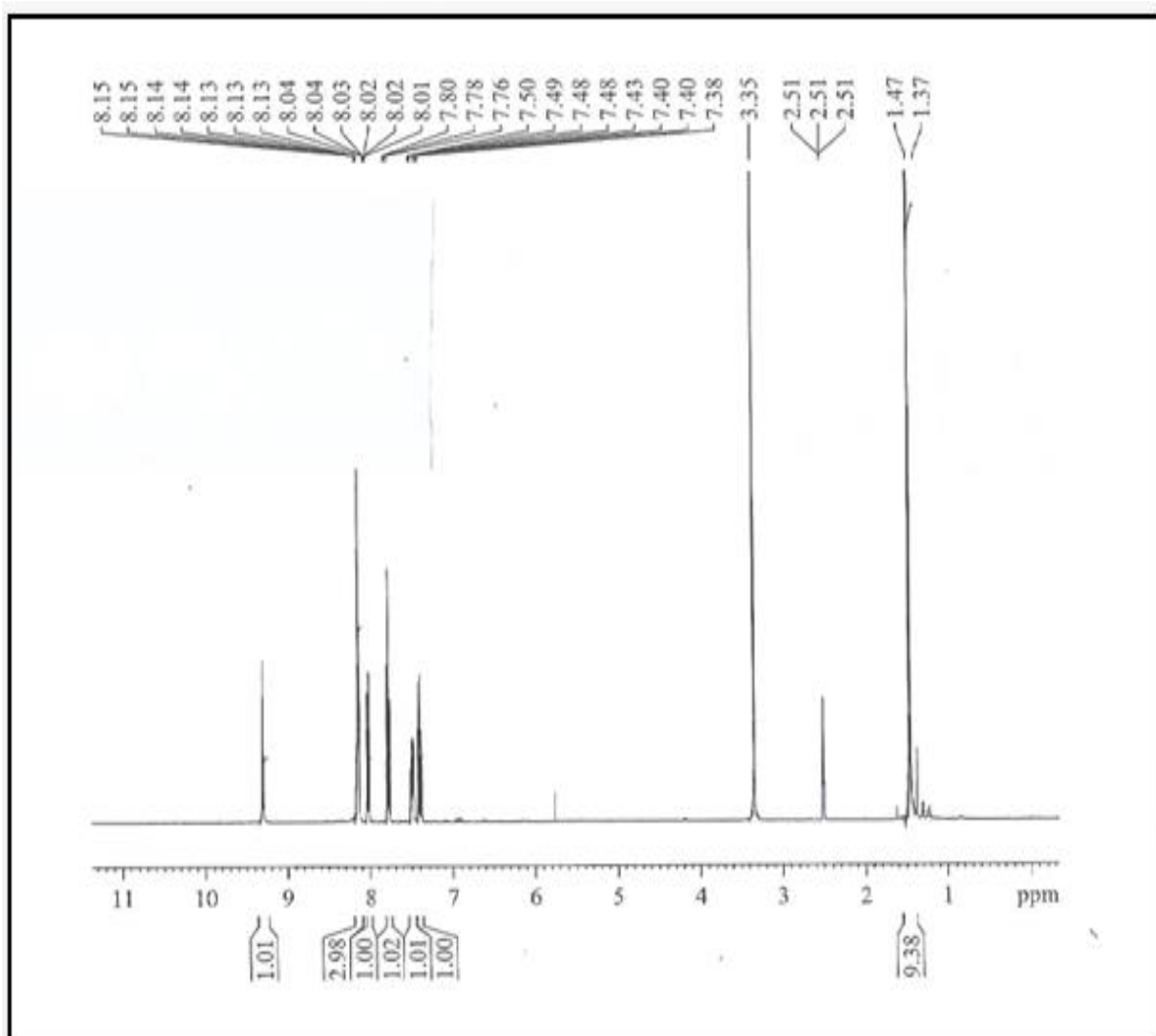


The normal phase HPLC profile of racemic standard product is shown in *figure 3.3*



*Figure 3.3 Chiral HPLC chromatogram of tert-butyl{5-[(4-cyanophenyl) (hydroxy) methyl]-2-fluorophenyl}carbamate*

$^1\text{H}$  NMR of substrate is presented in *figure 3.4*



*Figure 3.4*  $^1\text{H}$  NMR profile of tert-butyl[5-(4-cyanobenzoyl)-2-fluoro phenyl]carbamate

whereas the mass fragments of substrate and product as provided by supplier with LC-MS are displayed in *figure 3.5* and *figure 3.6* respectively

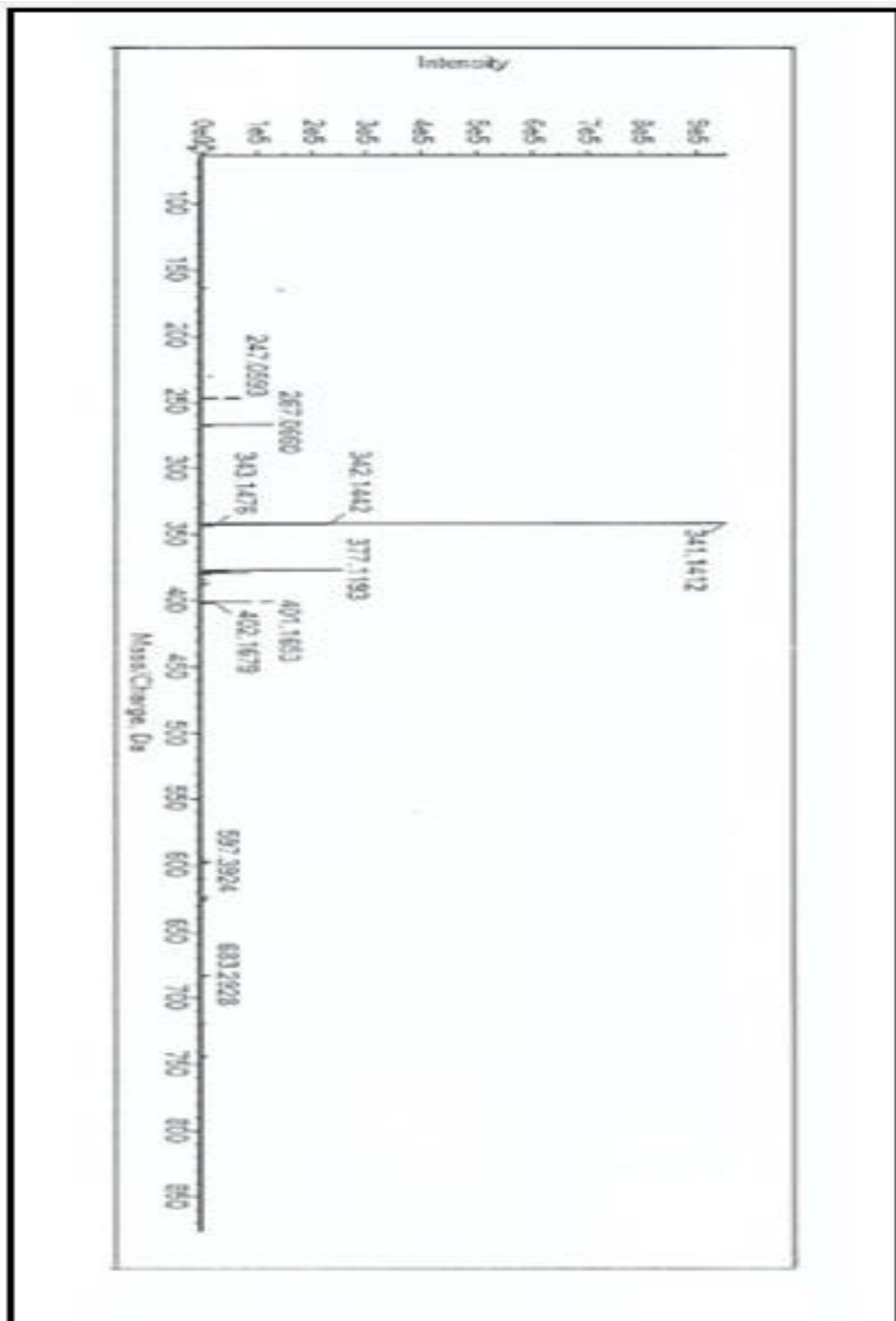


Figure 3.5 LC-MS spectra of tert-butyl[5-(4-cyanobenzoyl)-2-fluorophenyl] carbamate

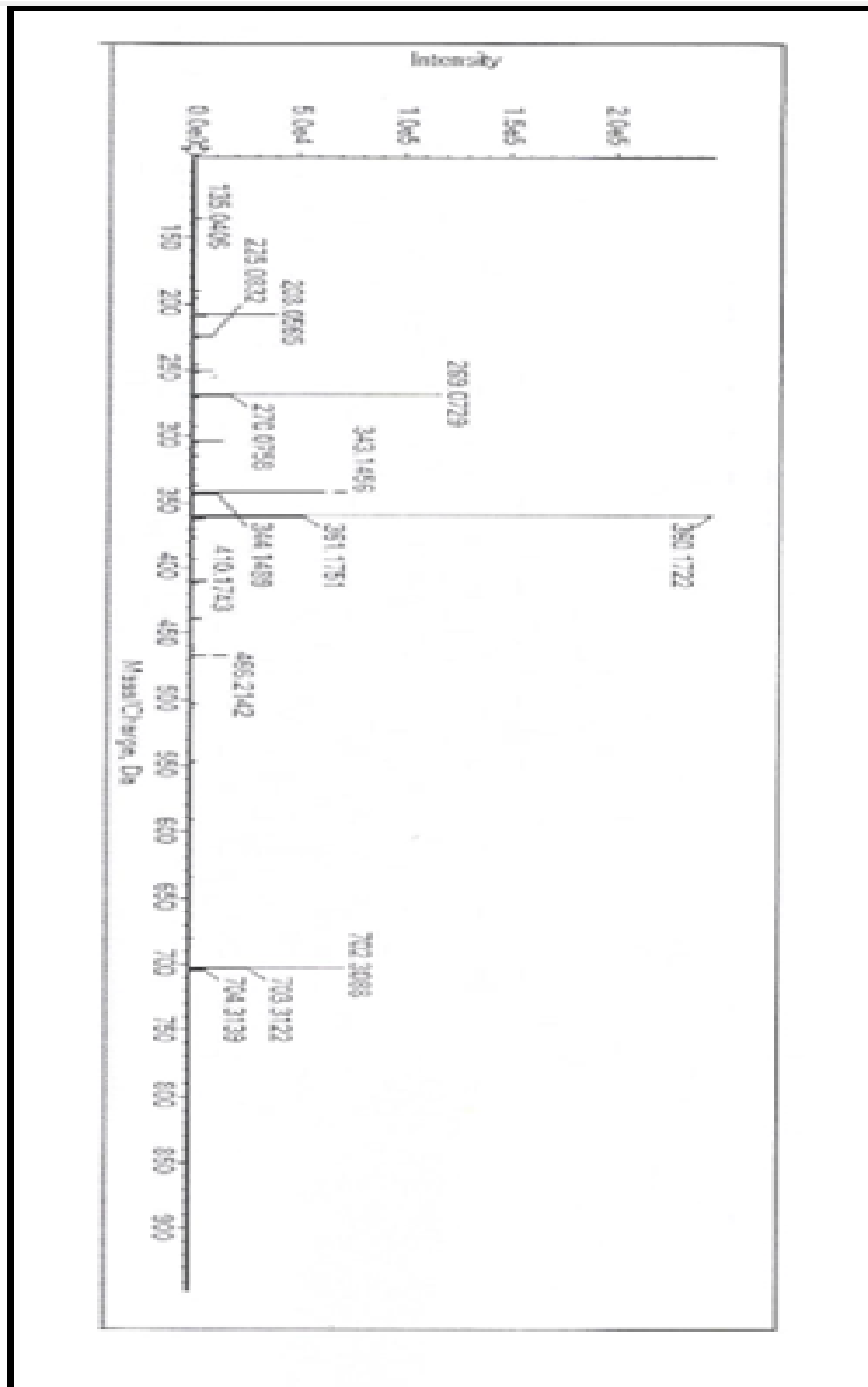


Figure 3.6 LC-MS spectra of *tert*-butyl{5-[(4-cyanophenyl)(hydroxy)methyl]-2-fluorophenyl} carbamate

### 3.3.1 Screening of ketoreductases for reduction of tert-butyl[5-(4-cyanobenzoyl)-2-fluorophenyl]carbamate to tert-butyl {5-[(4-cyanophenyl) (hydroxy) methyl] -2-fluorophenyl}carbamate

The reduction of tert-butyl[5-(4-cyanobenzoyl)-2-fluorophenyl]carbamate to tert-butyl{5-[(4-cyanophenyl)(hydroxy)methyl]-2-fluorophenyl}carbamate was carried with enzymatic approach using ketoreductases to overcome the hurdles associated with chemical route which comprises of harsh treatment with alkalises and acids which are corrosive in nature, processing at higher temperature, generation and discharge of compounds with toxic nature, protection of chemical groups, and many others, that may lead to reduced yield, productivity, and purity [67, 69]. The enzyme assisted approach may help in metal free reactions and gentle reaction conditions with highly specific, minimum energy requirement, generation of negligible by-product, and many others benefits listed in literature [80]. Herein, for the reduction of tert-butyl[5-(4-cyanobenzoyl)-2-fluorophenyl]carbamate to tert-butyl{5-[(4-cyanophenyl)(hydroxy) methyl]-2-fluoro phenyl}carbamate, 92 different ketoreductases from different sources and suppliers were screened at 100% loading of enzyme and 10% (V/V) *iso*-propyl alcohol as a co-solvent to dissolve substrate in the potassium phosphate buffer. The screening of enzymes can act as an entry point for industrial utilization of these ketoreductases for a wide array of reduction reaction for synthesizing specific and valuable chiral entities [69]. The schematic representation of this enzymatic reaction with glucose and glucose dehydrogenase system, and *iso*-propanol as co-factor recycling system for reduction reaction are displacement in *figure 3.7* and *figure 3.8*

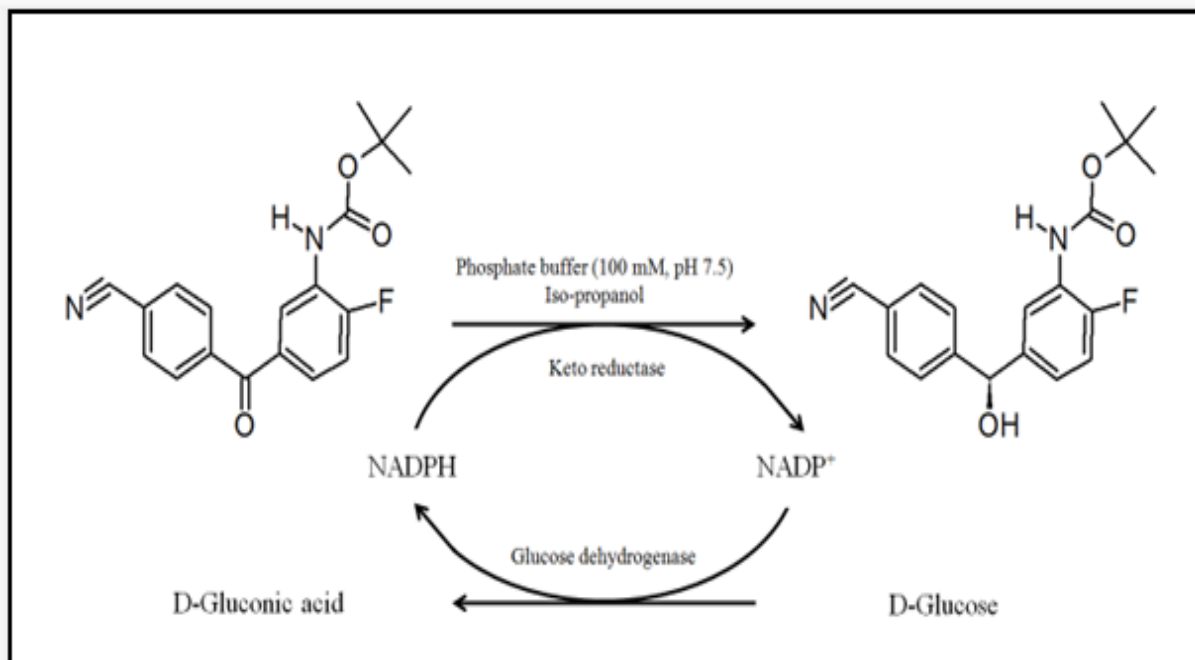


Figure 3.7 Reaction pathway for ketoreductase mediated chiral selective reduction of tert-butyl [5-(4-cyanobenzoyl)-2-fluorophenyl]carbamate to tert-butyl {5-[(S)-(4-cyanophenyl)(hydroxy)methyl]-2-fluorophenyl}carbamate using glucose and glucose dehydrogenase system

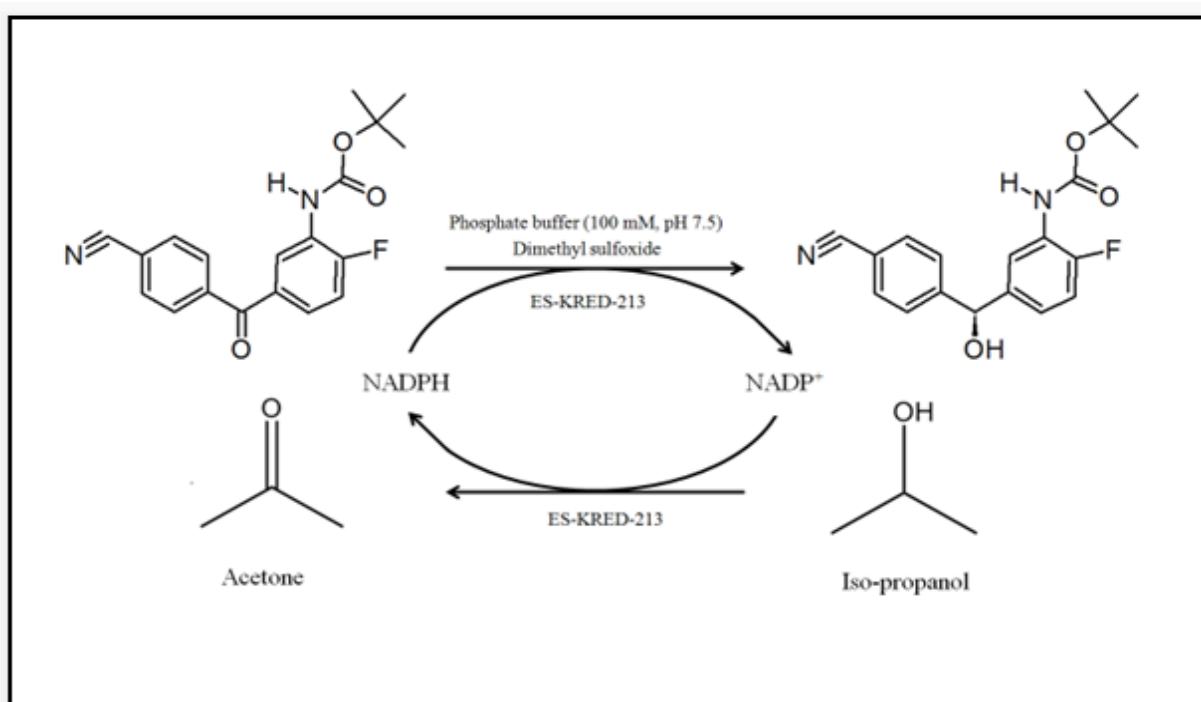


Figure 3.8 Reaction pathway for ketoreductase mediated chiral selective reduction of tert-butyl [5-(4-cyanobenzoyl)-2-fluorophenyl]carbamate to tert-butyl {5-[(S)-(4-cyanophenyl)(hydroxy)methyl]-2-fluorophenyl}carbamate using iso-propanol as co-factor recycling

Amongst the various ketoreductases screened for biotransformation, one enzyme from Codexis (KRED-P1-H01), ten from Enzyme Work (KRED-EW-102, KRED-EW-104, KRED-EW-105, KRED-EW-107, KRED-EW-108, KRED-EW-109, KRED-EW-111, KRED-EW-112, KRED-EW-118, and KRED-EW-123), and twenty two from SyncoZymes (ES- KRED-196, ES- KRED-197, ES- KRED-199, ES- KRED-200, ES- KRED-201, ES- KRED-202, ES- KRED-207, ES- KRED-208, ES- KRED-210, ES- KRED-211, ES- KRED-212, ES- KRED-213, ES- KRED-215, ES- KRED-216, ES- KRED-218, ES- KRED-219, ES- KRED-220, ES- KRED-221, ES- KRED-222, ES- KRED-223, ES- KRED-224, and ES- KRED-225) have shown prominent reduction of tert-butyl[5-(4-cyanobenzoyl)-2-fluorophenyl]carbamate to tert-butyl{5-[(4-cyano phenyl)(hydroxy)methyl]-2-fluorophenyl}carbamate (*table 3.1*).

*Table 3.1 Screening of ketoreductases for reduction of tert-butyl [5-(4-cyanobenzoyl)-2-fluorophenyl]carbamate to tert-butyl {5-[(S)-(4-cyanophenyl)(hydroxy)methyl]-2-fluorophenyl}carbamate*

Sr. No.	Name	Manufacturer	Conversion (%)	Chiral selectivity (%)	
				Isomer I	Isomer II
1	KRED-P1-H01	Codexis	75	≥99	-
2	KRED-EW-102	Enzyme Work	35	≥99	-
3	KRED-EW-104	Enzyme Work	51	≥99	-
4	KRED-EW-105	Enzyme Work	35	≥99	-
5	KRED-EW-107	Enzyme work	45	≥99	-
6	KRED-EW-108	Enzyme work	40	≥99	-

7	KRED-EW-109	Enzyme work	51	$\geq 99$	-
8	KRED-EW-111	Enzyme Work	55	$\geq 99$	-
9	KRED-EW-112	Enzyme Work	61	$\geq 99$	-
10	KRED-EW-118	Enzyme Work	52	$\geq 99$	-
11	KRED-EW-123	Enzyme Work	43	$\geq 99$	-
12	ES-KRED-196	Syncozyme	39	$\geq 99$	-
13	ES-KRED-197	Syncozyme	35	$\geq 99$	-
14	ES-KRED-199	Syncozyme	61	$\geq 99$	-
15	ES-KRED-200	Syncozyme	51	$\geq 99$	-
16	ES-KRED-201	Syncozyme	54	$\geq 99$	-
17	ES-KRED-202	Syncozyme	49	$\geq 99$	-
18	ES-KRED-207	Syncozyme	58	$\geq 99$	-
19	ES-KRED-208	Syncozyme	52	$\geq 99$	-
20	ES-KRED-210	Syncozyme	48	$\geq 99$	-
21	ES-KRED-211	Syncozyme	53	$\geq 99$	-
22	ES-KRED-212	Syncozyme	65	$\geq 99$	-
23	ES-KRED-213	Syncozyme	76	$\geq 99$	-
24	ES-KRED-215	Syncozyme	39	$\geq 99$	-
25	ES-KRED-216	Syncozyme	54	$\geq 99$	-
26	ES-KRED-218	Syncozyme	25	$\geq 99$	-
27	ES-KRED-219	Syncozyme	37	$\geq 99$	-



28	ES-KRED-220	Syncozyme	51	≥99	-
29	ES-KRED-221	Syncozyme	43	≥99	-
30	ES-KRED-222	Syncozyme	38	≥99	-
31	ES-KRED-223	Syncozyme	25	≥99	-
32	ES-KRED-224	Syncozyme	35	≥99	-
33	ES-KRED-225	Syncozyme	45	≥99	-

**Reaction conditions:** 20 mg substrate in 100 $\mu$ L iso-propanol solution, 20 mg enzyme (100% loading), 900  $\mu$ L buffer of potassium phosphate with pH 7.5, 0.1M containing 2 mM-NAD, 2 mM-NADP, 2 mg GDH, and 10 mg glucose, 1000 rpm, 35 $\pm$ 2<sup>0</sup>C. Conversion and chiral selectivity was determined by HPLC analysis.

Amongst all the ketoreductases screened, KRED-P1-H01 and ES-KRED-213 have shown a prominent conversion of >75% and chiral selectivity of > 99%. The other enzymes used in screening namely KRED-P1- A04, KRED-P1- A12, KRED-P1- B02, KRED-P1- B05, KRED-P1- B10, KRED-P1- B12, KRED-P1- C01, KRED-P1- H08, KRED-P2- B02, KRED-P2- C02, KRED-P2- C11, KRED-P2- D03, KRED-P2- D11, KRED-P2- D12, KRED-P2- G03, KRED-P2- H07, KRED-P3- B03, KRED-P3- G09, KRED-P3- H12, KRED- EW-101, KRED- EW-103, KRED- EW-106, KRED- EW-110, KRED- EW-113, KRED- EW-114, KRED- EW-115, KRED- EW-116, KRED- EW-117, KRED- EW-119, KRED- EW-120, KRED- EW-121, KRED- EW-122, KRED- EW-124, KRED-EW-125, ES- KRED-105, ES- KRED-106, ES- KRED-107, ES- KRED-108, ES- KRED-109, ES- KRED-110, ES- KRED-112, ES- KRED-116, ES- KRED-117, ES- KRED-118, ES- KRED-119, ES- KRED-120, ES- KRED-121, ES- KRED-122, ES- KRED-123, ES- KRED-124, ES- KRED-125, ES- KRED-198, ES- KRED-203, ES- KRED-204, ES -KRED-205, ES -KRED-206, ES -KRED-209, ES -KRED-214, AND ES -KRED-217 did not show any significant conversion for this reduction reaction.

Maximum conversion with some ketoreductases could be due to the desired specificity of substrate towards its active cleft [81]. The minor variations in the arrangement of amino acids in active cleft and structure of substrate are also major factors for specificity of enzymes [82]. In addition, the conservation of co-enzyme binding site and catalytic site, length, and composition of amino acids in loops also contributes to the substrate specificity of the different ketoreductases [83]. Amongst the various ketoreductases assessed, ES-KRED-213 was selected as an ideal enzyme for optimization and scale up studies because of its potential of highest conversion, and availability.

### 3.3.2 Effect of co-solvents

The reduction of *tert*-butyl[5-(4-cyanobenzoyl)-2-fluorophenyl]carbamate to *tert*-butyl{5-[(4-cyanophenyl)(hydroxy)methyl]-2-fluorophenyl}carbamate was carried out with ES-KRED-213 in different co-solvents for determination of best one for the optimization and scaleup studies to improve the practical feasibility of the developed process.

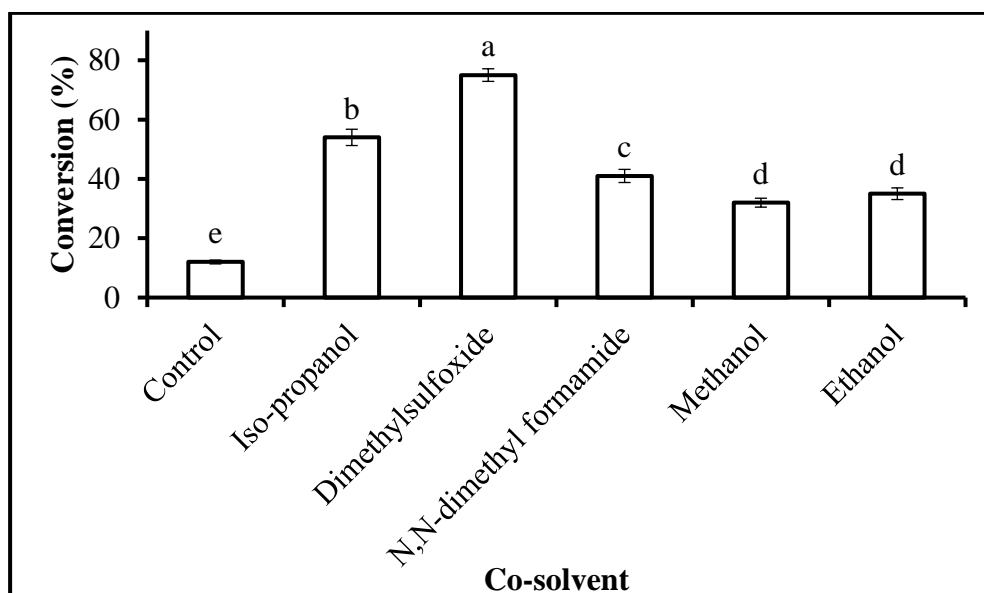


Figure 3.9 Effect of addition of co-solvents on chiral selective reduction of *tert*-butyl [5-(4-cyanobenzoyl)-2-fluorophenyl]carbamate to *tert*-butyl {5-[(*S*)-(4-cyanophenyl) (hydroxy) methyl]-2-fluorophenyl}carbamate

Co-solvents such as *iso*-propanol, dimethylsulfoxide, *N,N*-dimethylformamide, methanol and ethanol were screened at 10% concentration of the final reaction volume to assess the improvement in percent conversion of product (*figure 3.9*).

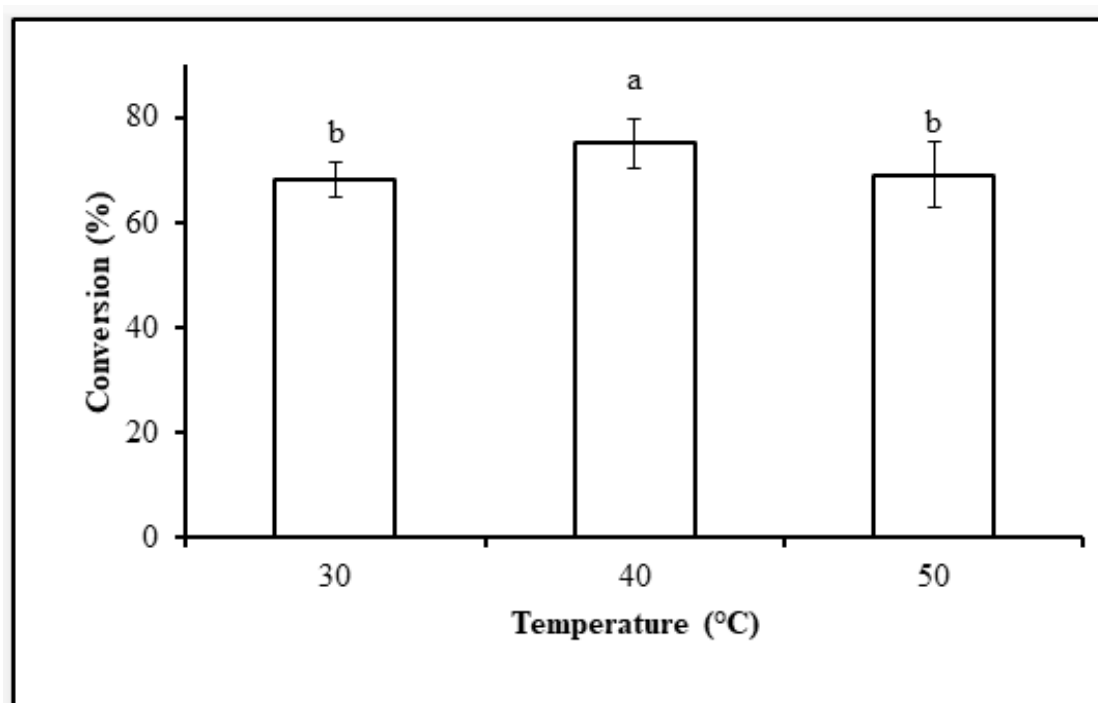
Screening of co-solvents is a pre-requisite for biotransformation and finding the best one is very important [84]. This is because the added co-solvents may also alter the selectivity of enzyme/s in some operating conditions and could have a keen influence on hydration layer surrounding the vicinity of enzymes, alter the structural conformation, and indirectly the activity and the formation of product [85]. These added co-solvents are also known to weaken the electrostatic interactions, minimize the surface area accessible to solvents and reduce the stability [86]. In addition, the co-solvents may also ease up the post reaction work-up and processing making a simple recovery of product [87].

A considerably higher conversion of  $75\pm 2.12\%$  was seen in dimethylsulfoxide subsequently followed by *iso*-propanol and *N,N*-dimethylformamide showing a conversion of  $54\pm 2.75\%$  and  $41\pm 2.21\%$ , respectively, and this was much higher over the control ( $12\pm 0.65\%$ ). Added co-solvents enhance the solubility of substrate making them more available for enzymes to smoothly proceed the reaction [88]. Previously, DMSO was also found to be a suitable co-solvent for ketoreductase and transaminase assisted biodeoximation of propiophenone oxime [89], reduction of 2-chloro-1-(2,4-dichloro phenyl)-ethanone to (*R*)-2-chloro-1-(2,4-dichloro phenyl) ethanol [90], reduction of *N,N*-dimethyl -3-keto-3-(2-thienyl)-1-propanamine to (*S*)-(-)-*N,N* - dimethyl-3-hydroxy -3-(2-thienyl)-1-propanamine [91], 3-hydroxy acetophenone to 3-[(1*R*)-1-hydroxyethyl]phenol [84], amongst many others.

### 3.3.3 Optimization of process parameters

#### 3.3.3.1 Incubation temperature

The incubation temperature is a crucial factor for biotransformation reactions as stability, activity and performance of the enzymes, along with solubility of substrate and product, and the reaction rate are directly commanded by it [92, 93]. The temperature domain of 30°C-50°C was with an reaction time for period of 12 hours was selected for the investigation. Statistically significant differences ( $p < 5\%$ ) were seen at varying incubation temperature for the reduction of substrate to product represented in *figure 3.10*



*Figure 3.10 Effect of temperature on chiral selective reduction of tert-butyl [5-(4-cyanobenzoyl)-2-fluorophenyl]carbamate to tert-butyl {5-[(S)-(4-cyanophenyl)(hydroxy) methyl]-2-fluoro phenyl}carbamate*

Highest conversion ( $75 \pm 4.68\%$ ) along with a chiral selectivity of  $> 99\%$  of tert-butyl[5-(4-cyanobenzoyl)-2-fluorophenyl]carbamate to tert-butyl{5-[(4-cyanophenyl)(hydroxy) methyl]-2-fluorophenyl}carbamate was visualized at 40°C

with ES-KRED-213. The conversion was less at 50<sup>0</sup>C, and this could be ascribed to decline in catalytic activity and performance of ES-KRED-213 at higher incubation temperature. The present findings are in accordance with previous findings by [82, 84, 91] wherein the optimum temperature for reduction with ketoreductases was 37<sup>0</sup>C, 25<sup>0</sup>C, and 37<sup>0</sup>C, respectively.

### 3.3.3.2 Medium pH

As like incubation temperature, the medium pH has a pivotal role in specific activity, performance, and stereoselectivity of enzymes [84, 93]. The pH of medium has a strong influence on the surface charge of enzyme and influences the electrostatic interactions and solubility of enzyme and substrate[92, 94]. The pH domain of 6-9 with an incubation temperature of at 40<sup>0</sup>C for 12 h was selected for this investigation. Maximum conversion (75±4.12%) with a chiral selectivity of > 99% was seen at pH 7.0 and considerable differences (p<5%) were seen at varying medium pH for the reduction of substrate represented in *figure 3.11*

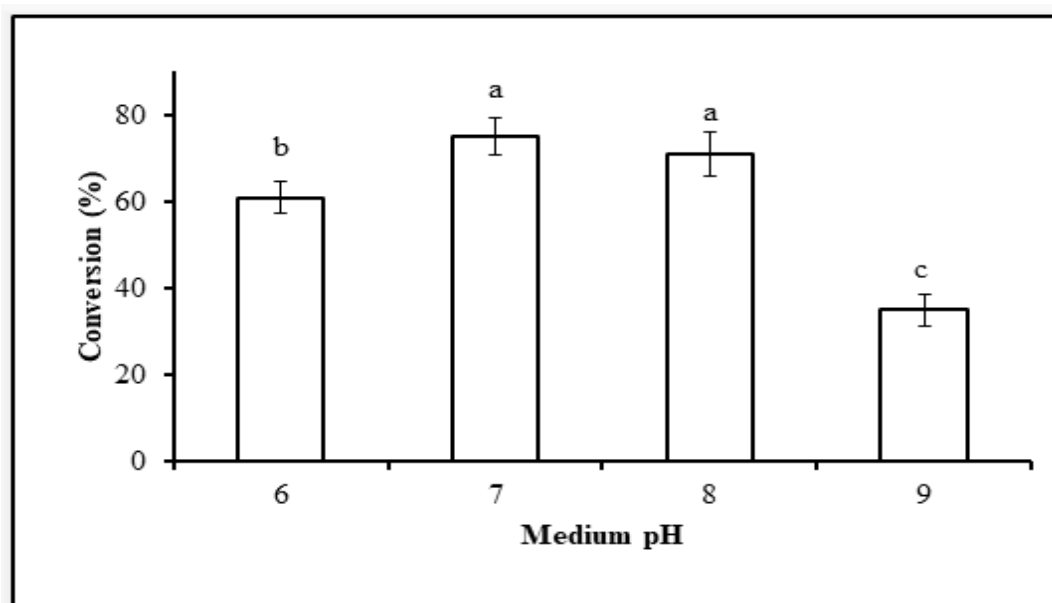


Figure 3.11 Effect of operating pH on chiral selective reduction of *tert*-butyl [5-(4-cyanobenzoyl)-2-fluorophenyl]carbamate to *tert*-butyl {5-[(*S*)-(4-cyanophenyl) (hydroxy) methyl]-2-fluoro phenyl}carbamate

The present findings of optimal pH are in correlation with previous findings by [95-97], wherein the ambient pH for reduction with ketoreductases was 6-7, 7.0, 7-8, and 7.7, respectively.

### 3.3.3.3 Enzyme loading

From economic perspective of process, it is a mandate to optimize the enzyme concentration required to carry out biotransformation reaction. The possession of the enzyme loading (%) was scrutinized by altering the enzyme addition from 5% to 20% at pH 7.0, with an reaction medium temperature of at 40<sup>0</sup>C for 12 hours. The enzyme loading had a direct role with the formation of product, and there was a steady rise in product formation with increasing enzyme concentration in the reaction mixture represented in *figure 3.12*

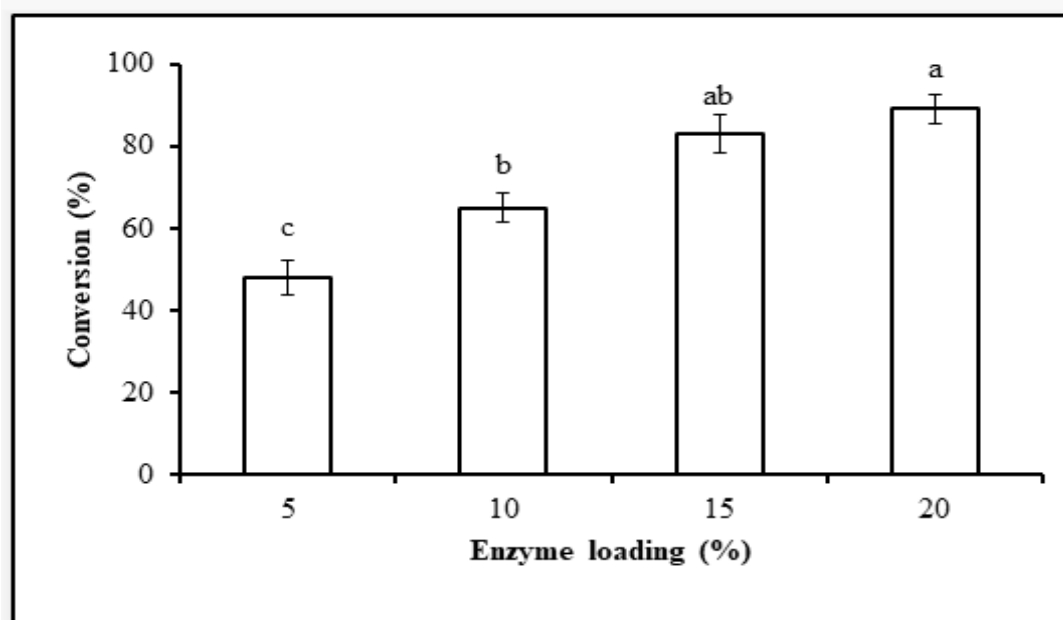


Figure 3.12 Effect of enzyme loading on chiral selective reduction of *tert*-butyl [5-(4-cyanobenzoyl)-2-fluorophenyl]carbamate to *tert*-butyl {5-[(*S*)-(4-cyanophenyl) (hydroxy) methyl]-2-fluoro phenyl}carbamate

Highest conversion of  $89\pm 3.6\%$  and  $83\pm 4.82\%$  with a chiral selectivity of  $>99\%$  was seen at 20% and 15% enzyme loading, while 10% enzyme loading displayed a comparably desirable conversion of  $65\pm 3.39\%$  and a chiral selectivity of  $>99\%$ , respectively.

#### **3.3.3.4 Substrate loading**

To develop the process the economically feasible process, it is necessary to examine the substrate loading (%) in the reaction mixture along with the enzyme loading. The effect of substrate loading (%) was calculated by assorted the substrate additions from 50 g/L to 150 g/L at 10% enzyme loading, pH 7.0, with an incubation temperature of at  $40^{\circ}\text{C}$  for 12 hours. A decline in the reaction conversion (%) from substrate to product was seen with an increase in substrate loading represented in *figure 3.13*

Maximum conversion of  $91\pm 4.5\%$  with a chiral selectivity of  $> 99\%$  was seen at 50 g/L concentration of substrate followed by 100 g/L and 150 g/L subsequently displaying  $75\pm 4.1\%$  and  $51\pm 4.2\%$  conversion and a chiral selectivity of  $>99\%$ , respectively.

At higher substrate loading the overall viscosity of reaction medium may give rise to decline mass transfer of the substrate to the active cleft of enzyme and leading to reduced conversion of product [85].

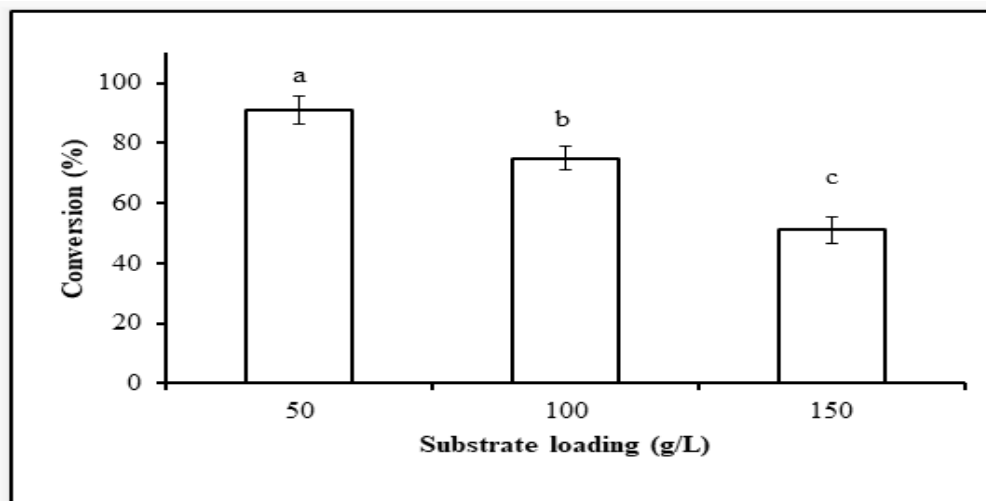


Figure 3.13 Consequences of substrate loading on chiral selective reduction of *tert-butyl [5-(4-cyanobenzoyl)-2-fluorophenyl]carbamate* to *tert-butyl {5-[(S)-(4-cyanophenyl) (hydroxy) methyl]-2-fluoro phenyl}carbamate*

### 3.3.4 Time course reactions on gram scale

The screening and process variable optimization investigations were performed at lower substrate concentration and higher enzyme loading. Now, with a perspective of scale-up, the gram scale studies were carried out [74]. The substrate loading needs to be higher and enzyme loading should be lower for technical and economic feasibility of process [86]. The selection criteria of processing parameters like temperature, pH, buffer strength, enzyme loading, substrate loading, co-solvent concentration, incubation time, and many others are among the factors for optimization of process to attain a specific product with desired specifications, and these are associated with reaction conditions to be used and characteristic properties of substrate and product, substrate [56]. The gram scale studies were performed by assessing the progression of reaction at varying temperature, enzyme loading, and substrate loading. To develop a cost effective and green process for enzyme mediated reduction of *tert-butyl[5-(4-cyanobenzoyl)-2-fluorophenyl]carbamate* to *tert-butyl{5-[(4-cyanophenyl) (hydroxy) methyl]-2-fluorophenyl}carbamate* with precise utilization of co-solvent (dimethylsulfoxide), the ambient conditions used



were 100 g/L substrate loading, 10% enzyme loading, pH 7.0, and reaction temperature of at 40°C. The enzyme loading and substrate loading were considered as 10% and 100 g/L for developing an economically feasible, industry viable and cost-effective process.

### 3.3.4.1 Progress of reaction with incubation temperature

The progression of reduction reaction at different incubation temperature was analysed because of its direct relation with rate of reaction, stability of enzyme and its activity, solubility of substrate and its product [74]. The reduction of tert-butyl[5-(4-cyanobenzoyl)-2-fluorophenyl]carbamate to tert-butyl{5-[(4-cyanophenyl)(hydroxy) methyl]-2-fluorophenyl}carbamate was studied at 30±2°C, 40±2°C, and 50±2°C at 10% ES-KRED-213 loading, 100 g/L substrate loading, pH 7.0 for 24 hours of incubation. During the early incubation period, a consistent and steady increase in conversion (%) was noticed with a rise in incubation temperature and this prominently got declined with a further incubation period was illustrated in *figure 3.14*

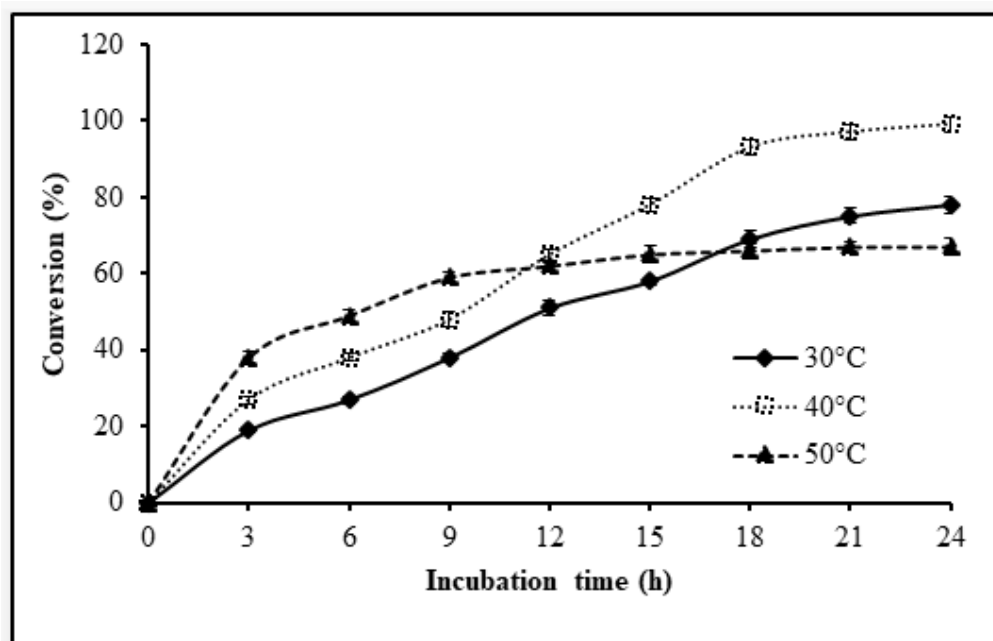


Figure 3.14 Time course of reaction on gram scale progression with temperature

After the incubation period of 24 hours, a conversion of  $78\pm 2.20\%$ ,  $99\pm 2.10\%$ , and  $67\pm 2.05\%$  was seen at  $30\pm 2^{\circ}\text{C}$ ,  $40\pm 2^{\circ}\text{C}$ , and  $50\pm 2^{\circ}\text{C}$ . The product formation was  $3.90\pm 0.11$  g/50 mL,  $4.95\pm 0.10$  g/50 mL, and  $3.35\pm 0.10$  g/50 mL, while the actual isolated product after work-up was 3.35 g, 4.16 g, and 2.95 g displaying an product yield of 67.08%, 83.16%, and 58.96% with respect to substrate loaded, and the yield of 86%, 84% and 88% with respect to the product formed after reaction at the respective incubation temperature of  $30\pm 2^{\circ}\text{C}$ ,  $40\pm 2^{\circ}\text{C}$ , and  $50\pm 2^{\circ}\text{C}$ . A slender decline in conversion (%), product formation (g/L), along with the product yield (%) at higher incubation temperature may be correlated with the lower stability enzyme at higher incubation temperature for longer period [55, 98].

#### **3.3.4.2 Progress of reaction with enzyme loading**

The reduction of tert-butyl[5-(4-cyanobenzoyl)-2-fluorophenyl]carbamate to tert-butyl{5-[(4-cyanophenyl)(hydroxy)methyl]-2-fluorophenyl}carbamate was studied at 5%, 10%, 15%, and 20% ES-KRED-213 loading, at  $40\pm 2^{\circ}\text{C}$ , 100 g/L substrate loading, pH 7.0 for 24 h of incubation. A biotransformation reaction was directly influenced by the concentration of ketoreductase loaded in the reaction mixture. This linear association could be ascertained with the availability of number of accessible active sites of enzyme to the substrate leading to conversion and formation of product [99, 100]. Highest conversion of 99.6% and 99.5% was seen at 20% and 15% enzyme loading after 15 h of incubation, while least conversion of 86% after 24 h incubation was seen at 5% enzyme loading was illustrated in *figure 3.15*

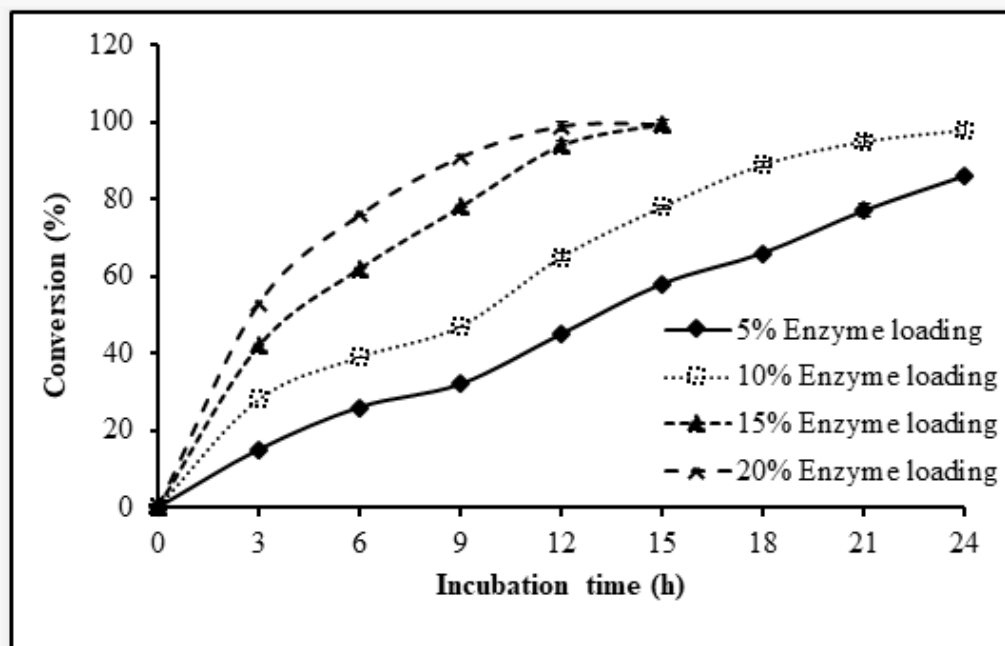


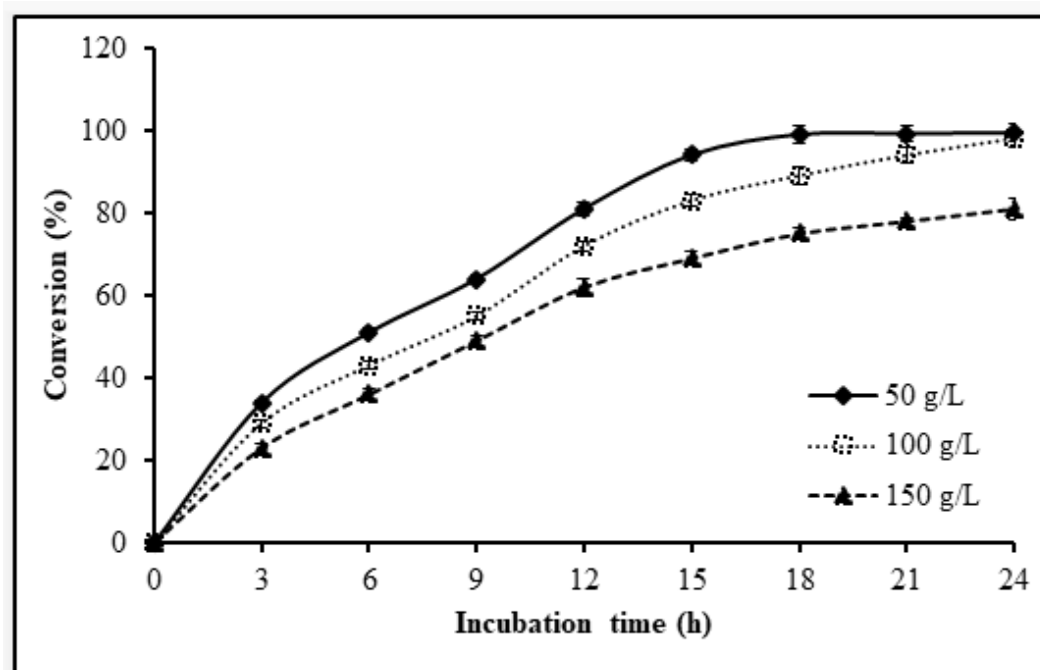
Figure 3.15 Time course of reaction on gram scale progression with enzyme loading

A considerably good conversion of 98% was also seen after 24 h with 10% enzyme loading. The final product formation at 5%, 10%, 15% and 20% enzyme loading were 4.3 g/ 50 mL, 4.9 g/ 50 mL, 4.98 g/ 50 mL, and 4.98 g/ 50 mL. The actual isolated product after work-up was 3.43 g, 4.21 g, 4.23 g, and 4.23 g displaying a product yield of 68.64%, 84.28%, 84.58% and 84.66% with respect to substrate loaded, while the yield of 88%, 86%, 85% and 85% with respect to the product formed after reaction at 5%, 10%, 15% and 20% enzyme loading, respectively.

### 3.3.4.3 Progress of reaction with substrate loading

For a reaction to get going, it is necessary to examine the substrate loading (%) in the reaction mixture along with the enzyme loading. The end results of substrate loading (%) was enumerated by changing the substrate addition from 50 g/L to 150 g/L at 10% enzyme loading, pH 7.0, with an incubation temperature of at 40°C for 24 hours. A gradual reduction in conversion of tert-butyl[5-(4-cyanobenzoyl)-2-fluorophenyl]carbamate to tert-butyl{5-[(4-cyanophenyl)(hydroxy)methyl]-2-fluoro

phenyl}carbamate was seen with an increase in substrate loading was displayed in *figure 3.16*



*Figure 3.16 Time course of reaction on gram scale progression with substrate loading*

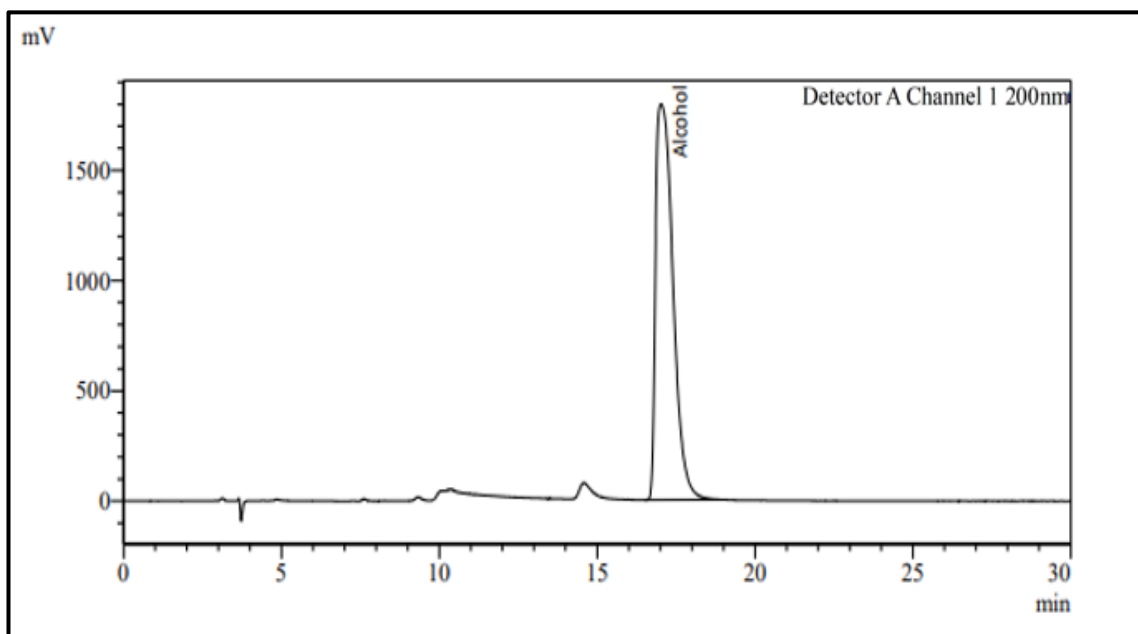
This could be due to the higher availability of substrate to lesser number of accessible active sites of enzyme [92, 93]. Maximum conversion of 99.4% and 98% was seen at 50g/L and 100g/L substrate loading after 24 hours of incubation, while least conversion of 81% after 24 hours incubation was seen at 150g/L substrate loading. The final product formation at 50g/L, 100g/L, and 150g/L substrate loading was 2.49 g/50mL, 4.90 g/50 mL, and 6.08 g/50mL with a product yield of 99.4%, 98%, and 81%, respectively with respect to the substrate. The actual isolated product after work-up was 3.39 g, 4.17 g, and 5.22 g displaying a product yield of 87%, 85%, and 86 with respect to the product formed after reaction at 50g/L, 100g/L, and 150g/L substrate loading, respectively.

### 3.3.5 Instrumental characterization of tert-butyl{5-[(4-cyanophenyl)(hydroxy)methyl]-2-fluorophenyl}carbamate

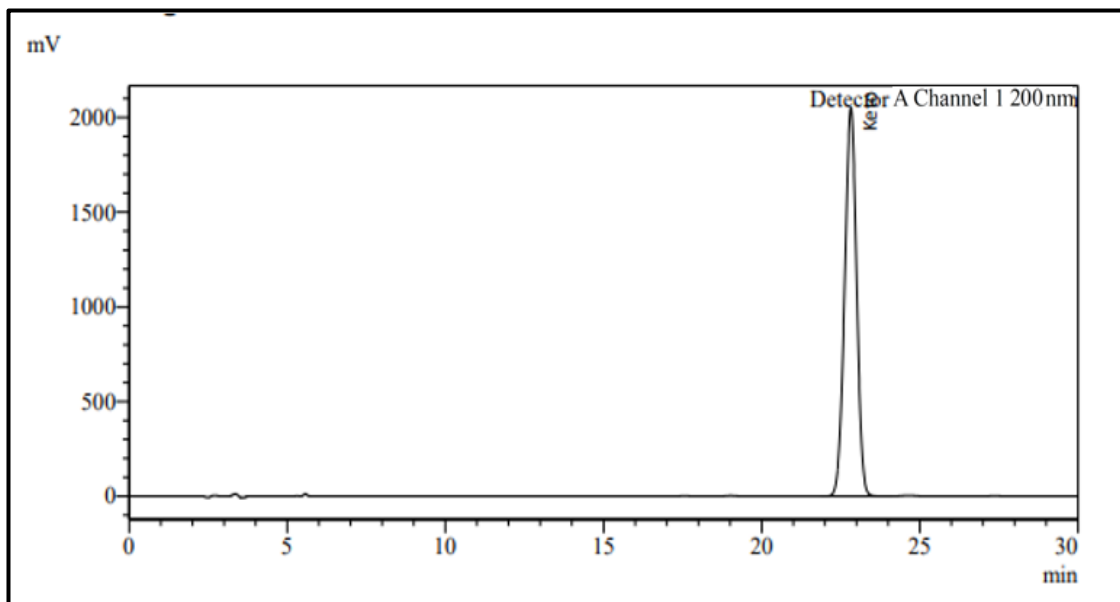
The instrumental characterization of the product was performed to confirm the formation of tert-butyl{5-[(4-cyanophenyl)(hydroxy)methyl]-2-fluorophenyl}carbamate with specific optical rotation, melting point and boiling point, LC-MS, ATR-FTIR,  $^1\text{H}$  NMR, and  $^{13}\text{C}$  NMR, along with the HPLC analysis.

#### 3.3.5.1 HPLC analysis

The liquid chromatography profile of tert-butyl{5-[(4-cyanophenyl)(hydroxy)methyl]-2-fluorophenyl}carbamate in HPLC had a retention time of 17.025 min (*Figure 3.17*). The retention time of tert-butyl[5-(4-cyanobenzoyl)-2-fluorophenyl]carbamate was 22.822 min on (*figure 3.18*)

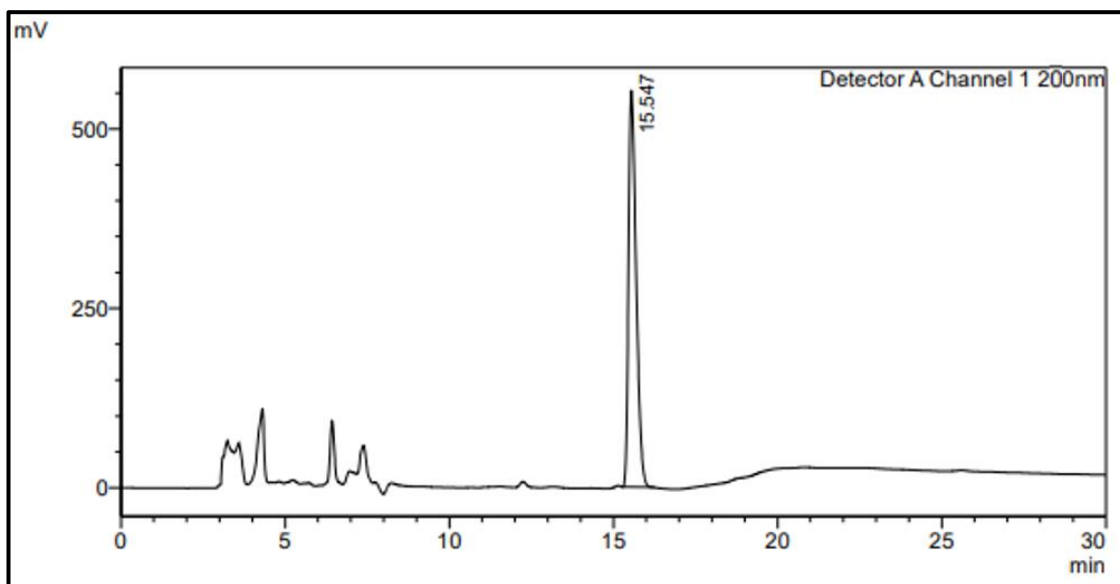


*Figure 3.17 HPLC profile of tert-butyl {5-[(S)-(4-cyanophenyl)(hydroxy)methyl]-2-fluorophenyl}carbamate*



*Figure 3.18 Reverse phase HPLC chromatogram of tert-butyl[5-(4-cyanobenzoyl)-2-fluorophenyl]carbamate*

The chiral analysis of recovered and purified product on normal phase chromatography indicated a single isomer with a retention time of 15.547 min (*figure 3.19*), which was assessed against the racemic standard showing two isomers at a retention time of 15.473 min and 16.056 min (*figure 3.20*)



*Figure 3.19 Normal phase HPLC chromatogram of single isomer of tert-butyl{5-[(4-cyano phenyl)(hydroxy)methyl]-2-fluorophenyl}carbamate*

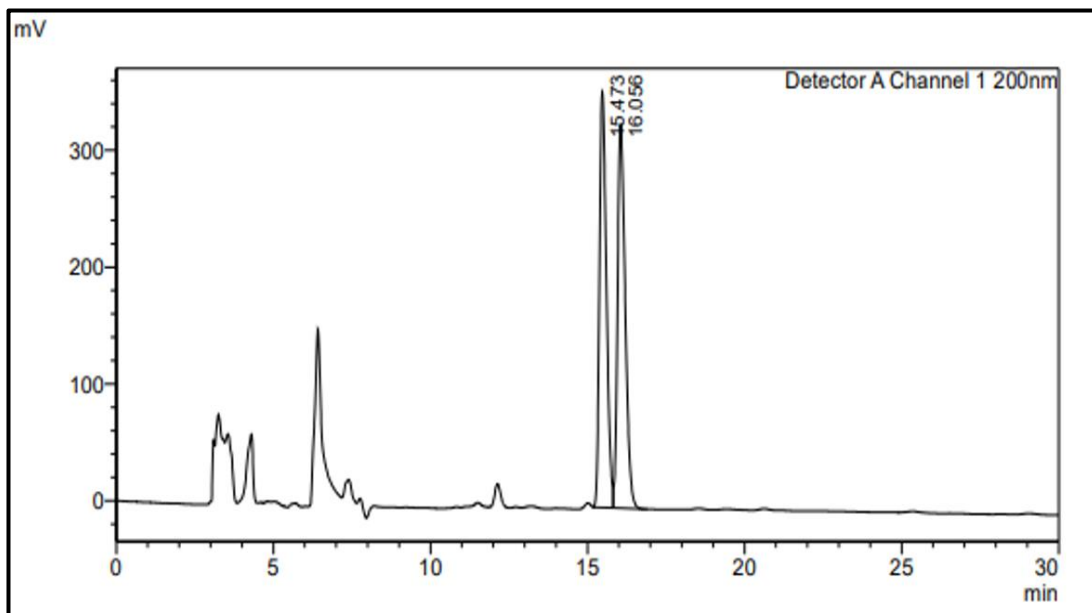


Figure 3.20 Normal phase HPLC chromatogram of racemic tert-butyl{5-[(4-cyanophenyl)(hydroxy)methyl]-2-fluorophenyl}carbamate

### 3.3.5.2 Specific optical rotation

The SOR of tert-butyl{5-[(4-cyanophenyl)(hydroxy)methyl]-2-fluorophenyl}carbamate was  $[\alpha]_D$  at 25<sup>0</sup>C: +30.5 [C=1, MDC].

### 3.3.5.3 Melting point and boiling point

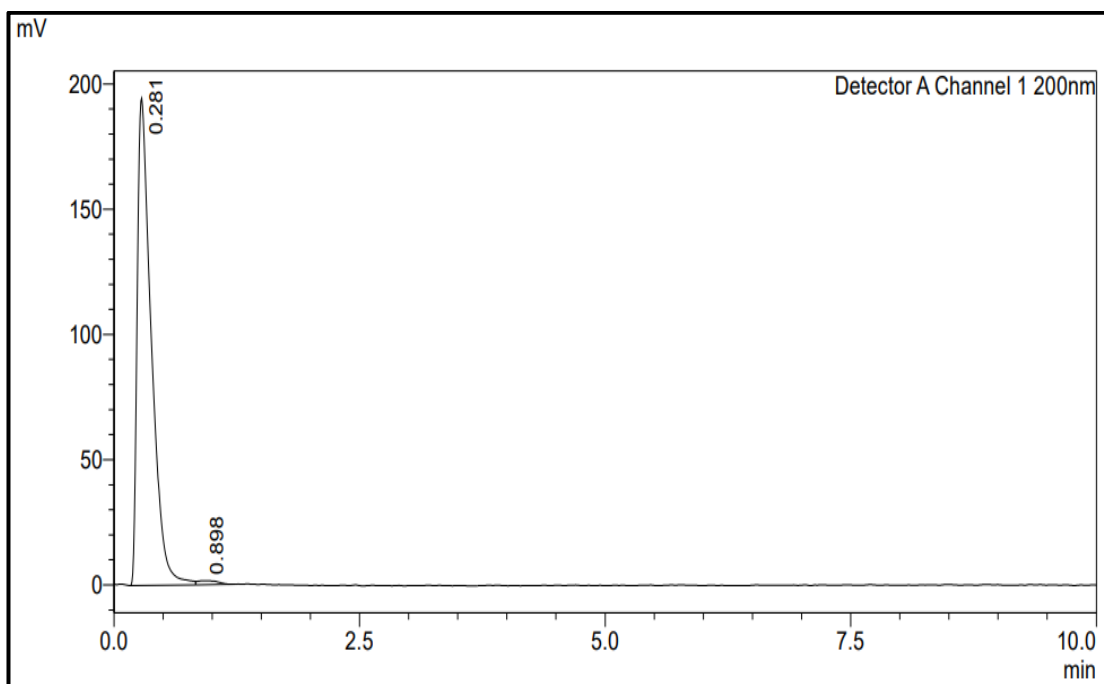
The melting and boiling point of tert-butyl{5-[(4-cyanophenyl)(hydroxy)methyl]-2-fluorophenyl}carbamate was analysed by digital melting point apparatus and found to be 57-59<sup>0</sup>C, and 115-117<sup>0</sup>C, respectively.

### 3.3.5.4 Mass by LC-MS analysis

The liquid chromatographic profile of tert-butyl{5-[(4-cyanophenyl)(hydroxy)methyl]-2-fluorophenyl}carbamate in LC-MS displayed a retention time of 0.281 min (*figure 3.21*)

The mass fragments of the purified compound were assessed by automated mass split in the instrument as shown in *figure 3.22* The mono-isotopic mass of tert-butyl{5-[(4-cyano phenyl)(hydroxy)methyl]-2-fluorophenyl}carbamate was 343 and this can also be confirmed by m/z of 343.09. The other m/z fragments of 342.91 and

343.68, 259.02, and 241.46 indicates the (M+H)<sup>+</sup> fragments with the acetonitrile and water adducts having molecular weights of 324, 217, and 199, respectively.



*Figure 3.21 LC profile of tert-butyl{5-[4-cyanophenyl](hydroxy)methyl]-2-fluorophenyl} carbamate in LC-MS*



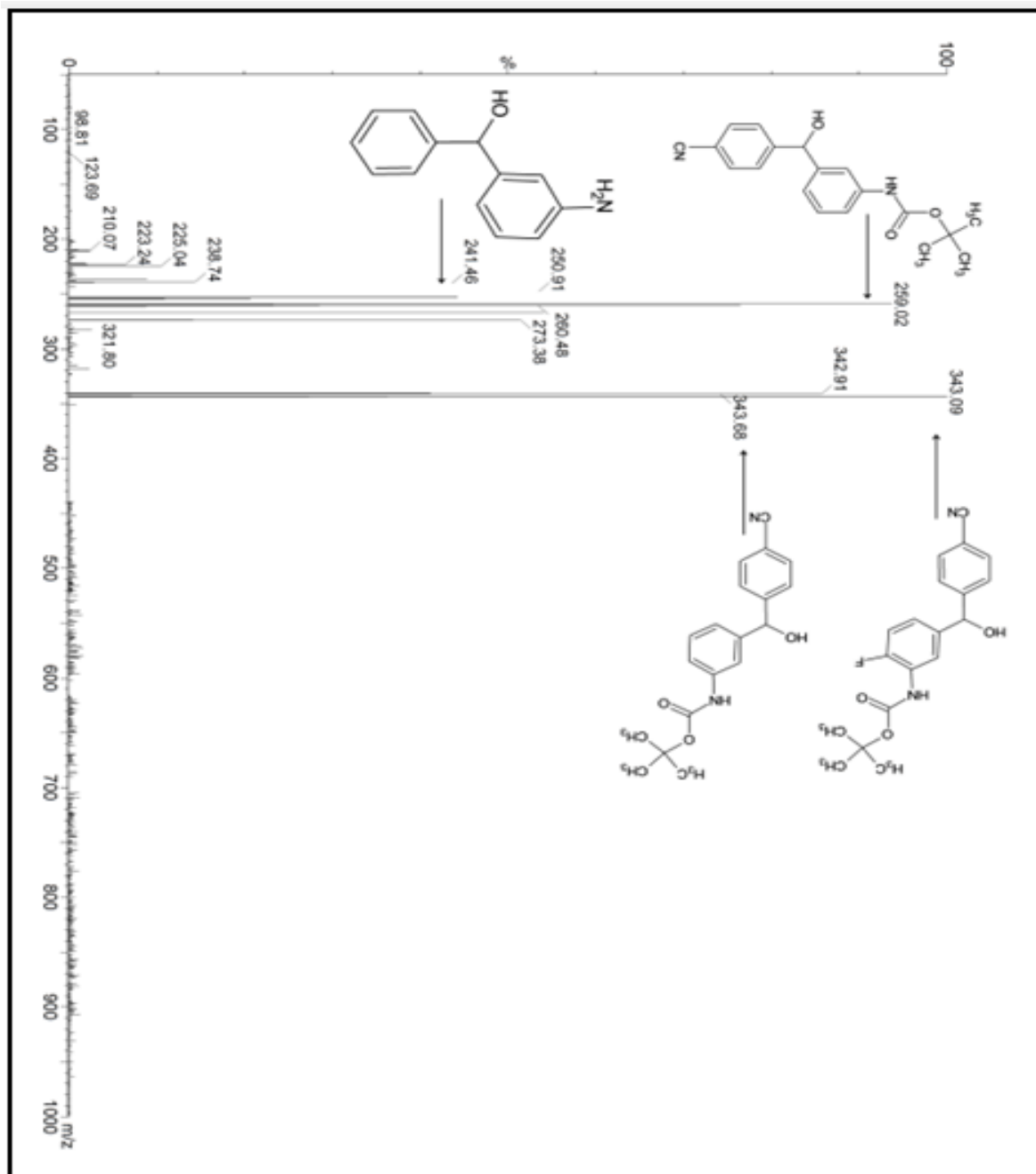


Figure 3.22 Mass fraction profile tert-butyl{5-[(4-cyanophenyl)(hydroxy)methyl]-2-fluorophenyl} carbamate

### 3.3.5.5 FTIR analysis

FTIR spectra of tert-butyl{5-[(4-cyanophenyl)(hydroxy)methyl]-2-fluorophenyl} carbamate is displayed in Figure 3.23. The occurrence of functional and characteristic peak at 1823 (1/cm) and 1770 (1/cm) signifies C=O stretching vibration, while the non-hydrogen linked amide A (N-H), amide-I (C=O), and

amide-II (N-H) regions can be confirmed by prominent peaks at 3411 (1/cm), 1691 (1/cm), and 1517 (1/cm). The presence of  $-C\equiv N$  functional group can be designated by functional peak at 2241 (1/cm). The presence of peaks at 3322 (1/cm) and 976 (1/cm) strongly signifies the stretching vibration and out of plane bend of -OH group, while the C-F stretching vibrations can be ascribed to sharp peaks at 1156 (1/cm) and 1142 (1/cm). The C-F stretching can be seen over a wide range in between 1360 (1/cm) to 1000 (1/cm). The vibrations of  $-CH=CH-$  bonds in benzene rings can be substantiated to peaks at 737 (1/cm) and 763 (1/cm), whereas the presence of peaks at 1716 (1/cm), 1371 (1/cm), and 1359 (1/cm) can be ascertained to BOC group, and 1256 (1/cm) can be corroborated to deformity vibrations of - C-H linkage in the  $-CH_3$  skeleton vibrations in the benzene ring.

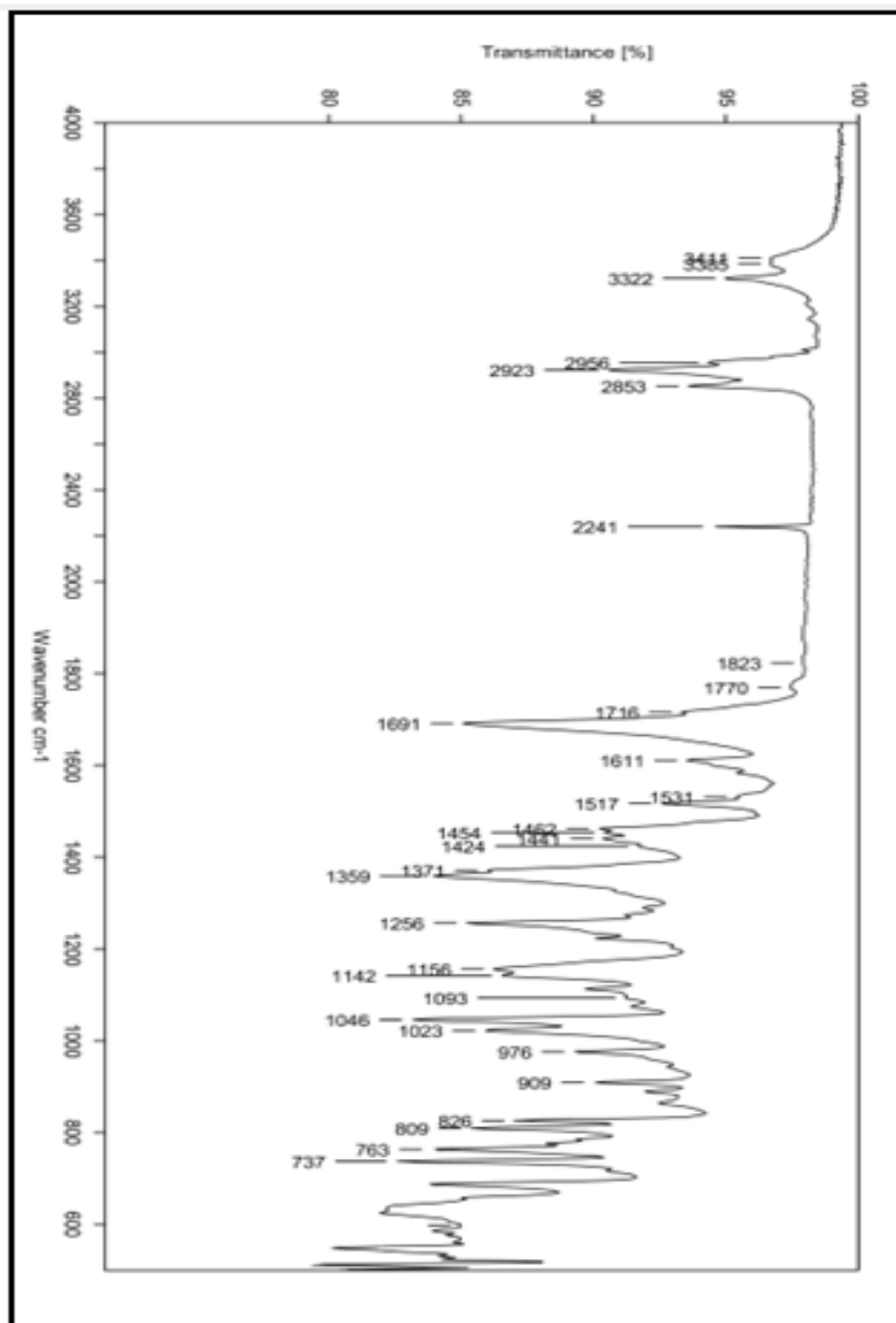


Figure 3.23 FTIR spectra of *tert*-butyl{5-[(4-cyanophenyl)(hydroxy)methyl]-2-fluorophenyl} carbamate

### 3.3.5.6 NMR analysis

The  $^1\text{H}$  and  $^{13}\text{C}$  NMR analysis of *tert*-butyl{5-[(4-cyanophenyl)(hydroxy)methyl]-2-fluorophenyl} carbamate performed in dimethylsulfoxide signified the presence of nineteen protons and nineteen carbon atoms in its structure, as displayed in *figure*

3.24 and *figure 3.25* respectively. The proton at  $\delta$ - 8.89, 7.80, and 1.44 showed a singlet peak;  $\delta$ 7.63-7.62, 6.16-6.18, and 5.75-5.76 displayed doublet peak;  $\delta$ - 7.11-7.15 has shown a triplet peak, while  $\delta$ - 7.70-7.63 has shown a multiplet.

$^1\text{H-NMR}$  (400 MHz, DMSO):  $\delta$ - 8.89, 7.80, 7.70, 7.68, 7.67, 7.63, 7.62, 7.55, 7.53, 7.51, 7.15, 7.13, 7.11, 6.18, 6.17, 5.76, 5.75, 1.44.

$^{13}\text{C-NMR}$  (101 MHz, DMSO):  $\delta$ -154.82, 153.45, 152.38, 147.56, 141.19, 131.51, 131.13, 129.96, 126.64, 126.52, 123.10, 123.03, 122.61, 119.29, 115.75, 115.56, 111.52, 79.75, 73.00, 28.46.

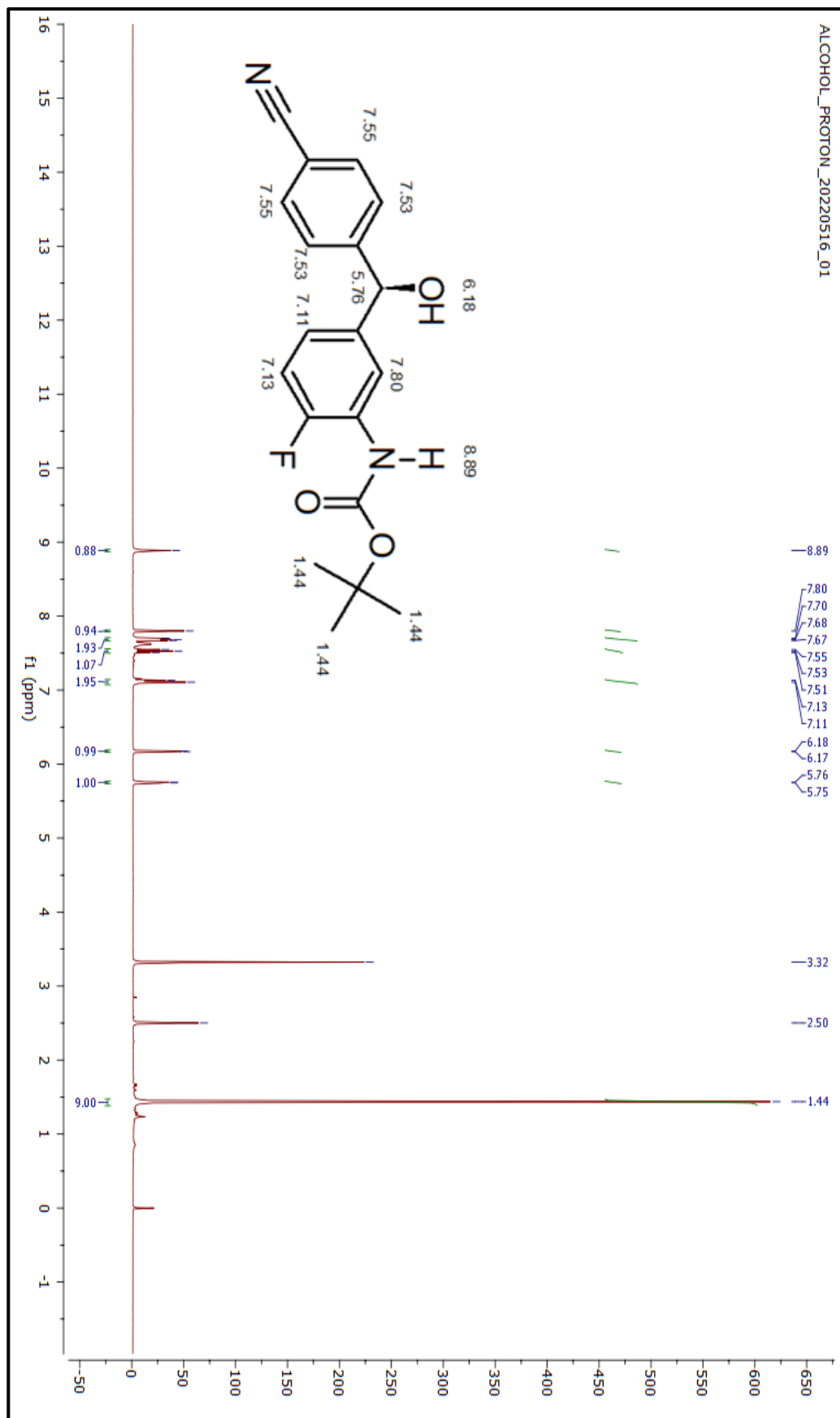


Figure 3.24 <sup>1</sup>H NMR in DMSO of tert-butyl {5-[(S)-(4-cyano phenyl)(hydroxy)methyl]-2-fluorophenyl}carbamate

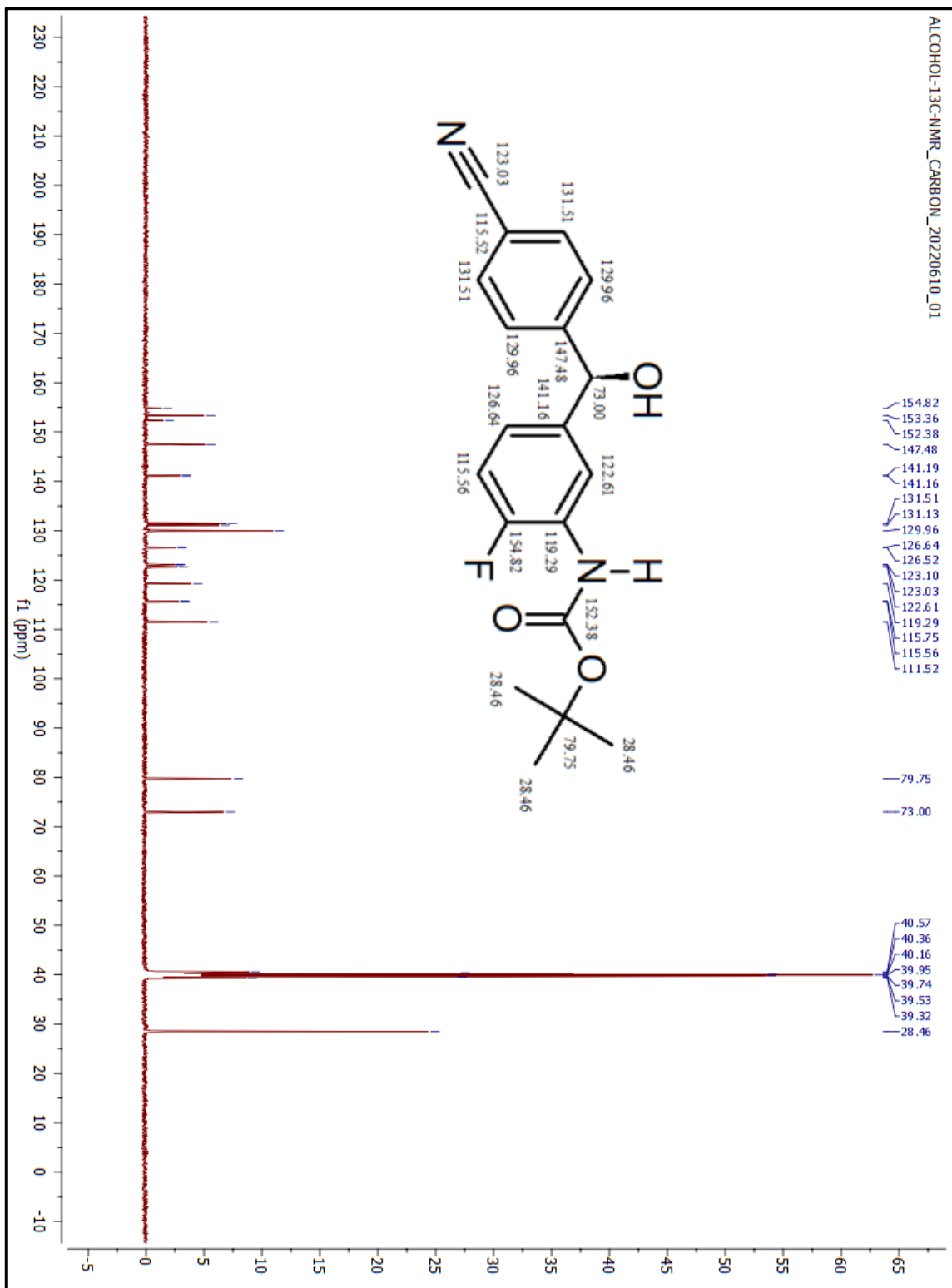


Figure 3.25  $^{13}\text{C}$  NMR in DMSO of tert-butyl {5-[(S)-(4-cyanophenyl) (hydroxy)methyl]-2-fluorophenyl}carbamate

The instrumental characterization of the formation of product and its data revealed it to be tert-butyl{5-[(4-cyanophenyl)(hydroxy)methyl]-2-fluorophenyl}carbamate

### 3.4 Conclusion

Ketoreductases from different sources were screened for reduction of tert-butyl[5-(4-cyanobenzoyl)-2-fluorophenyl]carbamate to tert-butyl{5-[(4-cyanophenyl)(hydroxy)methyl]-2-fluorophenyl}carbamate, and ES-KRED-213 was found to be the best one. The ES-KRED-213 gave best chiral selective reduction with 10% (V/V) dimethylsulfoxide as co-solvents, and had an optimum temperature 40°C, pH 7.0, 10% enzyme loading, and 100 g/L substrate loading as ambient parameter for maximum conversion in the said biotransformation reaction. The investigation of timely progress of reaction was performed on gram scale batches at different temperatures such as 30°C, 40°C, and 50°C, enzyme loading like 5%, 10%, 15% and 20%, and substrate loading 50g/L, 100g/L, and 150 g/L, and at optimal conditions (40°C, 10% enzyme loading, and 100 g/L substrate loading) conversion was 99.4%, and product formation of 4.90 g/50 mL. The actual product recovery after work-up was 4.17 g which corresponded to a product yield 85% with respect to the product formed after reaction. The purity of product formed with reverse phase HPLC was >99%, and the isomeric purity with normal phase HPLC was >99%. In addition, the finally recovered product was confirmed and characterized with HPLC analysis, specific optical rotation, melting point and boiling point, LC-MS, ATR-FTIR, <sup>1</sup>H NMR, and <sup>13</sup>C NMR. The confirmation of synthesized enantiomer of tert-butyl{5-[(4-cyanophenyl)(hydroxy)methyl]-2-fluorophenyl}carbamate needs to be performed with 2D NMR or single crystal characterization for better understanding of chiral nature.

## **CHAPTER-4**

# **SCREENING OF COMMERCIALY AVAILABLE TRANSAMINASES FOR THE CONVERSION OF 1-(3-METHYLPHENYL)ETHAN-1-ONE TO (1R)-(3-METHYLPHENYL)ETHAN-1-AMINE AND PROCESS OPTIMIZATION**



## Chapter 4

### 4.1 Introduction

(1*R*)-(3-methylphenyl)ethan-1-amine is an pivotal entity of different pharmaceutical drugs and a primary component in synthesis of therapeutics in different derivatized forms [101]. This includes (1*R*)-(3-methoxyphenyl)ethan-1-amine for Tecalcet hydrochloride which is an oral calcium receptor used for treatment of secondary hyperparathyroidism [102], (1*R*)-(1-naphthyl)ethanamine for Cinacalcet which helps to cure parathyroid carcinoma, tertiary hyperparathyroidism, and primary hyperparathyroidism [103], (*S*)- $\alpha$ -methylbenzylamines for Rivastigmine which is a cholinesterase inhibitor and most prominent drug for the curing of Alzheimer's and Parkinson's diseases during early stages [104], amongst many others. The enantiomerically pure 3-methylphenylethan-1-amine intermediates with  $-NH_2$  groups are generally synthesized by resolution of chiral acids with *p*-substituted 1-phenylethylamines by hydrogen phthalate or isopropylidene glycerol [105], diastereoselective reductive amination [106], transition metal mediated catalysis for asymmetric incorporation of organozinc species into imines [107], methyl lithium to chiral oxime ethers by nucleophilic additions [102], and many other methods documented in literature. In a recent review, [108] has explained different catalysts, route of synthesis, and the respective chemical approaches used for asymmetric amination of prochiral aldehydes and ketones to yield chiral and racemic amines used as active pharma ingredients.

The chemical amination/transamination approach is labor intensive, may need prevention of specific functional group, involvement of processing with harsh chemicals and conditions during its operation like acids and alkalis processing, discharge of toxic and hazardous waste, limited scope of substrate, and formation of a product with inferior quality, some impurities and reduced yield [52, 109, 110].

Now-a-days, biocatalysis based approach with transaminases have attracted the attention of researchers across globe as a greener opportunity to chemical route for direct transamination of pro-chiral aldehydes and ketones to amines precise enantiomeric selectivity (stereo-, chemo-, and regio-) of product [52, 111, 112]. Further, the chiral amines are predominantly used for bioactive natural products, agrochemicals, active pharmaceutical ingredients, and are vital pharmaceutical building entities. Due to this, there is a strategic interest in synthesis of chiral amines by development of biocatalytic strategies with wide acumen of applications [113]. For this, an array of enzymes has been practiced including different imine reductases, amine dehydrogenases, transaminases, monoamine oxidases, and ammonia lyases, and reductive aminases which have been discovered recently [114]. Transaminases with E.C. 2.6.1.X, generally termed as aminotransferases, are PLP (Pyridoxal-5-phosphate) dependent biocatalysts which are fold types I and IV family members, and predominantly involved in reversible shifting of -amino groups from designated donor to suitable -carbonyl acceptor [111, 115]. On account of synthesize chirally pure single enantiomer (either *R* or *S*), the transaminases have been employed for manufacturing of synthesis of an array of chiral synthons with commercial importance in food, pharma, and chemical sectors, and this has been broadly covered in recent reviews by [52, 116, 117]. The industrial vitality of transaminases can be apparently seen from the stats of accumulating number of research articles published and innovative patents filed by various industries and academia's, which highlights the methods, routes, and processes for synthesizing valuable intermediates and compounds.

For the application of transaminases and subsequent development of biotransformation process, the enzyme loading, substrate loading, reaction temperature, operating pH, agitation speed, time course of reaction, etc. are the

governing parameters. The optimization of these process variables could be performed by traditionally available approaches such as one factor at a time approach or statistical approach using response surface methodology (RSM) with different available designs [92]. Exploration of statistical optimization method has been a crucial area of focus owing to the bottlenecks in traditional optimization methods, like lack of information of the interactions effects that may occur amongst the operating parameters [118]. RSM is most frequently used statistical numerical approach that has been most commonly applied in various segments to optimize numerous sets of industrial processes [119]. Amongst the different designs available in RSM, the Box-Behnken and central composite designs are most frequently utilized due to requirement of fewer experiments to predict the associated response/s [120, 121]. Previously, BBD was used to optimize process for synthesis of glycinamides using proteases [122], biosynthesis of resveratrol from polydatin using  $\beta$ -glycosidase [123], conversion of red ginseng saponin to ginsenoside RB1 using enzyme viscoflow MG [124], synthesis of polyhydroxyalkanoates from Kraft lignin and lignosulfonate using microbial strain *Burkholderia* Sp. ISTR5 (R5) [125], amongst many others reported previously.

In the current research, we have used a systematic approach to synthesize chiral selective (1*R*)-(3-methylphenyl)ethan-1-amine *via* the transamination of 1-(3-methylphenyl) ethan-1-one using transaminase as a vital biocatalyst. Initially, different transaminases from various commercial suppliers were screened for desired bioconversion and the enzyme displaying best result was taken forward, followed by screening of different co-solvents. Subsequently, the optimization studies for development of process displaying maximum conversion with good product formation and higher yield was done with traditional approach such as one factor at a time and statistical approach such as Box Behnken RSM design approach using

enzyme loading, substrate loading, temperature, and pH as processing parameters. In addition, the recovered product was confirmed with different analytical techniques such as boiling point, LC-MS, <sup>1</sup>H NMR, and ATR-FTIR, along with RP-HPLC and chiral GC analyses. After this, ‘What If’ studies were also carried out by investigating timely progress of reaction on gram scale batches to check the effect of drastic change of process parameter on bioconversion process. According to the our knowledge and available information, the chiral selective transamination of 1-(3-methylphenyl)ethan-1-one to (1*R*)-(3-methylphenyl)ethan-1-amine using transaminases assisted approach, its process optimization, along with the ‘What If’ studies are being documented for the first time in literature.

## **4.2 Material and Methods**

### **4.2.1 Enzyme Screening for transamination of 1-(3-methylphenyl)ethan-1-one to (1*R*)-(3-methylphenyl)ethan-1-amine**

A total of 28 transaminases were screened for chiral selective transamination of 1-(3-methyl phenyl) ethan-1-one to (1*R*)-(3-methyl phenyl) ethan-1-amine. For this, transaminases enzyme (5 mg) was slowly dissolved in 0.9 mL of triethanolamine-hydrochloride buffers system with pH 8.5, 0.1 M possessing 1 M *iso*-propylamine and 2 mM pyridoxal-5-phosphate. To this, 1-(3-methylphenyl)ethan-1-one (10 mg mixed in 0.1 mL Dimethylsulfoxide) was mixed and the final reaction combination obtained was incubated on a static thermomixer for 24 hours at 45±2<sup>0</sup>C and 600-700 rotations per minute. The work up of the said biocatalytic reaction was performed with a procedure thoroughly explained by [126]. The collected organic layers were analysed for conversion on reverse phase HPLC and chiral purity on chiral GC.

### **4.2.2 Screening of co-solvents**

The influence of incorporation of various co-solvents namely dimethylsulfoxide, *iso*-propanol, *N, N*-dimethylformamide, methanol, ethanol and *tertiary*-butanol for the

chiral selective transamination of 1-(3-methylphenyl)ethan-1-one to (1*R*)-(3-methylphenyl) ethan-1-amine was determined at 10% volume in the triethanolamine-HCl buffer system (pH 8.5, 100 mM) possessing 1 M *iso*-propylamine and 2 mM pyridoxal-5-phosphate buffer with 10% transaminase (ATA-025). The 1-(3-methylphenyl)ethan-1-one was firstly dissolved in co-solvent, followed by addition to the reaction mass, and then enforcement at  $45\pm 2^{\circ}\text{C}$  and 600-700 rotations per minute for 24 hours.

#### **4.2.3 Optimization of process parameters**

The variables governing transamination of 1-(3-methylphenyl)ethan-1-one to (1*R*)-(3-methylphenyl)ethan-1-amine namely enzyme loading, substrate loading, operating pH, and temperature were improved with both approaches namely one-factor-at-a-time approach and statistical application using Box Behnken pattern of RSM.

##### **4.2.3.1 One factor at a time application**

The reaction mass containing 90 mL triethanolamine-hydrochloride buffer system with pH 8.5, and 0.1 M possessing 1 M *iso*-propylamine and 2 mM pyridoxal-5-phosphate, with transaminases (ATA-025), and substrate dissolved in 10 mL DMSO, followed by incubation at ambient temperature and pH conditions under continuous stirring at 250-280 rpm. The process parameters for transamination of 1-(3-methylphenyl)ethan-1-one to (1*R*)-(3-methylphenyl)ethan-1-amine such as enzyme loading (2.5, 5.0, 7.5, 10, 12.5 and 15%), substrate loading (25, 50, 75 and 100 g/L), temperature (30, 35, 40, 45, 50 and  $55^{\circ}\text{C}$ ) and operating pH (6.5, 7.0, 7.5, 8.0, 8.5, 9.0 and 9.5) were optimized one by one for maximum possible conversion. The product formed (g/L), product obtained (g/L), theoretical yield (%) and actual yield (%) were also enumerated.

#### 4.2.3.2 Statistical application using central composite pattern

The Box Behnken pattern of RSM with four non-dependent variables namely enzyme loading (EL, %), substrate loading (SL, g/L), temperature (T, °C) and operating pH (P) were used to achieve maximum conversion (%) and yield (%). A quadratic polynomial model was established by regression analysis for R as the responses for conversion (%) and yield (%), and represented as:

$$R = \beta_0 + \beta_1A + \beta_2B + \beta_3C + \beta_4D + \beta_5A^2 + \beta_6B^2 + \beta_7C^2 + \beta_8D^2 + \beta_9AB + \beta_{10}AC + \beta_{11}AD + \beta_{12}BC + \beta_{13}BD + \beta_{14}CD$$

Where R is the response for conversion (%) and yield (%),  $\beta_0$  to  $\beta_{14}$  signifies the regression coefficients, whereas A, B, C and D indicates the without dimension coded values for enzyme loading (EL, %), substrate loading (SL, g/L), temperature (T, °C) and operating pH (P), respectively (*Table 4.1*).

*Table 4.1 Experimental range levels of parameters for chiral selective transamination of 1-(3-methylphenyl)ethan-1-one to (1R)-(3-methylphenyl)ethan-1-amine*

Variable	Symbol	Coded factor levels		
		Low limit	Mid limit	Upper level
Enzyme loading (EL, %)	A	5	10	15
Substrate loading (SL, g/L)	B	25	50	75
Temperature (T, °C)	C	35	45	55
Operating pH (P)	D	6.5	8	9.5

The real values in the polynomial model were represented as coded values to express the comparative significance of each transamination parameter involved in the process and associated terms namely linear, interaction, and quadratic affects the respective response.

$$A = \left( \frac{EL - 10}{5} \right)$$

$$B = \left( \frac{SL - 50}{25} \right)$$

$$C = \left( \frac{T - 45}{10} \right)$$

$$D = \left( \frac{P - 8}{1.5} \right)$$

After the Box Behnken Design of RSM, a set of 29 experimental runs were performed by considering conversion (%) and yield (%) as responses. The interaction effect amongst the associated independent parameters namely enzyme loading (EL, %), substrate loading (SL, g/L), temperature (T, °C) and operating pH (P) on the conversion (R1) and yield (R2) as two responses after transamination reaction, and were assessed with four mathematical models namely linear model, quadratic model, polynomial model, and the cubic model, and the ideal fit was taken into account on the basis of high R<sup>2</sup>, and adjusted R<sup>2</sup> values, respectively.

On the basis of numerical optimization, the desirability function (D) was enumerated to determine the optimal point by combining all the process parameters namely enzyme loading (EL, %), substrate loading (SL, g/L), temperature (T, °C) and operating pH (P). It was performed to attain the highest possible overall desirability value as

$$\text{Overall desirability (D)} = (d_1^{r_1} \times d_2^{r_2} \times d_3^{r_3} \times d_4^{r_4} \times d_5^{r_5} \times d_6^{r_6})^{\left( \frac{1}{r_1+r_2+r_3+r_4+r_5+r_6} \right)}$$

This mentioned equation comprises of desirability values ( $d_i$ ) for every attribute associated with the reaction, and also includes linked factors and response ( $d_1$  till  $d_i$ ) together with their respective relative importance's ( $r_1$  to  $r_i$ ) on the 1 to 5 scale, respectively.

#### **4.2.4 Instrumental characterization**

The assessment of transamination of 1-(3-methylphenyl)ethan-1-one to (1*R*)-(3-methylphenyl)ethan-1-amine was done by enumeration of conversion (%) on reverse phase HPLC and chiral purity with chiral GC.

##### **4.2.4.1 Reverse phase HPLC**

The samples were diluted with acetonitrile: water (20:80 V/V) to make up the final concentration of sample 0.25 mg/mL, followed by removal of any turbidity (if any) by filtration from 0.45  $\mu$ m filter, and determination on C18 column using HPLC system. The HPLC conditions were 10  $\mu$ L injection volume,  $40 \pm 2^\circ\text{C}$  column temperature with flow rate of 1 mL/min, and detected at 210 nm, and a total run time of 25 min. The mobile phase used for analysis of conversion (%) contained 0.1% TFA in water as mobile phase A and acetonitrile as mobile phase B which was processed in gradient mode (time: 0.01 min, A=80 and B=20; 10 min, A= 40 and B= 60; 15 min, A= 20 and B= 80; 20 min, A= 20 and B= 80; and 25 min, A= 20 and B= 80).

##### **4.2.4.2 Chiral analysis by GC**

The chiral purity of isolated (1*R*)-(3-methylphenyl)ethan-1-amine was enumerated with GC on chiral column using GC system (Shimadzu LC-2030C 3D plus, Japan). Conditions at injector were - temperature:  $250^\circ\text{C}$ , split: 100:1, flow: 1.4 mL/min; Conditions at column oven were – temperature flow: $80^\circ\text{C}$  for 3 min,  $130^\circ\text{C}$  for 5 min.,  $200^\circ\text{C}$  for 0 min, total time-31.6 min; Conditions at detector (FID) were - temperature:  $300^\circ\text{C}$ ,  $\text{N}_2$  - 25mL/min,  $\text{H}_2$  - 30mL/min, and Air - 300mL/min.



#### **4.2.4.3 Confirmation and characterization of 1-(3-methylphenyl)ethan-1-one to (1R)-(3-methylphenyl)ethan-1-amine**

The characterization and confirmation of final recovered and purified product [(1R)-(3-methylphenyl)ethan-1-amine] and initial substrate [1-(3-methylphenyl)ethan-1-one] were done by HPLC, chiral purity with GC, melting point, ATR-FTIR, LC-MS and <sup>1</sup>H NMR. The melting point of 1-(3-methylphenyl)ethan-1-one and (1R)-(3-methylphenyl)ethan-1-amine was analysed on Digital Melting Point Apparatus (Labline, Mumbai, India). The unique, functional, characteristic, and structurally associated moieties in substrate and product were recorded on ATR-FTIR. LC-MS of both substrate and purified product was carried out on C18 column by using the same mobile phase as for RP-HPLC. The direct mass of both the compounds were seen with mass split of LCMS system. The number of protons present in both substrate and purified product were calculated by <sup>1</sup>H NMR by uniform dissolution in DMSO.

#### **4.2.5 Time course reactions on gram scale**

The ‘What If’ studies were performed by setting up biotransformation reactions on gram scale and analysing the periodic progress of transamination reaction by determining the conversion (%) after drastic change of process parameter. The major deviation was made from the optimal point by suddenly increasing and decreasing values of process parameter. The studies were performed by varying the enzyme loading (5%, 10% and 15%), substrate loading (25g/L, 50g/L, and 75g/L), temperature (35<sup>0</sup>C, 45<sup>0</sup>C, and 55<sup>0</sup>C) and medium pH (6.5, 8.0, and 9.5). In a reaction flask, 90 mL triethanolamine-HCl buffer (100 mM) possessing 1 M *iso*-propylamine and 2 mM pyridoxal-5-phosphate, and enzyme (ATA-025) were mixed, and incubated at 240-260 rpm. The conversion of 1-(3-methylphenyl)ethan-1-one to (1R)-(3-methylphenyl)ethan-1-amine was monitored periodically with HPLC. The

acetone generated during the advancement of transamination reaction was withdrawn by application of intermittent vacuum. After 24 h the reaction was stopped by reducing the pH up to 2.5-2.0 with 4 M HCl followed by addition of 10 g Hyflo powder (Celite 535) in the reaction mixture, stirring for 30 min, and filtration from Hyflo bed prepared on Whatman filter paper no. 42, and then Hyflo cake generated was washed with hot ethylacetate (45-50<sup>0</sup>C). The organic layer from the collected filtrate was recovered to remove any starting material using a separating funnel. After this, the pH of aqueous layer was increased up to 12-12.5 with 40% NaOH solution and then extracted in *iso*-propylacetate (40 mL × 3). The organic layers combined together were then given bicarbonate wash (10% sodium bicarbonate), brine wash (20% NaCl solution), water wash, activated carbon treatment (55-60<sup>0</sup>C for 0.5-1.0 h), and filtered through Hyflo bed and the filtrate was treated with sodium sulphate to remove traces of moisture, and finally distilled on rotary evaporator at 50-55<sup>0</sup>C under vacuum, and the product formed (g/L), product obtained (g/L), theoretical yield (%) and actual yield (%) were also estimated.

#### **4.2.6 Statistical analysis**

All the experiments in the present study were performed three times and the acquired findings are expressed as average ± standard errors. The observed data was processed and explored on Microsoft Excel, 2013, and SPSS Version16 by operating one way ANOVA to evaluate the differences in mean and statistically noteworthy differences amongst the achieved average values confirmed at a confidence interval of 95% and Dunnett's post hoc test.

### 4.3 Result and discussion

#### 4.3.1 Screening of transaminases for transamination of 1-(3-methylphenyl)ethan-1-one to (1R)-(3-methylphenyl)ethan-1-amine

The transamination of 1-(3-methylphenyl)ethan-1-one to (1R)-(3-methylphenyl)ethan-1-amine was performed with enzyme assisted route using transaminases to tackle the major issues associated with chemical route of synthesis. The chemical processes include harsh processing with acids and bases which have corrosive nature, protection of functional groups, treatment with high temperatures, discharge of toxic compounds generated during process, amongst many others and which may eventually cause reduction in purity, yield and productivity [67, 69]. The enzyme mediated route follows metal free conditions and uses mild reaction conditions which are generally safe and lead to higher specificity, generation of considerably lower by-product, nominal requirement of energy, and multiple others benefits documented in earlier text [80, 111].

In the said study, we have screened 28 different transaminases from Codexis for transamination of 1-(3-methylphenyl)ethan-1-one to (1R)-(3-methylphenyl)ethan-1-amine at 50% enzyme loading and DMSO (10% V/V) as a co-solvent for proper dissolution of substrate in triethanolamine-HCl buffer system with 0.1 M pH 8.5. Screening of enzymes is a pre-requisite for any biotransformation reaction and process, as it is an entry point for identification of the best hit (potential enzyme) for higher conversion with required enantiomer [127]. The route of synthesis of this enzymatic transamination reaction as a schematic representation with DMSO as co-solvent is represented in *figure 4.1*

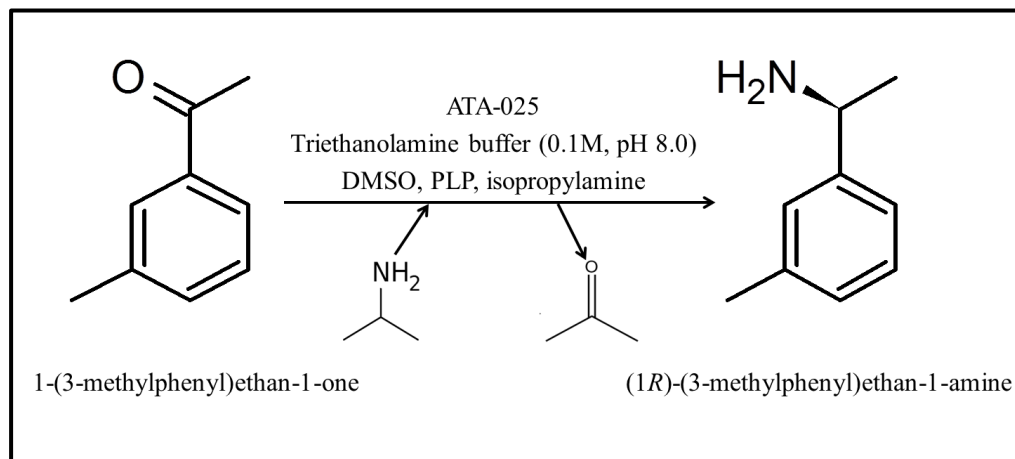


Figure 4.1 Route of synthesis for Chiral selective transamination of (1R)-(3-methyl phenyl) ethan-1-amine from 1-(3-methyl phenyl) ethan-1-one

Amongst the different transaminases from Codexis screened for transamination of 1-(3-methylphenyl)ethan-1-one to (1R)-(3-methylphenyl)ethan-1-amine, ATA-025, ATA-024, ATA-251, ATA-237, ATA-033, ATA-013, ATA-234, and ATA-415 have shown distinct conversion of 60.51%, 55.92%, 50.50%, 48.66%, 42.67%, 35.68%, 32.76%, and 24.89%, and chiral selectivity of  $\geq 98.5\%$ , respectively (table 4.2). ATA-237 and ATA-257 have shown formation of 'S-' enantiomer, while others have displayed formation of 'R-' enantiomer. Rest of the transaminases used for screening, namely ATA-200, ATA-238, ATA-254, ATA-256, ATA-260, ATA-303, ATA-412, ATA-P1-B04, ATA-P2-A01, ATA-P2-B01, ATA-007, ATA-113, ATA-117, ATA-217, ATA-301, ATA-P1-F03, ATA-P1-G05, ATA-P2-A07, ATA-P1-A06, and ATA-P1-G06 have displayed very less ( $\leq 10\%$ ) or negligible conversion during this transamination reaction.

Table 4.2 Transaminase screening screening for transamination of 1-(3-methyl phenyl)ethan-1-one to (1R)-(3-methyl phenyl)ethan-1-amine

Sr. No.	Enzyme	Conversion (%)	R-Isomer	S-Isomer
1	ATA-237	48.66		≥98.5%
2	ATA-234	32.76	≥98.5%	
3	ATA-251	50.50		≥98.5%
4	ATA-415	24.89	≥98.5%	
5	ATA-013	35.68	≥98.5%	
6	ATA-025	60.51	≥98.5%	
7	ATA-024	55.92	≥98.5%	
8	ATA-033	42.67	≥98.5%	

**Reaction conditions:** 10 mg Substrate (10 g/L, 10 mg mixed in 100  $\mu$ L DMSO), 5 mg enzyme (50% loading), 900  $\mu$ L of triethanolamine buffer (pH 8.5, 100 mM) containing 1 M iso-propylamine and 2 mM pyridoxal-5-phosphate,  $45\pm 2^{\circ}$ C and 600-700 rpm. Conversion was assessed by HPLC, and chiral analysis by GC.

Some transaminases have shown maximum conversion, while some displayed minimal, and this might be assumed specificity of experimental substrate towards the active catalytic site in enzyme structure [128]. The slight alterations in organization of amino acids in active domain, and structure and nature of substrate are other vital parameters that govern the specificity of enzymes [52]. Further, the structural

conformation of active cleft and co-enzyme binding region, and composition and length of amino acids in loops are other major factors that adds on to the altering substrate specificity of the different transaminases [115].

Amongst the numerous transaminases from Codexis screened, ATA-025 was considered as a suitable biocatalyst in transamination of 1-(3-methylphenyl)ethan-1-one to (1*R*)-(3-methylphenyl)ethan-1-amine for further process optimization, product characterization, and ‘What If’ studies, due of its potential of maximum conversion (%) and formation of desired ‘*R*-’ enantiomer.

#### **4.3.2 Screening of co-solvents**

The influence of different co-solvents on transamination of 1-(3-methylphenyl)ethan-1-one to (1*R*)-(3-methylphenyl)ethan-1-amine with ATA-025 was analysed to assess the best suitable co-solvent for protocol optimization and scale-up studies, and further enhance the practical acumen of developed process. Co-solvents namely dimethylsulfoxide, *iso*-propanol, *N,N*-dimethylformamide, *t*-butanol, methanol, and ethanol which are generally used were screened at 10% (V/V) to enumerate the enhancement in conversion (%) of product (*figure 4.2*)

Screening of co-solvents is a primary requirement for biocatalytic processes, as these added co-solvents have been reported to have a role in altering the enantioselectivity of products [129]. In addition, these co-solvents may interact with the hydration layer around the vicinity of enzyme, change the 3D conformation, reduce the strength of electrostatic interactions, reduce the accessible surface area to substrate, minimize stability, and eventually the enzyme performance, and product formation [92, 130]. Furthermore, they could also aid in easing up the post reaction processing and work-up and subsequently making the product recovery hassle-free [131].

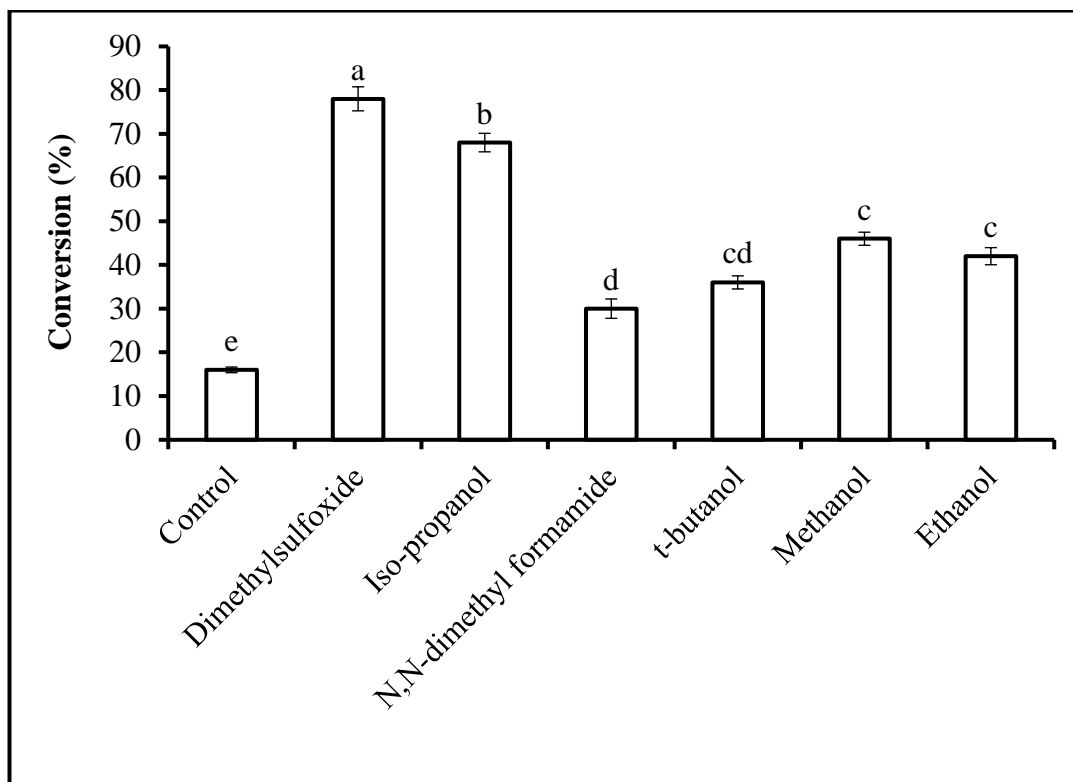


Figure 4.2 Effect of of co-solvents on chiral selective transamination of (1R)-(3-methyl phenyl) ethan-1-amine from 1-(3-methyl phenyl) ethan-1-one

During transamination of 1-(3-methylphenyl)ethan-1-one to (1R)-(3-methylphenyl) ethan-1-amine with ATA-025, a higher and lower conversion of  $78 \pm 2.75\%$  and  $30 \pm 2.21\%$  was observed with dimethylsulfoxide and *N,N*-dimethylformamide with an actual yield of  $59.76 \pm 1.15\%$ , and  $23.52 \pm 0.81$ , respectively, and these were considerably superior over the control which displayed  $16 \pm 0.65\%$  conversion and  $12.42 \pm 0.21\%$  yield. DMSO was observed to be a desired co-solvent during transamination mediated synthesis of 1-(3',4'-disubstituted phenyl) propan-2-amines [131], (*S*)-1-(5-fluoropyrimidin-2-yl)-ethanamine [132], (*R*)-3-amino-1-Boc-piperidine [126], Benzylamine derivatives [133], Sitagliptin intermediates [134], among many others documented in literature.

### 4.3.3 Optimization of process parameters

The transamination of 1-(3-methylphenyl)ethan-1-one to (1*R*)-(3-methylphenyl)ethan-1-amine was revolutionized by two approaches *viz.* the traditional approach using 1 factor at a time, and statistical approach of numeric optimization using Box Behnken Design of RSM. Amongst the numerous process parameters linked with transamination, enzyme loading (%), substrate loading (g/L), temperature (°C) and operating pH were taken into account for transamination of 1-(3-methyl phenyl) ethan-1-one to (1*R*)-(3-methyl phenyl) ethan-1-amine with ATA-025 as biocatalyst and DMSO (10% V/V) as co-solvent.

#### 4.3.3.1 1 factor at a time approach

The transamination of 1-(3-methylphenyl)ethan-1-one to (1*R*)-(3-methylphenyl)ethan-1-amine was directly associated with the enzyme loading. For the commercial practicability of biocatalytic operation, the optimization of enzyme loading (%) required for enzymatic biotransformation is must due to direct association of enzyme cost with the process [127]. The enzyme loading (%) range of 2.5% to 15% with an incubation duration of 24 h was considered for transamination, and statistically considerable differences ( $p < 5\%$ ) were observed (*figure 4.3*).



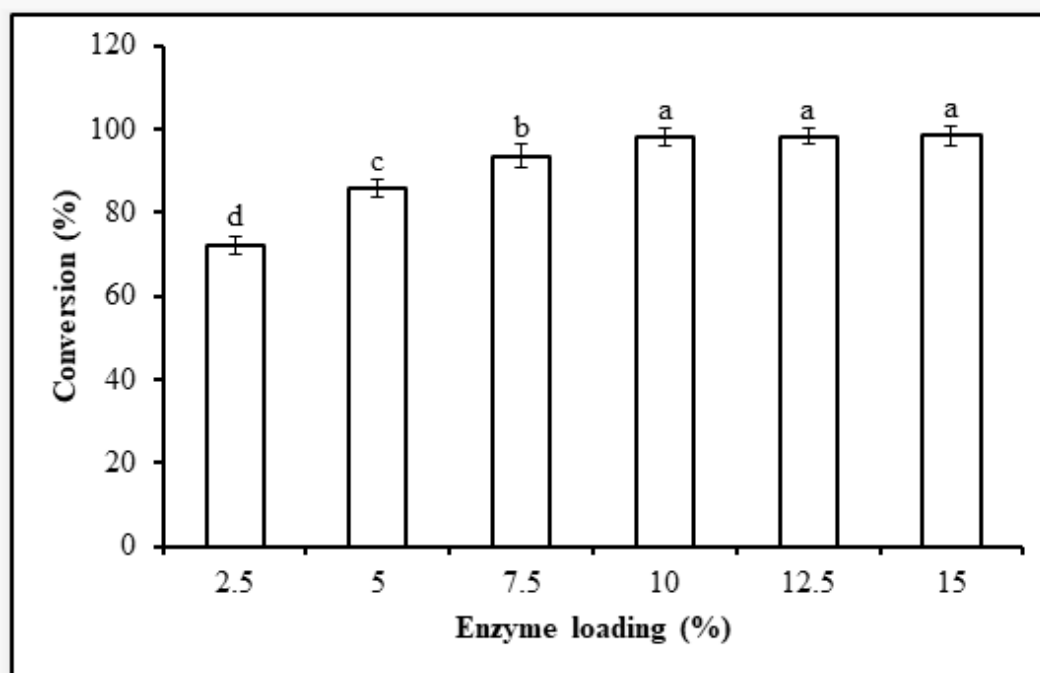


Figure 4.3 Influence of enzyme loading on chiral selective transamination of 1-(3-methylphenyl)ethan-1-one to (1R)-(3-methylphenyl)ethan-1-amine

A maximum conversion ( $98.30 \pm 2.51\%$ ) with more than  $\geq 98.5\%$  chiral selectivity of (1R)-(3-methylphenyl)ethan-1-amine was observed at enzyme loading above 10%, and the actual yield was  $78.1 \pm 0.58\%$ . At lower loading of transaminases ( $< 7.5\%$ ), the enzyme may be deficient to transform 1-(3-methylphenyl)ethan-1-one to (1R)-(3-methylphenyl) ethan-1-amine due to occupancy of active site with substrate. Additionally, at higher loading percentage ( $> 10\%$ ) of ATA-025 the conversion was approximately similar.

For a reaction to be driven actively, the incorporation of substrate in proper concentration must be considered along with the enzyme loading. The optimization of substrate loading was carried out in a range of 25g/L to 100g/L with an enzyme loading of 10% and an incubation period 24 h. There was a considerable variation ( $p \leq 5\%$ ) in conversion (%) at each studied substrate loading and a reduction in

conversion (%) of substrate was observed with an increase in substrate loading above 50 g/L (figure 4.4).

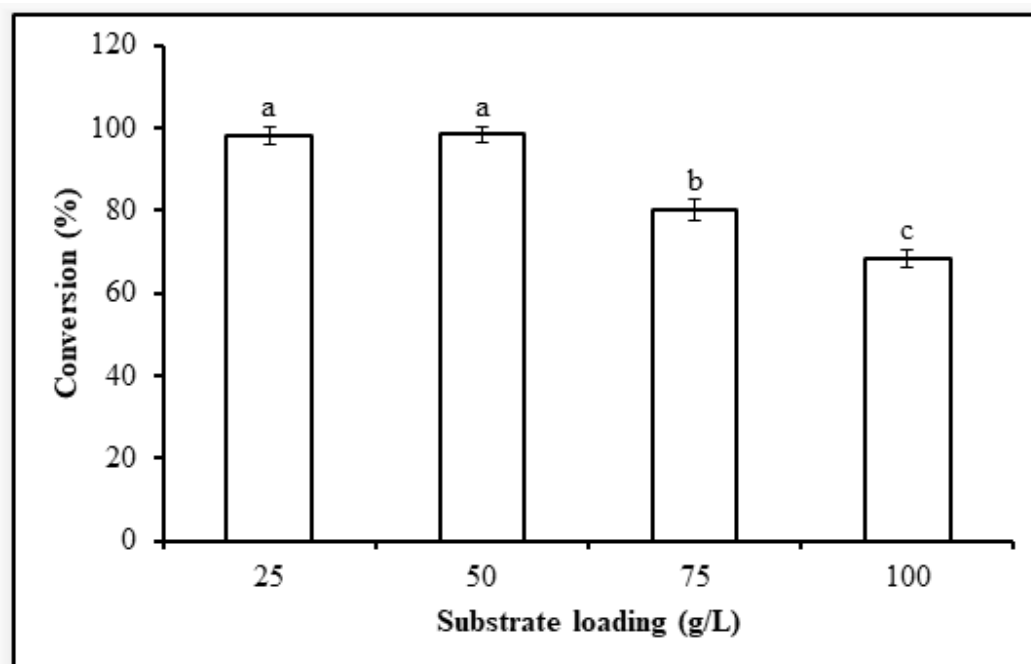
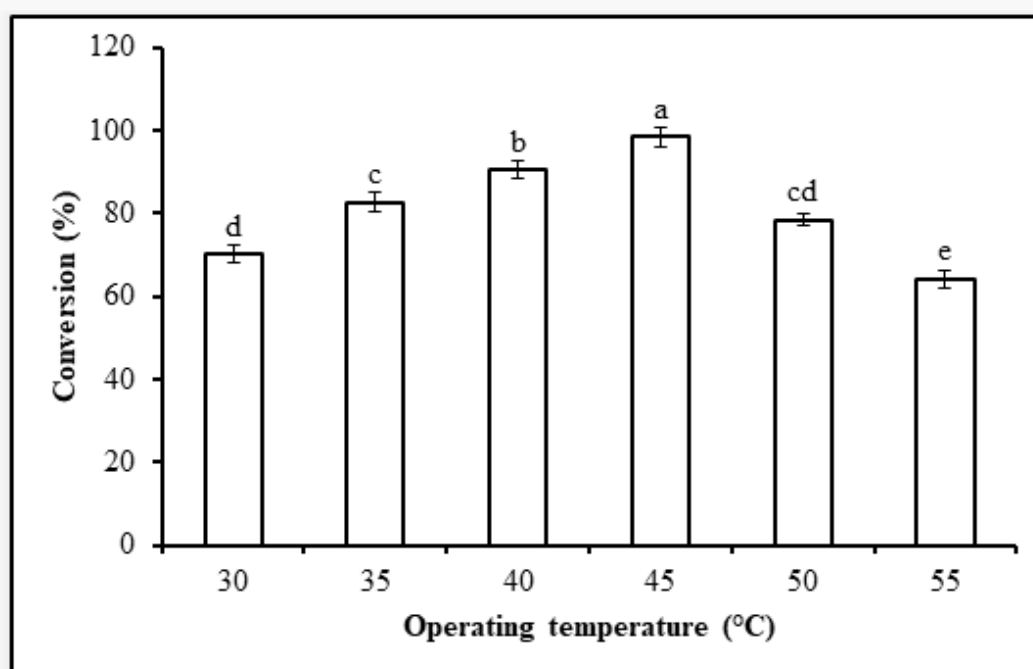


Figure 4.4 Influence of substrate loading on chiral selective transamination of 1-(3-methylphenyl)ethan-1-one to (1R)-(3-methylphenyl)ethan-1-amine

Maximum conversion ( $98.31 \pm 1.87\%$ ) with a chiral purity of  $\geq 98.5\%$  and actual yield of  $78.30 \pm 0.47\%$  of (1R)-(3-methylphenyl)ethan-1-amine was seen at 50 g/L substrate loading and 10% ATA-025 enzyme loading. With higher substrate loading, there is an increase in overall viscosity of reaction medium causing prominent depletion in the mass transfer of substrate towards active catalytic domain of enzyme [127, 135].

After the enzyme loading and substrate loading, the optimization of incubation temperature was carried out, as it is a critical variable for the biotransformation reactions due to its direct influence on activity, stability, and positive performance of biocatalyst [136]. Further, the solubility of product and substrate, rate of reaction and its kinetics are directly administered by it [137, 138]. The consequences of

incubation temperature was estimated in a temperature regime of 30°C-55°C at 10% enzyme loading, 50 g/L substrate loading for 24 h (*figure 4.5*).



*Figure 4.5 Influence of operating temperature on chiral selective transamination of 1-(3-methylphenyl)ethan-1-one to (1R)-(3-methylphenyl)ethan-1-amine*

There was a maximum conversion of  $98.33 \pm 2.20\%$  with a chiral purity of  $\geq 98.5\%$  and actual yield of  $77.30 \pm 0.55\%$  at  $45 \pm 2^\circ\text{C}$ , and statistically considerable differences ( $p \leq 5\%$ ) were observed at each studied temperature during transamination of 1-(3-methylphenyl)ethan-1-one to (1R)-(3-methylphenyl)ethan-1-amine with ATA-025. There was a prominent reduction in conversion above  $50^\circ\text{C}$  and below  $40^\circ\text{C}$ , and this could be attributed to reduction in catalytic performance of ATA-025 due to either thermal inactivation or availability of less energy for enzyme activation [92, 138]. The values of present optimal temperature domain are in close proximate with earlier findings in literature by [131, 132, 134, 137, 139], wherein the optimum temperature for synthesis of (*S*)-4-phenyl-butanamine, (*S*)-1-(5-Fluoropyrimidin-2-yl)-ethanamine, (*R*)-1-phenyl propan-2-amine, 4*R*)-amino-4-phenylbutanoic acid

(chiral sitagliptin intermediate), and 1-BOC-(3*R*)-aminopiperidine, was 50°C, 38°C, 30°C, 37°C, and 30°C, respectively.

Along with temperature, reaction mixture pH has an astonishing impact on performance, specific activity, and chiral selectivity of enzymes [140]. This plays a pivotal function in not only maintaining the electrostatic interactions among substrate and enzyme, and the surface charge of enzyme, but also the solubility of substrate and enzyme [141]. The continuous incubation at 45±2°C causes a decline in pH due to evaporation of *iso*-propylamine from the medium, and therefore pH value was compensated by automatic addition of 4M *iso*-propylamine on a pH stat [142]. The optimization of pH was carried out in a regime of 6.5 to 9.5 at 10% enzyme loading, 50 g/L substrate loading and an incubation temperature of 45±2°C for 24 h. Maximum conversion (98.23±2.31%) with a chiral selectivity of ≥98.5% and an actual product yield of 77.24±0.51% was recorded at pH 8.0 and considerably noticeable differences were observed different pH values (*figure 4.6*)

The values of optimal pH are closely associated with previous reports by [126, 131, 134, 135] wherein the optimum pH was 7.5, 8.0, 8.0 and 7.5 for synthesis of 1-BOC-3-aminopiperidine, (*S*)-1-phenoxypropan-2-amine, (*4R*)-amino-4-phenylbutanoic acid (chiral sitagliptin intermediate), (*R*)-1-phenylpropan-2-amine, respectively. The slight variation in pH values may be due to differences in strength and composition of buffer used, along with other incubation conditions and amine donors used.

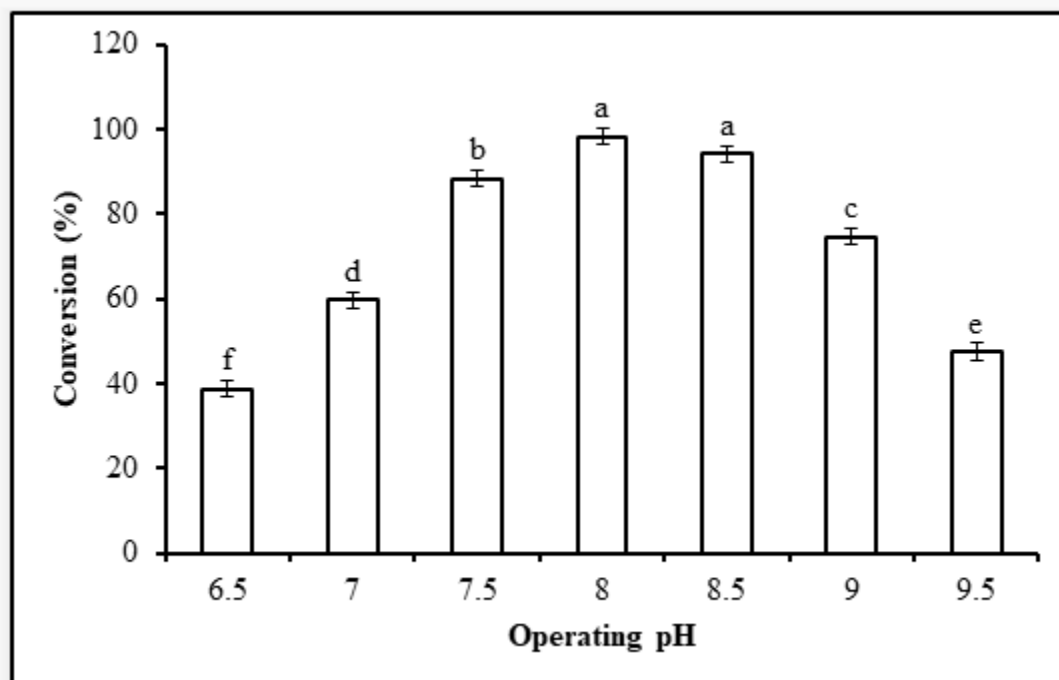


Figure 4.6 Influence of medium pH on chiral selective transamination of 1-(3-methylphenyl) ethan-1-one to (1R)-(3-methylphenyl)ethan-1-amine

The optimum parameters for the transamination of 1-(3-methylphenyl)ethan-1-one to (1R)-(3-methylphenyl)ethan-1-amine with the approach of one factor at a time were 10% ATA-025 loading, 50 g/L substrate loading,  $45\pm 2^\circ\text{C}$  and a pH of 8 yielding  $99.02\pm 2.61\%$  conversion and an actual yield of  $76.85\pm 1.01\%$ . The effect of transamination parameters on conversion, product formation, product recovery, and yield after the chiral selective transamination of 1-(3-methylphenyl)ethan-1-one to (1R)-(3-methylphenyl)ethan-1-amine is displayed in table 4.3

Table 4.2 Effect of transamination parameters on conversion, product formation, product recovery, and yield after of chiral selective transamination of 1-(3-methylphenyl)ethan-1-one to (1R)-(3-methylphenyl)ethan-1-amine

Parameter		Product formed (g/L)	Product obtained (g/L)	Theoretical yield (%)	Actual yield (%)
Enzyme loading (%)	2.5	3.639±0.112	2.838±0.90	72.77±0.63	56.76±0.56
	5.0	4.323±0.113	3.372±0.91	86.46±0.65	67.44±0.56
	7.5	4.714±0.135	3.724±1.07	94.29±0.75	74.48±0.67
	10.0	4.945±0.115	3.905±0.93	98.90±0.96	78.10±0.58
	12.5	4.946±0.094	3.858±0.75	98.91±0.53	77.16±0.47
	15.0	4.955±0.127	3.864±1.01	99.11±0.71	77.28±0.63
Substrate loading (g/L)	25	2.476±0.054	1.933±0.43	99.04±0.30	77.32±0.26
	50	4.956±0.094	3.915±0.75	99.12±0.53	78.3±0.47
	75	6.066±0.200	4.974±1.01	80.88±1.12	66.32±0.1.04
	100	6.901±0.195	5.660±0.98	69.01±1.07	56.6±0.999
Temperature (°C)	30	3.535±0.103	2.757±0.83	70.70±0.58	55.14±0.51
	35	4.165±0.116	3.165±0.93	83.31±0.65	63.30±0.59
	40	4.561±0.111	3.603±0.89	91.22±0.62	72.06±0.55
	45	4.951±0.111	3.865±0.89	99.03±0.62	77.30±0.55
	50	3.955±0.072	3.085±0.57	79.09±0.41	61.70±0.34
	55	3.234±0.113	2.460±0.91	64.68±0.64	49.20±.58

	6.5	1.950±0.092	1.483±0.73	39.00±0.51	29.66±0.46
	7.0	3.005±0.094	2.345±0.75	60.11±0.59	46.90±0.49
	7.5	4.450±0.096	3.516±0.77	88.99±0.54	70.32±0.48
pH	8.0	4.952±0.101	3.862±0.81	99.04±0.57	77.24±0.50
	8.5	4.746±0.099	3.703±0.80	94.91±0.56	74.06±0.49
	9.0	3.759±0.101	2.933±0.81	75.18±0.58	58.66±0.50
	9.5	2.395±0.108	1.796±0.86	47.90±0.61	35.92±0.54

1 factor at a time is schematic and simple method for optimizing a process but it doesn't reveals the assessment of interactions that may exist between the operation variables [121]. Herein, the gathered data from the 1 factor at a time process was utilized as a primary and raw data to design the experiments in Box Behnken Design on the basis of conversion (%) and yield (%) as the linked responses. The levels of experiments for each parameter to be utilized in Box Behnken Design were proposed based on the primary trials of one factor at a time.

#### 4.3.3.2 Statistical approach using Box Behnken Design

A Box Behnken Design with four variables *viz.* enzyme loading (%), substrate loading (g/L), temperature (°C) and operating pH was employed to achieve maximum substrate conversion (%) and actual yield (%). A total of 29 experimental set were run, proposed by Box Behnken Design for each transamination parameter and this consisted of linear, interaction, and quadratic term. The transamination was counted in terms of conversion of 1-(3-methylphenyl)ethan-1-one to (1R)-(3-

methylphenyl)ethan-1-amine and the process parameters (EL, SL, T and P) had a significant influence on it (*table 4.4*)

The interactions between the process variables namely enzyme loading (A), substrate loading (B), temperature (C), and pH (D), against two responses namely (R1) conversion (%) and (R2) yield (%) were estimated by using all the three models namely linear model, quadratic polynomials model, and cubic model, appropriately. The compatibility of these models was set by analysing their abilities to predict data under all the non-experimental and experimental conditions with minimal deviation, cooperatively with desired and significant *F*-value and *p*-value, respectively [118].

*Table 4.3 Combined transformation parameters according to Box Behnken design and the corresponding response as enzymatic conversion (%) and yield (%) in chiral selective transamination of 1-(3-methylphenyl)ethan-1-one to (1R)-(3-methylphenyl)ethan-1-amine*

Run	Enzyme loading (A, %)	Substrate loading (B, g/L)	Temperature (C, °C)	pH (D)	Conversion (R1, %)	Yield (R2, %)
1	5	25	45	8	94.20±0.23	71.23±0.48
2	15	25	45	8	98.40±0.15	75.40±0.36
3	5	75	45	8	66.81±.17	51.18±0.41
4	15	75	45	8	84.30±0.23	64.59±0.50
5	10	50	35	6.5	60.10±0.30	46.05±0.52
6	10	50	55	6.5	42.84±0.35	33.34±0.74



7	10	50	35	9.5	70.20±0.42	53.79±0.68
8	10	50	55	9.5	53.40±0.32	40.92±0.64
9	5	50	45	6.5	65.81±0.29	50.42±0.62
10	15	50	45	6.5	67.90±0.58	52.03±0.89
11	5	50	45	9.5	69.10±0.38	52.95±0.76
12	15	50	45	9.5	82.90±0.26	63.52±0.61
13	10	25	35	8	90.30±0.28	69.19±0.47
14	10	75	35	8	68.92±0.31	53.78±0.68
15	10	25	55	8	63.80±0.25	48.89±0.58
16	10	75	55	8	53.90±0.35	41.30±0.78
17	5	50	35	8	78.20±0.59	59.91±0.98
18	15	50	35	8	95.40±0.56	73.09±0.92
19	5	50	55	8	66.81±0.19	49.44±0.41
20	15	50	55	8	70.08±0.41	53.70±0.85
21	10	25	45	6.5	54.64±0.19	40.38±0.46
22	10	75	45	6.5	50.50±0.23	38.69±0.53
23	10	25	45	9.5	79.53±0.28	60.94±0.57
24	10	75	45	9.5	47.78±0.33	36.61±0.68
25	10	50	45	8	97.05±0.59	74.36±0.94
26	10	50	45	8	99.21±0.62	76.02±0.97
27	10	50	45	8	99.22±0.59	77.03±0.98

28	10	50	45	8	96.55±0.76	73.98±0.92
29	10	50	45	8	98.49±0.68	75.47±0.94

The data for lack of fit test describing the success or failure of model for conversion (%) and yield (%) is presented in *Table 4.5* and *Table 4.6*.

Response Surface Methodology (RSM) in combination was used to optimize the production of chiral selective transamination of 1-(3-methylphenyl)ethan-1-one. The enzyme loading, substrate loading, pH and temperature were chosen as the variables and the response selected was the yield of 1-(3-methylphenyl)ethan-1-one in present work. The Response surface plots (3D and 2D) representing the effect of interaction of enzyme loading and substrate loading shown in *figure 4.7*, enzyme loading and temperature shown in *figure 4.8*, enzyme loading and pH shown in *figure 4.9*, substrate loading and temperature shown in *figure 4.10*, substrate loading and pH shown in *figure 4.11*, and temperature and pH shown in *figure 4.12* on the response 1 (Conversion, %) during chiral selective transamination of (1*R*)-(3-methylphenyl)ethan-1-amine from 1-(3-methylphenyl)ethan-1-one

*Table 4.4 ANOVA for response surface quadratic model of response 1 (Conversion, %) in chiral selective transamination of 1-(3-methylphenyl)ethan-1-one to (1R)-(3-methylphenyl)ethan-1-amine*

Source	Sum of squares	df	Mean square	F-value	P-value	Prob > F
Model	8773.274	14	626.662	106.209	< 0.0001	Significant
A-Enzyme loading	280.817	1	280.817	47.594	< 0.0001	
B-Substrate loading	983.916	1	983.916	166.758	< 0.0001	
C-Temperature	1050.754	1	1050.754	178.086	< 0.0001	
D-pH	311.305	1	311.305	52.761	< 0.0001	
A <sup>2</sup>	12.516	1	12.5160	2.121	0.1673	
B <sup>2</sup>	972.240	1	972.240	164.779	< 0.0001	
C <sup>2</sup>	1904.282	1	1904.282	322.746	< 0.0001	
D <sup>2</sup>	4314.430	1	4314.430	731.227	< 0.0001	
AB	44.156	1	44.156	7.484	0.0161	
AC	48.511	1	48.511	8.222	0.0124	

AD	34.281	1	34.281	5.810	0.0303	
BC	32.948	1	32.948	5.584	0.0331	
BD	190.578	1	190.578	32.300	< 0.0001	
CD	0.0529	1	0.0529	0.009	0.9259	
Residual	82.604	14	5.9003			
Lack of Fit	76.460	10	7.646	4.978	0.0678	Not significant
Pure Error	6.144	4	1.536			
Cor Total	8855.877	28				

Response surface plots (3D and 2D) representing the consequences of interaction of enzyme load and substrate load displayed in *figure 4.7*, enzyme load and temperature represented in *figure 4.8*, enzyme load and pH displayed in *figure 4.9*, substrate load and temperature displayed in *figure 4.10*, substrate load and pH displayed in *figure 4.11*, and temperature and pH displayed in *figure 4.12* on the response 1 (Conversion, %) during chiral selective transamination of (1*R*)-(3-methyl phenyl) ethan-1-amine from 1-(3-methyl phenyl) ethan-1-one.

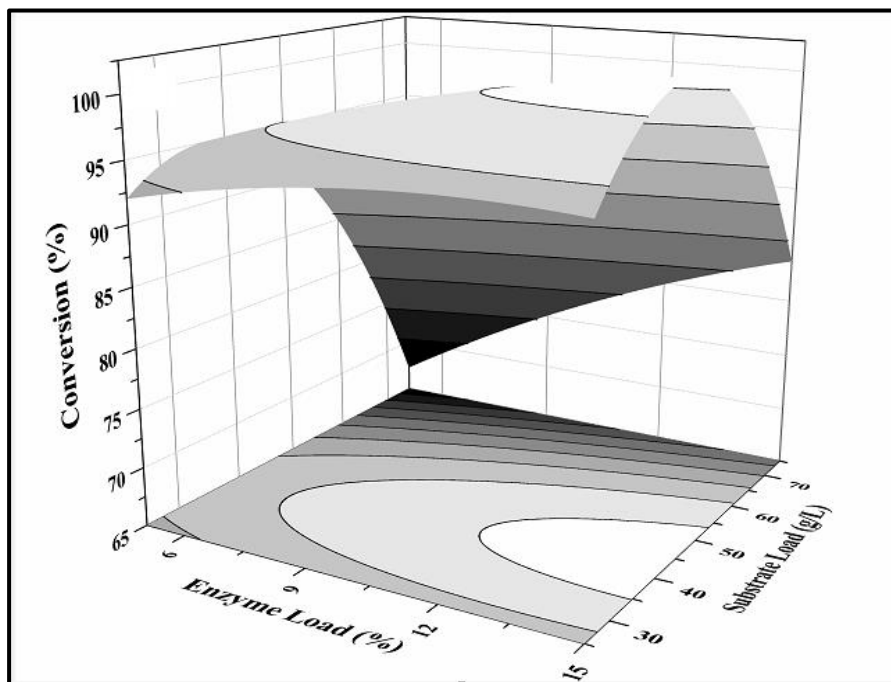


Figure 4.7 Response surface plots (3D and 2D) representing the consequences of interaction of enzyme load and substrate load on the response 1 (Conversion, %) during chiral selective transamination of (1R)-(3-methyl phenyl) ethan-1-amine from 1-(3-methyl phenyl) ethan-1-one

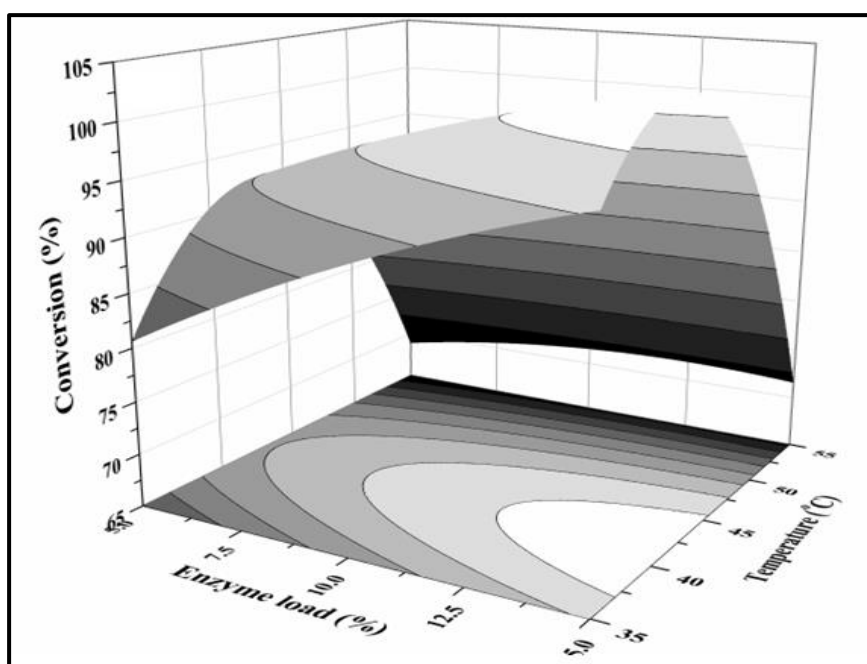


Figure 4.8 Response surface plots (3D and 2D) representing the consequences of interaction of enzyme load and temperature on the response 1 (Conversion, %) during chiral selective transamination of (1R)-(3-methyl phenyl) ethan-1-amine from 1-(3-methyl phenyl) ethan-1-one

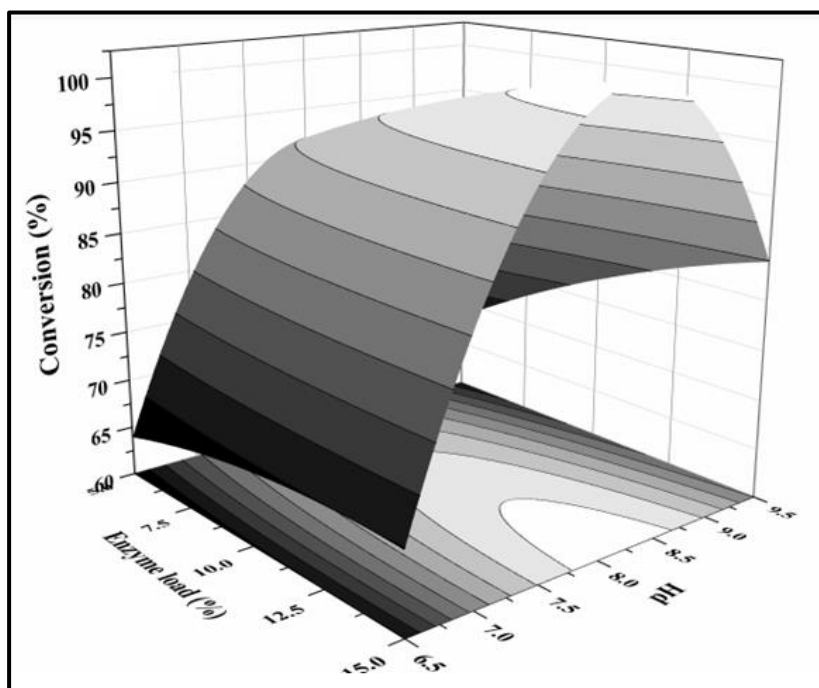


Figure 4.9 Response surface plots (3D and 2D) representing the consequences of interaction of enzyme load and pH on the response 1 (Conversion, %) during chiral selective transamination of (1R)-(3-methyl phenyl) ethan-1-amine from 1-(3-methyl phenyl) ethan-1-one

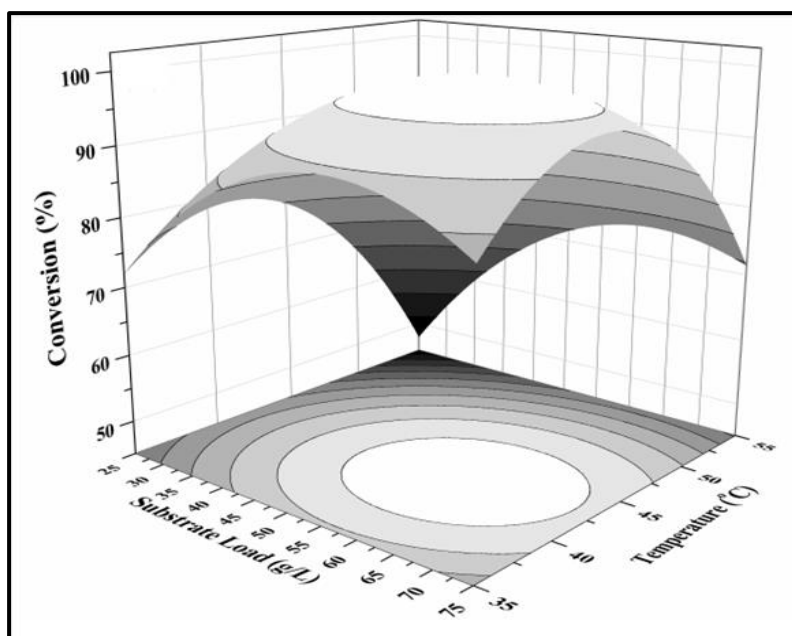


Figure 4.10 Response surface plots (3D and 2D) representing the consequences of interaction of substrate load and temperature on the response 1 (Conversion, %) during chiral selective transamination of (1R)-(3-methyl phenyl) ethan-1-amine from 1-(3-methyl phenyl) ethan-1-one

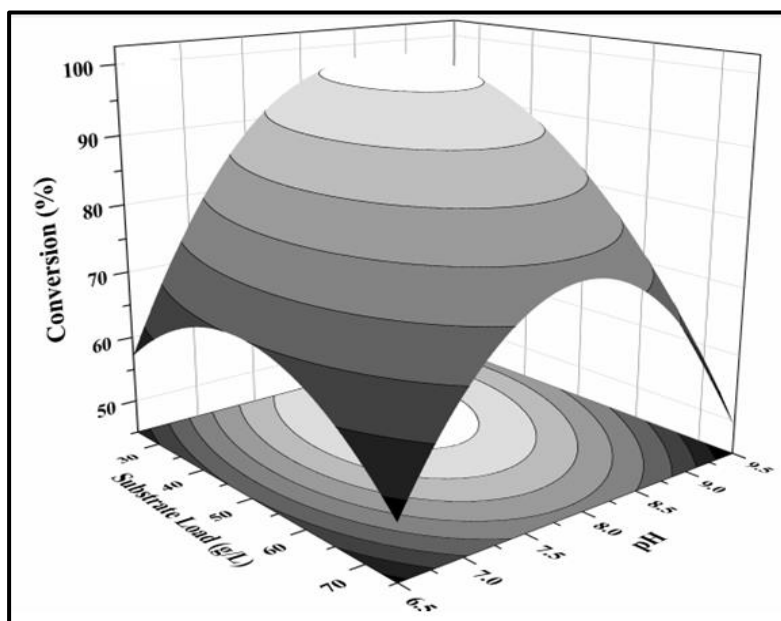


Figure 4.11 Response surface plots (3D and 2D) representing the consequences of interaction of substrate load and pH on the response 1 (Conversion, %) during chiral selective transamination of (1R)-(3-methyl phenyl) ethan-1-amine from 1-(3-methyl phenyl) ethan-1-one

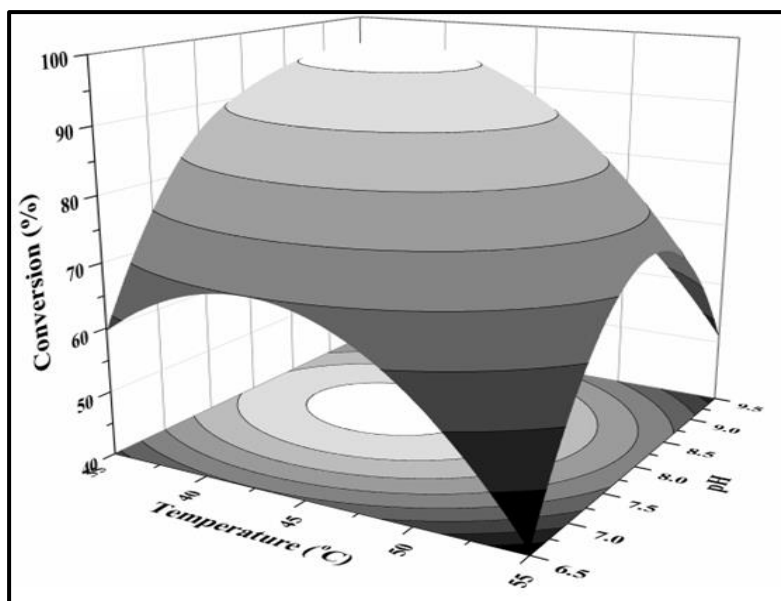


Figure 4.12 Response surface plots (3D and 2D) representing the consequences of interaction of temperature and pH on the response 1 (Conversion, %) during chiral selective transamination of (1R)-(3-methyl phenyl) ethan-1-amine from 1-(3-methyl phenyl) ethan-1-one

Response surface plots (3D and 2D) representing the consequences of interaction of enzyme load and substrate load displayed in *figure 4.13*, enzyme load and temperature displayed in *figure 4.14*, enzyme loading and pH shown in *figure 4.15*, substrate load and temperature displayed in *figure 4.16*, substrate load and pH displayed in *figure 4.17* and temperature and pH displayed in *figure 4.18* on the response 2 (Yield, %) during chiral selective transamination of (1*R*)-(3-methyl phenyl) ethan-1-amine from 1-(3-methyl phenyl) ethan-1-one.

*Table 4.5 ANOVA for response surface quadratic model of response 2 (Yield, %) in chiral selective transamination of 1-(3-methyl phenyl) ethan-1-one to (1*R*)-(3-methyl phenyl) ethan-1-amine*

Source	Sum of squares	Df	Mean square	F-value	P-value	Prob > F
Model	5182.707	14	370.193	76.586	< 0.0001	Significant
A-Enzyme loading	185.624	1	185.624	38.402	< 0.0001	
B-Substrate loading	531.425	1	531.425	109.942	< 0.0001	
C-Temperature	648.950	1	648.950	134.256	< 0.0001	
D-pH	190.475	1	190.475	39.406	< 0.0001	
A <sup>2</sup>	12.563	1	12.563	2.599	0.1292	
B <sup>2</sup>	591.912	1	591.9118	122.456	< 0.0001	



C <sup>2</sup>	1121.492	1	1121.492	232.0164	< 0.0001	
D <sup>2</sup>	2561.310	1	2561.310	529.889	< 0.0001	
AB	21.350	1	21.350	4.417	0.0542	
AC	19.902	1	19.902	4.117	0.0619	
AD	20.093	1	20.093	4.157	0.0608	
BC	15.302	1	15.302	3.166	0.0969	
BD	128.178	1	128.178	26.518	0.0001	
CD	0.0069	1	0.00687	0.0014	0.9704	
Residual	67.671	14	4.834			
Lack of Fit	61.552	10	6.155	4.023	0.0960	Not significant
Pure Error	6.120	4	1.530			
Cor Total	5250.379	28				

Response surface plots (3D and 2D) representing the consequences of interaction of enzyme load and substrate load displayed in *figure 4.13*, enzyme load and temperature displayed in *figure 4.14*, enzyme load and pH displayed in *figure 4.15*, substrate load and temperature displayed in *figure 4.16*, substrate load and pH displayed in *figure 4.17* and temperature and pH displayed in *figure 4.18* on the response 2 (Yield, %) during chiral selective transamination of (1*R*)-(3-methyl phenyl) ethan-1-amine from 1-(3-methyl phenyl) ethan-1-one.

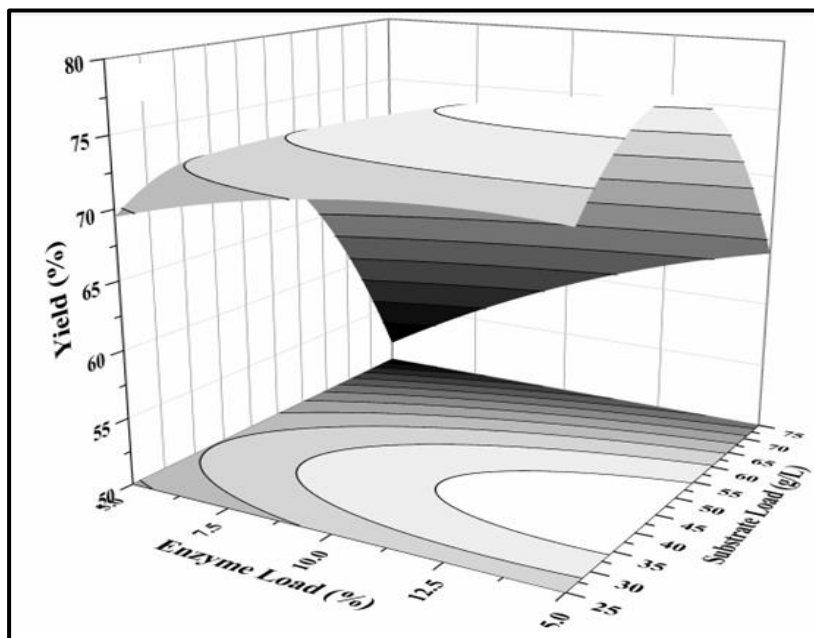


Figure 4.13 Response surface plots (3D and 2D) representing the consequences of interaction of enzyme load and substrate load on the response 2 (Yield, %) during chiral selective transamination of (1R)-(3-methyl phenyl) ethan-1-amine from 1-(3-methyl phenyl) ethan-1-one

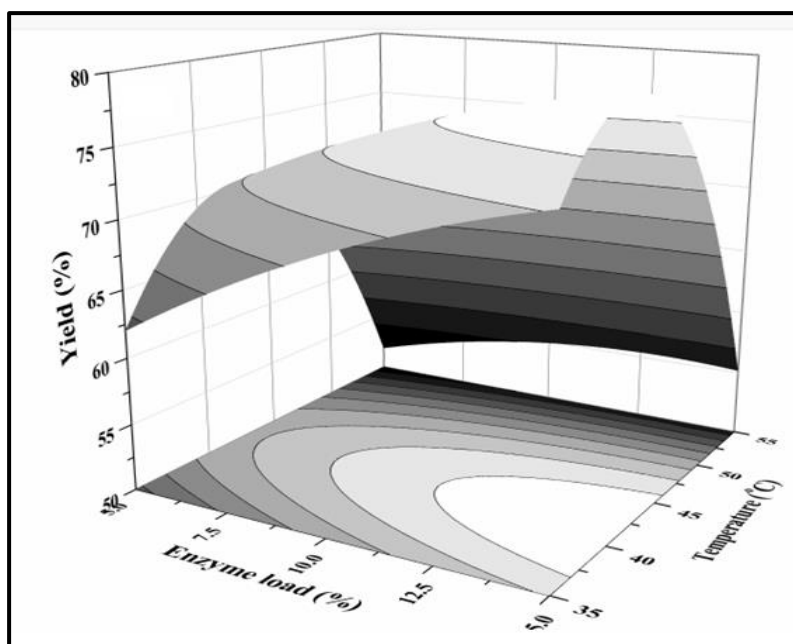


Figure 4.14 Response surface plots (3D and 2D) representing the consequences of interaction of enzyme load and temperature on the response 2 (Yield, %) during chiral selective transamination of (1R)-(3-methyl phenyl) ethan-1-amine from 1-(3-methyl phenyl) ethan-1-one

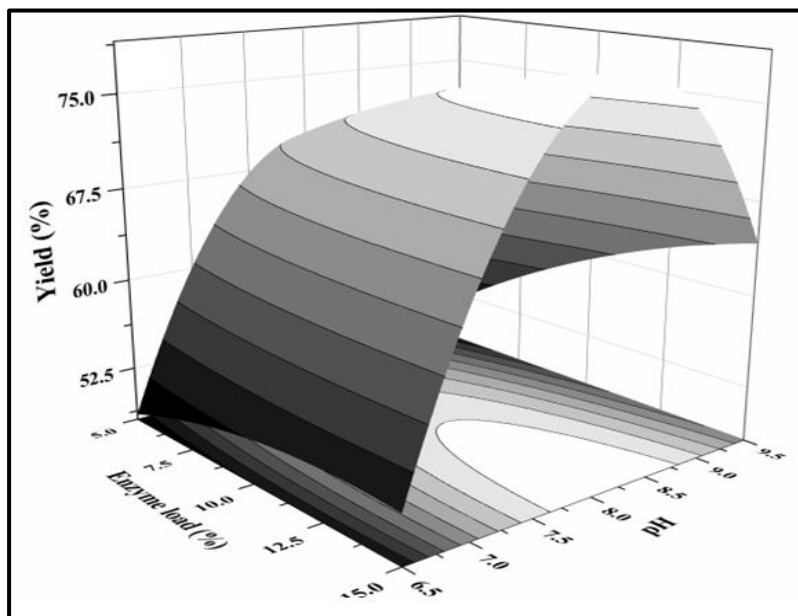


Figure 4.15 Response surface plots (3D and 2D) representing the consequences of interaction of enzyme load and pH on the response 2 (Yield, %) during chiral selective transamination of (1R)-(3-methyl phenyl) ethan-1-amine from 1-(3-methyl phenyl) ethan-1-one

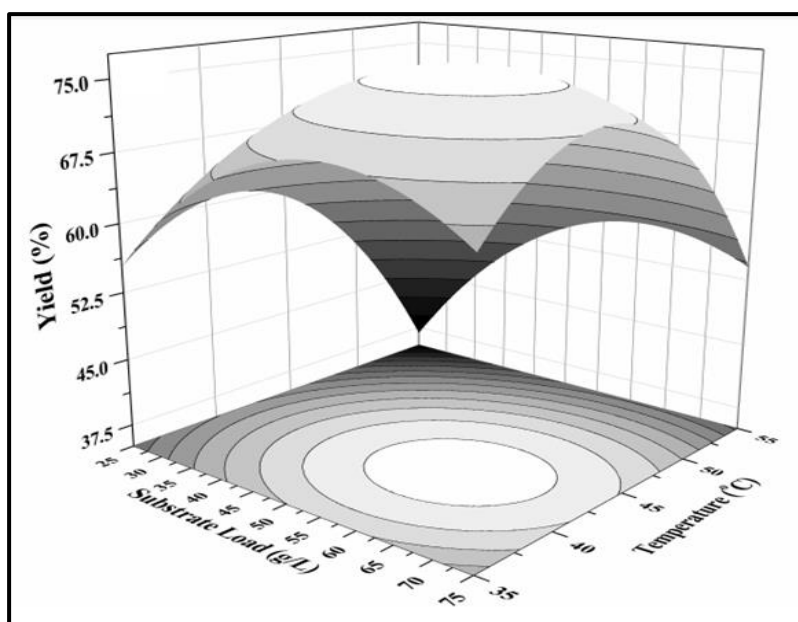


Figure 4.16 Response surface plots (3D and 2D) representing the consequences of interaction of substrate load and temperature on the response 2 (Yield, %) during chiral selective transamination of (1R)-(3-methyl phenyl) ethan-1-amine from 1-(3-methyl phenyl) ethan-1-one

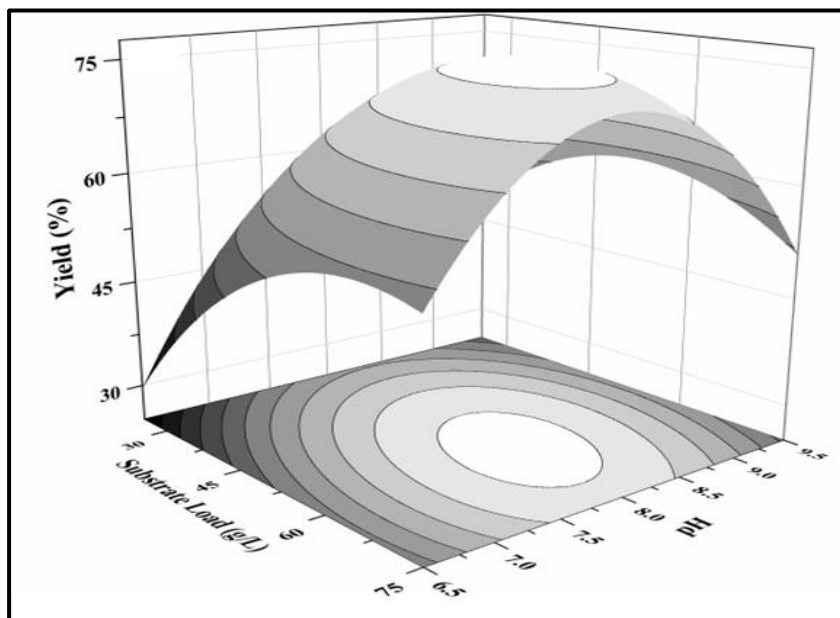


Figure 4.17 Response surface plots (3D and 2D) representing the consequences of interaction of substrate load and pH on the response 2 (Yield, %) during chiral selective transamination of (1R)-(3-methyl phenyl) ethan-1-amine from 1-(3-methyl phenyl) ethan-1-one

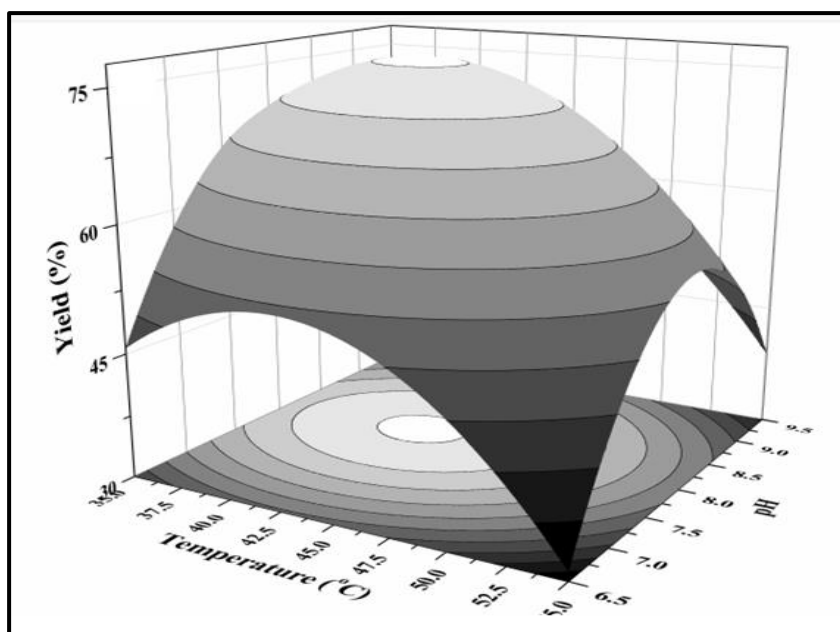


Figure 4.18 Response surface plots (3D and 2D) representing the consequences of interaction of temperature and pH on the response 2 (Yield, %) during chiral selective transamination of (1R)-(3-methyl phenyl) ethan-1-amine from 1-(3-methyl phenyl) ethan-1-one

The coded form of coefficients of all linear, square, and interaction terms in the model for conversion (R1, %) and yield (R2, %) has been summarized in *Table 4.6*, and the quadratic polynomial equation was developed by performing and assessing the experimental findings in set of triplicate.

$$R1 = 98.104 + 4.838 A - 9.055 B - 9.358 C + 5.093 D - 1.389 A^2 - 12.243 B^2 - 17.134 C^2 - 25.790 D^2 + 3.323 AB - 3.483 AC + 2.928 AD + 2.870 BC - 6.903 BD + 0.115 CD$$

$$R2 = 75.372 + 3.933 A - 6.655 B - 7.354 C + 3.984 D - 1.392 A^2 - 9.553 B^2 - 13.149 C^2 - 19.871 D^2 + 2.310 AB - 2.231 AC + 2.241 AD + 1.956 BC - 5.661 BD - 0.0415 CD$$

Where R1 and R2 are the response for conversion (%) and yield (%), whereas A, B, C and D indicating the dimensionless coded values for enzyme loading (EL, %), substrate load (SL, g/L), temperature (T, °C) and operating pH (P), respectively.

*Table 4.6 Coefficient of all the term in polynomial model at  $p < 0.05$  and the corresponding ANOVA data associated with the consequences of transamination parameters on conversion (%) and yield (%)*

Component estimates	Response-1 (Conversion, %)	Response-2 (Yield, %)
Intercept	98.104	75.372
A	4.838	3.933
B	-9.055	-6.655
C	-9.358	-7.354
D	5.093	3.984

A <sup>2</sup>	-1.389	-1.392
B <sup>2</sup>	-12.243	-9.553
C <sup>2</sup>	-17.134	-13.149
D <sup>2</sup>	-25.790	-19.871
AB	3.323	2.310
AC	-3.483	-2.231
AD	2.928	2.241
BC	2.870	1.956
BD	-6.903	-5.661
CD	0.115	-0.0415
<i>p</i> -value	<0.0001	<0.0001
<i>p</i> <sub>lof</sub> -value	0.068	0.096
<i>F</i> -value	106.21	76.47
<i>F</i> <sub>lof</sub> -value	4.98	4.02
R <sup>2</sup>	0.9907	0.9871
Adjusted R <sup>2</sup>	0.9813	0.9742
Predicted R <sup>2</sup>	0.9492	0.9307
C.V. (%)	3.2517	3.8450

The coefficients showed that both conversion (%) and yield (%) were remarkably influenced by linear terms in the quadratic equation  $p \leq 0.05$ . The proportionate

impact of the linear temperature term ( $^{\circ}\text{C}$ ) influenced both conversion and yield by direct decrement, followed by substrate loading. The negative linear terms means that the increment of parameter values lowers the response value of the accompanying reaction. On the other hand, the coefficients of linear terms pH and enzyme load were responsible for improving both responses.

Amongst all, the squared coefficients of three factors (substrate load, temperature, and pH) in the developed model noteworthy subscribed to the changes in conversion (%) and yield (%) from the reaction. Further, only exceptions have been realized for the squared term of enzyme load was not subscribing notable at  $p \leq 0.05$ . The negative coefficients of all the square term reflected the adverse effect, which shows the decrements in response values.

The interactive consequences amongst all the four factors (AB, AC, AD, BC, BD, and CD) on conversion (%) and yield (%) were significant at  $p \leq 0.05$ . Whereas amongst all, only two interaction terms (AB and BD) significantly influenced the change in yield (%). As expected, the positive coefficients of the term AB were the most influential in the positive side of the reaction, followed by AD and BC, while the enzyme load-temperature (AC), and substrate load-pH (BD) interactions negatively affected the reaction.

The interactions between the process parameters exhibited superior correlation ship with the quadratic polynomial model, as displayed from notable higher  $R^2$ , adjusted  $R^2$ , and predicted  $R^2$  values for conversion (%) and yield (%) which were 0.9907, 0.9813, and 0.9492, and 0.9871, 0.9742, and 0.9307, respectively (*Table 4.7*). The difference of  $\leq 0.2$  between actual, predicted, and adjusted  $R^2$  values defines the highly desirable fit of the model in the equation. The  $R^2$  values nearly equal to 1 specify an enhanced correlation between the observed values and predicted values [119, 120]. The observed  $p$ -values for the models of both the responses were

<0.0001, and the model  $F$ -values of 106.21 and 76.47 for conversion (%) and yield (%) respectively, signified a successful fitting of data for the observed responses and then described the acceptability of obtained data. Further, these values suggested the model to be remarkable and only a 0.01% chance that an  $F$ -value this wide could occur due to the noise. These values were also supported by an insignificant  $p$ -lack of fit value of 0.0678 and 0.0960 for respective conversion (%) and yield (%), and then described the acceptability of obtained data. Further, the developed models for conversion (%) and yield (%) had a coefficient of variation (CV) of 3.2517% and 3.8450%, respectively, and this reflected a superior precision and excellent reliability of experiments.

#### **4.3.3.3 Desirability based numeric optimization**

Desirability based numerical optimization using developed polynomial models was carried out by targeting to get the highest conversion and yield percentage which is summarized in *Table 4.7*. The relative importance ( $r_i$ ) ranged from 1 and 5 (least to most important) and was allotted to each parameter and response. Utmost conversion (%) and yield (%) were focussed by labeling maximum importance ( $r_i = 5$ ). However, while considering the cost of an enzyme, reaction parameters such as enzyme load should be as minimum as possible with best response values. Therefore, a lower enzyme load with  $r_i = 5$  was assigned for optimization. The optimal reaction parameters suggested during optimization were 5% enzyme load, 36.78 g/L substrate loading at 42.66 °C, and pH 8.18 with a desirability value of 0.813. The predicted results for at given optimal conditions were 96.12% conversion and 73.12% yield. The observed results were validated by comparing the predicted values vs. actual results. The practical results of the experiment were closely analogous to the suggested values. The reaction was carried out at 5% enzyme load, 37 g/L substrate loading at 43°C, and pH 8.2 and this displayed 97.25% conversion



and 74.52% yield. Therefore, it can be proposed that the optimal reaction conditions in the current investigation were adequate for similar studies.

*Table 4.7 The set of constraints for different factors and responses for developing the reaction conditions*

<b>Parameters</b>	<b>Target</b>	<b>Lower limit (Li)</b>	<b>Upper Limit (Ui)</b>	<b>Relative importance (ri)</b>	<b>Optimized conditions at D</b>	<b>Actual experimental conditions*</b>
<b>D= 0.813</b>						
A- Enzyme load (%)	Minimize	5	15	5	5.00	5
B- Substrate load (g/L)	In range	25	75	3	36.78	37
C- Temperature (°C)	In range	35	55	3	42.66	43
D- pH	In range	9.5	9.5	3	8.18	8.2
<b>Conversion (%)</b>	Maximize	33.34	77.03	5	96.115	97.25
<b>Yield (%)</b>	Maximize	42.84	99.22	5	73.12	74.52

#### **4.3.4 Instrumental characterization of 1-(3-methyl phenyl) ethan-1-one and (1R)-(3-methyl phenyl) ethan-1-amine**

The instrumental characterization was performed for confirming the formation of product [(1R)-(3-methyl phenyl) ethan-1-amine] from substrate [1-(3-methyl phenyl) ethan-1-one] after transamination with ATA-025 using analytical methods such as boiling point, LC-MS, <sup>1</sup>H NMR, and ATR-FTIR along with the HPLC and GC analysis.

##### **4.3.4.1 Boiling point**

The boiling point of 1-(3-methylphenyl)ethan-1-one and (1R)-(3-methylphenyl)ethan-1-amine was determined by a digital melting point apparatus and found to be 218-220°C, and 202-204°C, respectively.

##### **4.3.4.2 LC-MS analysis**

The liquid chromatogram profile of 1-(3-methylphenyl)ethan-1-one and (1R)-(3-methylphenyl)ethan-1-amine in LC-MS is displayed in *figure 4.19* and *figure 4.20*

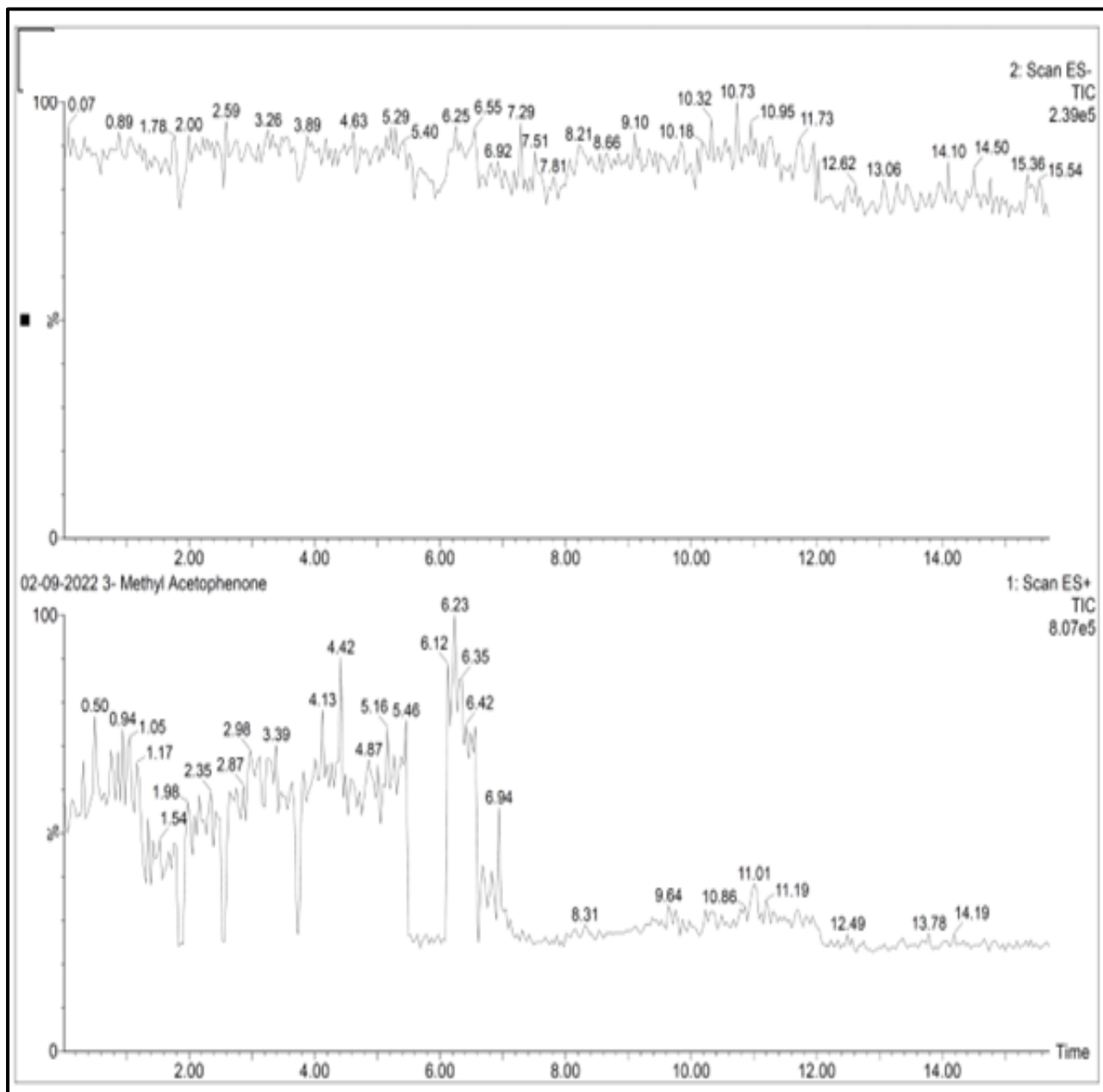


Figure 4.19 LC profile of 1-(3-methyl phenyl) ethan-1-one after LC-MS analysis

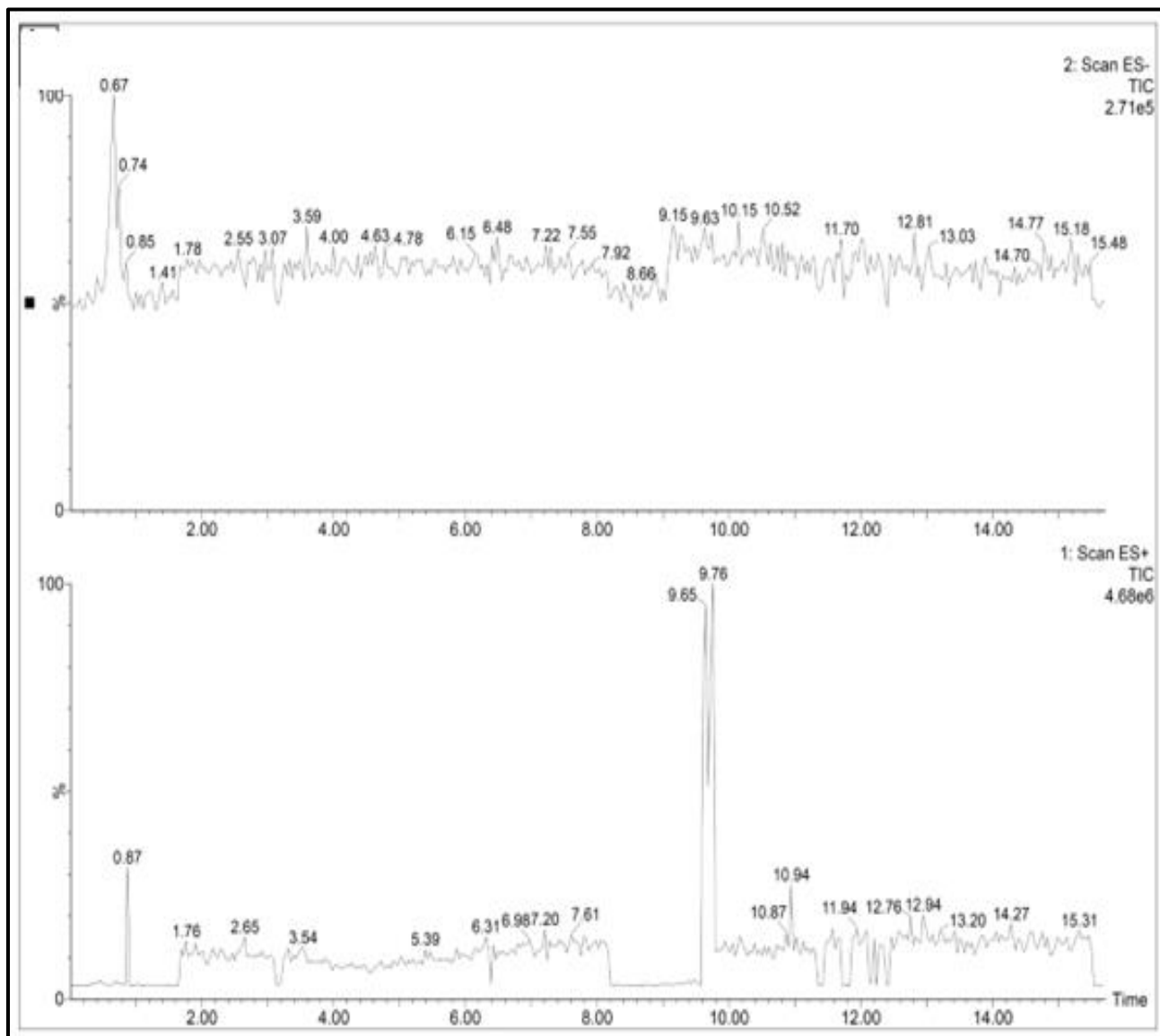


Figure 4.20 LC profile of (1R)-(3-methyl phenyl) ethan-1-amine after LC-MS analysis

The mass fragments of the both the purified compounds were analysed on automated mass split in the instrument (figure 4.21 and figure 4.22). The mono-isotopic mass of 1-(3-methylphenyl)ethan-1-one and (1R)-(3-methylphenyl)ethan-1-amine were 134 and 135, and this was confirmed by  $m/z$  of 135.53 and 136.72 indicating the respective  $(M+H)^+$  fragments.

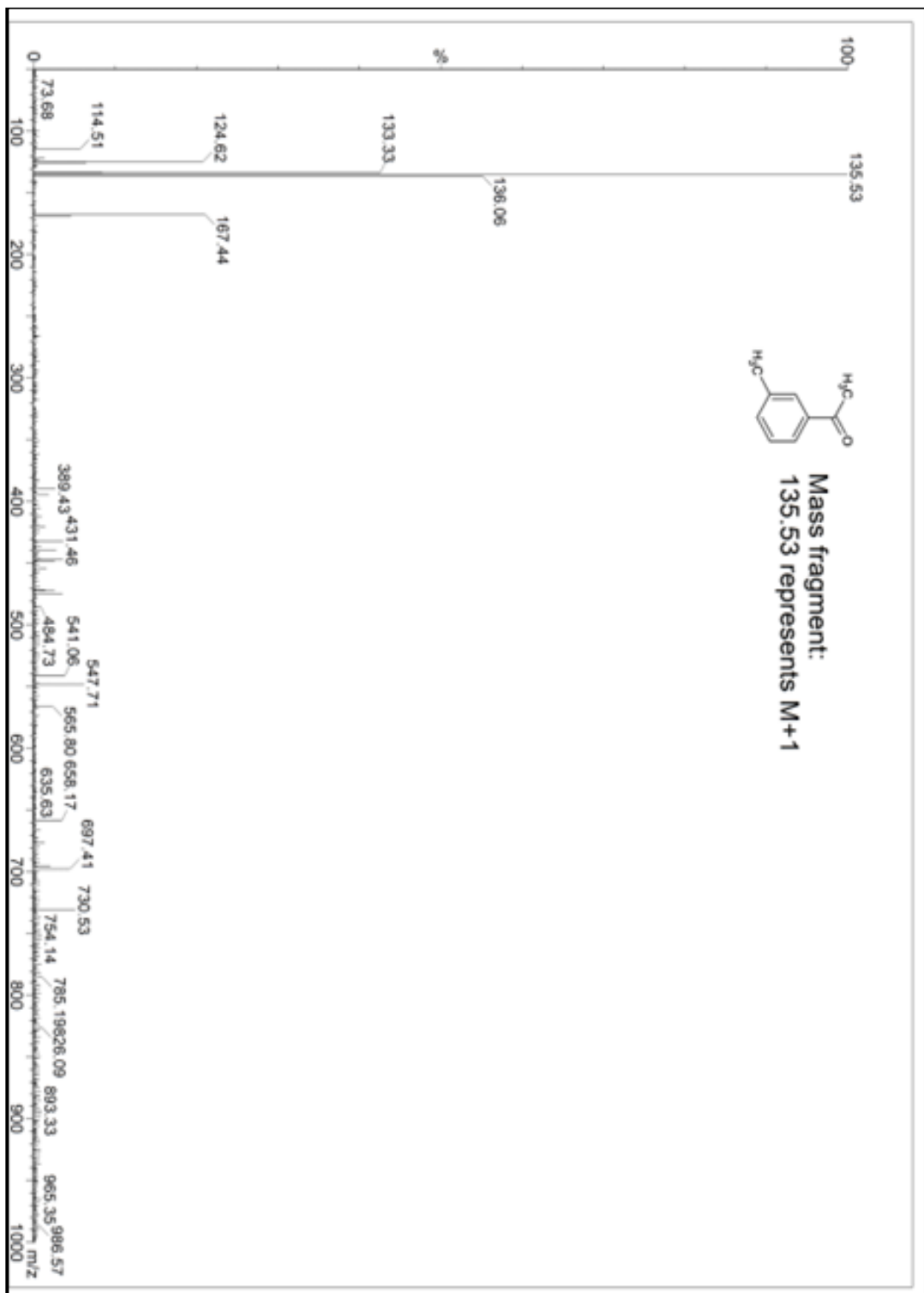


Figure 4.21 LC mass profile of 1-(3-methyl phenyl) ethan-1-one

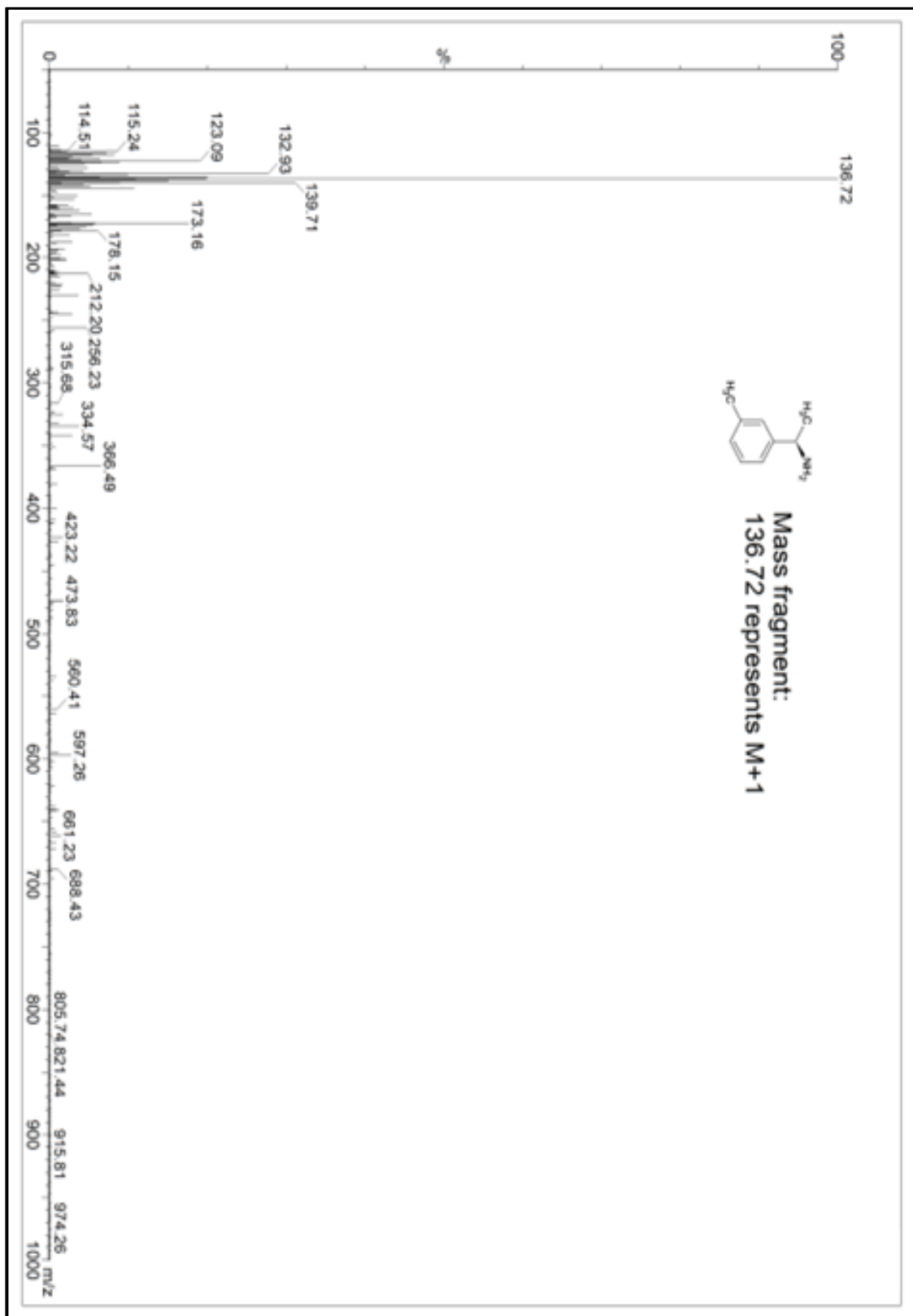


Figure 4.22 LC mass profile of (1R)-(3-methyl phenyl) ethan-1-amine

#### 4.3.4.3 NMR analysis

The  $^1\text{H}$  NMR analysis of 1-(3-methylphenyl)ethan-1-one and (1*R*)-(3-methylphenyl)ethan-1-amine performed in dimethylsulfoxide revealed the presence of ten and thirteen protons in their skeleton, as represented in *figure 4.23* and *figure 4.24*

$^1\text{H}$  NMR (400 MHz, DMSO) of 1-(3-methylphenyl)ethan-1-one :  $\delta$ 2.40 (3H, S), 2.60 (3H, S), 7.20-7.40 (2H, 7.40 (ddd,  $J=7.9, 1.5, 1.1$  Hz), 7.40 (ddd,  $J=8.2, 7.9, 0.4$  Hz)), 7.80-8.00 (2H, 7.92 (ddd,  $J=1.7, 1.5, 0.4$  Hz), 8.0 (ddd,  $J=8.2, 1.7, 1.1$ Hz))

$^1\text{H}$  NMR (400 MHz, DMSO) of (1*R*)-(3-methylphenyl)ethan-1-amine :  $\delta$ 1.20 (3H, d,  $J=6.5$ Hz), 2.20 (3H, S), 4.10 (1H, q,  $J=6.5$  Hz), 7.10-7.20 (3 Hz, 7.10 (ddd,  $J=7.9, 1.6, 1.5$  Hz), 7.01 (ddd,  $J=7.9, 1.5, 0.9$  Hz), 7.09 (ddd,  $J=1.6, 0.9, 0.5$  Hz)), 7.20 (1H, td,  $J=7.9, 0.5$  Hz)

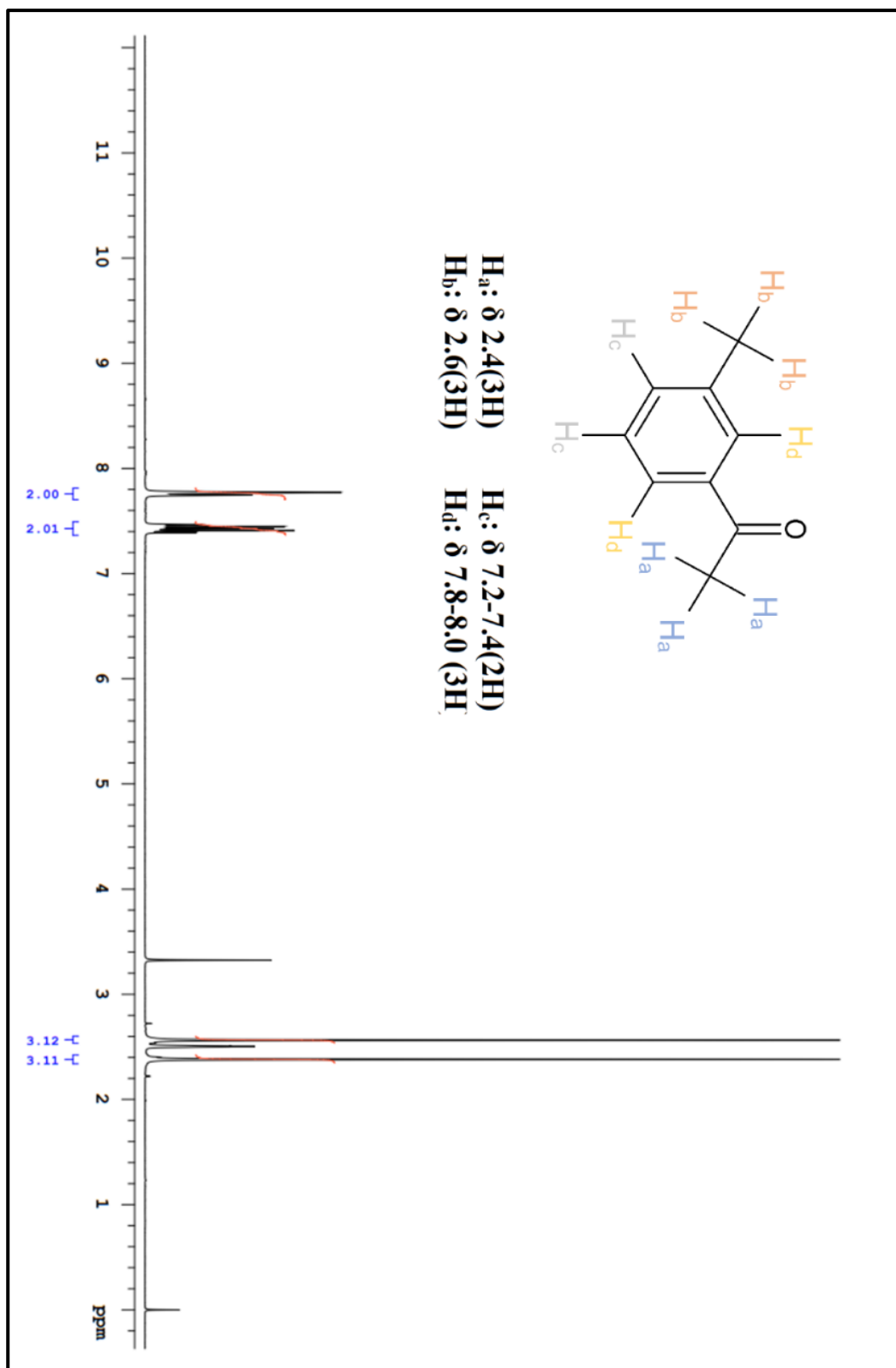


Figure 4.23  $^1H$  NMR spectra of 1-(3-methyl phenyl) ethan-1-one



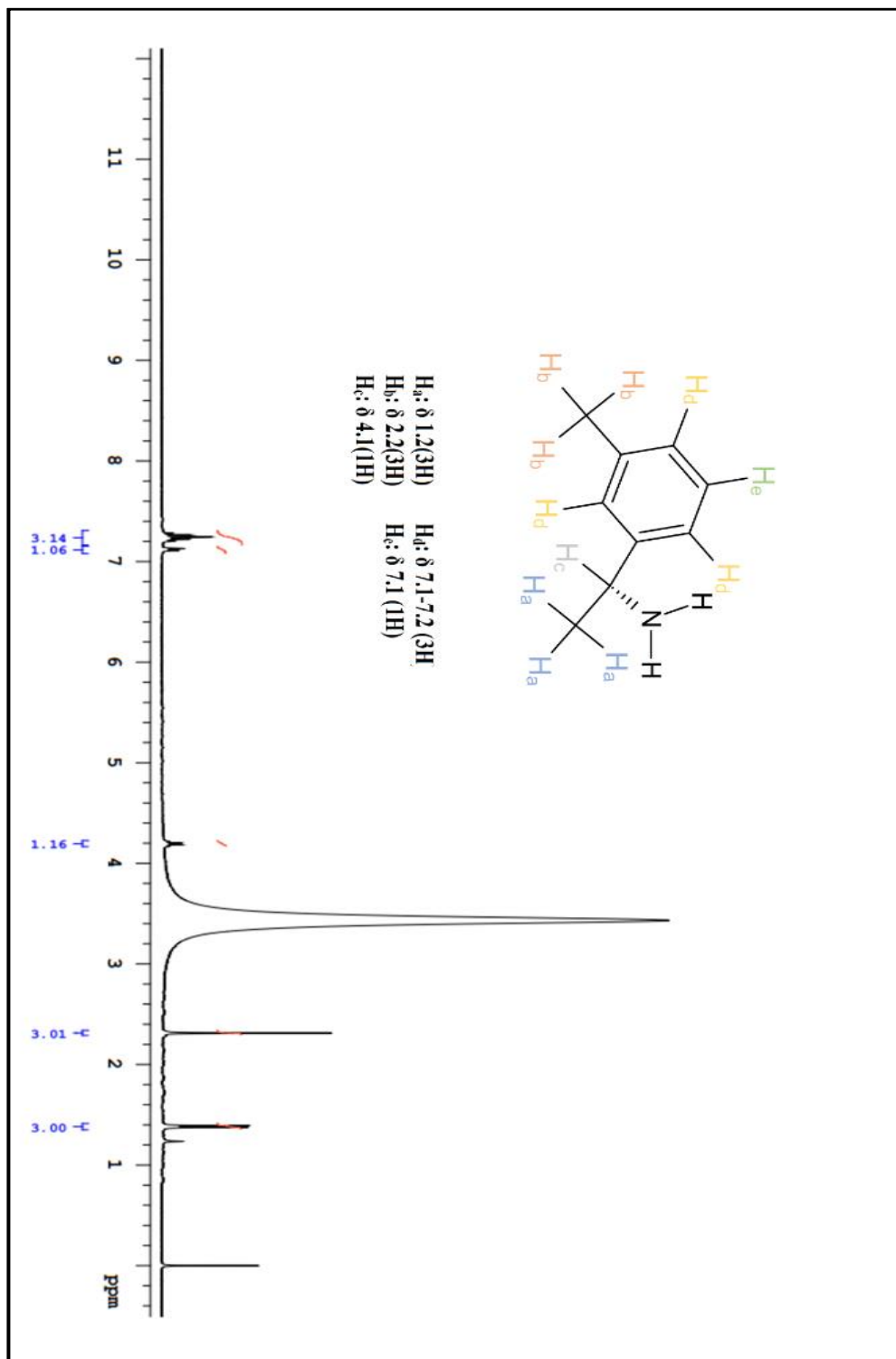


Figure 4.24  $^1H$  NMR spectra of (1R)-(3-methyl phenyl) ethan-1-amine

#### 4.3.4.4 FTIR analysis

The FTIR spectra of 1-(3-methylphenyl)ethan-1-one and (1*R*)-(3-methylphenyl)ethan-1-amine are represented in *figure 4.25* and *figure 4.26*. The presence of functional peaks at 3062 1/cm and 3004 1/cm represents =C-H aryl stretching vibrations, whereas distinct peaks at 2963 1/cm, 2922 1/cm and 2865 1/cm signifies the stretching vibrations in –CH alkyl. The major functional peak at 1680 1/cm indicates the presence of –C=O in 1-(3-methylphenyl)ethan-1-one, while aromatic C=C and bending in –CO=C could be ascertained by peaks at 1603 1/cm to 1425 1/cm, and 1273 1/cm. Further, the –CH of benzene rings could be designated by peaks at 784 1/cm to 690 1/cm. The successful transamination by ATA-025 in (1*R*)-(3-methylphenyl)ethan-1-amine could be confirmed by sharp peak at 3358 1/cm which can be designated to –NH<sub>2</sub> stretching. The functional peaks at 1638 1/cm, 1389 1/cm and 700 1/cm represents the scissoring nature of –NH<sub>2</sub>, stretching of –C-N bond and out of plane bending of –NH<sub>2</sub> group, respectively.

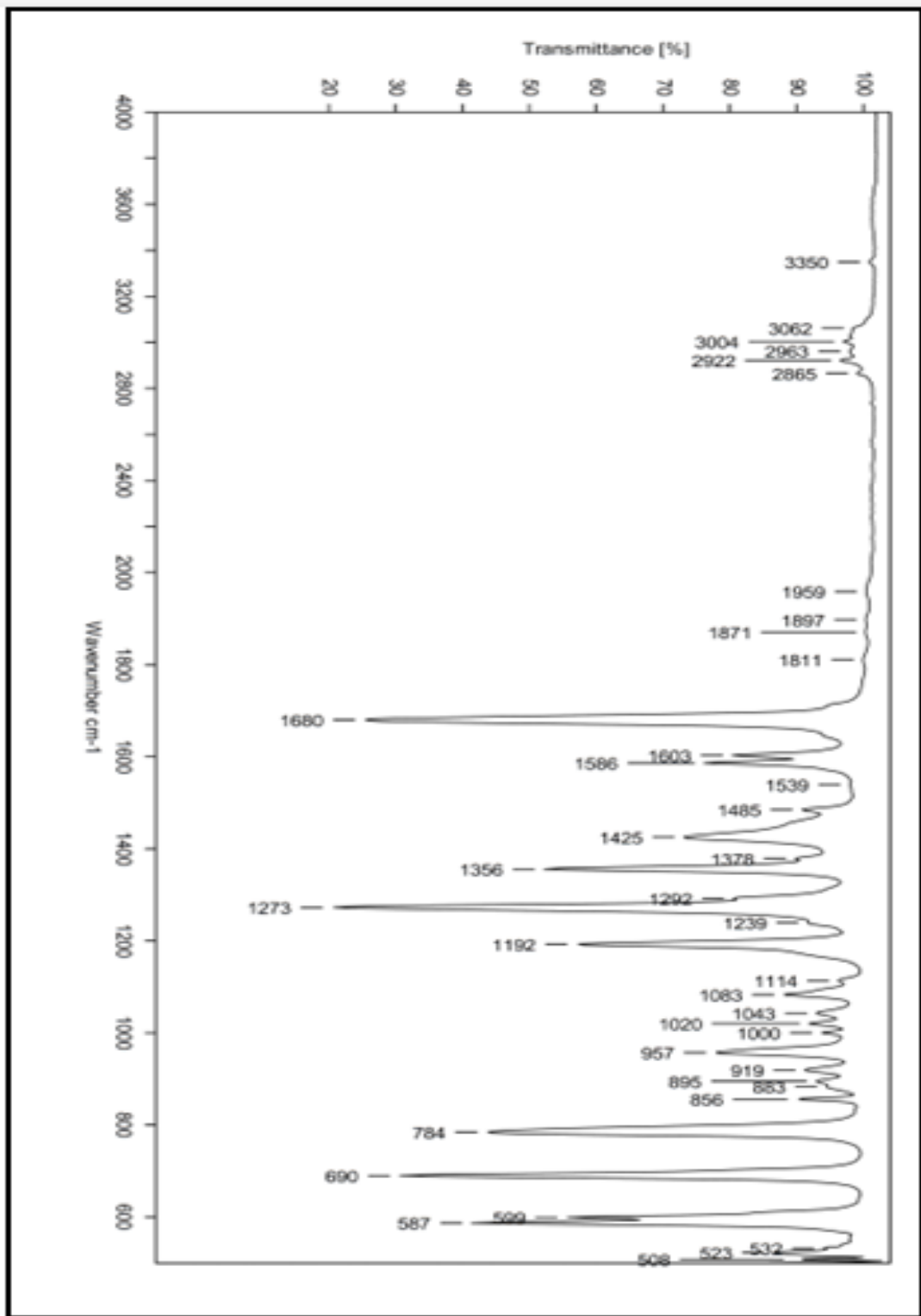


Figure 4.25 FTIR spectra of 1-(3-methylphenyl)ethan-1-one

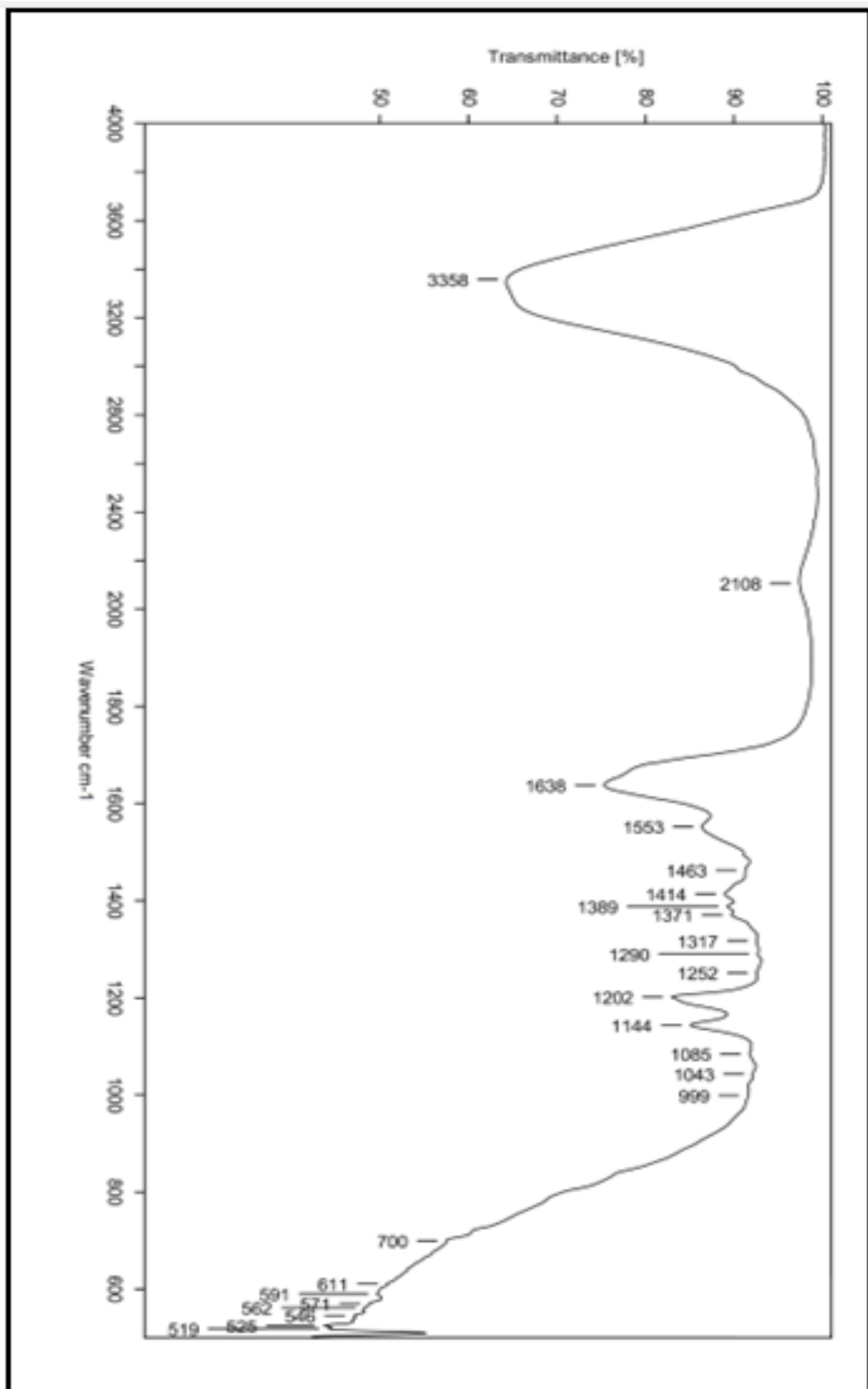
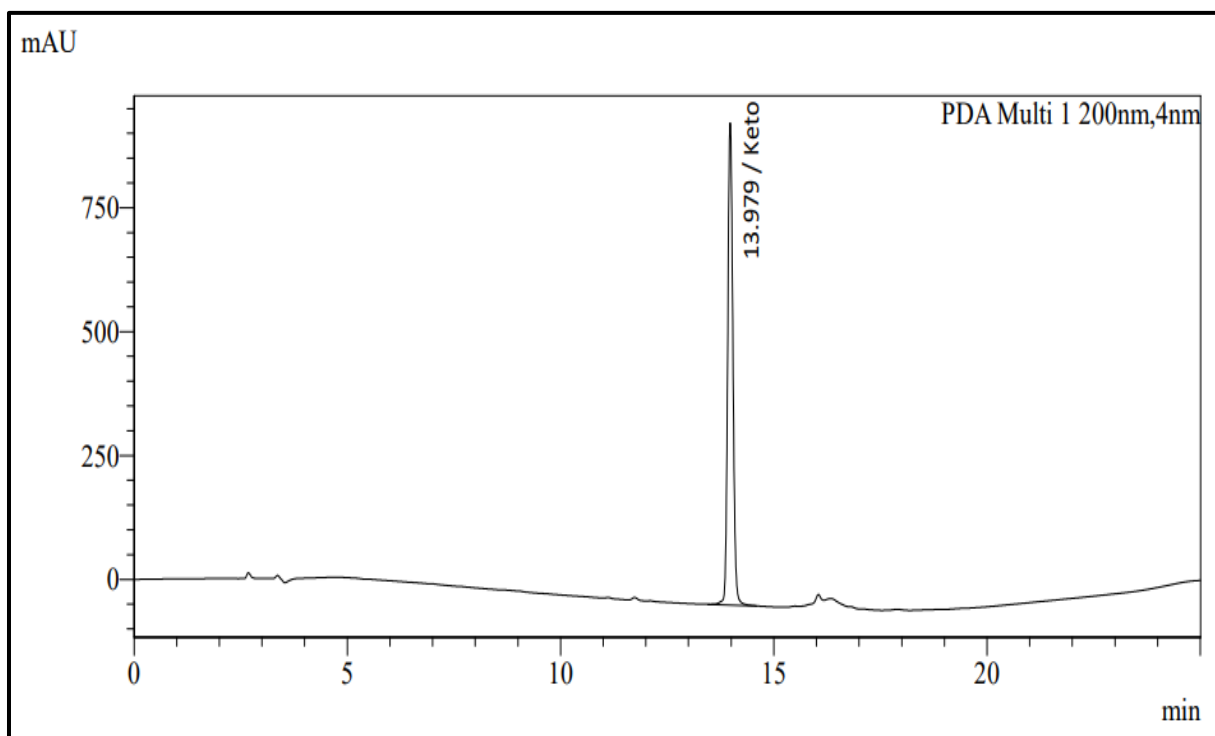


Figure 4.26 FTIR spectra of (1R)-(3-methylphenyl)ethan-1-amine

#### 4.3.4.5 HPLC analysis

The liquid chromatography profile of 1-(3-methylphenyl)ethan-1-one and (1*R*)-(3-methylphenyl)ethan-1-amine in HPLC presented a single peak at retention time of 13.979 min and 6.194 min (*figure 4.27* and *figure 4.28*). The intermittent sample with nearly 55-60% conversion of substrate to product is presented in *figure 4.29* and shows two distinct peaks of product (first) and substrate (second).



*Figure 4.27 RP-HPLC profile of 1-(3-methylphenyl)ethan-1-one*

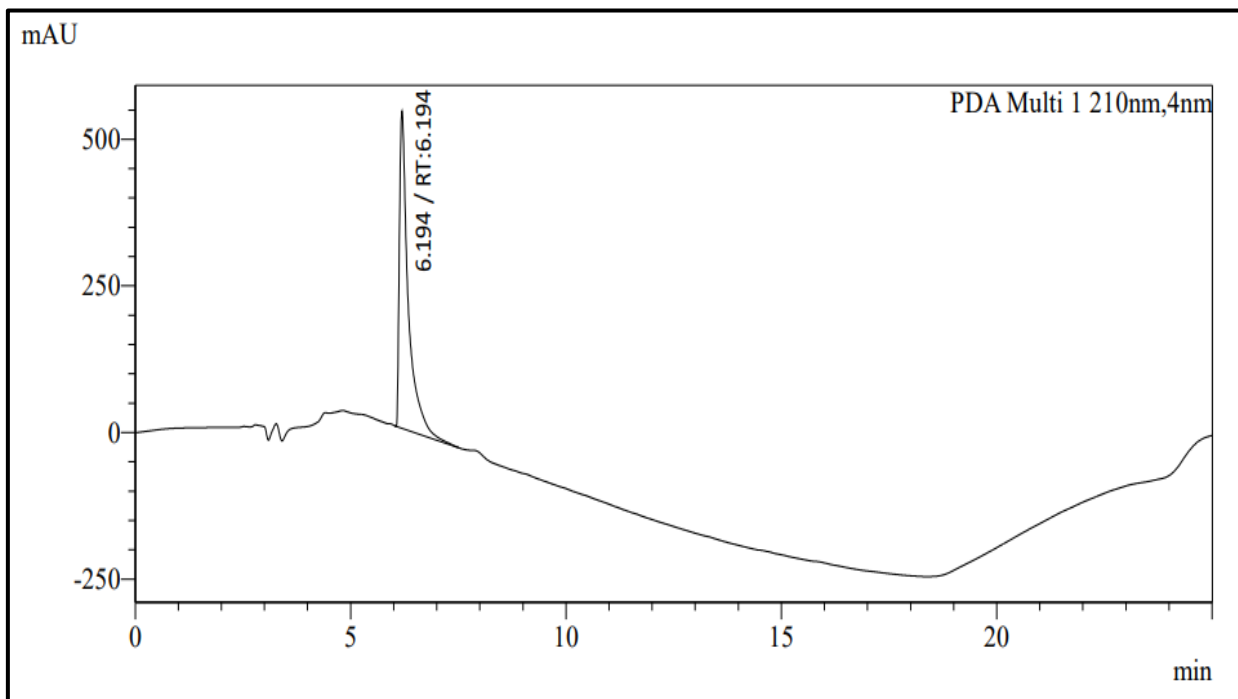


Figure 4.28 RP-HPLC profile of (1R)-(3-methylphenyl)ethan-1-amine

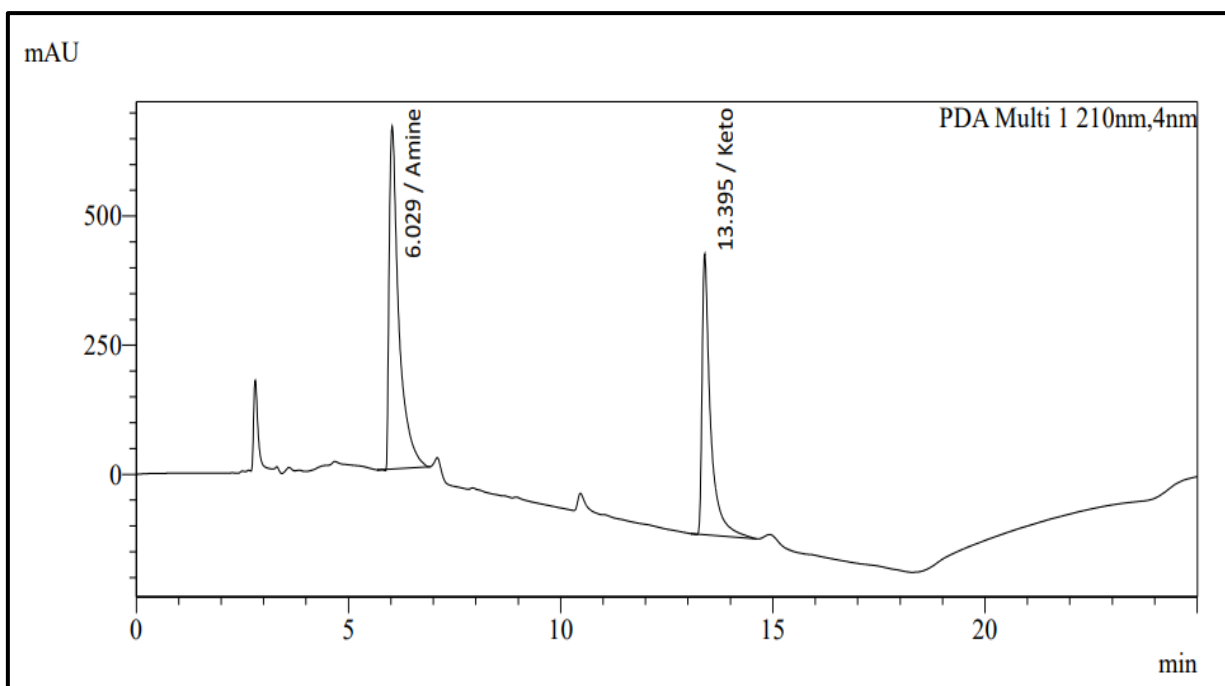


Figure 4.29 HPLC profile of transamination reaction with around 55-60% conversions

#### 4.3.4.6 Chiral analysis by GC

The chiral analysis of recovered and purified 3-methylphenylethan-1-amine on chiral gas chromatography displayed a single *R*-isomer with a chiral purity  $\geq 98.5\%$ , which was confirmed by a single peak at retention time of 12.106 minute (*figure 4.30*), which was compared against the racemic standard showing two isomers at a retention time of 12.107 minute and 12.395 minute (*figure 4.31*).

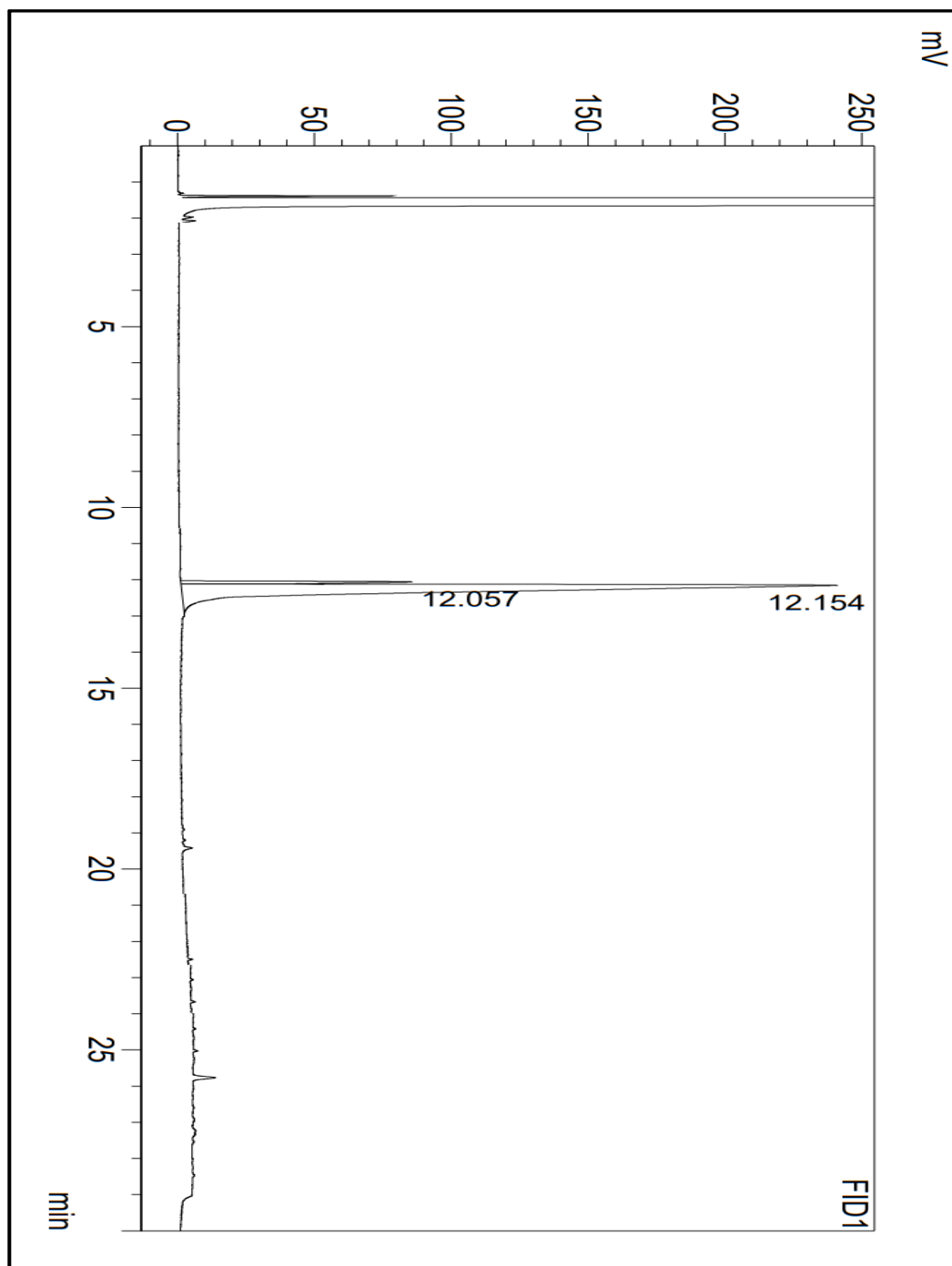


Figure 4.30 Chiral GC profile of (1*R*)-(3-methylphenyl)ethan-1-amine

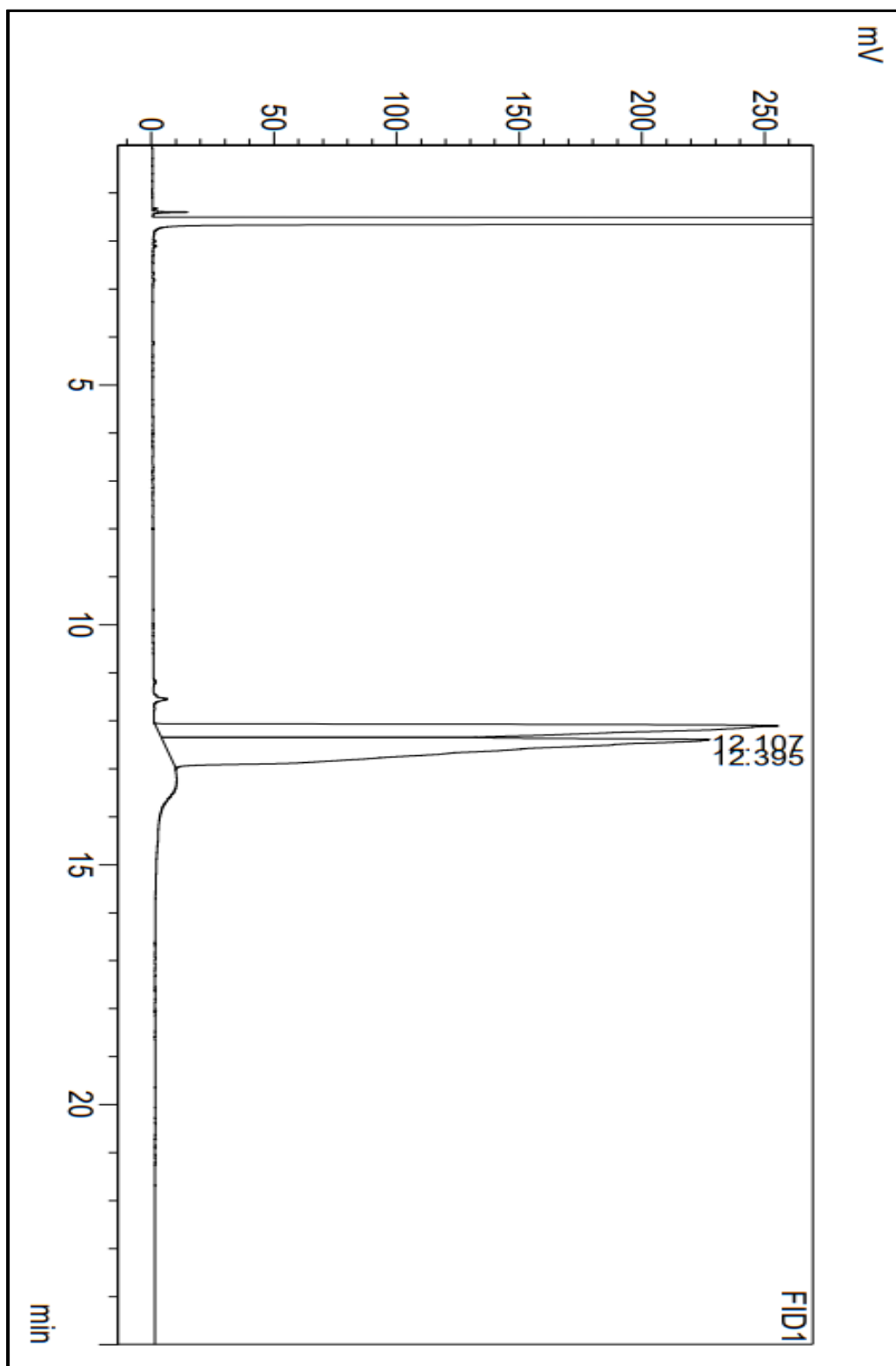


Figure 4.31 Chiral GC profile of (R,S)-(3-methylphenyl)ethan-1-amine



#### 4.3.5 Time course reactions on gram scale for ‘What If studies’

The ‘What If’ studies generally known as negative studies were performed by assessing the timely progress of reaction on gram scale with sudden change in the process variable from the optimal value. The investigation was performed at reactions points which may be attained due to flaws or errors (manuals and/or instrumental) occurring during operation. For the said transamination, we have selected lower and upper limits along with the optimal point of process variable that can extremely occur during controlled progress of reaction. The transamination reactions on gram scale were carried out by altering the enzyme loading (5%, 10% and 15%), substrate loading (25g/L, 50g/L, and 75g/L), temperature (35°C, 45°C, and 55°C) and medium pH (6.5, 8.0, and 9.5) domain and determining the progression of reaction by estimating conversion (%).

##### 4.3.5.1 Progress of reaction with enzyme loading

The transamination of 1-(3-methylphenyl)ethan-1-one to (1*R*)-(3-methylphenyl)ethan-1-amine was studied at ATA-025 loading of 5%, 10% and 15%, at 45±2°C, 50 g/L substrate loading, pH 8.0 for 24 hours of incubation. The progress of this transamination reaction had a directly relation with amount of ATA-025 loaded in the reaction mixture. If the addition of enzyme reduces below the optimal concentration (10%) then the reaction will progress slowly, while the higher loading above 10% will cause the reaction progress at a elevated rate and achieve conversion in less time. The 5% (lower level), 10% (actual point) and 15% enzyme loading (higher level) showed 81.18±2.24%, 98.38±2.31% and 98.96±2.66% conversion and the actual yield was 65.64±1.02%, 77.06±1.08% and 77.21±1.15%, respectively (*figure 4.32*).

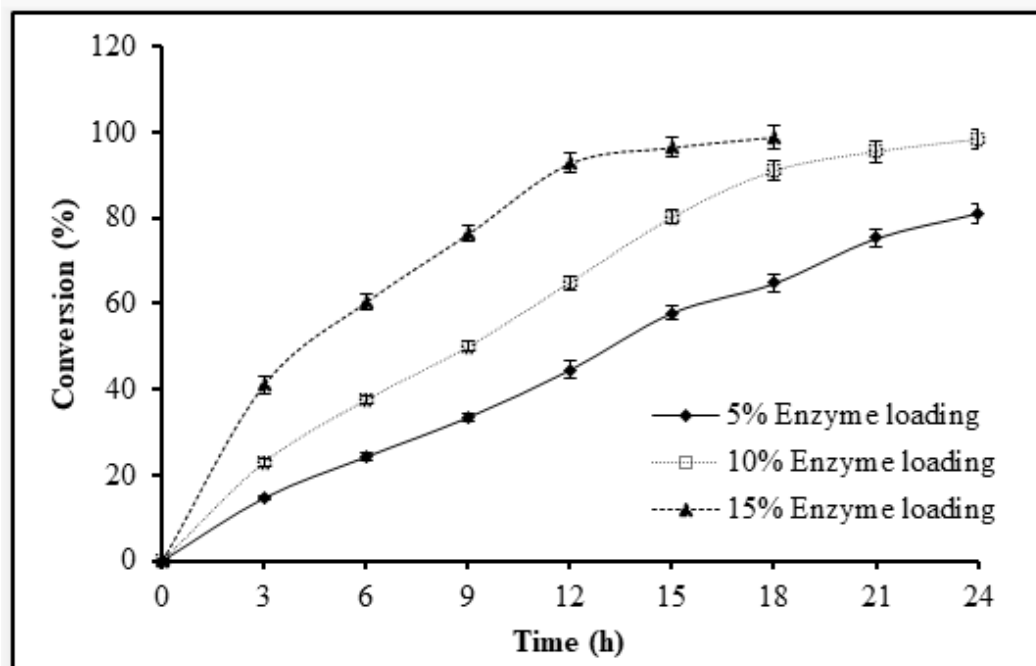


Figure 4.32 Consequences of enzyme loading in transamination of 1-(3-methylphenyl) ethan-1-one to (1R)-(3-methylphenyl)ethan-1-amine

If the addition of enzyme is lower, then reaction can be compensated by addition of some extra enzyme and continuing the process for some extra time with control of all parameters [143]. Further, if addition of enzyme is greater than the reaction can be harvested earlier [84, 144]. Both the conditions will add on to the processing cost.

#### 4.3.5.2 Progress of reaction with substrate loading

The transamination was assessed at substrate loading of 25, 50 and 75 g/L, at 10% enzyme loading,  $45 \pm 2^\circ\text{C}$ , pH 8.0 for 24 hours of incubation. With an increase in substrate loading a significant reduction in conversion (%) and progress of this transamination reaction was seen. If the addition of substrate reduces below the optimal level (25 g/L) then the reaction will proceed quickly, whereas higher substrate loading above 50% will cause the reaction progress slowly and achieve the conversion in higher time. The conversion (%) and actual yield (%) of (1R)-(3-methylphenyl)ethan-1-amine at 25g/L (lower level), 50g/L (actual point) and 75g/L

(higher level) were  $99.21\pm 2.08\%$ ,  $99.18\pm 2.08\%$  and  $78.52\pm 2.62\%$ , and  $77.32\pm 1.21\%$ ,  $78.30\pm 1.15\%$  and  $63.08\pm 0.98\%$ , respectively (figure 4.33).

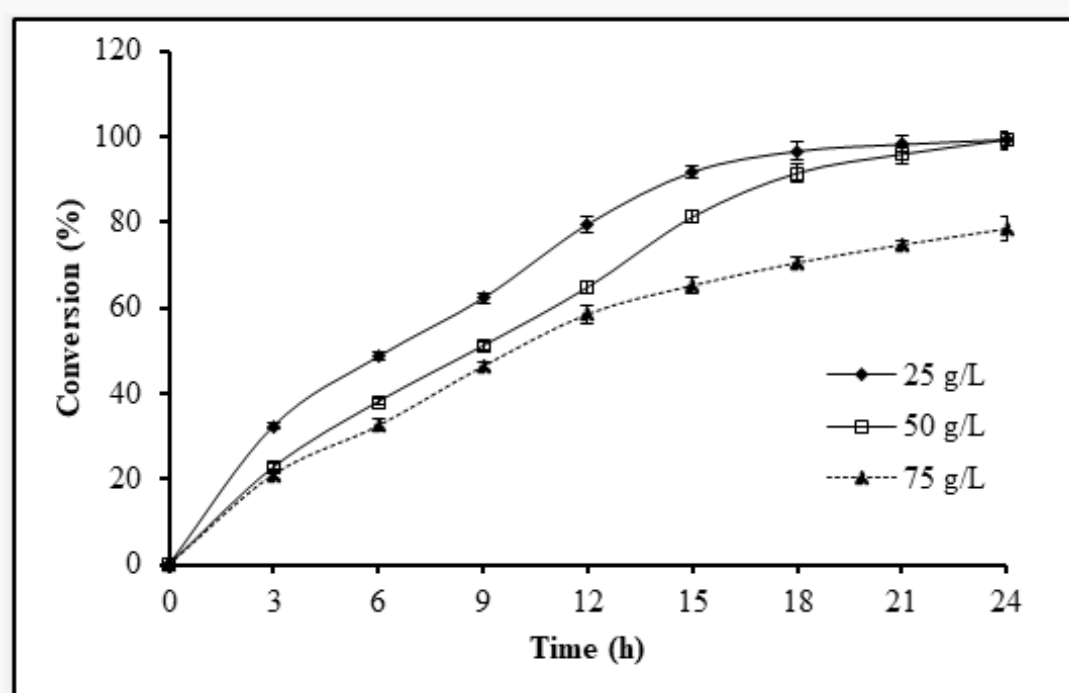


Figure 4.33 Consequences of substrate loading in transamination of 1-(3-methylphenyl) ethan-1-one to (1R)-(3-methylphenyl)ethan-1-amine

If the addition of substrate is lower, then reaction can be taken forward by incorporation of extra substrate and continuing the process for some extra time with control of all parameters [145]. On the other hand, if addition of substrate is higher than the reaction can be continued by increasing the reaction volume and indirectly diluting the substrate concentration to desired levels [84].

#### 4.3.5.3 Progress of reaction with temperature

The transamination of 1-(3-methylphenyl)ethan-1-one to (1R)-(3-methylphenyl)ethan-1-amine was analyzed at 35°C, 45°C, and 55°C, at 10% enzyme loading, 50 g/L substrate loading, pH 8.0 for 24 h of incubation. The conversion (%) and actual yield (%) at 35°C (lower level), 45°C (actual point) and 55°C (higher level) were

81.41±2.31%, 99.26±2.20% and 64.18±2.25%, and 63.30±0.84%, 77.30±1.76% and 49.20±0.79%, respectively (figure 4.34).

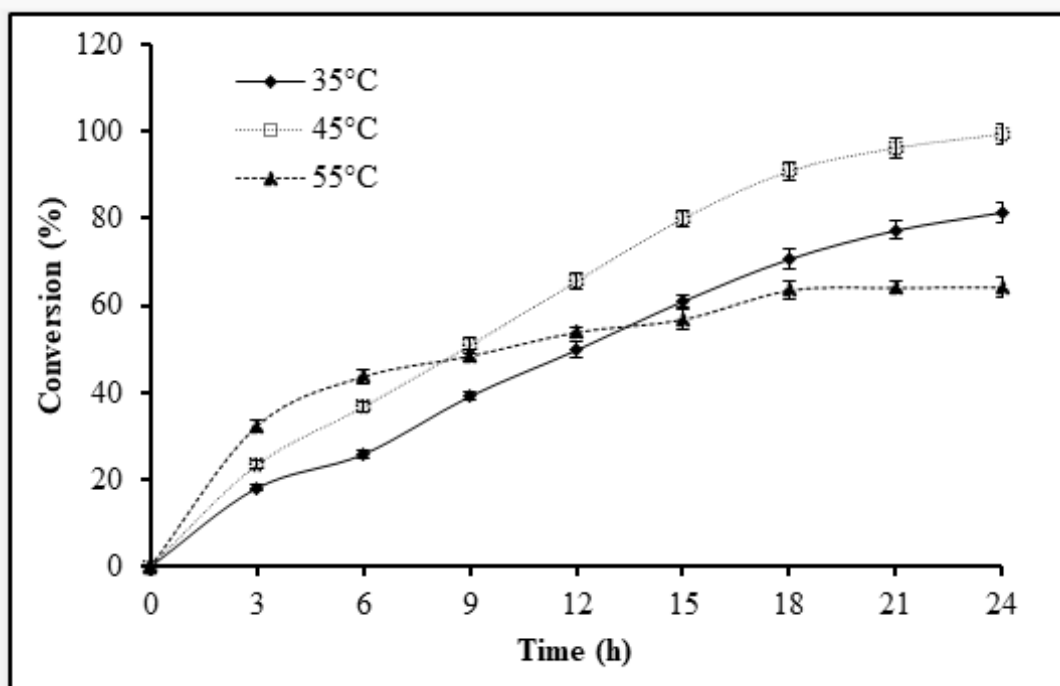


Figure 4.34 Consequences of operating temperature in transamination of 1-(3-methyl phenyl)ethan-1-one to (1R)-(3-methylphenyl)ethan-1-amine

If the temperature reduces below optimum point, then reaction can be taken forward by continuing the incubation but the time required for completion will be much longer. This can be compensated by increasing the temperature till ambient point followed by incubation till end point. Alternatively, if the temperature is more the enzyme may get inactivated due excess heat [92, 140]. This reaction can be compensated by reducing the temperature till ambient point, and adding certain amount of enzyme and maintaining a desired pH value followed by incubation till end point.

#### 4.3.5.4 Progress of reaction with medium pH

The transamination was assessed at pH values of 6.5, 8.0 and 9.5, at 10% enzyme loading, 50 g/L substrate loading, 45±2°C, and pH 8.0 for 24 hours of incubation.

The conversion (%) and actual yield (%) of (1*R*)-(3-methylphenyl)ethan-1-amine at 6.5 (lower level) and 9.5 (higher level) were 38.78±1.91%, 99.13±1.98% and 47.52±2.01%, and 29.60±0.69%, 77.24±1.14% and 35.92±0.98%, respectively (figure 4.35).

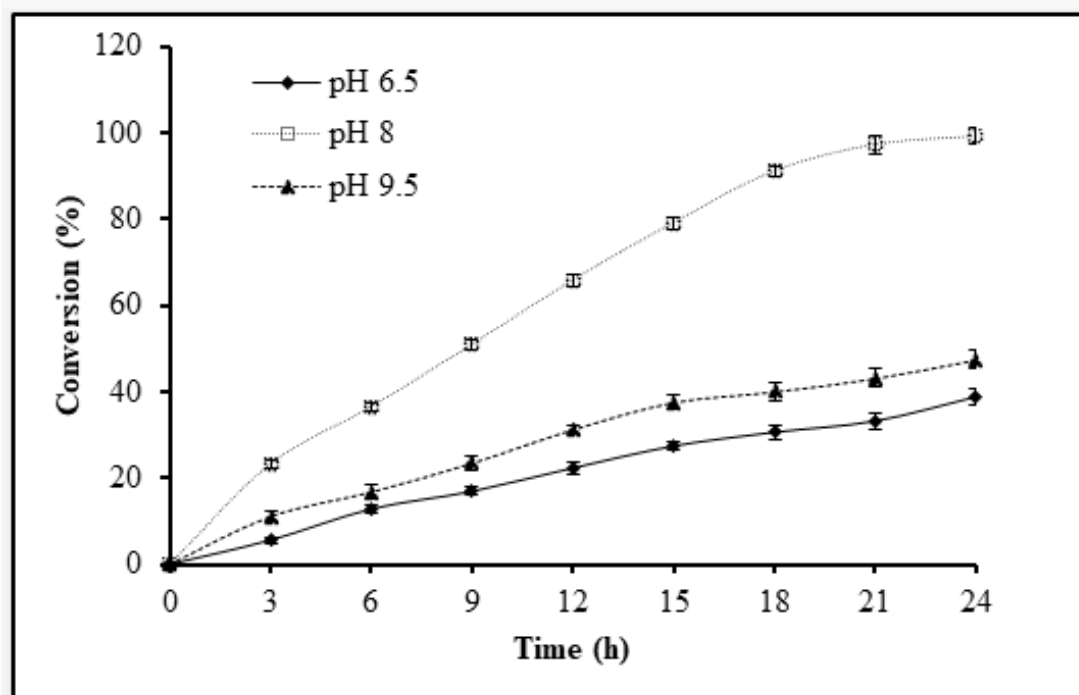


Figure 4.35 Consequences of medium pH in transamination of 1-(3-methylphenyl)ethan-1-one to (1*R*)-(3-methylphenyl)ethan-1-amine

If there is a drastic reduction or increment in pH from the optimum point, then the enzyme may lose its activity based on severity of pH variation [146]. In these cases, the reaction can be taken forward by adjusting the pH with 4M *iso*-propylamine or 6N HCl to a desired point and incorporating certain amount of enzyme followed by incubation till end point with strict maintenance of processing parameters [147].

#### 4.4 Conclusion

Different commercial transaminases were screened for chiral selective transamination of (1*R*)-(3-methyl phenyl) ethan-1-amine from 1-(3-methyl phenyl)

ethan-1-one. ATA-025 was found to be the best enzyme for chiral selective transamination with 10% (V/V) dimethylsulfoxide as an effective co-solvent. The process was then optimized with 1 factor at a time approach and Box-Behnken design of RSM, and the optimal parameters were 10% ATA-025 loading, 50 g/L substrate loading,  $45\pm 2^\circ\text{C}$  and a pH of 8 yielding  $99.02\pm 2.61\%$  conversion,  $\geq 98.5\%$  chiral selectivity, and an actual yield of  $76.85\pm 1.01\%$ , and 5% ATA-025 loading, 36.78 g/L substrate loading,  $42.66^\circ\text{C}$  and a pH of 8.2 yielding 96.12% conversion,  $\geq 98.5\%$  chiral selectivity, and an actual yield of 73.12%, respectively. The isolated and purified product was confirmed instrumentally with RP-HPLC, and chiral purity with Chiral-GC, and then characterized with instrumental methods using boiling point, LC-MS, ATR-FTIR, and  $^1\text{H}$  NMR. The findings of 'What If' studies (generally termed as negative studies) performed by investigating timely progress of reaction on gram scale batches by drastically changing the process parameters revealed a drastic reduction in the conversion (%) and yield (%) of final product and further needs subsequent modification in process variables to achieve desired results. The chiral amine synthesized by facile and novel enzymatic approach with an optimized process could be further used for synthesis of various active pharma entities.

## **CHAPTER-5**

**SCREENING OF COMMERCIALY AVAILABLE NITRILASES FOR  
THE CONVERSION OF 2-CHLORO ISONICOTINONITRILE TO 2-  
CHLORO ISONICOTINIC ACID AND PROCESS OPTIMIZATION**

## Chapter 5

### 5.1 Introduction

2-Chloroisonicotinic acid is a vital pharmaceutical ingredient due to its unique anti-inflammatory property [148], and acts as a primary derivative in synthesis of active drug intermediates like Homocamptothecin derivative and anticancer agent Diflomotecan [149], (phenylmorpholinyl)pyrimidinones [150], trans-N-[1-(2-fluorophenyl)-3-pyrazolyl]-3-oxospiro-[6-azaisobenzofuran-1(3H),10-cyclohexane]-40-carboxamide [151], and 11-oxo-11 H-pyrido[2,1-b]quinazoline-7-CA [152], as well as some monocomposite films. The 2-chloroisonicotinic acid is synthesized by using isonicotinic-N-oxide, phosphorous pentachloride and phosphorous oxychloride [153]. This method requires harsh chemicals and conditions during operation and this leads to product with very less yield and some impurities. Further, there are risks during processing and operation, may add on to environmental burdens, and may also cause deterioration of process reactor [67]. Nowadays, biocatalysis based alternative to chemical process and/or synthesis for hydroxylation by nitrilases are becoming highly popular, due to stereo-, chemo-, and regio- selectivity, and substrate specificity [154].

Nitrilases (E.C. 3.5.5.1) belong to hydrolases class of enzymes which has acquired tremendous focus due to unique capability of hydrolyzing a wide array of nitriles and yielding important CA and amides by carbon chain extension at ambient processing conditions [155]. The wide application of nitrilases including synthesis of CA, drug intermediates, nicotinamides, cyanoverlamide, and valuable amides like acrylamide with specific chiral center have been explored in a review by [154]. Although nitrilases are green, versatile, and specific biocatalysts for numerous catalytic and transformation process and reactions, their stability during process and unit operations along with kinetic and thermal instability, and reusability are major



bottlenecks for exploring them on commercial scale [98, 156]. The mentioned challenges and/or problems for application of nitrilases can be resolved by stabilization and immobilization. The various approaches previously used for immobilization of nitrilases includes entrapment in polysaccharide matrices like agar, carrageenan, and alginate [157], encapsulation in zeolite imidazole framework-90 [158], covalent attachment on SiO<sub>2</sub> nanoparticles [159], cross linking using glutaraldehyde [160, 161], and more of the same.

In current times, the cross-linked aggregates of enzymes (CLEAs) gathered invigorating awareness of worldwide researchers to ameliorate as one step direct carrier independent crosslinking or immobilization process [160, 162]. In addition to simplicity, facile nature and robustness, the retardation to heat, organic solvents, and proteolysis are extra added features [163]. The preparation protocol for CLEAs is unique as it can be performed with partially purified enzyme/s. Further, the enzyme/s can be partially purified and immobilized in single unit operation of the preparation process [164]. Previous reports have stated a superior volumetric productivity, better operational stability, ease in recovery for repeated application, and eco-friendly nature of CLEAs for desired industrial applications over the native free form [165]. Although CLEAs have numerous benefits, the limitations such as (i) a broad distribution of of particle size, (ii) poor mechanical stability, (iii) non-uniform crystallinity cannot be ignored [166]. These problems mainly alter the reaction kinetics, mass transfer, leaching out of enzymes, and drop in enzyme activity [160, 161].

The formation of CLEAs is carried out by firstly precipitating the enzyme in active state under non-denaturing conditions followed by covalent cross linking with bifunctional cross-linking entity such as citric acid, formaldehyde, and glutaraldehyde [167, 168]. Solutions or enzyme formulations with lower content of

protein can be also be processed with additives like bovine serum albumin, polylysine, and other proteins [164]. It is worth noticing that the activity of CLEAs with lower activity can also be enhanced with application of surfactants such as Triton X-100, sodium dodecyl sulphonate, and Tween 80 [169]. Further, the parameters involved in governing the characteristic features of CLEAs are amount of protein loading, nature and concentration of additives and precipitant used, concentration of cross linker, period of cross linking, pH and temperature of medium used for CLEAs preparation [138]. Therefore, the optimization of parameters used for CLEAs preparation is utmost importance, and this can be achieved by one variable at a time method or statistical method using response surface methodology as an approach [92]. Earlier, the one variable at a time method was used for preparation of acrylamidase-CLEAs [138], cutinase-CLEAs [170], nitrilase-CLEAs [160, 171], formate dehydrogenase-CLEAs [172], lipase-CLEAs [173], amongst many others. On the other side, statistical method using response surface methodology was previously used for lipase-CLEAs [92],  $\beta$ -mannanase-CLEAs [165], cellulase-CLEAs [174], esterase-CLEAs [175], hydroxy nitrile lyase-CLEAs [176], amongst others reported in literature.

Here in the said investigation, we have firstly screened different nitrilases for hydroxylation of 2-chloro isonicotinonitrile to 2-chloro isonicotinic acid. The best enzyme hit was taken forward to introduce superior pH stability, thermal stability and reusability by carrier free immobilization with glutaraldehyde. The nitrilase-CLEAs were prepared by screening the best precipitating agent and optimizing glutaraldehyde concentration and period of cross linking. Further, instrumental characterization such as particle size, SEM, FTIR, and SDS PAGE analysis followed by enzyme kinetics, pH and temperature optima and stability also studied. Finally, the prepared nitrilase-CLEAs were assessed as a biocatalyst for hydroxylation of 2-

chloroisonicotinonitrile to 2-chloroisonicotinic acid, and the effect of parameters involved in hydroxylation (enzyme loading and temperature) were investigated with progression of incubation period. According to the information and knowledge, the described section *i.e.*, hydroxylation of 2-chloro isonicotinonitrile to 2-chloro isonicotinic acid is being reported for the first time in literature.

## **5.2 Material and methods**

### **5.2.1 Screening of nitrilases for hydroxylation of 2-chloro isonicotinonitrile to 2 – chloro isonicotinic acid**

A total of 40 nitrilases were screened for hydroxylation of 2-chloro isonicotinonitrile to 2-chloro isonicotinic acid. For this, nitrilase (25 mg) was added slowly in 900  $\mu$ L of potassium phosphate buffer pH 7.5, 0.1M with proper care to prevent foam formation. After this, substrate (50 mg dissolved in 100  $\mu$ L dimethyl sulfoxide) was added slowly to above, and the resulting reaction mass was incubated at  $30\pm 2^{\circ}\text{C}$  on a thermomixer for 24 hours and 1000 rpm. The reaction was stopped by adjusting the pH to 2-2.5 with 6 M solution of HCl, and the samples were extracted in dichloromethane ( $3 \times 1$  mL). The collected organic layers were pooled together and dried under reduced pressure by evaporation. Further, the dried samples were dissolved and diluted to a final concentration of 0.25 mg/mL with a mixture of 0.1% TFA in water (55%) and acetonitrile (45%), followed by filtration through 0.45  $\mu$ m filter, and analyzed on C18 column (Inert sustain AQ-C18 (5 $\mu$ m  $\times$  4.6  $\times$  250 mm)) HPLC system (Shimadzu LC-2030C 3D plus, Japan). The mobile phase used was 0.1% TFA in water: acetonitrile :: 55:45, column temperature was  $30\pm 2^{\circ}\text{C}$ , flow rate was 1 mL/min, and detection at 210 nm with a run time of 20 min. The enzyme yielding maximum product formation was selected for preparation of CLEAs and further scale-up studies.

## 5.2.2 Preparation of nitrilase-CLEAs

### 5.2.2.1 Step 1: Precipitation of nitrilase

Various miscible organic solvents like acetone, acetonitrile, 1,4-dioxane, N,N-dimethylformamide, dimethylsulfoxide, ethanol, *iso*-propanol, methanol, and *n*-propanol were screened for the precipitation of nitrilase in active form [161]. For this, chilled organic solvents were added drop wise from the side of tube to a chilled enzyme solution (5 mg/mL in 0.1M potassium phosphate buffer pH 7.5, 0.127 U/mg), and incubated on ice bath with intermittent shaken. These tubes were then centrifuged (Remi centrifuge, Model C-24PLUS, Remi Elektrotechnik, Ltd., Vasai, India) at  $6000 \times g$ , for 10 min at  $4 \pm 2^\circ\text{C}$ . The collected precipitate was assessed for nitrilase activity and the activity recovery of nitrilase after precipitation was enumerated as

$$\begin{aligned} & \text{Nitrilase activity recovery (\%)} \\ &= \frac{\text{Activity of nitrilase after precipitation}}{\text{Activity of nitrilase in free form}} \times 100 \end{aligned}$$

### 5.2.2.2 Step 2: Cross-linking of nitrilase

The optimization of cross-linking of nitrilase with glutaraldehyde was performed with one variable at a time approach by considering two parameters namely glutaraldehyde concentration (5-45 mM) and cross-linking time (0-140 min) for the best probable recovery of nitrilase. The nitrilase-CLEAs formation after cross-linking with glutaraldehyde with optimal concentration and ambient time were recovered by centrifugating at  $6000 \times g$ , for 10 min at  $4 \pm 2^\circ\text{C}$ , and were assessed for its activity. The activity recovery of nitrilase after cross linking was enumerated as

$$\text{Nitrilase activity recovery (\%)} = \frac{\text{Activity of nitrilase in CLEAs}}{\text{Activity of nitrilase in free form}} \times 100$$

### 5.2.3 Determination of nitrilase activity and protein content

The standard activity of free nitrilase and nitrilase-CLEAs was calculated by using mandelonitrile (30 mM) as a substrate as explained by [177]. In a reaction mixture of 2 mL, nitrilase (5 mg) was added slowly in 1.8 mL of potassium phosphate buffer (pH 7.0, 0.1M) with proper care to prevent foam formation followed by addition of substrate (200  $\mu$ L in DMSO). The resulting reaction mixture was incubated on a thermomixer for 30 min at  $30\pm 2^\circ\text{C}$  and 1000 rpm. The reaction was stopped by adding 100  $\mu$ L 2 M HCl solution, and the samples were extracted in dichloromethane ( $3 \times 1$  mL). The organic layers were collected, combined and dried by evaporation under reduced pressure. Further, the dried samples were dissolved and diluted to a final concentration of 0.25 mg/mL with a mixture of 0.1% TFA in water (60%) and acetonitrile (40%), followed by filtration through 0.45  $\mu$ m filter, and analyzed on C18 column on a HPLC. The mobile phase used was 0.1% TFA in water : acetonitrile :: 60:40, column temperature was  $30\pm 2^\circ\text{C}$ , flow rate was 1 mL/min, and detection at 210 nm with a run time of 20 min. One unit of nitrilase activity was defined as the quantity of enzyme required for production of 1  $\mu$ mol of mandelic acid per min at standard defined conditions of pH, temperature, and buffer strength. The soluble protein content was quantified by Bradford method [178].

### 5.2.4 Instrumental characterization

The size of prepared nitrilase-CLEAs was estimated with DLS-Particle size analyzer as statistical diameter. The shape, structure and morphology of external surface of nitrilase-CLEAs was seen with SEM. The distinctive variations in functional, characteristic and structural groups of free nitrilase and nitrilase-CLEAs were studied with ATR-FTIR spectrophotometer. The comparative molecular weight of free nitrilase and nitrilase-CLEAs was determined by SDS-PAGE assembly using

12% polyacrylamide (1:29:1:: bisacrylamide:acrylamide) in 250 mM glycine and 25 mM tris electrophoretic buffer (pH 8.2, 0.1% SDS).

### **5.2.5 Kinetic parameters of free nitrilase and nitrilase-CLEAs**

The kinetic parameters of free nitrilase and nitrilase-CLEAs were enumerated by determining the activities at different concentrations of mandelonitrile in a regime of 1-20 mM. The Michaelis-Menten equation and Lineweaver-Burk double reciprocal plot were utilized for estimation of kinetic parameters.

### **5.2.6 Biochemical characterization**

#### **5.2.6.1 pH optima and pH stability**

The pH optima were determined by measuring the activity of free nitrilase and nitrilase-CLEAs at  $30\pm 2^\circ\text{C}$  in 100 mM buffers systems with varying pH regime (4-10). The pH stability was quantified by incubating free nitrilase and nitrilase-CLEAs in 100 mM buffers with a varying pH domain of 4-10 for 24 h at  $30\pm 2^\circ\text{C}$ .

#### **5.2.6.2 Temperature optima and thermal stability**

The temperature optima were analyzed by measuring the activity of free nitrilase and nitrilase-CLEAs in 100 mM potassium phosphate buffer (pH 7.0) in varying temperature domain of 25-65°C. Further, the thermal stability was determined by incubating free nitrilase and nitrilase-CLEAs in 100 mM potassium phosphate buffer (pH 7.0) with a varying temperature domain of 4-10 for 24 h at  $30\pm 2^\circ\text{C}$ .

#### **5.2.6.3 Application of free-nitrilase and nitrilase-CLEAs for hydroxylation of 2-chloro isonicotinitrile to 2-chloro isonicotinic acid**

The reaction set-up with pH stat was adjusted. The substrate was prepared by adding 50 g of 2-chloroisonicotinonitrile in 50 mL dimethyl sulfoxide. In a reaction vessel, 450 mL potassium phosphate buffer (100 mM, pH 7.5) was added and stirring was started and temperature was maintained at  $30\pm 2^\circ\text{C}$ . The pH stat was started and

maintained at 7.5 with 10% NaOH solution, followed by addition of 5 g enzyme (10%). Further, the reaction was initiated by slow addition of substrate (within 1-2 h) with continuous stirring and maintenance of pH. The reaction was monitored for 24 h by HPLC (as mentioned above). The reaction mixture was filtered through Whatman filter paper no. 42 to isolate the nitrilase-CLEAs. This filtration step was excluded for free nitrilase. The pH of the filtrate was adjusted to 11-12 with 20% NaOH solution, followed by extraction in dichloromethane ( $2 \times 1$  volume) to remove un-reacted 2-chloroisonicotinonitrile. Further, the pH of collected aqueous layer was adjusted to 2-2.5 with 6 M HCl solution, and this was extracted in dichloromethane ( $3 \times 1$  volume). The collected organic layers were combined and distilled on rotary evaporator (model RV 8V, IKA® India Private Limited, Bangalore) at 45-50°C under vacuum. The product i.e. 2-chloroisonicotinic acid was recovered, dried in vacuum tray dryer for 20-22 h at 45-50°C under vacuum, and the yield was calculated on molar basis. Finally, the effect of reaction parameters namely enzyme loading (5%, 10% and 20%) and temperature (25°C, 30°C, 35°C and 40°C) linked with hydroxylation process were optimized with one factor at a time approach.

#### **5.2.6.4 Instrumental characterization of 2-chloroisonicotinonitrile and 2-chloroisonicotinic acid**

Along with HPLC, the confirmation of 2-chloroisonicotinonitrile and 2-chloroisonicotinic acid was done by FTIR,  $^1\text{H}$  NMR, AND LC-MS analysis. The FITR was performed on ATR-FTIR. LC-MS was carried out by using the same mobile phase on C18 column. (LCMS 2020, Shimadzu, Japan)).  $^1\text{H}$  NMR was recorded on NMR (Varian 400 MR, NMR spectrometer, USA) by dissolving both the compounds in DMSO.

### **5.2.7 Reusability studies of nitrilase-CLEAs**

The reusability potential of nitrilase-CLEAs was assessed by their subsequent use in repeated batches of hydroxylation reaction as mentioned above. The recovery of nitrilase-CLEAs was done by filtration and then washing by 0.1M potassium phosphate buffer of pH 7.5 to remove any impurities adhered on them. After each batch, the conversion (%), product (g/L) and yield (%) were calculated.

### **5.2.8 Statistical analysis**

All the experimental reactions were carried out three times and the obtained findings are expressed as average  $\pm$  standard errors. The resultant data was examined on Microsoft Excel, 2013, and SPSS Version16 by using one way ANOVA to assess the differences in mean and statistically significant differences amongst the observed average values established at  $p \leq 5\%$  and Dunnett's post hoc test.

## **5.3 Results and discussion**

### **5.3.1 Screening of nitrilases for hydroxylation of 2-chloro isonicotinitrile to 2-chloroiso nicotinic acid**

The hydroxylation of 2-chloro isonicotinitrile to 2-chloro isonicotinic acid was carried out by enzymatic pathway using nitrilase to overcome the limitations of chemical route which include harsh treatment with corrosive acids and alkalies, high processing temperature, discharge of toxic compounds, amongst many others, leading to lower yield, and purity [67]. The enzymatic route may impart higher specificity, metal free reactions under mild conditions, minimum requirement of energy, less by product formations, and many others. For the hydroxylation of 2-chloro isonicotinitrile to 2-chloro isonicotinic acid, 40 nitrilases were screened at 50% enzyme loading and 10% dimethylsulfoxides as co-solvent in the potassium phosphate buffer. Amongst the nitrilases investigated, ES-NIT-102, ES-NIT-103, ES-NIT-129, ES-NIT-131, ES-NIT-132 and ES-NIT-138 have shown promising



conversion of 90%, 85%, 80%, 71%, 29%, and 78% after 24 hours of incubation, and the yield at the end of the reaction was 86.9%, 82.1%, 77.3%, 68.6%, 28%, and 75.3%, respectively (*Table 5.1*).

*Table 5.1 Screening of nitrilases for hydroxylation of 2-chloro isonicotinitrile to 2-chloro isonicotinic acid*

Sr. No.	Enzyme	Time (h)	Conversion (%)	Yield (%)
1	ES-NIT-102	24	90	86.9
2	ES-NIT-103	24	85	82.1
3	ES-NIT-129	24	80	77.3
4	ES-NIT-131	24	71	68.6
5	ES-NIT-132	24	29	28
6	ES-NIT-138	24	78	75.3

*Reaction conditions: 50 mg substrate (50g/L, in 10% DMSO solution), 25 mg enzyme (50% loading), 900  $\mu$ L potassium phosphate buffer of pH 7.5, 0.1M, 1000 rpm, 30°C. Conversion was determined by HPLC analysis. Yield was calculated on molar basis.*

The other enzymes used in screening namely ES-NIT-101, ES-NIT-104, ES-NIT-105, ES-NIT-106 ES-NIT-107, ES-NIT-108, ES-NIT-109, ES-NIT-110, ES-NIT-111, ES-NIT-112, ES-NIT-113, ES-NIT-114, ES-NIT-115, ES-NIT-116, ES-NIT-117, ES-NIT-118, ES-NIT-119, ES-NIT-120, ES-NIT-121, ES-NIT-122, ES-NIT-123, ES-NIT-124, ES-NIT-125, ES-NIT-126, ES-NIT-127, ES-NIT-128, ES-NIT-130, ES-NIT-133, ES-NIT-134, ES-NIT-135, ES-NIT-136, ES-NIT-137, ES-NIT-139, ES-NIT-140 did not show any significant conversion during this hydroxylation reaction.

The higher conversion with the best enzymes could be due to the desired specificity of substrate towards its active cleft [81]. Nitrilase may show activity towards either

aliphatic nitriles, aromatic nitriles, or arylacetonitriles, and some on all [179]. In aliphatic nitriles, the short chain aliphatic di-nitriles are preferred over the medium-chain aliphatic mononitriles and aliphatic substituted mononitriles. Whereas, in aromatic nitriles, mono cyclic aromatic nitriles are more selective than the hetero cyclic aromatic nitriles [180]. This specificity could also be due to the action of specific enzymes on the specific structure of the substrate moieties [181]. Further, [182] stated that different nitrilases may act in a different way on dinitriles but they may not show similar catalytic effect on similar substrate.

From the different nitrilases studied, ES-NIT-102 was selected as an ideal candidate for carrier free immobilization because of its ability to convert maximum substrate and yield highest product formation. In addition, the selected enzyme also showed desired results for hydroxylation of 2-chloro isonicotinonitrile to 2-chloro isonicotinic acid (described below). The carrier free immobilization was performed by cross-linking the enzyme moieties together using glutaraldehyde as a bifunctional agent. Further, mandelonitrile was used as a substrate for determination of optimization parameters during preparation of nitrilase-CLEAs, its kinetics study, and biochemical characterization [183, 179].

### **5.3.2 Preparation of nitrilase-CLEAs**

The main stages engaged during preparation of CLEAs of enzymes are aggregation of proteins in their active form by precipitation followed by cross-linking with each other using a desired bi-functional agent. Here, the activity of nitrilase was determined by analyzing the conversion of mandelonitrile to mandelic acid. The standard HPLC profiles of mandelonitrile (0.25 mg/mL in 0.1% trifluoroacetic acid in water (60%) and acetonitrile (40%)), mandelic acid (0.25 mg/mL in 0.1% TFA in water (60%) and acetonitrile (40%)), and enzymatic reaction with around 90% conversion are shown in *figure 5.1, 5.2, and 5.3*

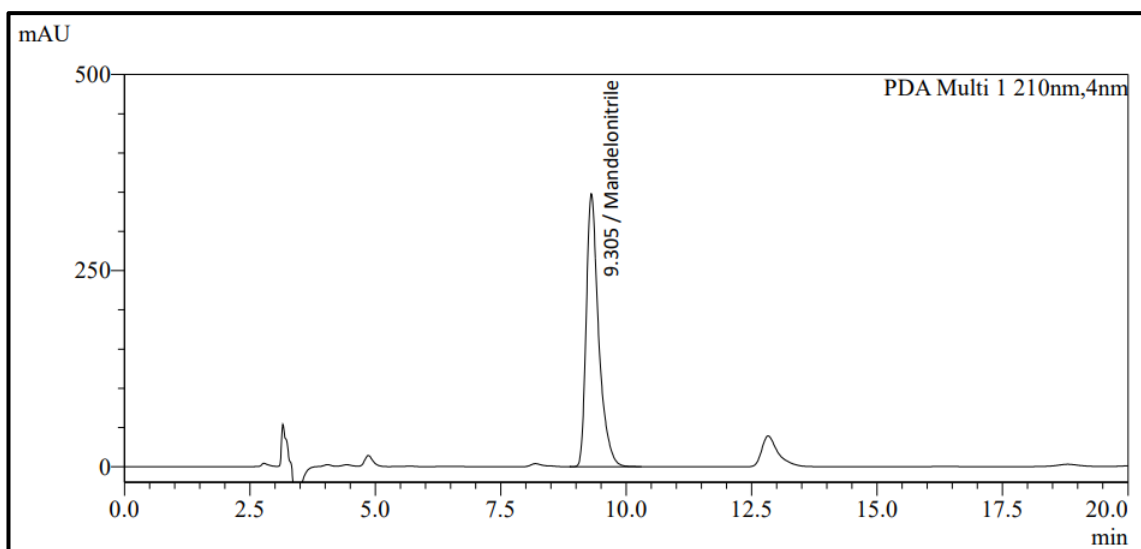


Figure 5.1 Chromatograms of standard mandelonitrile (0.25 mg/mL in 0.1% TFA in water (60%) and acetonitrile (40%)) on HPLC

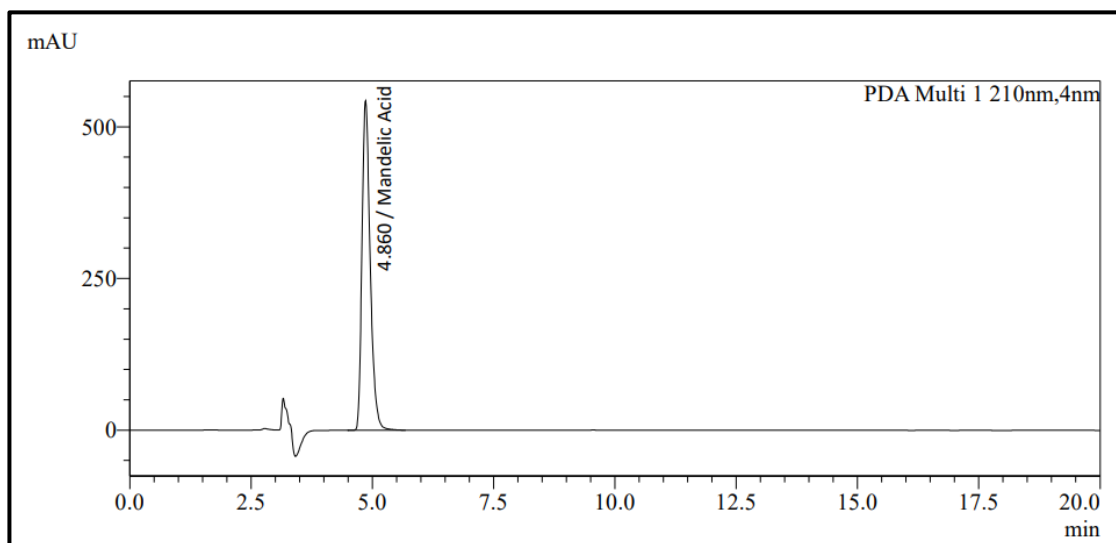


Figure 5.2 Chromatograms of standard mandelic acid (0.25 mg/mL in 0.1% TFA acid in water (60%) and acetonitrile (40%)) on HPLC

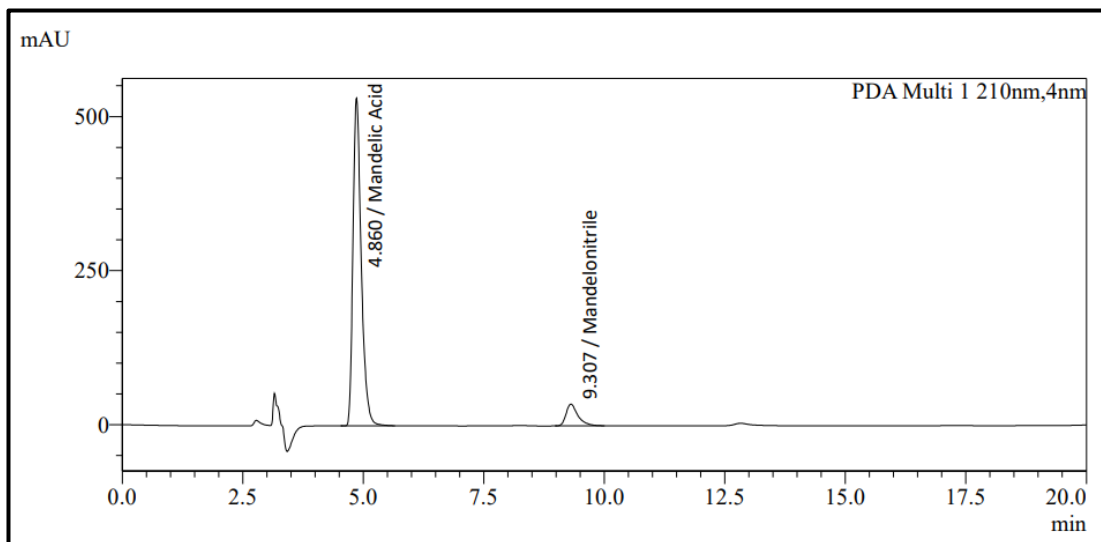


Figure 5.3 Chromatograms of enzymatic reaction with around 90% conversion on HPLC system

### 5.3.3 Precipitation of nitrilase

During precipitation *i.e.*, the first stage, enzymes are converted into aggregated state (*i.e.* insoluble form) from the free state (*i.e.* soluble form). For the maintenance of active state along with the native conformation a desired precipitating agent with proper concentration is a pre-requisite. Herein, different miscible organic solvents like acetone, acetonitrile, 1,4-dioxane, N, N-dimethylformamide, dimethylsulfoxide, ethanol, *iso*-propanol, methanol, and *n*-propanol were screened for precipitation of ES-NIT-102 in active state. Highest activity recovery of  $91 \pm 5.41\%$  and  $85 \pm 4.92\%$  with an actual activity of  $0.115 \pm 0.007$  U/mg and  $0.108 \pm 0.006$  U/mg were seen with *iso*-propanol and *n*-propanol, while least recovery of  $45.62 \pm 2.68\%$  and  $21.33 \pm 2.08\%$  with an actual activity of  $0.058 \pm 0.003$  U/mg and  $0.027 \pm 0.003$  U/mg with N, N-dimethylformamide, and acetonitrile, respectively (figure 5.4)

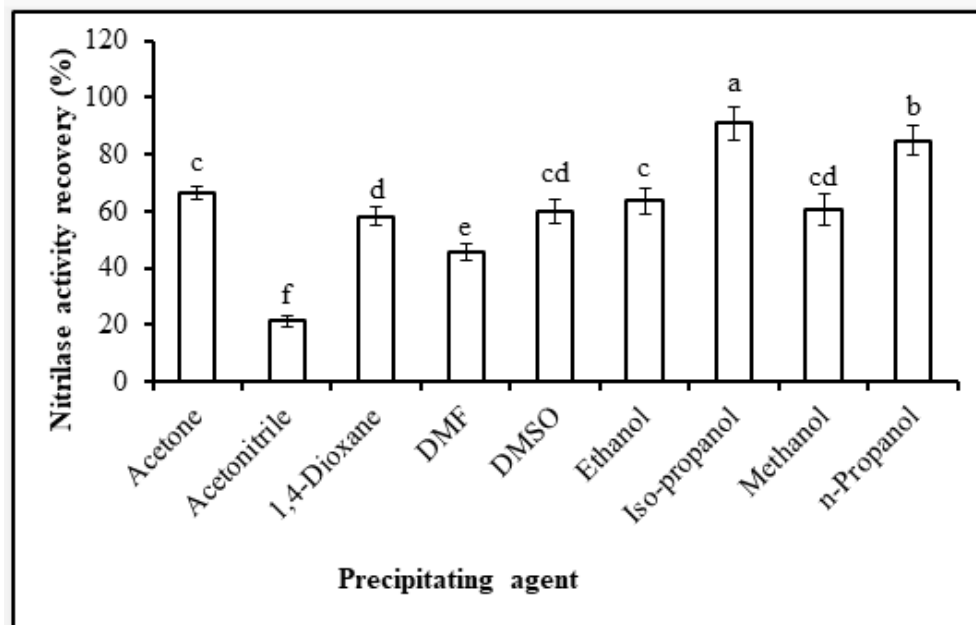


Figure 5.4 Consequences of miscible organic solvents on the recovery of nitrilase activity

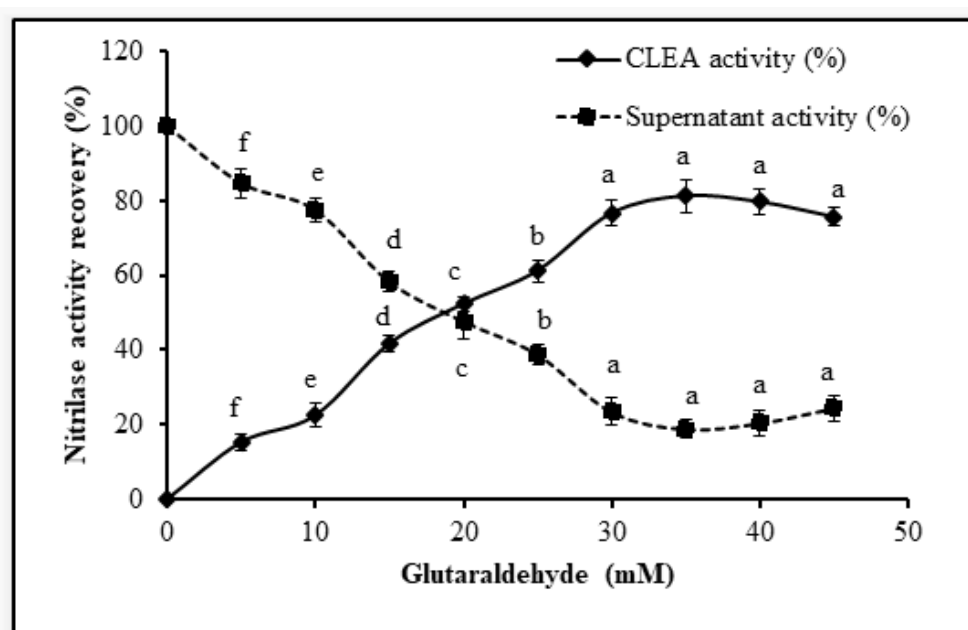
The miscible organic solvents are known for removal the aqueous layer present in the vicinity of enzyme forcing different attraction dipolar charges and electrostatic forces to cause aggregation. These solvents may also cause a displacement of polarity of the liquid medium and lead to dispersion of hydrophobic domains that may hamper the enzyme activity. This water layer plays a crucial part in maintenance of structural conformation, and hence the activity of enzyme [170]. A substantial reduction in nitrilase activity may be due to loss of active 3D structural conformation caused by deep penetration of these solvents. Previously, *iso*-propanol was also found to the best precipitating agent for nitrilase [160, 161] and it was also suitable for other enzymes like lipase [184], and cellulase from fermentation broth [185].

#### 5.3.4 Cross-linking of nitrilase

During cross linking *i.e.* the second stage, enzymes are attached with each other using a bi-functional cross linking agent such as glutaraldehyde, epichlorohydrin or

glyoxyl-containing compounds, ethylene glycol-N-hydroxysuccinimide, genipin, and many others [162, 186]. Herein, glutaraldehyde was utilized as a cross linking agent for ES-NIT-102 because of unique features like low cost, abundant availability, ease in handling and processing, and predominant ability to introduce covalent linkages with a wide array of enzymes [67, 165].

For preparing the CLEAs of nitrilase, two parameters namely glutaraldehyde concentration and period of cross-linking were optimized by 1 factor at a time aspect. The concentration of cross linking agent has a major impact on particle size, shape and operational stability of the prepared CLEAs [187]. The ambient concentration of glutaraldehyde (mM) for firm cross linking of nitrilase with each other in its active state was 35 mM. The residual activity and actual activity of ES-NIT-102 after cross linking at this concentration were  $81.26 \pm 4.51\%$  and  $0.103 \pm 0.006$  U/mg, respectively (*figure 5.5*).

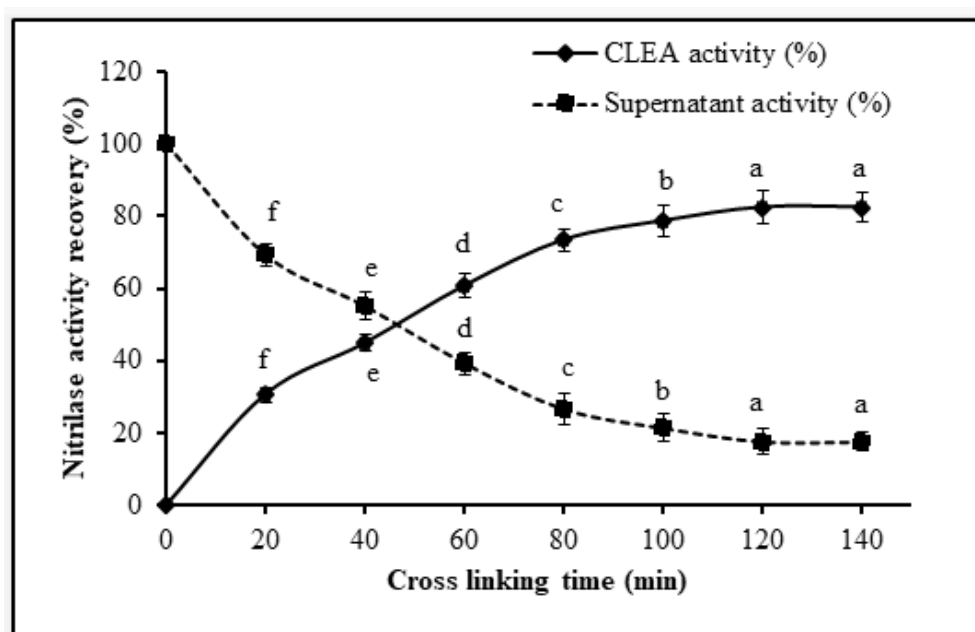


*Figure 5.5 Consequences of glutaraldehyde concentration (mM), on the preparation of nitrilase-CLEAs*

For effective activity of nitrilase, the Glu-Lys-Cys is a conformational catalytic triad, and the disturbances in this triad will hamper the active performance of the enzyme

[188]. At higher glutaraldehyde content (above 40 mM), all the nitrilase molecules could have got cross-linked with each other which might have caused excess molecular crowding due to distortion in the structural conformation. On the other hand, lower glutaraldehyde content (below 25 mM) could have not been sufficient to cross link all the nitrilases together. Previously, [160, 161, 171] reported an ambient concentration of 30 mM, 125 mM, and 20 mM for preparation of nitrilase-CLEAs from different microbial sources.

Cross linking period is other pivotal factor that majorly affects the robustness, rigidity and activity recovery of the enzyme CLEAs. The ambient duration required for cross linking nitrilase with each other in its active state was 120 min. The residual activity and actual activity of nitrilase after cross linking with 35 mM glutaraldehyde for 120 min were  $82.36 \pm 4.45\%$  and  $0.105 \pm 0.005$  U/mg, respectively (*figure 5.6*)



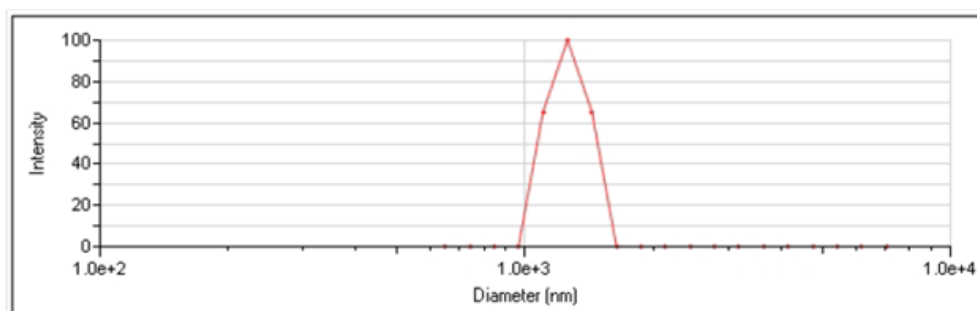
*Figure 5.6 Consequences of Cross-linking time (min) on the preparation of nitrilase-CLEAs*

A cross linking duration below or above ambient cross-linking time resulted in sparingly lower residual activity and actual activity of nitrilase. After a shorter period (below 100 min) the cross linking was incomplete, whereas prolonged cross-linking period (above 120 min) may have caused excess cross-linking and impeded the active cleft of nitrilase [93, 187].

### 5.3.5 Instrumental characterization of Nitrilase CLEAs

#### 5.3.5.1 Particle size and morphology of nitrilase-CLEAs

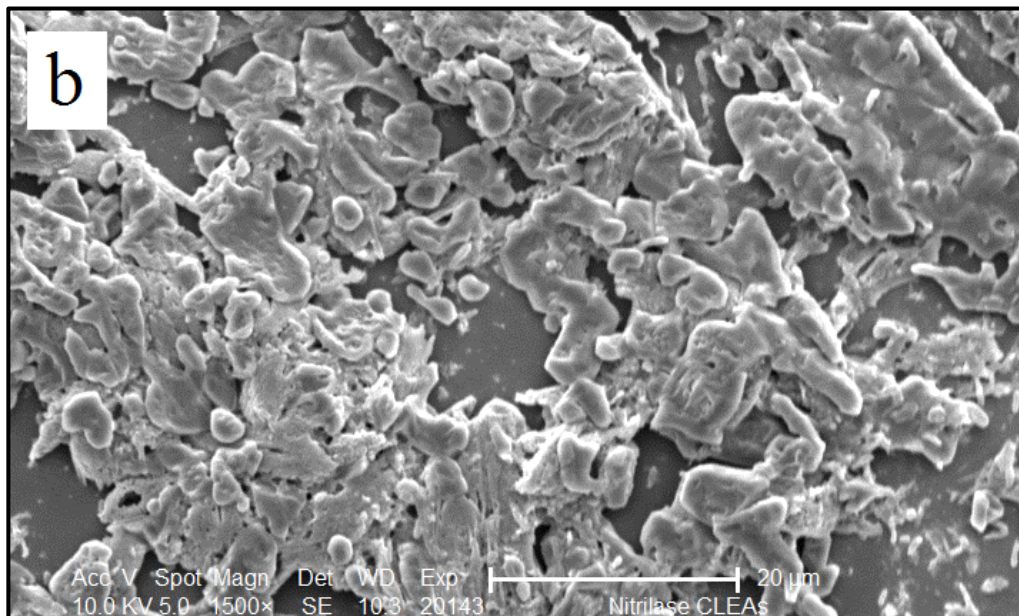
The verification of cross linking with glutaraldehyde after aggregate formation of nitrilase with *iso*-propanol was assessed by analysis of particle size and surface morphology. Particle size analysis revealed the formation of wide range of aggregates and the average particle size was 1544.93 nm and polydispersity index was 0.271 (*figure 5.7*).



*Figure 5.7 Instrumental characterization particle size distribution of nitrilase-CLEAs*

The scanning electron microscopy studies indicated the presence of abundant pores on the surface nitrilase CLEAs (*figure 5.8*)





*Figure 5.8 Scanning electron microscopic image of nitrilase-CLEAs at 1500 × magnification*

Previously, similar morphology of CLEAs was reported for nitrilase-CLEAs [160], acrylamidase CLEAs [138], formate dehydrogenase CLEAs [172], and lipase CLEAs [92].

The porosity and size of CLEAs is not only associated with type and amount of cross-linking agent and additives used, but also the steps and process followed during preparation [171]. Further, CLEAs are differentiated as Type-I (ball like spherical structures) and Type-II (less defined structures with more hydrophilicity) on the basis of degree of glycosylation of enzymes [165, 189]. The structure of prepared nitrilase-CLEAs was in a close resemblance with Type-II structure. In addition, CLEAs with less defined and large structure (Type-II) may have constrictions for transfer of substrate to active site of enzyme and vice versa. On the other hand, CLEAs with defined and small structure (Type-I) may possess challenges during recovery from the medium [121, 165].

### 5.3.5.2 FTIR analysis

The FTIR of free nitrilase (ES-NIT-102) and nitrilase-CLEAs displayed a distinguishing spectrum of usual protein with primary functional peaks in 3400–3300 (1/cm) and 1700–1600 (1/cm) region which specified the stretching of OH and/or stretching vibration of NH, CO=N–H binding, and peptide linkages, while the minor peaks at 597(1/cm) indicated S-S linkages, respectively (*figure 5.9*).

Further, cross linking of nitrilase with each other by glutaraldehyde caused a reduction in intensity of functional peaks 3400–3300 (1/cm) and 1700–1600 (1/cm). A shift in amide I bond from 1630 (1/cm) to 1640 (1/cm) due to imine reaction amongst the amino group of enzyme and aldehyde group of glutaraldehyde was also noticed. This reduction in the intensities of peak proved the alterations in conformation amide domain of enzyme structure [93]. Similar findings were also reported after preparation of  $\beta$ -mannanase CLEAs [165], and acrylamidase-CLEAs [138].

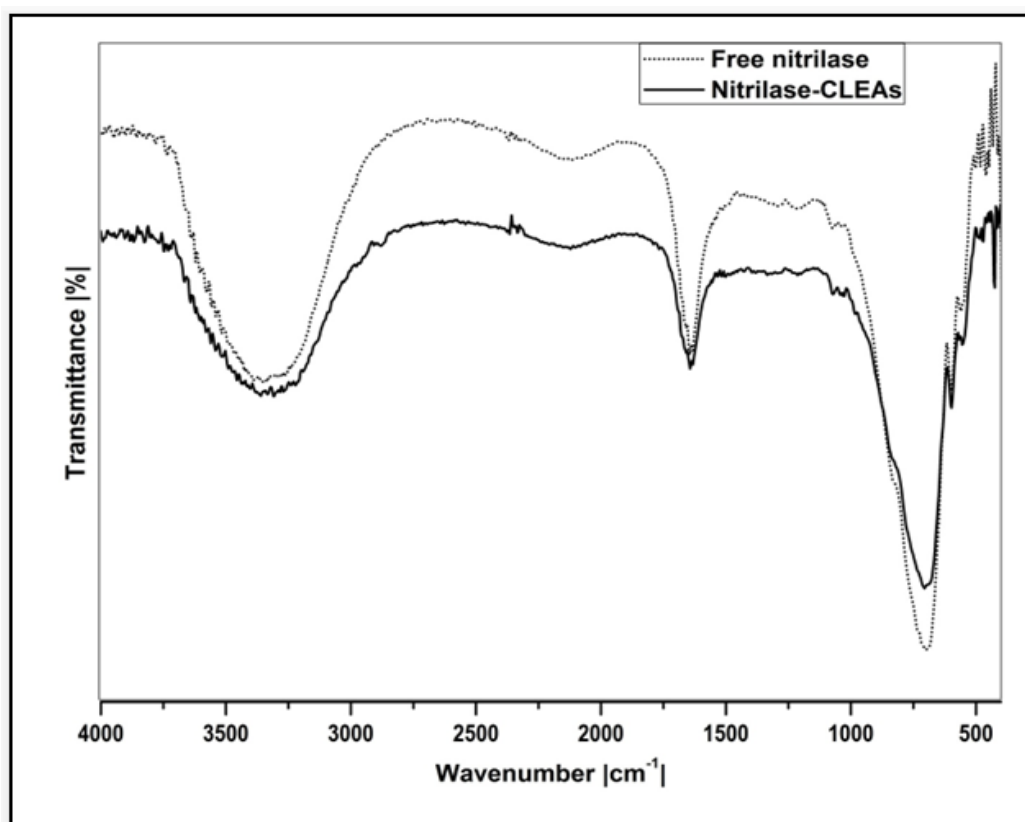
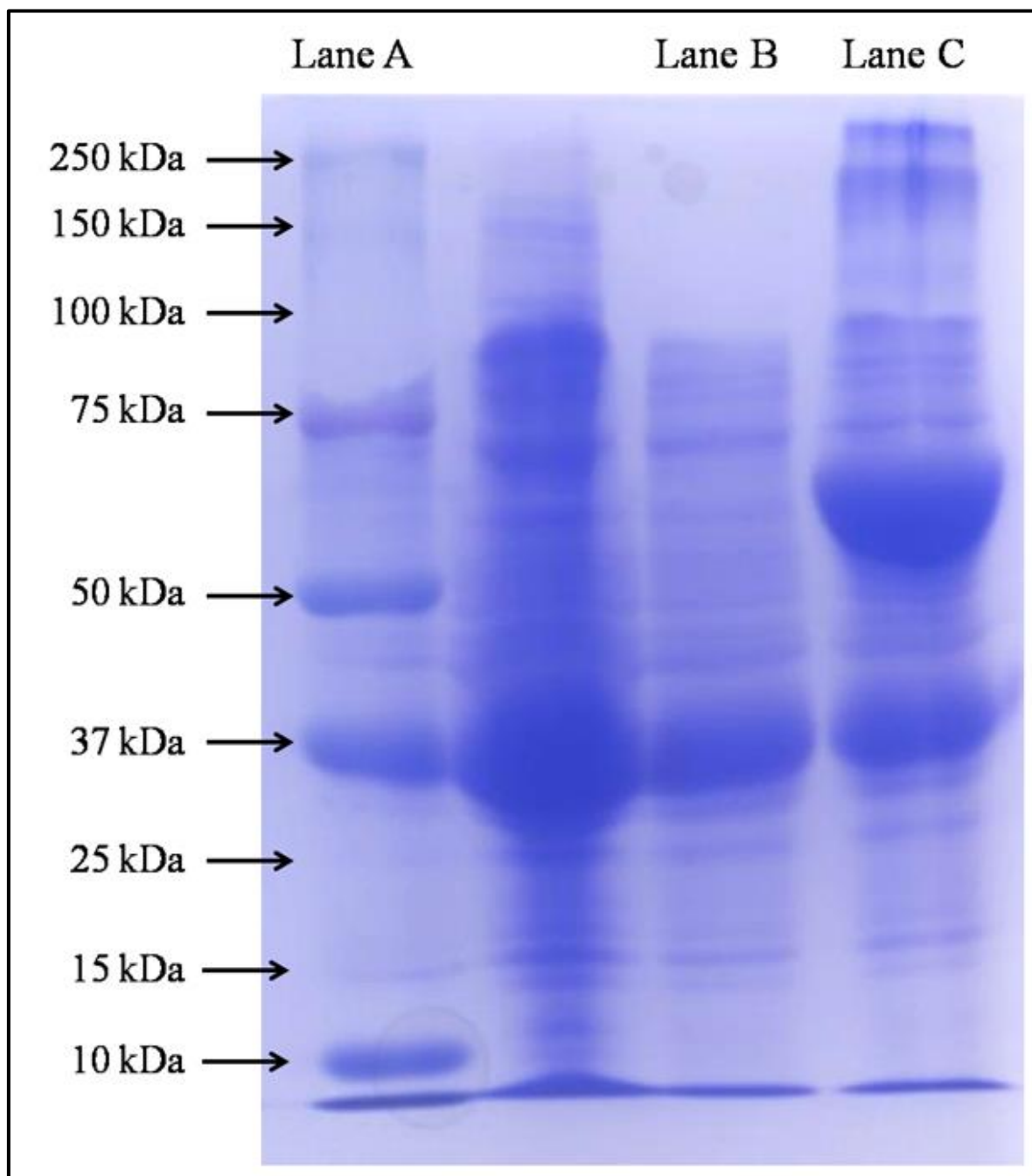


Figure 5.9 FTIR spectra of free nitrilase and nitrilase-CLEAs

### 5.3.5.3 SDS PAGE analysis

The molecular weight of free nitrilase (ES-NIT-102) and nitrilase-CLEAs was enumerated by comparing the distance migrated against the proteins with standard molecular weight in the gel. The free nitrilase showed a single prominent band whereas nitrilase-CLEAs showed four distinguishing bands with molecular weight of ~70 kDa, ~100 kDa, ~150 kDa, and ~250 kDa, (*figure 5.10*).

The molecular weight of free nitrilase was found to be ~ 37 kDa. Cross linking of nitrilase with each other using glutaraldehyde forms large molecules with higher molecular weight of ~70 kDa, ~100 kDa, ~150 kDa, and ~250 kDa, indicating successful formation of nitrilase-CLEAs. Previous reports have indicated variations in molecular weight of nitrilase and they may differ with sources. The molecular weight of nitrilase from *Arthrobacter aurescens* CYC705 was 36.7 kDa [180], nitrilase from *Pyrococcus* sp. M24D13 was 38.5 kDa [190], nitrilase from recombinant *E.coli* was 37 kDa [159], nitrilase from *Thermotoga maritima* MSB8 was 30.07 kDa [182], and nitrilase from *Paraburkholderia phymatum* was 37 kDa [98]. On the other hand, similar literature was documented after preparation of CLEAs with other enzymes such as acrylamidase [138],  $\beta$ -mannanase [165], lipase [191] amongst many others.



*Figure 5.10 SDS-PAGE analysis of free nitrilase and nitrilase-CLEAs. Lane A: standard molecular weight markers, Lane B: free nitrilase, and Lane C: nitrilase-CLEAs*

### **5.3.6 Kinetic constants**

The kinetic constants of free nitrilase (ES-NIT-102) and nitrilase-CLEAs were enumerated by Michaelis-Menten equation and using Lineweaver-Burk double reciprocal plot with a varying concentration of substrate (*figure 5.11*).

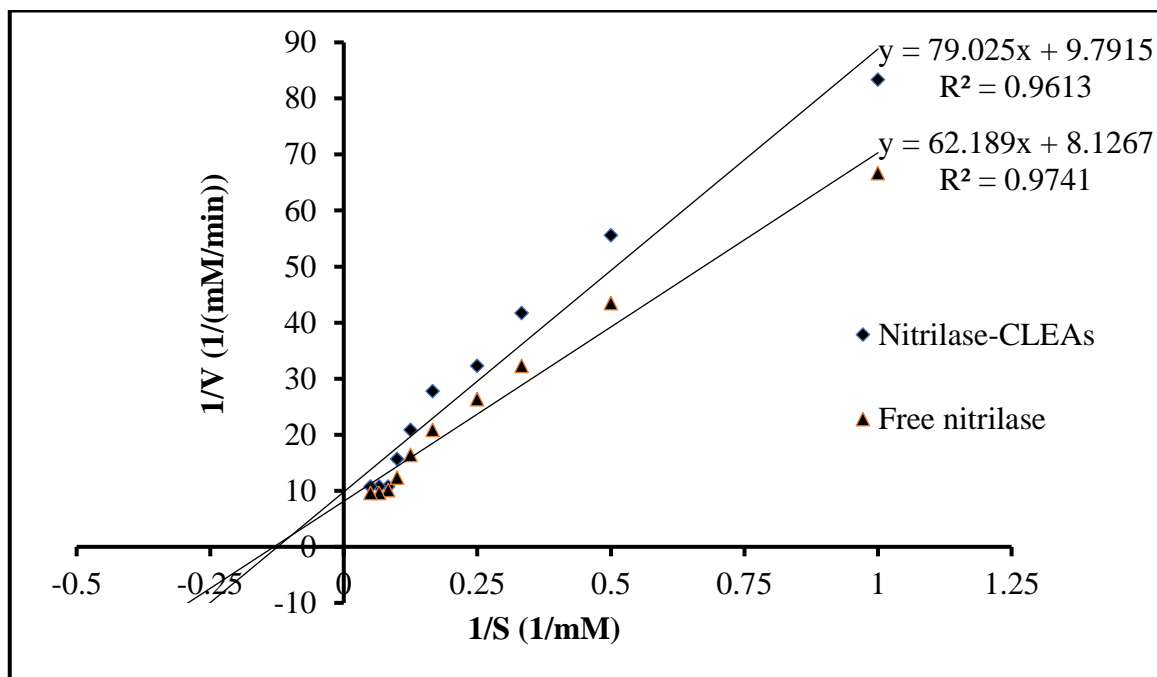


Figure 5.11 Lineweaver-Burk plot for determination of kinetic parameters of free nitrilase and nitrilase-CLEAs

The  $K_m$  values of free nitrilase and nitrilase-CLEAs were  $7.65 \pm 0.31$  mM and  $8.07 \pm 0.39$  mM. An increase in  $K_m$  values after cross linking with glutaraldehyde indicated a reduction in affinity of substrate to enzyme, and this may lead to an increased hurdle for movement of substrate to catalytic domain of the enzyme [185]. This can be further associated with a decline in conformational flexibility of enzyme after cross linking with each other and thus successively causing alterations in microenvironment in the nearby vicinity of the active domain of the enzyme [192]. The  $V_{max}$  values of free nitrilase and nitrilase-CLEAs were 0.123 and 0.102 mM/min. A slight decline in  $V_{max}$  values after cross linking may lead to a decrease in conversion of initial substrate to desired product. The current results are in accordance with previous findings of nitrilase-CLEAs and immobilized nitrilase by [155, 160, 177]. A similar phenomenon was previously recorded for esterase-CLEAs [175],  $\beta$ -mannanase-CLEAs [165], formate dehydrogenase-CLEAs [172],

acrylamidase-CLEAs [138], hydroxy nitrile lyase-CLEAs [176], and lipase-CLEAs [92].

### 5.3.7 Biochemical characterization

The reaction parameters usually practiced for carrying out enzyme mediated transformations are generally mild. The evaluation of biochemical parameters such as pH and temperature optima, along with pH and thermal stability are a prerequisite for best performance of biocatalysts, and subsequently attain subsequently higher conversion and yields of desired product/s.

#### 5.3.7.1 pH optima and pH stability

The determination of optimum pH for free nitrilase and nitrilase-CLEAs was carried out by analyzing the activity in a wide pH regime ranging from 4.0-10 at 40°C (figure 5.12).

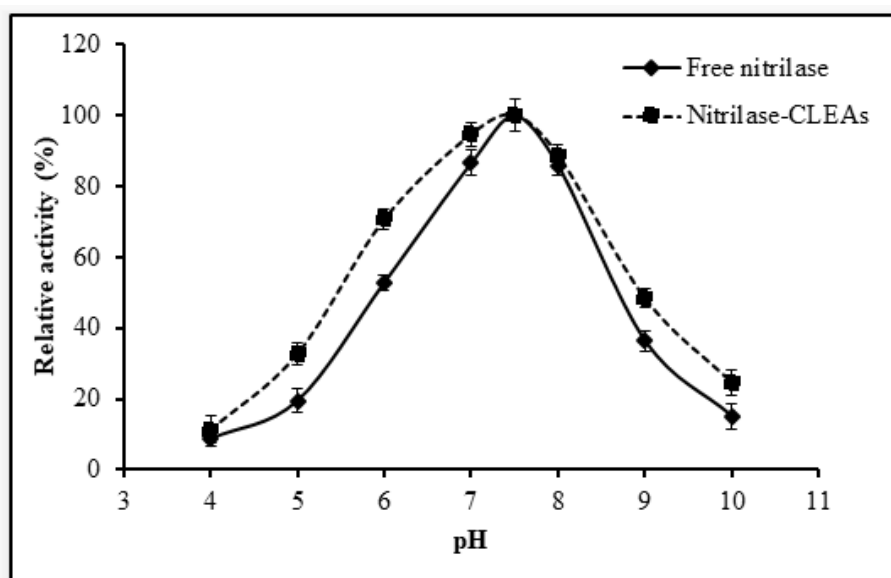
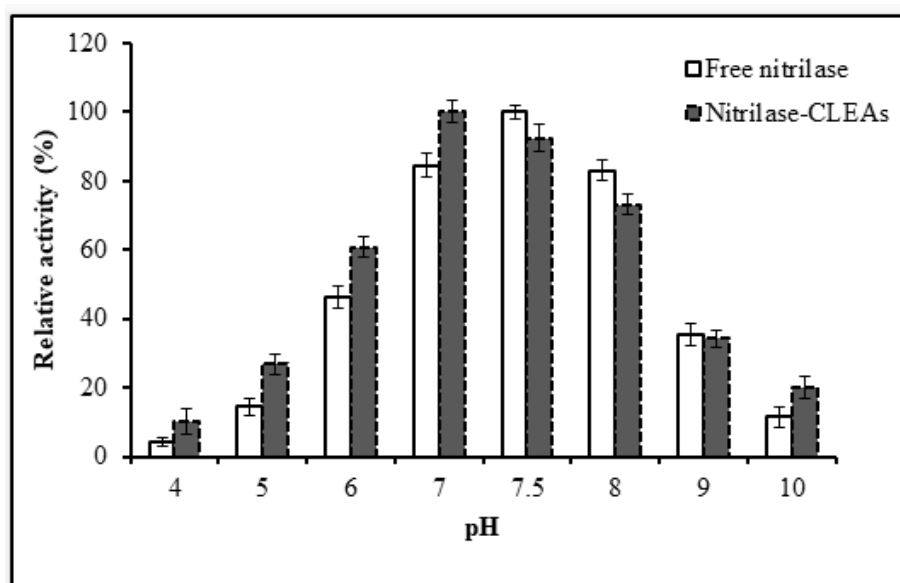


Figure 5.12 Consequences of operating pH on activity of free nitrilase and nitrilase-CLEAs

The results revealed that the activity of both the nitrilases increased from the pH 6.0 to pH 7.5, and highest activity of both free nitrilase and nitrilase-CLEAs was seen at

pH 7.0 in 0.1M buffer of potassium phosphate. Nitrilase-CLEAs exhibited a better activity under both acidic and alkaline over the free nitrilase. Further, the pH stability study revealed a higher stability of nitrilase-CLEAs under acidic conditions, while free nitrilase to be stable under alkaline conditions. The free nitrilase in pH regime of 7-8 and nitrilase-CLEAs in the pH range 6-8 retained more than 50% of their initial activities (*figure 5.13*).



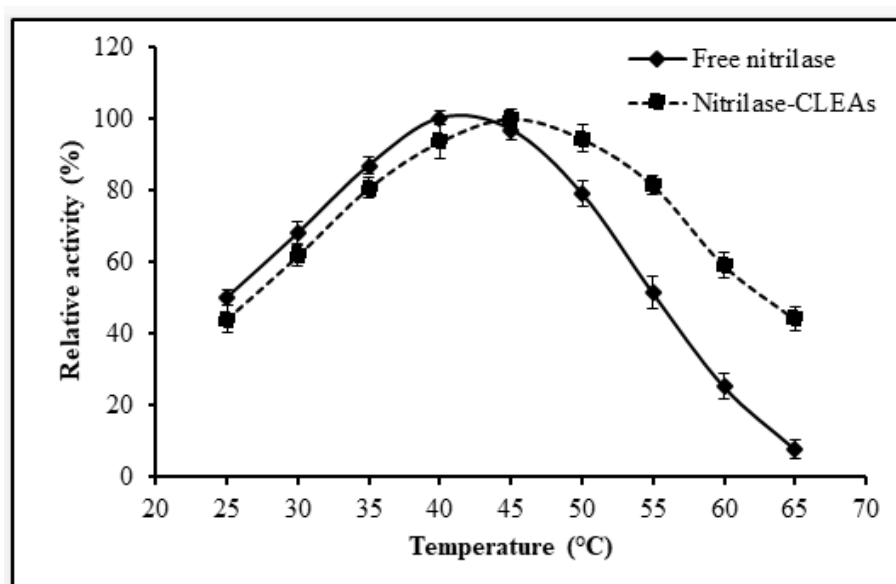
*Figure 5.13 pH stability of free nitrilase and nitrilase-CLEAs*

The current observation agrees with earlier report by [159], and [193]. The interaction of glutaraldehyde and free amino groups of enzymes nitrilase is by the development of Schiff bases and this may lead to transformation of its original ionization state and/or electrostatic charge/s, folding, and native conformation of enzyme [173].

### 5.3.7.2 Temperature optima and thermal stability

The determination of optimum temperature for free nitrilase and nitrilase-CLEAs was carried out by analyzing the activity in a wide temperature regime ranging from 25-65°C at pH 7.0 in 100 mM potassium phosphate buffer (*figure 5.14*).

The results revealed that free nitrilase and nitrilase-CLEAs displayed variations in sensitivities, and the optimum temperature was 40°C for and 45°C. The increase in optimum temperature by 5°C for nitrilase-CLEAs can be corroborated with the stability provided by strong covalent bond amongst glutaraldehyde and the aggregated enzymes [159, 185]



*Figure 5.14 Consequences of operating temperature on activity of free nitrilase and nitrilase-CLEAs*

A comparative investigation of thermal stability of free nitrilase and nitrilase-CLEAs was carried out in a temperature regime of 35-55°C in 100 mM potassium phosphate buffer of pH 7.0 (*figure 5.15* and *figure 5.16*).



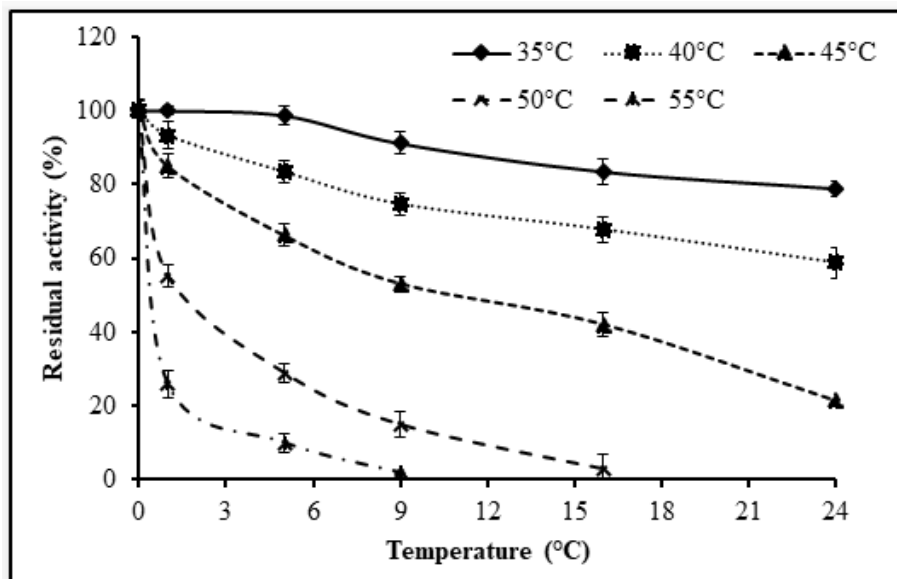


Figure 5.15 Thermal stability of free nitrilase

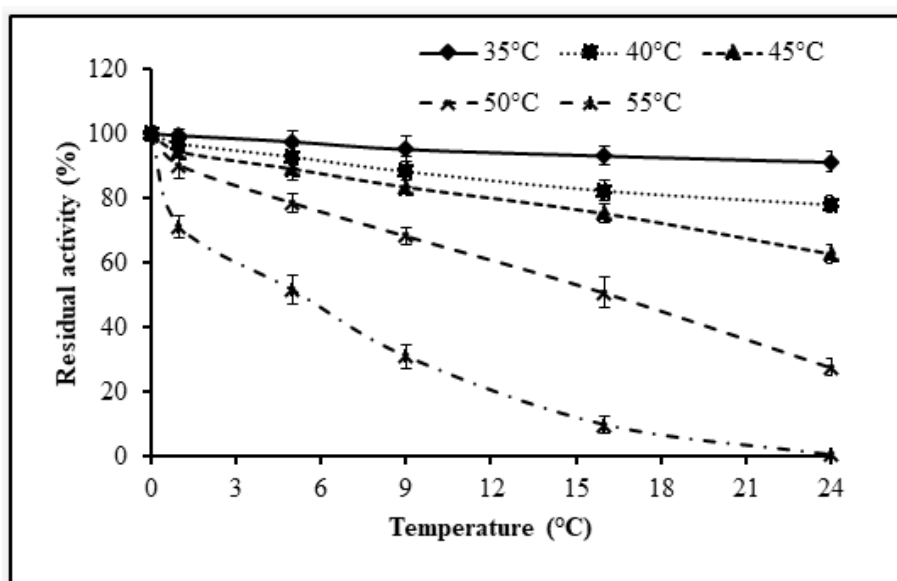


Figure 5.16 Thermal stability of nitrilase-CLEAs

The activity of both free nitrilase and nitrilase-CLEAs reduced gradually with a rise in temperature and incubation time. The residual activity of nitrilase-CLEAs has reduced less and at a slow rate than free nitrilase, and this could be due enhanced thermal stability. The free nitrilase have retained 78.89%, 58.65%, 21.21%, 2.89%,

and 1.80% activity after incubation for 24 h, 24 h, 24 h, 16 h, and 9 h at 35°C, 40°C, 45°C, 50°C, and 55°C, respectively. On the other hand, nitrilase-CLEAs were more tolerant to heat treatment as evident from the superior activities at time duration at each studied temperature. The subsequent residual activities of nitrilase-CLEAs at 35°C, 40°C, 45°C, 50°C, and 55°C after 24 hours of incubation were 91.34%, 78.08%, 62.73%, 27.66%, and 0.52%, respectively. Similar profile for thermal stability of free and nitrilase and nitrilase-CLEAs was previously recorded by [160] at 30°C and 50°C, [188] at 20-45°C, [171] at 4°C, 25°C, 37°C and 45°C, [55] at 26°C, 30°C, and 40°C, and [187] at 30°C, 40°C, and 50°C, respectively.

### **5.3.8 Hydroxylation of 2-chloro-4-cyanopyridine (2-chloro isonicotinitrile) to 2-chloro pyridine-4-carboxylic acid (2-chloro isonicotinic acid)**

The selection criteria of variables such as pH, temperature, enzyme loading, incubation time, amongst many others for optimization of process to obtain a desired product with required specifications are depended on characteristic features of product, substrate and reaction conditions that are possible to be followed [56]. Herein, the hydroxylation of 2-chloroisonicotinonitrile to 2-chloroisonicotinic acid was carried out at different nitrilase-CLEAs loading (5%, 10, and 20%) at  $30\pm 2^\circ\text{C}$ , and different temperature ( $25\pm 2^\circ\text{C}$ ,  $30\pm 2^\circ\text{C}$ ,  $35\pm 2^\circ\text{C}$ , and  $40\pm 2^\circ\text{C}$ ) at 10% enzyme loading. The progression of reaction with increasing incubation period was monitored by HPLC. The schematic presentation of nitrilase assisted reaction pathway for hydroxylation of 2-chloroisonicotinonitrile to 2-chloroisonicotinic acid is displayed in *figure 5.17*.

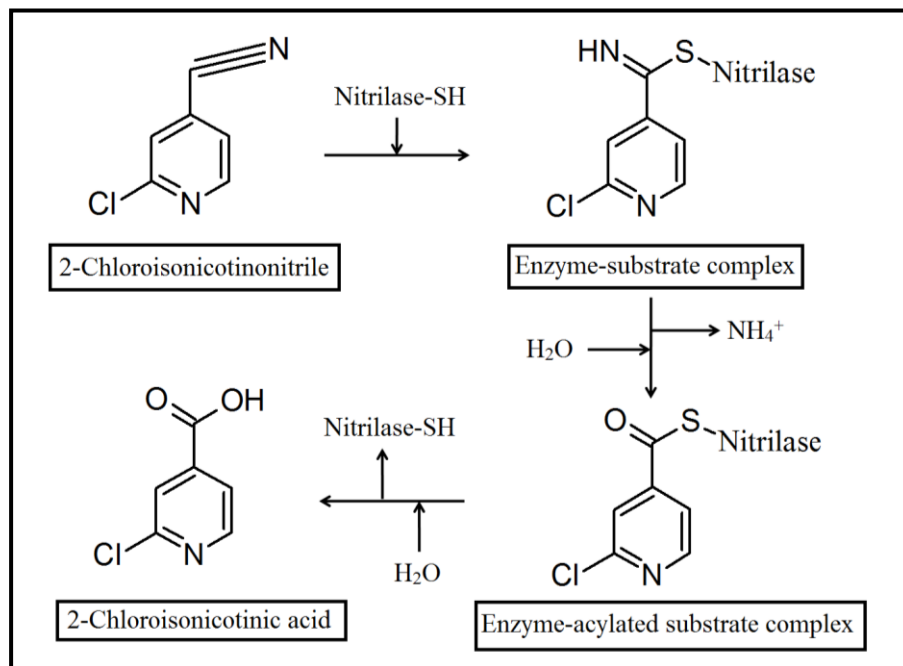


Figure 5.17 Reaction pathway of hydroxylation of 2-chloroisonicotinonitrile to 2-chloroisonicotinic acid with nitrilase

Moreover, the standard HPLC profiles of 2-chloroisonicotinonitrile (0.25 mg/mL 0.1% TFA in water (55%) and acetonitrile (45%)), 2-chloroisonicotinic acid (0.25 mg/mL in 0.1% TFA in water (55%) and acetonitrile (45%)), and enzymatic reaction with around 40% conversion are shown in figure 5.18, 5.19, and 5.20

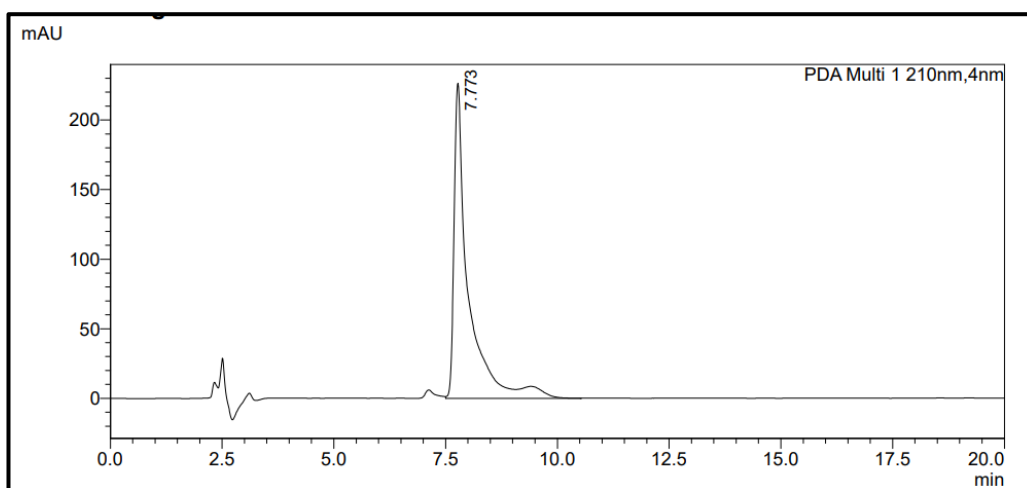
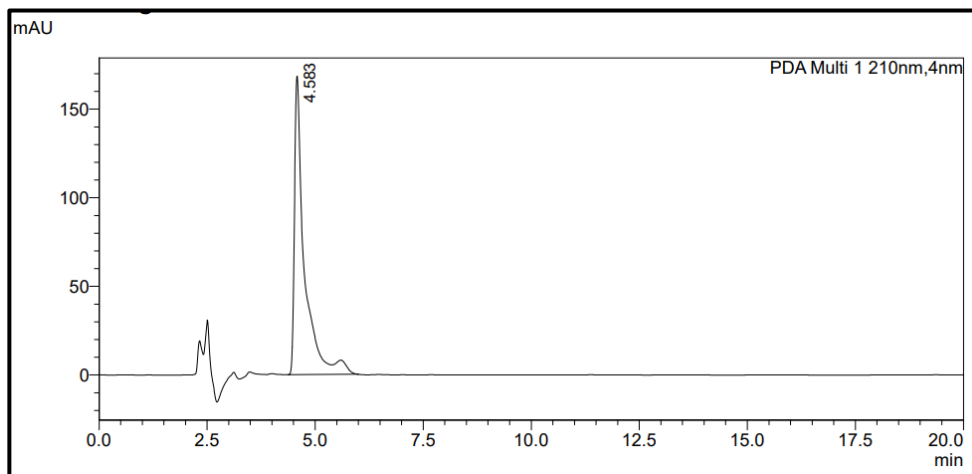
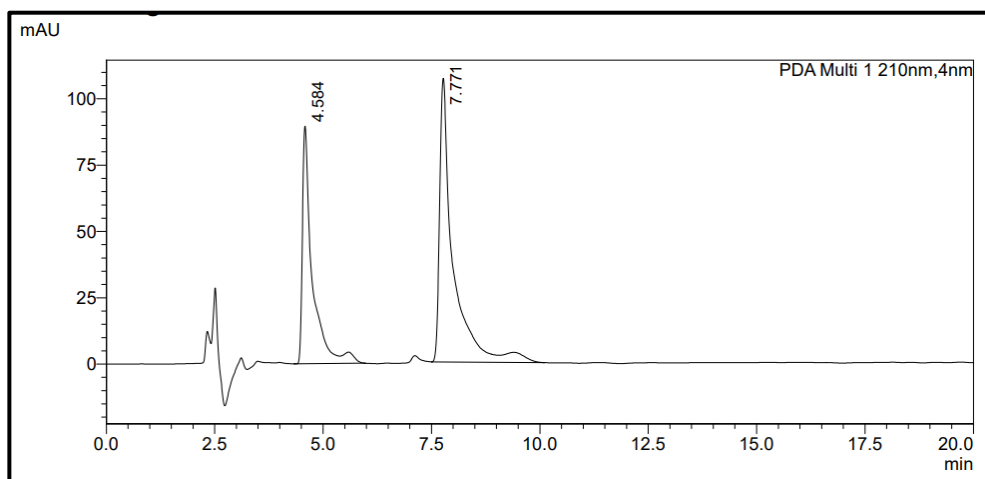


Figure 5.18 Chromatograms of standard 2-chloroisonicotinonitrile (0.25 mg/mL in 0.1% TFA in water (60%) and acetonitrile (40%)) on HPLC system



*Figure 5.19 Chromatograms of standard 2-chloroisonicotinic acid (0.25 mg/mL in 0.1% TFA in water (60%) and acetonitrile (40%)) on HPLC system*

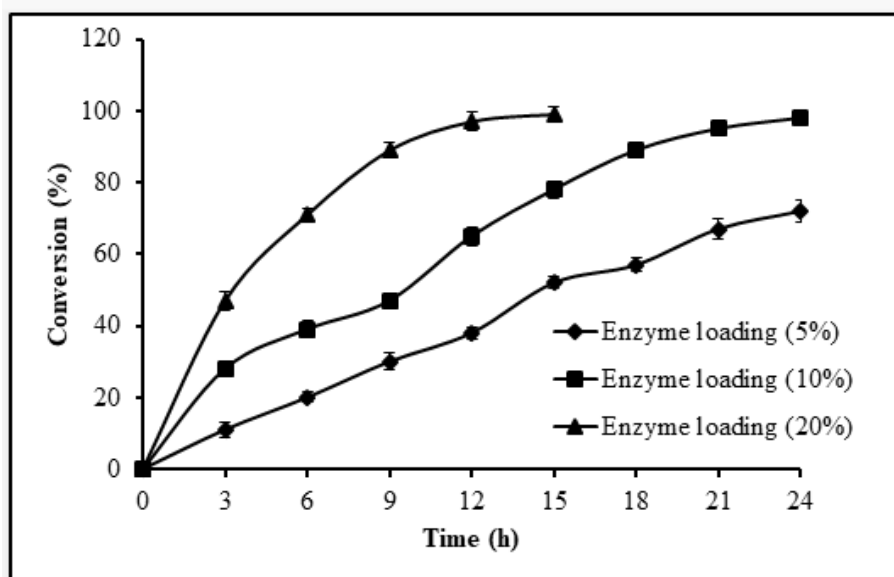


*Figure 5.20 Chromatograms of enzymatic reaction with around 40% conversion on HPLC system*

### **5.3.8.1 Effect of enzyme loading**

The hydroxylation of 2-chloro isonicotinitrile to 2-chloro isonicotinic acid was directly affected by the amount of nitrilase-CLEAs loaded. This could be attributed to the fact that product formation is linearly associated with the number of accessible active sites of enzyme to the substrate [99, 100]. Maximum conversion of 99% was seen at 20% loading of nitrilase-CLEAs after 15 hours, while minimum conversion

of 72% after 24 hours incubation was seen at 5% loading (*figure 5.21*). A considerably fair conversion of 98% was also seen with 10% loading after 24 h of incubation. The final product formation at 5%, 10% and 20% nitrilase-CLEAs loading was 69.59g/L, 94.72 g/L, and 95.69 g/L with a product yield of 61.20%, 83.30%, and 84.15%, respectively.



*Figure 5.21 Effect of nitrilase-CLEAs loading on conversion of 2-chloroisonicotinonitrile to 2-chloroisonicotinic acid*

### 5.3.8.2 Effect of reaction temperature

The influence of incubation temperature on the progression of the hydroxylation reaction was analyzed due to its direct effect on rate of reaction, solubility of respective substrate and its corresponding product, and stability of enzyme and its activity. The hydroxylation of 2-chloroisonicotinonitrile to 2-chloroisonicotinic acid was carried out at  $25\pm 2^\circ\text{C}$ ,  $30\pm 2^\circ\text{C}$ ,  $35\pm 2^\circ\text{C}$ , and  $40\pm 2^\circ\text{C}$  at nitrilase-CLEAs loading of 10% for 24 h. A steady and consistent increase in conversion was seen with an increase in temperature in the early phase and which significantly got reduced with further progression of reaction (*figure 5.22*) [194]. The conversion was 85%, 98%, 80%, and 72% at  $25\pm 2^\circ\text{C}$ ,  $30\pm 2^\circ\text{C}$ ,  $35\pm 2^\circ\text{C}$ , and  $40\pm 2^\circ\text{C}$  after 24 h with a product

formation of 82.16 g/L, 94.72 g/L, 77.32 g/L, and 69.59 g/L with a product yield of 72.25%, 83.30%, 68%, and 61.20%, respectively.

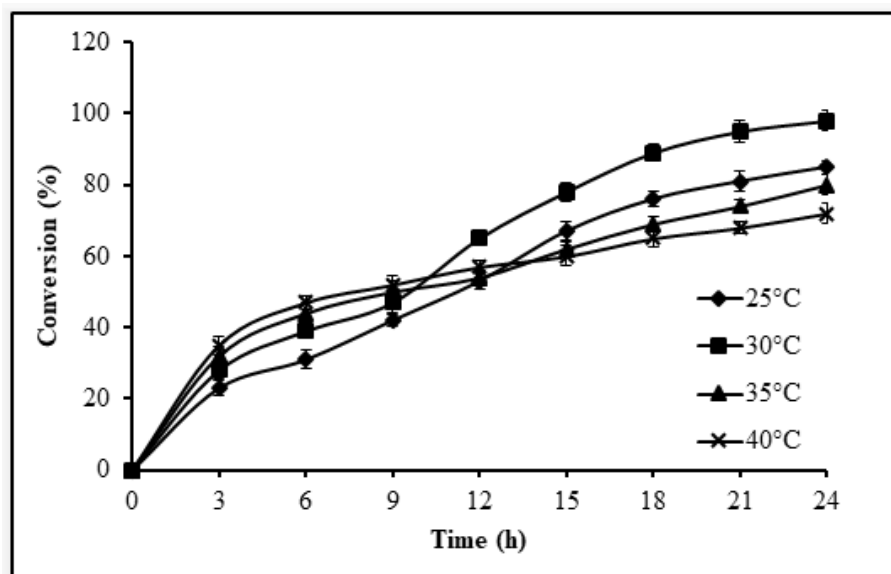


Figure 5.22 Effect of temperature with incubation time on conversion of 2-chloro isonicotinitrile to 2-chloroisonicotinic acid using nitrilase CLEA

The slight reduction in conversion, product formation, and yield at higher temperature may be corroborated with the fact that enzyme progressively loses its activity at elevated temperature with prolonged incubation period [55, 98].

### 5.3.9 Instrumental characterization of 2-chloro isonicotinitrile to 2-chloro isonicotinic acid

The instrumental characterization was performed to confirm the formation of 2-chloro isonicotinic acid from 2-chloro isonicotinitrile with ATR-FTIR,  $^1\text{H}$  NMR, and LC-MS analysis.

#### 5.3.9.1 Functional group confirmation by FTIR

The FTIR spectra of 2-chloroisonicotinitrile and 2-chloroisonicotinic acid is presented in figure 5.23

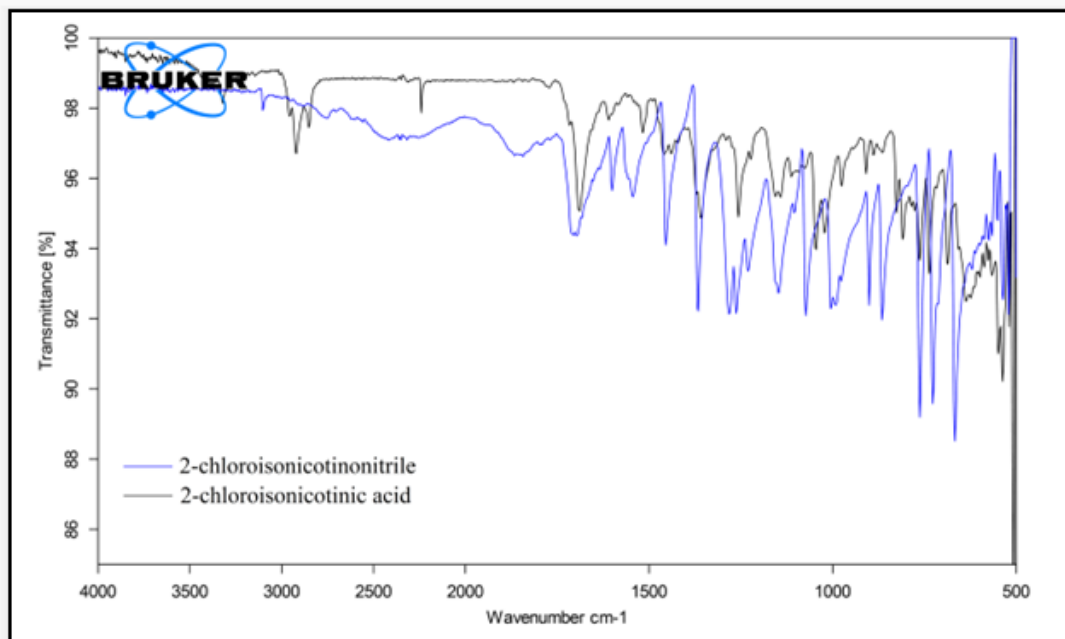


Figure 5.23 FTIR spectra of 2-chloroisonicotriole and 2-chloroisonicotinic acid

The presence of characteristic peak at 1590-1660 ( $1/\text{cm}$ ) and 1500 ( $1/\text{cm}$ ) indicated C-C and C-N in the pyridine rings. The presence of CN (nitrile) group in substrate was confirmed by prominent peak at 2250 ( $1/\text{cm}$ ), while its conversion to  $-\text{COOH}$  (carboxylic group) was investigated by distinct peaks at 3000 ( $1/\text{cm}$ ) and 1720 ( $1/\text{cm}$ ) revealing  $-\text{OH}$  stretching and  $\text{C}=\text{O}$  presence. The presence of  $\text{C}=\text{C}$  in pyridine was ascertained by peak at 1700 ( $1/\text{cm}$ ). Finally, the presence of  $\text{C}-\text{Cl}$  in the structure was revealed by sharp peak at 750 ( $1/\text{cm}$ ).

#### 5.3.9.2 Mass confirmation by LC-MS

The liquid chromatogram profile of 2-chloroisonicotinic acid in LC-MS was same as that obtained in HPLC with a retention time of 4.475 min (*figure 5.24*)

The mass fragments of the compound were determined by mass split in the instrument (*figure 5.25*).

The mono-isotopic mass of 2-chloroisonicotinic acid is 156.9 and this can also be confirmed by  $m/z$  of 156.87. The  $m/z$  fragments at 79.79, 114.77, 124.42, and

158.33 indicates the (M+H)<sup>+</sup> of pyridine ring, chloro-pyridine, pyridine CA, chloropyridine CA, respectively.

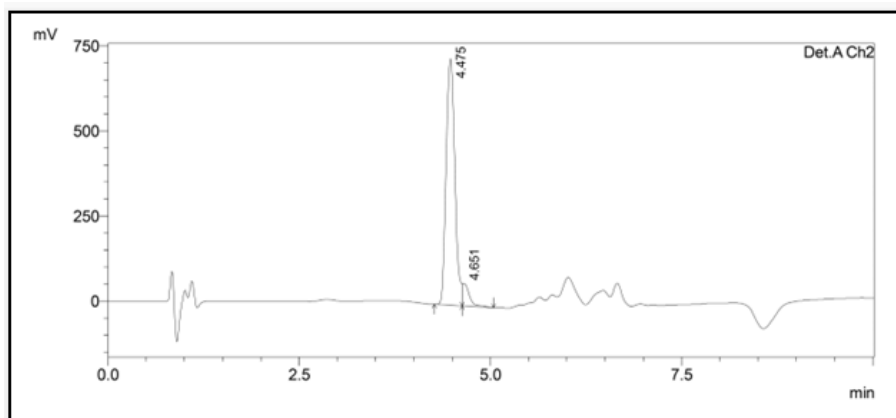


Figure 5.24 LC profile of 2-chloroisonicotinic acid in LC-MS

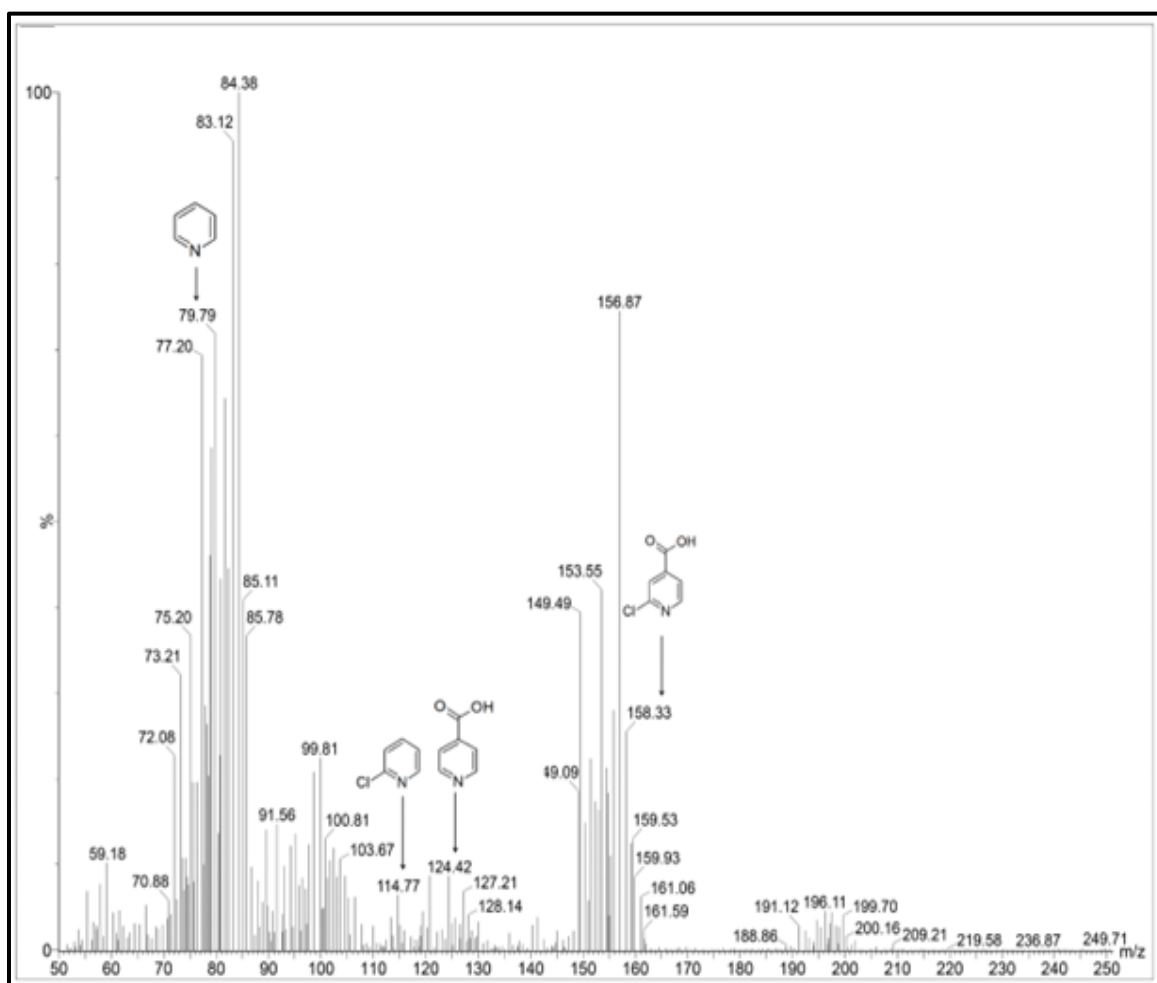


Figure 5.25 Mass fractions of 2-chloroisonicotinic acid on LC-MS spectra



### 5.3.9.3 Structural confirmation by NMR

NMR studies revealed the presence of three and four protons in 2-chloroisonicotinonitrile and 2-chloroisonicotinic acid, respectively. In the substrate (2-chloroisonicotinonitrile), the proton at 3<sup>rd</sup> position gives a singlet peak (S) at 8.28 ppm, equivalent to single proton, and the proton present at the 5<sup>th</sup> position gives doublet of doublet (dd) at 7.94 ppm equivalent to single proton, and proton present at the 6<sup>th</sup> position also gives doublet of doublet (dd) at 8.68 ppm and equivalent to single proton (*figure 5.26*). <sup>1</sup>H NMR (400 MHz, *d*<sub>6</sub>, DMSO): δ7.94 (dd, 1H, J = 1.44 Hz, 1.44 Hz), δ8.26 (S, 1H), δ8.66 (dd, 1H, J = 5.0 Hz, J = 5.08 Hz).

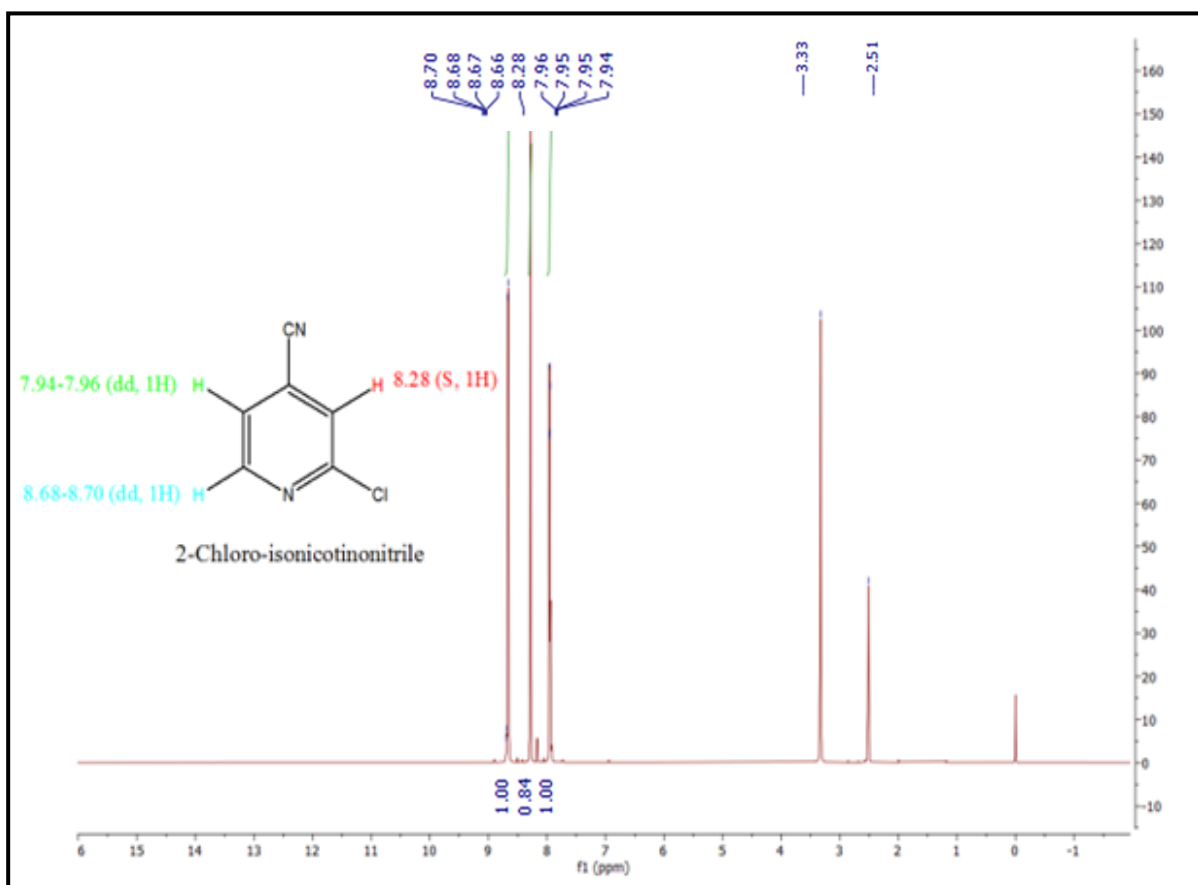
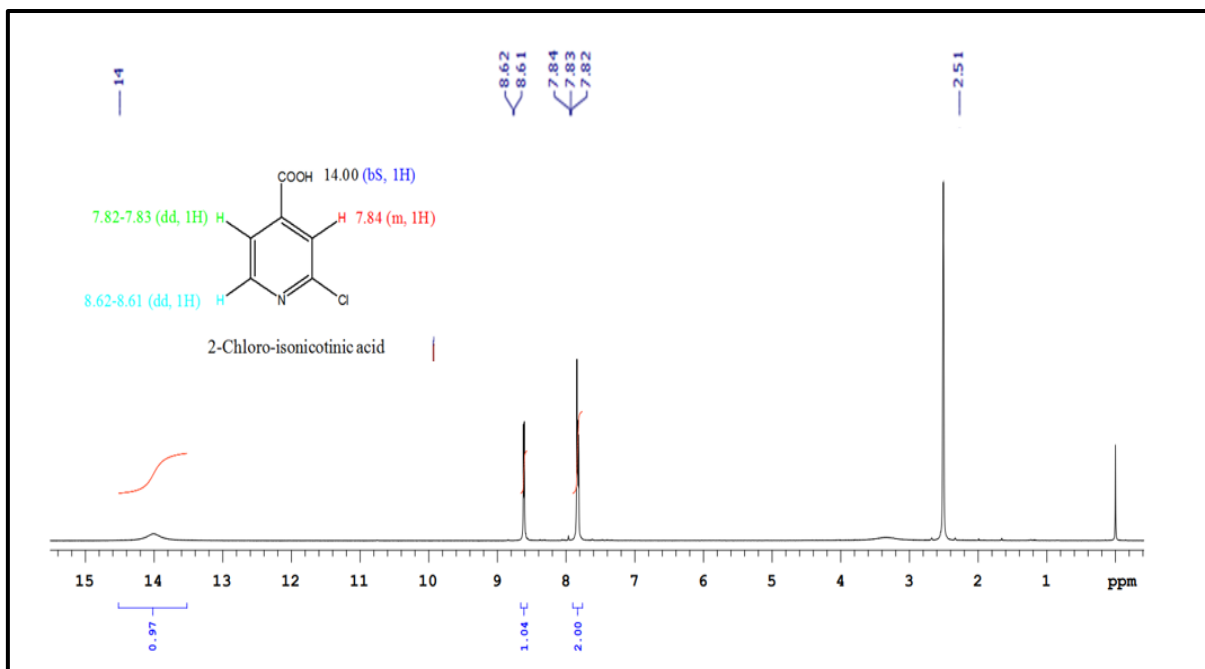


Figure 5.26 <sup>1</sup>H NMR spectra of 2-chloroisonicotinonitrile

In the product (2-chloroisonicotinic acid), the proton at 5<sup>th</sup> position gives the doublet at 8.61 ppm which is equivalent to single proton (S), and the proton present at the 3<sup>rd</sup>

and 6<sup>th</sup> position were merged and gives multiplet at 7.82 and these were equivalent to two protons *figure 5.27*).

<sup>1</sup>H NMR (400 MHz, *d*<sub>6</sub>, DMSO): δ7.82 (m, 2H), δ8.61 (d, 1H, J = 4.63 Hz), δ14.00 (bS, 1H) (bS, 1H).



*Figure 5.27* <sup>1</sup>H NMR spectra of 2-chloroisonicotinic acid

### 5.3.10 Reusability of nitrilase-CLEAs

The assessment of reusability of nitrilase-CLEAs was done for five consecutive cycles for a hydroxylation reaction performed in batch mode (*Table 5.2*).

*Table 5.2 Reusability profile of nitrilase-CLEAs for hydroxylation of 2-chloro isonicotinonitrile to 2-chloro isonicotinic acid indicating conversion of substrate to product (%), product formation (g/L) and product yield (%)*

<b>Cycle</b>	<b>Conversion (%)</b>	<b>Product (g/L)</b>	<b>Yield (%)</b>
1	100±0	96.65±2.45	84.99±2.59
2	92±2.32	87.88±1.95	77.28±2.35
3	81±1.85	75.53±2.03	66.42±2.24
4	55±2.01	50.03±1.83	43.99±2.11
5	30±1.75	25.24±2.20	22.2±2.03

There was continuous reduction in conversion of substrate to product, product formation, and yield of product with each subsequent batch. Herein, the nitrilase-CLEAs were efficient in converting 2-chloroisonicotinonitrile to 2-chloroisonicotinic acid till the third batch where the conversion was 81%, product formation was 75.53 g/L and yield was 66.42%, this was substantially less than the findings of first batch. In the fifth batch, the conversion reduced to 30% from 100%, product formation declined to 25.24 g/L from 96.65 g/L, and yield got down to 22.2% from 84.99%, when compared to the first batch. The present findings agreed with the previous reports by [160, 161, 171] indicating a reusability for five, fifteen, seven cycles, respectively. The continuous decline in the nitrilase-CLEAs after each progressive batch might be because of leach out of enzyme moieties from CLEA structure, generation of CLEA clumps, and/or reduced loading of enzymes caused by low shear resistance [67, 195]. In addition, the factors such as mechanical and physical forces exerted on nitrilase-CLEAs because of compression and firmness during/after

centrifugation and/or filtration could have also added up in hampering of nitrilase activity [185, 196]

#### **5.4. Conclusion**

Nitrilases were screened for hydroxylation of 2-chloro isonicotinonitrile to 2-chloroisonicotinic acid. ES-NIT-102 was chosen for CLEA preparation with glutaraldehyde concentration and cross linking period as operating parameters. The prepared nitrilase-CLEAs were characterized with particle size, SEM, FTIR, and SDS PAGE, and they displayed superior enzyme kinetics, enhanced pH and temperature stability, with a shift in optimal temperature by 5°C. Finally, the nitrilase-CLEAs were used for hydroxylation of 2-chloroisonicotinonitrile to 2-chloroisonicotinic acid with optimized conditions of 10% enzyme loading at 30°C displaying 98% conversion, 94.72 g/L product formation, and 83.30% recovery of yield after 24 h. Further, the reusability studies revealed nitrilase-CLEAs to be catalytically stable for 3 cycles with 81% conversion, 75.53 g/L product formation and 66.42% yield. The initial substrate and recovered product were characterized by HPLC, FTIR, LC-MS, and <sup>1</sup>H NMR, and displayed >99% purity. Lastly, this facile process for recovery, stabilization, and reusability of nitrilases could be explored as an efficient, simple, compatible, economic and green approach for other applications of nitrilases in pharmaceutical, food and fine chemical for synthesis of molecules with desired structural properties.

## **CHAPTER-6**

### **SUMMARY AND FUTURE PROSPECTS**

## Chapter 6

### 6.1. Summary

Industrial revolution is become invitation to various types of life-threatening diseases across globally. As per the reports and literature the active pharmaceutical intermediates are mostly chiral and show the better interaction towards the biological sites. Additionally, in current pharmaceuticals market around 50% active pharmaceutical intermediates are chiral in nature. It is necessary to separate the biologically active isomer from the racemate (racemic mixture) to avoid the side effects of non-biologically active isomer.

Previously, biologically active isomers were separated by researchers with establishing the separation techniques such as diastereomer formation which uses harsh chemicals, adverse reaction conditions and yielding very low yield of desired isomer.

Now a days, it is very essential to design and develop, inexpensive, selective, efficient, and effective resolution of biologically active isomer at ambient reaction condition which favours principles of green chemistry. From the literature it was observed that biocatalytic processes are effective for achieving this purpose. Considering above points, it was considered globally to develop most effective and economic biocatalytic resolution of biologically active isomer or active pharmaceutical intermediates in development of potential active pharmaceutical intermediates.

The current research work includes development of process for chiral selective synthesis of active pharmaceutical intermediates using reductase and transaminase enzymes whereas nitrilase enzymes study performed to understand recycling of enzymes for achieving economic feasibility of the process. The results achieved

during the research work found to be fast, selective, reproducible and economic. The details of the conclusion with chapter wise mentioned herein.

*In Chapter 3*, chiral selective synthesis of tert-butyl{5-[(4-cyanophenyl)(hydroxy)methyl]-2-fluorophenyl}carbamate from tert-butyl[5-(4-cyanobenzoyl)-2-fluorophenyl]carbamate) using reductase enzyme. For this reported literature referred and interpreted for the screening of the protocol development. Screened ~92 commercially available enzymes and 33 enzymes show considerable conversion. ES-KRED-213 found best hit with 76% conversion and 100% chiral selectivity. The process optimised with ES-KRED-213 studying parameters such as effect of cosolvent and process parameter includes incubation temperature, incubation pH, enzyme loading and substrate loading. Process consistency and downstream is optimise to check quality of the desired product with analytical techniques. The purity and chiral purity of chiral selective tert-butyl{5-[(4-cyanophenyl)(hydroxy)methyl]-2-fluorophenyl}carbamate performed. Purity by reverse phase HPLC using Ascentis Express (C18 (2.7  $\mu\text{m}$   $\times$  4.6  $\times$  150 mm)) and observed  $\geq 99\%$  whereas chiral purity by normal phase HPLC using CHIRALCEL® OJ-RH (5  $\mu\text{m}$   $\times$  4.6  $\times$  150 mm) and observed  $\geq 99.9\%$  selective. Specific optical rotation  $[\alpha]_{\text{D}}$  at 25<sup>0</sup>C: +30.5 [C=1, MDC] obtained. The further characterization include determination of melting point and boiling point and obtained result are 57-59<sup>0</sup>C, and 115-117<sup>0</sup>C respectively. LC-MS performed to check the mass and found 342.0 m/z, FTIR performed to confirm the functional group and finally, NMR checked for structural elucidation of the tert-butyl{5-[(4-cyanophenyl)(hydroxy)methyl]-2-fluoro phenyl}carbamate

The developed process is operated at ambient temperature and chiral resolution observed without using harsh chemicals and adverse reaction condition with

improved yield effectively. The consistency of the process was checked by performing experiments in triplicate.

*In Chapter 4*, The synthesis of (1*R*)-(3-methylphenyl)ethan-1-amine from of 1-(3-methylphenyl)ethan-1-one using transaminase enzyme. For this reported literature referred and interpreted for the screening of the protocol development. Screened ~28 commercially available enzymes and 8 enzymes show considerable conversion. ATA-025 found best hit with 60.5% conversion and 98.5% chiral selectivity. The process optimised with ATA-025 using two approaches (one factor at a time and statistical approach by Box Behnken Design).

The purity and chiral purity of (1*R*)-(3-methylphenyl)ethan-1-amine was performed on reverse phase HPLC using Atlantis® T3 (C18 (5  $\mu\text{m}$   $\times$  4.6  $\times$  250 mm)) and obtained  $\geq$  99% whereas chiral purity performed on GC using CP-Chirasil Dex CB (Length 25m,  $\times$  Film 0.25 $\mu\text{m}$   $\times$  Diameter 0.25 mm) and observed chiral purity ~99% for (1*R*)-(3-methylphenyl)ethan-1-amine

The further characterization includes boiling point which was found 202-204°C. LC-MS performed to check the mass and the observed value was 136.7342.0 m/z, FTIR performed to confirm the functional group and finally NMR checked for structural elucidation of the (1*R*)-(3-methylphenyl)ethan-1-amine.

The developed process is operated at ambient temperature and chiral resolution observed without using harsh chemicals, adverse reaction condition with improved yield effectively. The consistency of the process was checked by performing experiments in triplicate.

*In Chapter 5*, The synthesis of 2-chloroisonicotinic acid from 2-chloroisonicotinonitrile using nitrilase enzyme for this reported literature referred and interpreted for the screening of the protocol development and CLEA preparation.



Screened ~40 commercially available enzymes and 6 enzymes show considerable conversion. ES-NIT-102 found best hit with 86.9% conversion. The CLEA was prepared with best hit enzyme (ES-NIT-102). The recycling efficiency checked till 5 cycles and found that enzymes show 3 recycling after that enzyme activity slowly falls.

Optimization of CLEAs synthesis by screening precipitating solvent and cross-linking agent and cross-linking time reaction. Process optimization studied such as effect of cosolvent and process parameters includes incubation temperature, incubation pH, enzyme loading and substrate loading. Consistency of the process with yield after downstream established.

Synthesized ES-NIT-102-CLEAs was characterized by particle size distribution and scanning electron microscope. Cross-linking was confirmed by ATR-FTIR and molecular weight was determined by SDS-PAGE. Further biochemical characterization such as optimum pH and thermal stability comparison to free enzyme checked and found that ES-NIT-102 CLEAs shows improved stability comparative to free enzyme (ES-NIT-102).

Application of ES-NIT-CLEAs was performed in the synthesis of 2-chloroisonicotinic acid from 2-chloroisonicotinonitrile and isolated the 2-chloroisonicotinic acid. The Purity of 2-chloroisonicotinic acid was performed on reverse phase HPLC using HPLC column: Inert sustain AQ-C18 (5 $\mu$ m  $\times$  4.6  $\times$  250 mm) and observed purity was  $\geq$ 99%. The further characterization includes LC-MS performed to check the mass, it is found to be 156.7 m/z, FTIR performed to confirm the functional group and finally NMR checked for structural elucidation of 2-chloroisonicotinic acid.

The developed process is operated at ambient temperature with effective recycling ES-NIT-102 CLEAs till 3 cycles after this enzyme activity slowly falls. The consistency of the process is checked by performing experiments in triplicate.

## **6.2 Future prospects**

Biocatalysis is recently becoming the prime focus for the synthesis of chiral intermediates of API, because of its green, inexpensive chemistry and highly selective towards the chiral center. Naturally, existing enzymes sustainably synthesize the pharma, agriculture and fine chemicals chiral intermediates.

The presented thesis work has focused on the “Application of Biocatalysts for the Sustainable Potential Drugs” with the help of reductase, transaminase and nitrilase enzymes. Several aspects of enzymes biocatalysis, from the development of greener and eco-friendly process to the broadening of our current understanding towards the sustainable potential drugs., In chemical processes most molecules exist as racemic mixtures. Enantiomers of racemic compounds can often exhibit diverse pharmacological and therapeutic properties. In fact, different drugs usually have their biological activity based mainly on one enantiomer. The findings compiled in this thesis contribute to advance the utility and the basic understanding of process development, particularly with respect to the isolation of one enantiomer having biological activity. Also covers enzyme stability and implementation of CLEA for recycling the enzyme for reducing the step cost. Expected further research efforts both in industry and academic helps in implementing the biocatalytic process from 5-10% to 50% as compared to classical chemical processes. This application of biocatalyst works on prochiral center for the resolution of chiral building blocks of pharma, agriculture and fine chemicals intermediates. Such methods double the yield of enantiopure alcohols and amines compared to classical chemical synthesis.

The presented work has competitive with established chemical synthetic approaches under both the safety and atom economy perspectives. In this thesis work, the processes developed will hopefully aid the values to process safety and economically favourable process which also deals with the environment safety. In conclusion, the content of this thesis will hopefully direct future research in both industry and academia to access chiral alcohols, amines through safer and simpler routes relying on more stable, versatile and efficient process via more rational approaches.

There is various enzyme which need to explore in terms of industrial application. Mostly, these enzymes such as (reductase, transaminase and nitrilase) are applied for the synthesis API and its intermediate. However, the conditions mentioned in the study can be widely used for the screening reactions using reductase, transaminase and nitrilase enzymes. For the synthesis of chiral alcohols, amine and chiral acids. To further explore enzyme uses in pharmaceutical industries testing of enzymes towards intermediates of API, Agricultural and fine chemicals are ongoing in our laboratory. This exploratory work will open a new venue for the bio-catalysis industrial application.

## **REFERENCES**

## REFERENCES

- [1] K. Faber, *Biotransformations in organic chemistry: a textbook*, no. 660.634 F334B. Springer, 2011.
- [2] A. J. J. Straathof and P. Adlercreutz, *Applied biocatalysis*. CRC Press, 2000.
- [3] M. J. Snider and R. Wolfenden, "The rate of spontaneous decarboxylation of amino acids," *J Am Chem Soc*, vol. 122, no. 46, pp. 11507–11508, 2000.
- [4] R. Wolfenden and M. J. Snider, "The depth of chemical time and the power of enzymes as catalysts," *Acc Chem Res*, vol. 34, no. 12, pp. 938–945, 2001.
- [5] A. S. Bommarius and B. R. Riebel-Bommarius, *Biocatalysis: fundamentals and applications*. John Wiley & Sons, 2004.
- [6] R. N. Patel, "Synthesis of chiral pharmaceutical intermediates by biocatalysis," *Coord Chem Rev*, vol. 252, no. 5–7, pp. 659–701, 2008.
- [7] M. A. Kiss, É. Sefanovits-Bányai, Á. Tóth, and L. Boross, "Extractive Synthesis of Ethyl-Oleate Using Alginate Gel Co-Entrapped Yeast Cells and Lipase Enzyme," *Eng Life Sci*, vol. 4, no. 5, pp. 460–464, 2004.
- [8] M. Balat, H. Balat, and C. Öz, "Progress in bioethanol processing," *Prog Energy Combust Sci*, vol. 34, no. 5, pp. 551–573, 2008.
- [9] R. M. Kelly and H. Waldmann, "Biocatalysis and biotransformation-Editorial overview," *Curr Opin Chem Biol*, vol. 3, no. 1, pp. 9–10, 1999.
- [10] N. S. Çolak, E. Şahin, E. Dertli, M. T. Yilmaz, and O. Taylan, "Response surface methodology as optimization strategy for asymmetric bioreduction of acetophenone using whole cell of *Lactobacillus senmaizukei*," *Prep Biochem Biotechnol*, vol. 49, no. 9, pp. 884–890, 2019.

- [11] R. N. Patel *et al.*, “Enantioselective microbial reduction of substituted acetophenones,” *Tetrahedron Asymmetry*, vol. 15, no. 8, pp. 1247–1258, 2004.
- [12] A. A. Koesoema, D. M. Standley, T. Senda, and T. Matsuda, “Impact and relevance of alcohol dehydrogenase enantioselectivities on biotechnological applications,” *Appl Microbiol Biotechnol*, vol. 104, no. 7, pp. 2897–2909, 2020.
- [13] K. Nakamura, R. Yamanaka, T. Matsuda, and T. Harada, “Recent developments in asymmetric reduction of ketones with biocatalysts,” *Tetrahedron Asymmetry*, vol. 14, no. 18, pp. 2659–2681, 2003.
- [14] R. Kuncham *et al.*, “Biocatalytic ketone reduction—a study on screening and effect of culture conditions on the reduction of selected ketones,” *International Letters of Natural Sciences*, vol. 1, 2014.
- [15] N. Harms, G. E. de Vries, K. Maurer, J. Hoogendijk, and A. H. Stouthamer, “Isolation and nucleotide sequence of the methanol dehydrogenase structural gene from *Paracoccus denitrificans*,” *J Bacteriol*, vol. 169, no. 9, pp. 3969–3975, 1987.
- [16] J. Vonck and E. F. van Bruggen, “Architecture of peroxisomal alcohol oxidase crystals from the methylotrophic yeast *Hansenula polymorpha* as deduced by electron microscopy,” *J Bacteriol*, vol. 174, no. 16, pp. 5391–5399, 1992.
- [17] E. Keinan, E. K. Hafeli, K. K. Seth, and R. Lamed, “Thermostable enzymes in organic synthesis. 2. Asymmetric reduction of ketones with alcohol dehydrogenase from *Thermoanaerobium brockii*,” *J Am Chem Soc*, vol. 108, no. 1, pp. 162–169, 1986.
- [18] C. W. Bradshaw, W. Hummel, and C. H. Wong, “*Lactobacillus kefir* alcohol dehydrogenase: a useful catalyst for synthesis,” *J Org Chem*, vol. 57, no. 5, pp. 1532–1536, 1992.

- [19] T. Matsuda, T. Harada, N. Nakajima, and K. Nakamura, "Mechanism for improving stereoselectivity for asymmetric reduction using acetone powder of microorganism," *Tetrahedron Lett*, vol. 41, no. 21, pp. 4135–4138, 2000.
- [20] K. Nakamura, S. Kondo, N. Nakajima, and A. Ohno, "Mechanistic study for stereochemical control of microbial reduction of  $\alpha$ -keto esters in an organic solvent," *Tetrahedron*, vol. 51, no. 3, pp. 687–694, 1995.
- [21] K. Goldberg, K. Schroer, S. Lütz, and A. Liese, "Biocatalytic ketone reduction—a powerful tool for the production of chiral alcohols—part I: processes with isolated enzymes," *Appl Microbiol Biotechnol*, vol. 76, no. 2, pp. 237–248, 2007.
- [22] C. Hiraoka *et al.*, "Screening, substrate specificity and stereoselectivity of yeast strains, which reduce sterically hindered isopropyl ketones," *Tetrahedron Asymmetry*, vol. 17, no. 24, pp. 3358–3367, 2006.
- [23] D. Zhu, H. T. Malik, and L. Hua, "Asymmetric ketone reduction by a hyperthermophilic alcohol dehydrogenase. The substrate specificity, enantioselectivity and tolerance of organic solvents," *Tetrahedron Asymmetry*, vol. 17, no. 21, pp. 3010–3014, 2006.
- [24] B. El-Zahab, D. Donnelly, and P. Wang, "Particle-tethered NADH for production of methanol from CO<sub>2</sub> catalyzed by coimmobilized enzymes," *Biotechnol Bioeng*, vol. 99, no. 3, pp. 508–514, 2008.
- [25] V. Höllrigl, K. Otto, and A. Schmid, "Electroenzymatic asymmetric reduction of rac-3-methylcyclohexanone to (1S, 3S)-3-methylcyclohexanol in organic/aqueous media catalyzed by a thermophilic alcohol dehydrogenase," *Adv Synth Catal*, vol. 349, no. 8-9, pp. 1337–1340, 2007.

- [26] K. Nakamura and R. Yamanaka, "Light-mediated regulation of asymmetric reduction of ketones by a cyanobacterium," *Tetrahedron Asymmetry*, vol. 13, no. 23, pp. 2529–2533, 2002.
- [27] D. Mandal, A. Ahmad, M. I. Khan, and R. Kumar, "Enantioselective bioreduction of acetophenone and its analogs by the fungus *Trichothecium* sp.," *J Mol Catal B Enzym*, vol. 27, no. 2–3, pp. 61–63, 2004.
- [28] J. M. Woodley, "Choice of biocatalyst form for scalable processes." Citeseer, 2006.
- [29] J. B. van Beilen and Z. Li, "Enzyme technology: an overview," *Curr Opin Biotechnol*, vol. 13, no. 4, pp. 338–344, 2002.
- [30] Y. Xie, J.-H. Xu, W.-Y. Lu, and G.-Q. Lin, "Adzuki bean: a new resource of biocatalyst for asymmetric reduction of aromatic ketones with high stereoselectivity and substrate tolerance," *Bioresour Technol*, vol. 100, no. 9, pp. 2463–2468, 2009.
- [31] M. Matsuda, T. Yamazaki, K. Fuhshuku, and T. Sugai, "First total synthesis of modiolide A, based on the whole-cell yeast-catalyzed asymmetric reduction of a propargyl ketone," *Tetrahedron*, vol. 63, no. 36, pp. 8752–8760, 2007.
- [32] M. Gelo-Pujic, F. le Guyader, and T. Schlama, "Microbial and homogenous asymmetric catalysis in the reduction of 1-[3, 5-bis (trifluoromethyl) phenyl] ethanone," *Tetrahedron Asymmetry*, vol. 17, no. 13, pp. 2000–2005, 2006.
- [33] D. J. Pollard and J. M. Woodley, "Biocatalysis for pharmaceutical intermediates: the future is now," *Trends Biotechnol*, vol. 25, no. 2, pp. 66–73, 2007.
- [34] A. Miyadera, K. Satoh, and A. Imura, "Efficient synthesis of a key intermediate of DV-7751 via optical resolution or microbial reduction," *Chem Pharm Bull (Tokyo)*, vol. 48, no. 4, pp. 563–565, 2000.



- [35] F. Hollmann, D. J. Opperman, and C. E. Paul, "Biocatalytic reduction reactions from a chemist's perspective," *Angewandte Chemie International Edition*, vol. 60, no. 11, pp. 5644–5665, 2021.
- [36] A. Friberg, T. Johanson, J. Franzén, M. F. Gorwa-Grauslund, and T. Frejd, "Efficient bioreduction of bicyclo [2.2. 2] octane-2, 5-dione and bicyclo [2.2. 2] oct-7-ene-2, 5-dione by genetically engineered *Saccharomyces cerevisiae*," *Org Biomol Chem*, vol. 4, no. 11, pp. 2304–2312, 2006.
- [37] Z. Guo, Y. Chen, A. Goswami, R. L. Hanson, and R. N. Patel, "Synthesis of ethyl and t-butyl (3R, 5S)-dihydroxy-6-benzyloxy hexanoates via diastereo-and enantioselective microbial reduction," *Tetrahedron Asymmetry*, vol. 17, no. 10, pp. 1589–1602, 2006.
- [38] S. R. Wallner *et al.*, "Stereoselective anti-Prelog reduction of ketones by whole cells of *Comamonas testosteroni* in a 'substrate-coupled' approach," *J Mol Catal B Enzym*, vol. 55, no. 3–4, pp. 126–129, 2008.
- [39] I. A. Kaluzna, B. D. Feske, W. Wittayanan, I. Ghiviriga, and J. D. Stewart, "Stereoselective, biocatalytic reductions of  $\alpha$ -chloro- $\beta$ -keto esters," *J Org Chem*, vol. 70, no. 1, pp. 342–345, 2005.
- [40] J. v Comasseto, L. F. Assis, L. H. Andrade, I. H. Schoenlein-Crusius, and A. L. M. Porto, "Biotransformations of ortho-, meta-and para-aromatic nitrocompounds by strains of *Aspergillus terreus*: Reduction of ketones and deracemization of alcohols," *J Mol Catal B Enzym*, vol. 39, no. 1–4, pp. 24–30, 2006.
- [41] Y. Yang, D. Zhu, T. J. Piegat, and L. Hua, "Enzymatic ketone reduction: mapping the substrate profile of a short-chain alcohol dehydrogenase (YMR226c) from *Saccharomyces cerevisiae*," *Tetrahedron Asymmetry*, vol. 18, no. 15, pp. 1799–1803, 2007.

- [42] E. B. Kurbanoglu, K. Zilbeyaz, M. Ozdal, M. Taskin, and N. I. Kurbanoglu, "Asymmetric reduction of substituted acetophenones using once immobilized *Rhodotorula glutinis* cells," *Bioresour Technol*, vol. 101, no. 11, pp. 3825–3829, 2010.
- [43] W.-Y. Lou, W. Wang, R.-F. Li, and M.-H. Zong, "Efficient enantioselective reduction of 4'-methoxyacetophenone with immobilized *Rhodotorula* sp. AS2. 2241 cells in a hydrophilic ionic liquid-containing co-solvent system," *J Biotechnol*, vol. 143, no. 3, pp. 190–197, 2009.
- [44] P. Soni and U. C. Banerjee, "Enantioselective reduction of acetophenone and its derivatives with a new yeast isolate *Candida tropicalis* PBR-2 MTCC 5158," *Biotechnology Journal: Healthcare Nutrition Technology*, vol. 1, no. 1, pp. 80–85, 2006.
- [45] D. Koszelewski, K. Tauber, K. Faber, and W. Kroutil, " $\omega$ -Transaminases for the synthesis of non-racemic  $\alpha$ -chiral primary amines," *Trends Biotechnol*, vol. 28, no. 6, pp. 324–332, 2010.
- [46] M. S. Malik, E.-S. Park, and J.-S. Shin, "Features and technical applications of  $\omega$ -transaminases," *Appl Microbiol Biotechnol*, vol. 94, no. 5, pp. 1163–1171, 2012.
- [47] R. N. Patel, "Biocatalysis: Synthesis of key intermediates for development of pharmaceuticals," *ACS Catal*, vol. 1, no. 9, pp. 1056–1074, 2011.
- [48] R. N. Patel, "Biocatalysis for synthesis of pharmaceuticals," *Bioorg Med Chem*, vol. 26, no. 7, pp. 1252–1274, 2018.
- [49] D. Ghislieri and N. J. Turner, "Biocatalytic approaches to the synthesis of enantiomerically pure chiral amines," *Top Catal*, vol. 57, no. 5, pp. 284–300, 2014.

- [50] H.-U. Blaser, "Chirality and its implications for the pharmaceutical industry," *Rendiconti Lincei*, vol. 24, no. 3, pp. 213–216, 2013.
- [51] I. Slabu, J. L. Galman, R. C. Lloyd, and N. J. Turner, "Discovery, engineering, and synthetic application of transaminase biocatalysts," *ACS Catal*, vol. 7, no. 12, pp. 8263–8284, 2017.
- [52] S. A. Kelly *et al.*, "Application of  $\omega$ -transaminases in the pharmaceutical industry," *Chem Rev*, vol. 118, no. 1, pp. 349–367, 2018.
- [53] S. Mathew and H. Yun, " $\omega$ -Transaminases for the production of optically pure amines and unnatural amino acids," *ACS Catal*, vol. 2, no. 6, pp. 993–1001, 2012.
- [54] A. J. M. Howden and G. M. Preston, "Nitrilase enzymes and their role in plant–microbe interactions," *Microb Biotechnol*, vol. 2, no. 4, pp. 441–451, 2009.
- [55] A. Malandra *et al.*, "Continuous hydrolysis of 4-cyanopyridine by nitrilases from *Fusarium solani* O1 and *Aspergillus niger* K10," *Appl Microbiol Biotechnol*, vol. 85, no. 2, pp. 277–284, 2009.
- [56] L. Martínková and V. Křen, "Biotransformations with nitrilases," *Curr Opin Chem Biol*, vol. 14, no. 2, pp. 130–137, 2010.
- [57] L. F. Solares, R. Brieva, M. Quirós, I. Llorente, M. Bayod, and V. Gotor, "Enzymatic resolution of a quaternary stereogenic centre as the key step in the synthesis of (S)-(+)-citalopram," *Tetrahedron Asymmetry*, vol. 15, no. 2, pp. 341–345, 2004.
- [58] R. Vedantham, V. P. R. Vetukuri, A. Boini, M. Khagga, and R. Bandichhor, "Improved one-pot synthesis of citalopram diol and its conversion to citalopram," *Org Process Res Dev*, vol. 17, no. 5, pp. 798–805, 2013.

- [59] C. Pramanik *et al.*, “Process Development of Citalopram/Escitalopram Oxalate: Isolation and Synthesis of Novel Impurities,” *Org Process Res Dev*, vol. 16, no. 5, pp. 824–829, 2012.
- [60] H. Yin, P.-Q. Luan, Y.-F. Cao, J. Ge, and W.-Y. Lou, “Coupling metal and whole-cell catalysis to synthesize chiral alcohols,” *Bioresour Bioprocess*, vol. 9, no. 1, pp. 1–7, 2022.
- [61] T. Zhao, Z. Shen, and S. Sheng, “The efficacy and safety of nefopam for pain relief during laparoscopic cholecystectomy: A meta-analysis,” *Medicine*, vol. 97, no. 10, 2018.
- [62] T. Touge, H. Nara, M. Fujiwhara, Y. Kayaki, and T. Ikariya, “Efficient access to chiral benzhydrols via asymmetric transfer hydrogenation of unsymmetrical benzophenones with bifunctional oxo-tethered ruthenium catalysts,” *J Am Chem Soc*, vol. 138, no. 32, pp. 10084–10087, 2016.
- [63] R. Newar *et al.*, “Amino Acid-Functionalized Metal-Organic Frameworks for Asymmetric Base–Metal Catalysis,” *Angewandte Chemie International Edition*, vol. 60, no. 19, pp. 10964–10970, 2021.
- [64] E. J. Corey, R. K. Bakshi, and S. Shibata, “Highly enantioselective borane reduction of ketones catalyzed by chiral oxazaborolidines. Mechanism and synthetic implications,” *J Am Chem Soc*, vol. 109, no. 18, pp. 5551–5553, 1987.
- [65] V. S. Shende, P. Singh, and B. M. Bhanage, “Recent trends in organocatalyzed asymmetric reduction of prochiral ketones,” *Catal Sci Technol*, vol. 8, no. 4, pp. 955–969, 2018.

- [66] L. Zheng, X. Zhang, Y. Bai, and J. Fan, "Using algae cells to drive cofactor regeneration and asymmetric reduction for the synthesis of chiral chemicals," *Algal Res*, vol. 35, pp. 432–438, Nov. 2018.
- [67] J. Chapman, A. E. Ismail, and C. Z. Dinu, "Industrial Applications of Enzymes: Recent Advances, Techniques, and Outlooks," *Catalysts 2018, Vol. 8, Page 238*, vol. 8, no. 6, p. 238, Jun. 2018.
- [68] E. L. Noey *et al.*, "Origins of stereoselectivity in evolved ketoreductases," *Proc Natl Acad Sci U S A*, vol. 112, no. 51, pp. E7065–E7072, Dec. 2015.
- [69] M. Voss *et al.*, "Multi-faceted Set-up of a Diverse Ketoreductase Library Enables the Synthesis of Pharmaceutically-relevant Secondary Alcohols," *ChemCatChem*, vol. 13, no. 6, pp. 1538–1545, Mar. 2021.
- [70] J. Zheng, "Structural Biology of Tailoring Domains in Polyketide Synthases," *Comprehensive Natural Products III*, pp. 47–60, 2020.
- [71] C. Huang *et al.*, "Ketoreductase Catalyzed (Dynamic) Kinetic Resolution for Biomanufacturing of Chiral Chemicals," *Front Bioeng Biotechnol*, vol. 10, Jun. 2022.
- [72] H. Puetz, E. Puchl'ová, K. Vranková, and F. Hollmann, "Biocatalytic oxidation of alcohols," *Catalysts*, vol. 10, no. 9, p. 952, 2020.
- [73] P. D. de María, G. de Gonzalo, and A. R. Alcántara, "Biocatalysis as Useful Tool in Asymmetric Synthesis: An Assessment of Recently Granted Patents," *Biocatalysis*, p. 5, 2019.
- [74] N. K. Modukuru *et al.*, "Development of a Practical, Biocatalytic Reduction for the Manufacture of (S)-Licarbazepine Using an Evolved Ketoreductase," *Org Process Res Dev*, vol. 18, no. 6, pp. 810–815, Jun. 2014.

- [75] X. J. Zhang *et al.*, “Efficient production of an ezetimibe intermediate using carbonyl reductase coupled with glucose dehydrogenase,” *Biotechnol Prog*, vol. 37, no. 1, p. e3068, Jan. 2021.
- [76] K. B. Vega *et al.*, “Chemoenzymatic Synthesis of Apremilast: A Study Using Ketoreductases and Lipases,” *J Braz Chem Soc*, vol. 32, no. 5, pp. 1100–1110, Apr. 2021.
- [77] C. Liang, Y. Nie, X. Mu, and Y. Xu, “Gene mining-based identification of aldo-keto reductases for highly stereoselective reduction of bulky ketones,” *Bioresour Bioprocess*, vol. 5, no. 1, pp. 1–8, Jul. 2018.
- [78] X. M. Gong, Z. Qin, F. L. Li, B. B. Zeng, G. W. Zheng, and J. H. Xu, “Development of an Engineered Ketoreductase with Simultaneously Improved Thermostability and Activity for Making a Bulky Atorvastatin Precursor,” *ACS Catal*, vol. 9, no. 1, pp. 147–153, Jan. 2019.
- [79] A. Halama, J. Jirman, O. Boušková, P. Gibala, and A. K. Jarrah, “Improved process for the preparation of montelukast: Development of an efficient synthesis, identification of critical impurities and degradants,” *Org Process Res Dev*, vol. 14, no. 2, pp. 425–431, 2010.
- [80] B. O. Burek, A. W. H. Dawood, F. Hollmann, A. Liese, and D. Holtmann, “Process intensification as game changer in enzyme catalysis,” *Frontiers in Catalysis*, vol. 2, 2022.
- [81] C. Vergne-Vaxelaire *et al.*, “Nitrilase activity screening on structurally diverse substrates: Providing biocatalytic tools for organic synthesis,” *Adv Synth Catal*, vol. 355, no. 9, pp. 1763–1779, Jun. 2013.

- [82] S. F. Haq *et al.*, “A strategy to identify a ketoreductase that preferentially synthesizes pharmaceutically relevant (S)-alcohols using whole-cell biotransformation,” *Microb Cell Fact*, vol. 17, no. 1, pp. 1–14, 2018.
- [83] J. Ko, I. Kim, S. Yoo, B. Min, K. Kim, and C. Park, “Conversion of methylglyoxal to acetol by *Escherichia coli* aldo-keto reductases,” *J Bacteriol*, vol. 187, no. 16, pp. 5782–5789, 2005.
- [84] S. Jothi and S. Vuppu, “Taguchi analysis and asymmetric keto-reduction of acetophenone and its derivatives by soil filamentous fungal isolate: *Penicillium rubens* VIT SS1,” *Prep Biochem Biotechnol*, vol. 50, no. 10, pp. 1042–1052, 2020.
- [85] S. J. Marathe, N. N. Shah, S. R. Bajaj, and R. S. Singhal, “Esterification of anthocyanins isolated from floral waste: Characterization of the esters and their application in various food systems,” *Food Biosci*, vol. 40, p. 100852, 2021.
- [86] Q. Xu, X. Xu, H. Huang, and S. Li, “Efficient synthesis of (R)-2-chloro-1-phenylethol using a yeast carbonyl reductase with broad substrate spectrum and 2-propanol as cosubstrate,” *Biochem Eng J*, vol. 103, pp. 277–285, 2015.
- [87] Z. Li, H. Yang, J. Liu, Z. Huang, and F. Chen, “Application of ketoreductase in asymmetric synthesis of pharmaceuticals and bioactive molecules: an update (2018–2020),” *The Chemical Record*, vol. 21, no. 7, pp. 1611–1630, 2021.
- [88] G. de Gonzalo, “Biocatalysed reductions of  $\alpha$ -ketoesters employing Cyrene<sup>TM</sup> as cosolvent,” *Biocatal Biotransformation*, pp. 1–6, 2021.
- [89] R. S. Correia Cordeiro, N. Ríos-Lombardía, F. Morís, R. Kourist, and J. González-Sabín, “One-pot transformation of ketoximes into optically active alcohols and amines by sequential action of laccases and ketoreductases or  $\omega$ -transaminases,” *ChemCatChem*, vol. 11, no. 4, pp. 1272–1277, 2019.

- [90] Y. Shang, Q. Chen, X. Kong, Y. Zhang, J. Xu, and H. Yu, "Efficient Synthesis of (R)-2-Chloro-1-(2, 4-dichlorophenyl) ethanol with a Ketoreductase from *Scheffersomyces stipitis* CBS 6045," *Adv Synth Catal*, vol. 359, no. 3, pp. 426–431, 2017.
- [91] R. Pei, X. Fu, L. Tian, S.-F. Zhou, and W. Jiang, "Enhancing the biocatalytic synthesis of chiral drug intermediate by rational design an aldo-keto reductase from *Bacillus megaterium* YC4-R4," *Enzyme Microb Technol*, p. 110074, 2022.
- [92] A. B. Muley, S. Awasthi, P. P. Bhalerao, N. L. Jadhav, and R. S. Singhal, "Preparation of cross-linked enzyme aggregates of lipase from *Aspergillus niger*: process optimization, characterization, stability, and application for epoxidation of lemongrass oil," *Bioprocess Biosyst Eng*, vol. 44, no. 7, pp. 1383–1404, 2021.
- [93] A. B. Muley, S. A. Chaudhari, S. B. Bankar, and R. S. Singhal, "Stabilization of cutinase by covalent attachment on magnetic nanoparticles and improvement of its catalytic activity by ultrasonication," *Ultrason Sonochem*, vol. 55, pp. 174–185, 2019.
- [94] T. Sun, B. Li, Y. Nie, D. Wang, and Y. Xu, "Enhancement of asymmetric bioreduction of N, N-dimethyl-3-keto-3-(2-thienyl)-1-propanamine to corresponding (S)-enantiomer by fusion of carbonyl reductase and glucose dehydrogenase," *Bioresour Bioprocess*, vol. 4, no. 1, pp. 1–10, 2017.
- [95] J. Wang, P. Cheng, Y. Wu, A. Wang, F. Liu, and X. Pei, "Discovery of a new NADPH-dependent aldo-keto reductase from *Candida orthopsilosis* catalyzing the stereospecific synthesis of (R)-pantolactone by genome mining," *J Biotechnol*, vol. 291, pp. 26–34, 2019.
- [96] H. Yu, S. Qiu, F. Cheng, Y.-N. Cheng, Y.-J. Wang, and Y.-G. Zheng, "Improving the catalytic efficiency of aldo-keto reductase KmAKR towards t-butyl 6-cyano-



- (3R, 5R)-dihydroxyhexanoate via semi-rational design,” *Bioorg Chem*, vol. 90, p. 103018, 2019.
- [97] J. Zhang, T. Pu, Y. Xu, J. Huang, D. Chen, and L. Shao, “Synthesis of dehydroepiandrosterone by co-immobilization of keto reductase and glucose dehydrogenase,” *Journal of Chemical Technology & Biotechnology*, vol. 95, no. 9, pp. 2530–2536, 2020.
- [98] C. Teepakorn *et al.*, “Nitrilase immobilization and transposition from a micro-scale batch to a continuous process increase the nicotinic acid productivity,” *Biotechnol J*, vol. 16, no. 10, p. 2100010, 2021.
- [99] S.-P. Zou, J.-W. Huang, Y.-P. Xue, and Y.-G. Zheng, “Highly efficient production of 1-cyanocyclohexaneacetic acid by cross-linked cell aggregates (CLCAs) of recombinant *E. coli* harboring nitrilase gene,” *Process Biochemistry*, vol. 65, pp. 93–99, 2018.
- [100] X.-H. Zhang, Z.-Q. Liu, Y.-P. Xue, Y.-S. Wang, B. Yang, and Y.-G. Zheng, “Production of R-mandelic acid using nitrilase from recombinant *E. coli* cells immobilized with tris (hydroxymethyl) phosphine,” *Appl Biochem Biotechnol*, vol. 184, no. 3, pp. 1024–1035, 2018.
- [101] X. Tan, S. Gao, W. Zeng, S. Xin, Q. Yin, and X. Zhang, “Asymmetric synthesis of chiral primary amines by ruthenium-catalyzed direct reductive amination of alkyl aryl ketones with ammonium salts and molecular H<sub>2</sub>,” *J Am Chem Soc*, vol. 140, no. 6, pp. 2024–2027, 2018.
- [102] N. Yamazaki, M. Atobe, and C. Kibayashi, “Nucleophilic addition of methyllithium to chiral oxime ethers: asymmetric preparation of 1-(aryl) ethylamines and application to a synthesis of calcimimetics (+)-NPS R-568 and its thio analogue,” *Tetrahedron Lett*, vol. 42, no. 30, pp. 5029–5032, 2001.

- [103] R. Han, X. Cao, H. Fang, J. Zhou, and Y. Ni, "Structure-based engineering of  $\omega$ -transaminase for enhanced catalytic efficiency toward (R)-(+)-1-(1-naphthyl) ethylamine synthesis," *Molecular Catalysis*, vol. 502, p. 111368, 2021.
- [104] M. Fuchs *et al.*, "Improved chemoenzymatic asymmetric synthesis of (S)-Rivastigmine," *Tetrahedron*, vol. 68, no. 37, pp. 7691–7694, 2012.
- [105] M. Pallavicini, E. Valoti, L. Villa, and O. Piccolo, "Resolution of ortho- and meta-substituted 1-phenylethylamines with isopropylidene glycerol hydrogen phthalate," *Tetrahedron Asymmetry*, vol. 12, no. 7, pp. 1071–1075, 2001.
- [106] M. Hu, F.-L. Zhang, and M.-H. Xie, "Novel convenient synthesis of rivastigmine," *Synth Commun*, vol. 39, no. 9, pp. 1527–1533, 2009.
- [107] A. A. Boezio, J. Pytkowicz, A. Côté, and A. B. Charette, "Asymmetric, catalytic synthesis of  $\alpha$ -chiral amines using a novel bis (phosphine) monoxide chiral ligand," *J Am Chem Soc*, vol. 125, no. 47, pp. 14260–14261, 2003.
- [108] S. Simić, E. Zukić, L. Schermund, K. Faber, C. K. Winkler, and W. Kroutil, "Shortening synthetic routes to small molecule active pharmaceutical ingredients employing biocatalytic methods," *Chem Rev*, vol. 122, no. 1, pp. 1052–1126, 2021.
- [109] K. K. Popov *et al.*, "Reductive Amination Revisited: Reduction of Aldimines with Trichlorosilane Catalyzed by Dimethylformamide— Functional Group Tolerance, Scope, and Limitations," *J Org Chem*, vol. 87, no. 2, pp. 920–943, 2021.
- [110] M. Jouffroy, T. Nguyen, M. Cordier, M. Blot, T. Roisnel, and R. Gramage-Doria, "Iridium-Catalyzed Direct Reductive Amination of Ketones and Secondary Amines: Breaking the Aliphatic Wall," *Chemistry—A European Journal*, vol. 28, no. 36, p. e202201078, 2022.

- [111] D. Patil, "M.; Grogan, G.; Bommarius, A.; Yun, H," *Recent Advances in  $\omega$ -Transaminase-Mediated Biocatalysis for the Enantioselective Synthesis of Chiral Amines. Catalysts*, vol. 8, no. 7, p. 254, 2018.
- [112] Abu, R. "ChemCatChem, vol 7, p. 3094-3105, 2015; (b) Meier, R. J.; Gundersen, MT; Woodley, JM; Schürmann, M., p. 2594-2597, 2015.
- [113] S. A. Kelly, S. Mix, T. S. Moody, and B. F. Gilmore, "Transaminases for industrial biocatalysis: novel enzyme discovery," *Appl Microbiol Biotechnol*, vol. 104, no. 11, pp. 4781–4794, 2020.
- [114] J. Shin and B. Kim, "Asymmetric synthesis of chiral amines with  $\omega$ -transaminase," *Biotechnol Bioeng*, vol. 65, no. 2, pp. 206–211, 1999.
- [115] E. E. Ferrandi and D. Monti, "Amine transaminases in chiral amines synthesis: recent advances and challenges," *World J Microbiol Biotechnol*, vol. 34, no. 1, pp. 1–10, 2018.
- [116] A. Basso and S. Serban, "Industrial applications of immobilized enzymes—A review," *Molecular Catalysis*, vol. 479, p. 110607, 2019.
- [117] J. F. Rocha, A. F. Pina, and S. F. Sousa, "Cerqueira NMFSA," *PLP-dependent enzymes as important biocatalysts for the pharmaceutical, chemical and food industries: a structural and mechanistic perspective. Catal Sci Technol*, vol. 9, no. 18, pp. 4864–4876, 2019.
- [118] P. R. More and S. S. Arya, "Intensification of bio-actives extraction from pomegranate peel using pulsed ultrasound: Effect of factors, correlation, optimization and antioxidant bioactivities," *Ultrason Sonochem*, vol. 72, p. 105423, 2021.

- [119] Z. Z. Ariffin, M. N. Saat, and N. T. Zulkifle, "A review on response surface methodology optimization in microbial biotransformation," *Science Letters*, vol. 16, no. 2, pp. 64–72, 2022.
- [120] K. Mulchandani, A. B. Muley, and R. S. Singhal, "Assessment of eight *Morus indica* cultivars for 1-deoxynojirmycin content, antioxidant and anti-diabetic potential: optimization of ultrasound assisted process for bioactive enriched leaf extract," *Journal of Food Measurement and Characterization*, pp. 1–15, 2022.
- [121] A. B. Muley, A. B. Pandit, R. S. Singhal, and S. G. Dalvi, "Production of biologically active peptides by hydrolysis of whey protein isolates using hydrodynamic cavitation," *Ultrason Sonochem*, vol. 71, p. 105385, 2021.
- [122] A. Sahu, P. S. Badhe, R. Adivarekar, M. R. Ladole, and A. B. Pandit, "Synthesis of glycinamides using protease immobilized magnetic nanoparticles," *Biotechnology Reports*, vol. 12, pp. 13–25, 2016.
- [123] X.-H. Fan *et al.*, "Magnetically immobilized edible *Bacillus natto* for the biotransformation of polydatin to resveratrol and its bioactivity assessment," *Ind Crops Prod*, vol. 161, p. 113213, 2021.
- [124] H. J. Kang, J. W. Lee, T. W. Park, H. Y. Park, and J. Park, "Biotransformation of Ginsenoside Rd from Red Ginseng Saponin using Commercial  $\beta$ -glucanase," *Journal of the Society of Cosmetic Scientists of Korea*, vol. 46, no. 4, pp. 349–360, 2020.
- [125] R. Morya, A. Sharma, M. Kumar, B. Tyagi, S. S. Singh, and I. S. Thakur, "Polyhydroxyalkanoate synthesis and characterization: A proteogenomic and process optimization study for biovalorization of industrial lignin," *Bioresour Technol*, vol. 320, p. 124439, 2021.

- [126] A. Petri, V. Colonna, and O. Piccolo, "Asymmetric synthesis of a high added value chiral amine using immobilized  $\omega$ -transaminases," *Beilstein Journal of Organic Chemistry*, vol. 15, no. 1, pp. 60–66, 2019.
- [127] A. G. Khatik, A. K. Jain, and A. B. Muley, "Preparation, characterization and stability of cross linked nitrilase aggregates (nitrilase–CLEAs) for hydroxylation of 2-chloroisonicotinonitrile to 2-chloroisonicotinic acid," *Bioprocess Biosyst Eng*, vol. 45, no. 9, pp. 1559–1579, 2022.
- [128] E. Y. Bezsudnova, V. O. Popov, and K. M. Boyko, "Structural insight into the substrate specificity of PLP fold type IV transaminases," *Appl Microbiol Biotechnol*, vol. 104, no. 6, pp. 2343–2357, 2020.
- [129] L. Skalden *et al.*, "Two subtle amino acid changes in a transaminase substantially enhance or invert enantioselectivity in cascade syntheses," *ChemBioChem*, vol. 16, no. 7, pp. 1041–1045, 2015.
- [130] F. Guo and P. Berglund, "Transaminase biocatalysis: optimization and application," *Green Chemistry*, vol. 19, no. 2, pp. 333–360, 2017.
- [131] Á. Lakó, Z. Molnár, R. Mendonça, and L. Poppe, "Transaminase-mediated synthesis of enantiopure drug-like 1-(3', 4'-disubstituted phenyl) propan-2-amines," *RSC Adv*, vol. 10, no. 67, pp. 40894–40903, 2020.
- [132] R. Semproli *et al.*, "Use of Immobilized Amine Transaminase from *Vibrio fluvialis* under Flow Conditions for the Synthesis of (S)-1-(5-Fluoropyrimidin-2-yl)-ethanamine," *ChemCatChem*, vol. 12, no. 5, pp. 1359–1367, 2020.
- [133] J. L. Galman, D. Gahloth, F. Parmeggiani, I. Slabu, D. Leys, and N. J. Turner, "Characterization of a putrescine transaminase from *Pseudomonas putida* and its

- application to the synthesis of benzylamine derivatives,” *Front Bioeng Biotechnol*, vol. 6, p. 205, 2018.
- [134] T. P. Khobragade, S. Sarak, A. D. Pagar, H. Jeon, P. Giri, and H. Yun, “Synthesis of Sitagliptin Intermediate by a Multi-Enzymatic Cascade System Using Lipase and Transaminase With Benzylamine as an Amino Donor,” *Front Bioeng Biotechnol*, vol. 9, 2021.
- [135] C. M. Heckmann, L. J. Gourlay, B. Dominguez, and F. Paradisi, “An (R)-selective transaminase from *Thermomyces stellatus*: stabilizing the tetrameric form,” *Front Bioeng Biotechnol*, vol. 8, p. 707, 2020.
- [136] Y. Feng *et al.*, “Development of an efficient and scalable biocatalytic route to (3 R)-3-aminoazepane: a pharmaceutically important intermediate,” *Org Process Res Dev*, vol. 21, no. 4, pp. 648–654, 2017.
- [137] T. Börner *et al.*, “Explaining operational instability of amine transaminases: substrate-induced inactivation mechanism and influence of quaternary structure on enzyme–cofactor intermediate stability,” *ACS Catal*, vol. 7, no. 2, pp. 1259–1269, 2017.
- [138] N. H. Kulkarni, A. B. Muley, D. K. Bedade, and R. S. Singhal, “Cross-linked enzyme aggregates of arylamidase from *Cupriavidus oxalaticus* ICTDB921: process optimization, characterization, and application for mitigation of acrylamide in industrial wastewater,” *Bioprocess Biosyst Eng*, vol. 43, no. 3, pp. 457–471, 2020.
- [139] A. Petri, V. Colonna, and O. Piccolo, “Asymmetric synthesis of a high added value chiral amine using immobilized  $\omega$ -transaminases,” *Beilstein Journal of Organic Chemistry*, vol. 15, no. 1, pp. 60–66, 2019.

- [140] P. Kelefiotis-Stratidakis, T. Tyrikos-Ergas, and I. v Pavlidis, "The challenge of using isopropylamine as an amine donor in transaminase catalysed reactions," *Org Biomol Chem*, vol. 17, no. 7, pp. 1634–1642, 2019.
- [141] E. Y. Bezsudnova, T. N. Stekhanova, A. O. Ruzhitskiy, and V. O. Popov, "Effects of pH and temperature on (S)-amine activity of transaminase from the cold-adapted bacterium *Psychrobacter cryohalolentis*," *Extremophiles*, vol. 24, no. 4, pp. 537–549, 2020.
- [142] D. Hülsewede, J. Dohm, and J. von Langermann, "Donor Amine Salt-Based Continuous in situ-Product Crystallization in Amine Transaminase-Catalyzed Reactions," *Adv Synth Catal*, vol. 361, no. 11, pp. 2727–2733, 2019.
- [143] L. Martínez-Montero, J. H. Schrittwieser, and W. Kroutil, "Regioselective biocatalytic transformations employing transaminases and tyrosine phenol lyases," *Top Catal*, vol. 62, no. 17, pp. 1208–1217, 2019.
- [144] J. T. Kohrt *et al.*, "Application of Flow and Biocatalytic Transaminase Technology for the Synthesis of a 1-Oxa-8-azaspiro [4.5] decan-3-amine," *Org Process Res Dev*, vol. 26, no. 3, pp. 616–623, 2021.
- [145] S. J. Novick *et al.*, "Engineering an amine transaminase for the efficient production of a chiral sacubitril precursor," *ACS Catal*, vol. 11, no. 6, pp. 3762–3770, 2021.
- [146] M. Doeker, L. Grabowski, D. Rother, and A. Jupke, "In situ reactive extraction with oleic acid for process intensification in amine transaminase catalyzed reactions," *Green Chemistry*, vol. 24, no. 1, pp. 295–304, 2022.
- [147] A. W. H. Dawood *et al.*, "Isopropylamine as Amine Donor in Transaminase-Catalyzed Reactions: Better Acceptance through Reaction and Enzyme Engineering," *ChemCatChem*, vol. 10, no. 18, pp. 3943–3949, 2018.

- [148] M. v Pavlova, A. I. Mikhalev, M. E. Kon'shin, M. v Vasilyuk, and V. P. Kotegov, "Synthesis and Antiinflammatory Activity of Isonicotinic and Cinchoninic Acid Derivatives," *Pharm Chem J*, vol. 36, no. 8, pp. 425–427, 2002.
- [149] R. Peters, M. Althaus, C. Diolez, A. Rolland, E. Manginot, and M. Veyrat, "Practical formal total syntheses of the homocamptothecin derivative and anticancer agent diflomotecan via asymmetric acetate aldol additions to pyridine ketone substrates," *J Org Chem*, vol. 71, no. 20, pp. 7583–7595, 2006.
- [150] K. Fukunaga *et al.*, "2-(2-Phenylmorpholin-4-yl) pyrimidin-4 (3H)-ones; A new class of potent, selective and orally active glycogen synthase kinase-3 $\beta$  inhibitors," *Bioorg Med Chem Lett*, vol. 23, no. 24, pp. 6933–6937, 2013.
- [151] Y. Haga *et al.*, "Discovery of trans-N-[1-(2-fluorophenyl)-3-pyrazolyl]-3-oxospiro [6-azaisobenzofuran-1 (3H), 1'-cyclohexane]-4'-carboxamide, a potent and orally active neuropeptide Y Y5 receptor antagonist," *Bioorg Med Chem*, vol. 17, no. 19, pp. 6971–6982, 2009.
- [152] C. F. Schwender, B. R. Sunday, and D. J. Herzig, "11-Oxo-11H-pyrido [2, 1-b] quinazoline-8-CA, an orally active antiallergy agent," *J Med Chem*, vol. 22, no. 1, pp. 114–116, 1979.
- [153] A. N. Kost, P. B. Terent'ev, L. A. Golovleva, and A. A. Stolyarchuk, "Synthesis of substituted pyridinecarboxylic acids and study of their properties," *Pharm Chem J*, vol. 1, no. 5, pp. 235–240, 1967.
- [154] J.-D. Shen, X. Cai, Z.-Q. Liu, and Y.-G. Zheng, "Nitrilase: a promising biocatalyst in industrial applications for green chemistry," *Crit Rev Biotechnol*, vol. 41, no. 1, pp. 72–93, 2021.



- [155] Y. Asano and P. Kaul, "Hydrolysis and Reverse Hydrolysis: Selective Nitrile Hydrolysis using Nitrilase and its Related Enzymes," *Ref. Module Chem. Mol. Sci. Chem. Eng*, vol. 7, p. 122, 2012.
- [156] N. Xiong, Y. Dong, D. Xie, Z. Li, Y.-P. Xue, and Y.-G. Zheng, "Immobilization of Escherichia coli cells harboring a nitrilase with improved catalytic properties through polyethylenimine-induced silicification on zeolite," *Int J Biol Macromol*, vol. 193, pp. 1362–1370, 2021.
- [157] H.-J. Federsel, T. S. Moody, and S. J. C. Taylor, "Recent trends in enzyme immobilization—concepts for expanding the biocatalysis toolbox," *Molecules*, vol. 26, no. 9, p. 2822, 2021.
- [158] H. Peng *et al.*, "Encapsulation of Nitrilase in Zeolitic Imidazolate Framework-90 to Improve Its Stability and Reusability," *Appl Biochem Biotechnol*, pp. 1–14, 2022.
- [159] L.-Q. Jin, D.-J. Guo, Z.-T. Li, Z.-Q. Liu, and Y.-G. Zheng, "Immobilization of nitrilase on bioinspired silica for efficient synthesis of 2-hydroxy-4-(methylthio) butanoic acid from 2-hydroxy-4-(methylthio) butanenitrile," *J Ind Microbiol Biotechnol*, vol. 43, no. 5, pp. 585–593, 2016.
- [160] P. Kaul, A. Stolz, and U. emsp14C Banerjee, "Cross-linked amorphous nitrilase aggregates for enantioselective nitrile hydrolysis," *Adv Synth Catal*, vol. 349, no. 13, pp. 2167–2176, 2007.
- [161] J. Qiu, E. Su, W. Wang, and D. Wei, "Efficient asymmetric synthesis of dN-formyl-phenylglycine via cross-linked nitrilase aggregates catalyzed dynamic kinetic resolution," *Catal Commun*, vol. 51, pp. 19–23, 2014.

- [162] M. Bilal, J. Cui, and H. M. N. Iqbal, "Tailoring enzyme microenvironment: State-of-the-art strategy to fulfill the quest for efficient bio-catalysis," *Int J Biol Macromol*, vol. 130, pp. 186–196, 2019.
- [163] J. D. Cui and S. R. Jia, "Optimization protocols and improved strategies of cross-linked enzyme aggregates technology: current development and future challenges," *Crit Rev Biotechnol*, vol. 35, no. 1, pp. 15–28, 2015.
- [164] R. A. Sheldon, "CLEAs, combi-CLEAs and 'smart' magnetic CLEAs: Biocatalysis in a bio-based economy," *Catalysts*, vol. 9, no. 3, p. 261, 2019.
- [165] S. Behera, M. J. Dev, and R. S. Singhal, "Cross-linked  $\beta$ -Mannanase Aggregates: Preparation, Characterization, and Application for Producing Partially Hydrolyzed Guar Gum," *Appl Biochem Biotechnol*, vol. 194, no. 5, pp. 1981–2004, 2022.
- [166] S. Ren *et al.*, "Recent progress in multienzymes co-immobilization and multienzyme system applications," *Chemical Engineering Journal*, vol. 373, pp. 1254–1278, 2019.
- [167] J. Cui, T. Lin, Y. Feng, Z. Tan, and S. Jia, "Preparation of spherical cross-linked lipase aggregates with improved activity, stability and reusability characteristic in water-in-ionic liquid microemulsion," *Journal of Chemical Technology & Biotechnology*, vol. 92, no. 7, pp. 1785–1793, 2017.
- [168] J. Cui, Y. Zhao, R. Liu, C. Zhong, and S. Jia, "Surfactant-activated lipase hybrid nanoflowers with enhanced enzymatic performance," *Sci Rep*, vol. 6, no. 1, pp. 1–13, 2016.
- [169] K. Gupta, A. K. Jana, S. Kumar, and M. M. Jana, "Solid state fermentation with recovery of Amyloglucosidase from extract by direct immobilization in cross linked

- enzyme aggregate for starch hydrolysis,” *Biocatal Agric Biotechnol*, vol. 4, no. 4, pp. 486–492, 2015.
- [170] S. A. Chaudhari and R. S. Singhal, “A strategic approach for direct recovery and stabilization of *Fusarium* sp. ICT SAC1 cutinase from solid state fermented broth by carrier free cross-linked enzyme aggregates,” *Int J Biol Macromol*, vol. 98, pp. 610–621, 2017.
- [171] S. Kumar, U. Mohan, A. L. Kamble, S. Pawar, and U. C. Banerjee, “Cross-linked enzyme aggregates of recombinant *Pseudomonas putida* nitrilase for enantioselective nitrile hydrolysis,” *Bioresour Technol*, vol. 101, no. 17, pp. 6856–6858, 2010.
- [172] M. H. Kim, S. Park, Y. H. Kim, K. Won, and S. H. Lee, “Immobilization of formate dehydrogenase from *Candida boidinii* through cross-linked enzyme aggregates,” *J Mol Catal B Enzym*, vol. 97, pp. 209–214, 2013.
- [173] C. Miao *et al.*, “Synthesis and properties of porous CLEAs lipase by the calcium carbonate template method and its application in biodiesel production,” *RSC Adv*, vol. 9, no. 51, pp. 29665–29675, 2019.
- [174] M. N. Gupta and V. S. Bisaria, “Effectiveness of cross-linked enzyme aggregates of cellulolytic enzymes in hydrolyzing wheat straw,” *J Biosci Bioeng*, vol. 126, no. 4, pp. 445–450, 2018.
- [175] Y. v Samoylova, K. N. Sorokina, A. v Piligaev, and V. N. Parmon, “Preparation of stable cross-linked enzyme aggregates (CLEAs) of a *Ureibacillus thermosphaericus* esterase for application in malathion removal from wastewater,” *Catalysts*, vol. 8, no. 4, p. 154, 2018.

- [176] D. Yildirim, S. S. Tükel, and D. Alagöz, “Crosslinked enzyme aggregates of hydroxynitrile lyase partially purified from *Prunus dulcis* seeds and its application for the synthesis of enantiopure cyanohydrins,” *Biotechnol Prog*, vol. 30, no. 4, pp. 818–827, 2014.
- [177] X. Yang *et al.*, “Self-assembly amphipathic peptides induce active enzyme aggregation that dramatically increases the operational stability of nitrilase,” *RSC Adv*, vol. 4, no. 105, pp. 60675–60684, 2014.
- [178] N. Bradford, “A rapid and sensitive method for the quantitation microgram quantities of a protein isolated from red cell membranes,” *Anal. Biochem*, vol. 72, no. 248, p. e254, 1976.
- [179] N. Thakur, N. K. Sharma, S. Thakur, and T. C. Bhalla, “Bioprocess development for the synthesis of 4-aminophenylacetic acid using nitrilase activity of whole cells of *Alcaligenes faecalis* MTCC 12629,” *Catal Letters*, vol. 149, no. 10, pp. 2854–2863, 2019.
- [180] W. Cai, E. Su, S. Zhu, Y. Ren, and D. Wei, “Characterization of a nitrilase from *Arthrobacter aurescens* CYC705 for synthesis of iminodiacetic acid,” *J Gen Appl Microbiol*, vol. 60, no. 6, pp. 207–214, 2014.
- [181] K. Zhang, T. Pan, L. Wang, H. Wang, Y. Ren, and D. Wei, “Screening and characterization of a nitrilase with significant nitrile hydratase activity,” 2022.
- [182] Z. Chen *et al.*, “Expression and characterization of a novel nitrilase from hyperthermophilic bacterium *Thermotoga maritima* MSB8,” *J Microbiol Biotechnol*, vol. 25, no. 10, pp. 1660–1669, 2015.
- [183] W. Jiang *et al.*, “Production of (R)-(-)-mandelic acid with nitrilase immobilized on D155 resin modified by l-lysine,” *Biochem Eng J*, vol. 127, pp. 32–42, 2017.

- [184] X. Xing *et al.*, “CALB immobilized onto magnetic nanoparticles for efficient kinetic resolution of racemic secondary alcohols: long-term stability and reusability,” *Molecules*, vol. 24, no. 3, p. 490, 2019.
- [185] A. B. Muley, K. H. Mulchandani, and R. S. Singhal, “Immobilization of enzymes on iron oxide magnetic nanoparticles: synthesis, characterization, kinetics and thermodynamics,” in *Methods in Enzymology*, vol. 630, Elsevier, 2020, pp. 39–79.
- [186] M. Bilal, J. Cui, and H. M. N. Iqbal, “Tailoring enzyme microenvironment: State-of-the-art strategy to fulfill the quest for efficient bio-catalysis,” *Int J Biol Macromol*, vol. 130, pp. 186–196, 2019.
- [187] Z.-J. Zhang *et al.*, “Efficient production of (R)-(-)-mandelic acid using glutaraldehyde cross-linked *Escherichia coli* cells expressing *Alcaligenes sp.* nitrilase,” *Bioprocess Biosyst Eng*, vol. 37, no. 7, pp. 1241–1248, 2014.
- [188] J. Qiu, E. Su, W. Wang, and D. Wei, “Efficient asymmetric synthesis of dN-formyl-phenylglycine via cross-linked nitrilase aggregates catalyzed dynamic kinetic resolution,” *Catal Commun*, vol. 51, pp. 19–23, 2014.
- [189] R. Schoevaart *et al.*, “Preparation, optimization, and structures of cross-linked enzyme aggregates (CLEAs),” *Biotechnol Bioeng*, vol. 87, no. 6, pp. 754–762, 2004.
- [190] G. v Dennett and J. M. Blamey, “A new thermophilic nitrilase from an Antarctic hyperthermophilic microorganism,” *Front Bioeng Biotechnol*, vol. 4, p. 5, 2016.
- [191] M. T. de Martino *et al.*, “Compartmentalized cross-linked enzymatic nano-aggregates (c-CLE n A) for efficient in-flow biocatalysis,” *Chem Sci*, vol. 11, no. 10, pp. 2765–2769, 2020.

- [192] D. K. Bedade, A. B. Muley, and R. S. Singhal, "Magnetic cross-linked enzyme aggregates of acrylamidase from *Cupriavidus oxalaticus* ICTDB921 for biodegradation of acrylamide from industrial waste water," *Bioresour Technol*, vol. 272, pp. 137–145, 2019.
- [193] V. Vejvoda *et al.*, "Purification and characterization of nitrilase from *Fusarium solani* IMI196840," *Process Biochemistry*, vol. 45, no. 7, pp. 1115–1120, 2010.
- [194] A. Toprak, S. S. Tükel, and D. Yildirim, "Stabilization of multimeric nitrilase via different immobilization techniques for hydrolysis of acrylonitrile to acrylic acid," *Biocatal Biotransformation*, vol. 39, no. 3, pp. 221–231, 2021.
- [195] R. A. Sheldon, A. Basso, and D. Brady, "New frontiers in enzyme immobilisation: robust biocatalysts for a circular bio-based economy," *Chem Soc Rev*, vol. 50, no. 10, pp. 5850–5862, 2021.
- [196] V. Chauhan *et al.*, "An insight in developing carrier-free immobilized enzymes," *Front Bioeng Biotechnol*, vol. 10, pp 794411 2022.